

Spring 1991

# Models of macro-scale hydrology for use in global change research: Tests on two tropical river systems

Charles Joseph Vorosmarty  
*University of New Hampshire, Durham*

Follow this and additional works at: <https://scholars.unh.edu/dissertation>

---

## Recommended Citation

Vorosmarty, Charles Joseph, "Models of macro-scale hydrology for use in global change research: Tests on two tropical river systems" (1991). *Doctoral Dissertations*. 1657.  
<https://scholars.unh.edu/dissertation/1657>

This Dissertation is brought to you for free and open access by the Student Scholarship at University of New Hampshire Scholars' Repository. It has been accepted for inclusion in Doctoral Dissertations by an authorized administrator of University of New Hampshire Scholars' Repository. For more information, please contact [nicole.hentz@unh.edu](mailto:nicole.hentz@unh.edu).

## INFORMATION TO USERS

This manuscript has been reproduced from the microfilm master. UMI films the text directly from the original or copy submitted. Thus, some thesis and dissertation copies are in typewriter face, while others may be from any type of computer printer.

**The quality of this reproduction is dependent upon the quality of the copy submitted.** Broken or indistinct print, colored or poor quality illustrations and photographs, print bleedthrough, substandard margins, and improper alignment can adversely affect reproduction.

In the unlikely event that the author did not send UMI a complete manuscript and there are missing pages, these will be noted. Also, if unauthorized copyright material had to be removed, a note will indicate the deletion.

Oversize materials (e.g., maps, drawings, charts) are reproduced by sectioning the original, beginning at the upper left-hand corner and continuing from left to right in equal sections with small overlaps. Each original is also photographed in one exposure and is included in reduced form at the back of the book.

Photographs included in the original manuscript have been reproduced xerographically in this copy. Higher quality 6" x 9" black and white photographic prints are available for any photographs or illustrations appearing in this copy for an additional charge. Contact UMI directly to order.

# U·M·I

University Microfilms International  
A Bell & Howell Information Company  
300 North Zeeb Road, Ann Arbor MI 48106-1346 USA  
313 761-4700 800 521-0600



**Order Number 9131299**

**Models of macro-scale hydrology for use in global change  
research: Tests on two tropical river systems**

**Vörösmarty, Charles Joseph, Ph.D.**

**University of New Hampshire, 1991**

**Copyright ©1991 by Vörösmarty, Charles Joseph. All rights reserved.**

**U·M·I**  
300 N. Zeeb Rd.  
Ann Arbor, MI 48106



MODELS OF MACRO-SCALE HYDROLOGY FOR USE  
IN GLOBAL CHANGE RESEARCH:  
TESTS ON TWO TROPICAL RIVER SYSTEMS

BY

Charles Joseph Vörösmarty  
B.S., Cornell University, 1977  
M.S., University of New Hampshire, 1983

DISSERTATION

Submitted to the University of New Hampshire  
in Partial Fulfillment of  
the Requirements for the Degree of

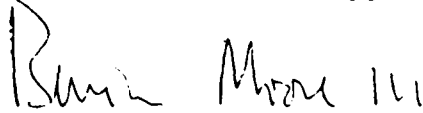
Doctor of Philosophy

in

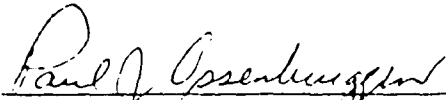
Engineering

May, 1991

This dissertation has been examined and approved.



\_\_\_\_\_  
Dissertation director, Berrien Moore, III  
Director of Institute for the Study of  
Earth, Oceans and Space



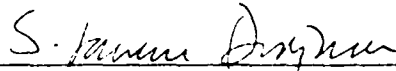
\_\_\_\_\_  
Paul Ossenbruggen, Associate Professor  
Civil Engineering



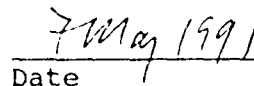
\_\_\_\_\_  
William B. Bowden, Assistant Professor  
Forest Resources



\_\_\_\_\_  
Theodore Loder, Associate Professor  
Earth Sciences



\_\_\_\_\_  
S. Lawrence Dingman, Professor  
Earth Sciences



\_\_\_\_\_  
Date

ALL RIGHTS RESERVED

c 1991

Charles Joseph Vorosmarty

## ACKNOWLEDGEMENTS

The research reported upon in this dissertation is in every sense of the word multi-disciplinary. It is the product of a long-term collaborative research effort to understand how humans have altered the Earth's physical, biological and geochemical cycles. This document is the culmination of numerous fruitful discussions with my colleagues both in the United States and abroad. I first wish to acknowledge the input of collaborating scientists at the Ecosystems Center of the Marine Biological Laboratory (Woods Hole, Massachusetts, USA) -- B. Bergquist, D. Kicklighter, J. Melillo, K. Nadelhoffer, B. J. Peterson, J. Raich, E. B. Rastetter, D. Rudnick and Paul Steudler. I wish also to thank C. J. Willmott of the University of Delaware and B. Choudhury of the Goddard Space Flight Center (Greenbelt, Maryland USA) for the thoughts they shared on water balance modeling and data sets. Members of the Water Resources Program at the International Institute for Applied Systems Analysis (Laxenburg, Austria) deserve special thanks. Prof. Z. Kaczmarek, K. A. Salewicz, C. Gandolfi, S. Kuuika, H. Leenaers, D. Miranov, and Y. Samarskaya all fostered a true spirit of cooperative research. J. R. Barnes of the Institute of Cultural Affairs (Harare,



Zimbabwe) supplied much-needed encouragement and editorial prowess. At the University of New Hampshire, A. Grace, E. Lent, S. Morin, S. Palmer, T. Stearns, H. Tennyson and S. Wallace provided critical assistance in the preparation of graphics and literature citations. Special recognition goes to C. Ransom who drew this document into a coherent whole. I also wish to recognize W. Chomentowski, M. P. Gildea, A. Grace, F. Rubin, D. Skole, and C. Smith for their insights on Geographic Information Systems. I am grateful to my dissertation committee for their support and critical comments on this research -- W. B. Bowden, S.L. Dingman, T. Loder, B. Moore III, and P. Ossenbruggen. I am fortunate to have participated in the Engineering Systems Design Program, headed by Prof. C. Taft, whose creative approach to multi-disciplinary education provided the necessary intellectual environment in which to pursue this research. Sincerest thanks go out to my father Charles and my son Daniel, who provided patience and support during the last challenging days of my graduate education. Finally, this work has been supported in part by the National Aeronautics and Space Administration, Grant NAGW-714, NAGW-1888 and Contract NA55-30558, and by the US Environmental Protection Agency, Grant No. CR816278010.

TABLE OF CONTENTS

ACKNOWLEDGMENTS . . . . . iii  
LIST OF TABLES . . . . . ix  
LIST OF FIGURES . . . . . xi  
LIST OF PLATES . . . . . xiv  
ABSTRACT . . . . . xvi

CHAPTER	PAGE
INTRODUCTION . . . . .	1
I.    HYDROLOGY AND THE CONCEPT OF GLOBAL CHANGE . . . . .	8
Introduction . . . . .	8
The Role of Water at the Earth's Surface . . . . .	11
Climatic Balances . . . . .	11
Biogeochemical Processing . . . . .	12
Weathering and Constituent Transport . . . . .	12
Habitat . . . . .	13
Water Resources for Human Development . . . . .	14
Anthropogenic Disturbance of the Hydrologic Cycle . . . . .	14
Climate Change . . . . .	15
Land Use Effects . . . . .	18
Water Resources Systems . . . . .	20
Macro-Scale Hydrology Models . . . . .	21
Summary . . . . .	24
II.   CONTINENTAL-SCALE MODELS OF WATER BALANCE AND FLUVIAL TRANSPORT: AN APPLICATION TO SOUTH	

AMERICA . . . . .	25
Introduction . . . . .	25
Model Development . . . . .	30
Water Balance Model: Structure . . . . .	31
Water Balance Model: Required Data . . . . .	37
Water Transport Model: Structure and Parameterization . . . . .	42
Results and Discussion . . . . .	53
Water Balance Model: General Hydrologic Regimes in South America . . . . .	53
Water Balance Model: Detailed Calculations at the Continental Scale . . . . .	57
Soil Moisture . . . . .	57
Evapotranspiration . . . . .	64
Runoff . . . . .	71
Water Balance Model: Amazon/Tocantins Drainage Basin . . . . .	77
Water Transport Model: Amazon/Tocantins River . . . . .	78
Comparison to Observed Hydrographs . . . . .	79
Mainstem/tributary Interactions . . . . .	87
Sensitivity to Transfer and Flooding Parameters . . . . .	90
Future Research Needs . . . . .	93
Summary and Conclusions . . . . .	96

III. MODELING BASIN-SCALE HYDROLOGY IN SUPPORT OF PHYSICAL CLIMATE AND GLOBAL BIOGEOCHEMICAL STUDIES: AN EXAMPLE USING THE ZAMBEZI RIVER . . . . .	100
Introduction . . . . .	100
Site Description . . . . .	104
Catchment-Scale Hydrologic Models . . . . .	109
Brief Overview of Models . . . . .	110
Water Balance Model . . . . .	114
Supporting Data and Technical Considerations . . . . .	114
The Algorithm . . . . .	122
Water Transport Model . . . . .	126
Supporting Data and Technical Considerations . . . . .	126
The Algorithm . . . . .	134
Anthropogenic Disturbance: An Important Component of the Terrestrial Water Cycle . . . . .	141
Impoundment . . . . .	142
Land Degradation . . . . .	147
Climate Change . . . . .	153
Summary and Conclusions . . . . .	159
IV. FURTHER TESTS OF A MACRO-SCALE HYDROLOGY MODEL IN TROPICAL RIVER SYSTEMS . . . . .	163
Introduction . . . . .	163
Site Description and Biophysical Data Sets . . . . .	164
Model Description . . . . .	185

Water Balance Model . . . . .	185
Water Transport Model . . . . .	189
Model Performance Tests . . . . .	192
Results and Discussion . . . . .	195
Preliminary Calibration--Water Balance . . . . .	195
Preliminary Calibration--Fluvial Transport . . . . .	201
Enhanced Parameterization--Water Balance . . . . .	206
Enhanced Parameterization--Fluvial Transport . . . . .	216
Summary and Conclusions . . . . .	224
V. CONCLUSIONS . . . . .	228
REFERENCES . . . . .	233
APPENDIX . . . . .	251

## LIST OF TABLES

Table		Page
I-1	Distribution of Global Water Pools (from Strahler and Strahler 1973) . . . . .	10
II-1	Relationships Linking Vegetation Class, Soil Texture, Rooting Depth and Moisture Capacities of Soil . . . . .	39
II-2	Distribution of South American Ecosystems . . . . .	41
II-3	Model-Generated Discharges for the Mainstem Amazon and Tocantins . . . . .	85
II-4	Model-Generated Discharges for Major Amazon River Tributaries . . . . .	86
II-5	Influence of Tributary Inputs on the Behavior of the Mainstem Amazon River . . . . .	88
III-1	Drainage Areas Reported for the Zambezi River System . . . . .	107
III-2	Required Data Sets for Water Balance Model . . . . .	115
III-3	Observed Mean Annual Discharges . . . . .	121
III-4	Wetlands in the Zambezi River System . . . . .	131
III-5	Floodwave Translation . . . . .	137
III-6	Characteristics of Major Impoundments . . . . .	145
III-7	Simulated Impact of 2x CO <sub>2</sub> on Precipitation in the Zambezi Basin . . . . .	156
IV-1	Cumulative Drainage Area for Subcatchments of the Zambezi River System . . . . .	167
IV-2	Biophysical Attributes of the 12 Subbasins of the Zambezi River System. The basin names refer to those given in Plate 1 . . . . .	170
IV-3	Relationships Linking Vegetation Class, Soil Texture, Rooting Depth and Moisture Capacities of Soil . . . . .	174

IV-4	Mean Annual Discharge for Selected Subcatchments of the Zambezi . . . . .	193
IV-5	Amazon/Tocantins River Model Performance Tests (after Vörösmarty et. al. 1989) . . . . .	202
IV-6	Zambezi River Model Performance Tests, Based on Preliminary Water Balance Adjustment . . . . .	204
IV-7	Water Budgets with Precipitation Inputs Adjusted by Subbasin. All Other Inputs are Assigned Default Values . . . . .	213
IV-8	Water Budgets with Potential ET Adjusted by Subbasin. All Other Inputs are Assigned Default Values . . . . .	214
IV-9	Water Budgets with Available Water Capacities Adjusted by Subbasin. All Other Inputs are Assigned Default Values . . . . .	215
IV-10	Zambezi River Model Performance Tests, Based on Refined Water Balance Adjustment and Selective Floodplain Inundation . . . . .	219

## LIST OF FIGURES

Figure		Page
I-1	Key Elements of the Terrestrial Water Cycle . . .	9
I-2	Major Agents of Anthropogenic Change and Their Interactions . . . . .	16
II-1	Modeling Efforts in the Study of Global Biogeochemical Cycles . . . . .	27
II-2	Structure of the Global Hydrologic Model, Showing the Relationship between Water Balance and Water Transport Models and a Set of Gridded Data Sets . . . . .	28
II-3	The Water Balance Model Showing Pools and Water Transfers . . . . .	32
II-4	Relation of Fluvial Transfer Coefficient, $K(\text{month}^{-1})$ , to a Length Scale, $S$ , Analogous to Sinuosity . . . . .	50
II-5	Water Balance Model Calculations for Representative $0.5^{\circ}$ Grid Cells in South America . . . . .	55
II-6	The Major Geographic Regions of South America . . . . .	58
II-7	The Relationship Between Precipitation (millimeters per year) and Calculated Mean Annual Soil Moisture (millimeters) for Grid Cells of the South American Continent . . . . .	61
II-8	Correspondence Between Soil Moisture Estimates Made by the Water Balance Model and Willmott and Rowe (1986) . . . . .	63
II-9	The Relationship Between Precipitation and Computed Evapotranspiration for Grid Cells of the South American Continent . . . . .	67
II-10	Correspondence Between Evapotranspiration Determined by the Water Balance Model, Korzoun et. al. [1977] and Willmott and Rowe [1986] . . . . .	69



II-11	The Relationship Between Precipitation and Model-Derived Runoff for Grid Cells of the South American Continent . . . . .	73
II-12	Correspondence Between Runoff Estimates Made by the Water Balance Model and Korzoun et. al. (1977) . . . . .	76
II-13	Modeled and Observed Discharge Hydrographs for Selected Sites in the Amazon and Tocantins River System . . . . .	80
II-14	Normalized Discharge Hydrographs Comparing WTM Calculations (lines) to Observations (bars) at Selected Sites within the Amazon and Tocantins Drainage Basin . . . . .	83
II-15	Model Results Showing the Effect of Variation in the Fluvial Transfer Coefficient (K), the Flood Initiation ( $C_f$ ), and the Flooding Exchange Parameter ( $r_f$ ) on the Discharge Hydrograph at Obidos . . . . .	91
III-1	Map of the Zambezi River System . . . . .	105
III-2	Precipitation Patterns in the Zambezi Basin .	108
III-3	Overall Organization of the Catchment Modeling Analysis . . . . .	111
III-4	Simulated Topology of the Zambezi River System at 0.5 x 0.5 degree (latitude x longitude) Spatial Resolution . . . . .	112
III-5	Comparison of Site-Specific and Continental -Scale Data Sets for Air Temperature, Precipitation, and Irradiance (sunshine) for a Grid Cell Located in the Kafue Basin . . . .	118
III-6	Alternative Calculation Schemes for Determining Potential Evapotranspiration . .	119
III-7	Long-term Discharge Hydrographs from Four Sites in the Zambezi Drainage Basin with Relatively Reliable Data Quality . . . . .	129
III-8	Grid Cell Locations Having Appreciable Areas of Wetland . . . . .	130
III-9	Inferred Floodwave Attenuation on the Upper Zambezi . . . . .	133

III-10	Water Balance Model Sensitivity to Change in the Water Holding Capacity of Soils . . .	149
IV-1	Key Features of the Zambezi River Drainage System . . . . .	165
IV-2	Simulated Topology of the Zambezi River System at 0.5 degree (latitude x longitude) Spatial Resolution . . . . .	168
IV-3	Structure of the Global Hydrologic Model, Showing the Relationship Between Water Balance and Water Transport Models and a Set of Gridded Data Sets . . . . .	186
IV-4	Model Performance Using WBM and Existing Biophysical Data Sets. Systematic Overestimates Are Apparent. The Relationship Depicted Is: $\text{pred} = 2.837 \text{ obs} + 55.31$ , $r^2 = 0.97$ . Observed Data for Mean Annual Discharge Are from Table III . . . . .	196
IV-5	Best Model Performance for Mean Annual Runoff Using WBM and Adjusted Precipitation ( $\text{pred} = 1.00 \text{ obs} + 79.9$ ; $r^2 = 0.95$ ) . . . . .	200
IV-6	Best Model Performance for Monthly Discharge Using Linked WBM/WTM, Corrected Biophysical Data Sets and Observed Data from the Livingstone, Itezhi-Tezhi and Lupata Sites . . . . .	205
IV-7	Monthly Timeseries Predicted by Linked WBM/WTM and Corrected Biophysical Data Sets at Three Discharge Monitoring Stations . . .	207
IV-8	Grid Cells Having Appreciable Areas of Wetland . . . . .	217
IV-9	Best Model Performance for Monthly Discharge Using Linked WBM/WTM, Corrected Biophysical Data Sets and Observed Data from the Livingstone, Itezhi-Tezhi and Lupata Sites . . . . .	220
IV-10	Monthly Timeseries Predicted by Linked WBM/WTM and Corrected Biophysical Data Sets at Three Discharge Monitoring Stations . . .	222

## LIST OF PLATES

Plate		Page
II-1	Field Capacities Used by the Water Balance Model at 0.5° Spatial Resolution . . .	43
II-2	Available Water Capacity (Field Capacity Minus Wilting Point) Computed by the Water Balance Model at 0.5° Spatial Resolution . . .	44
II-3	Mean Annual and Monthly Soil Moisture Predicted by the Water Balance Model at 0.5° Spatial Resolution . . . . .	59
II-4	Mean Annual and Monthly Evapotranspiration Predicted by the Water Balance Model at 0.5° Resolution . . . . .	65
II-5	Mean Annual and Monthly Runoff Predicted by the Water Balance Model at 0.5° Resolution . . .	72
IV-1	Subcatchments of the Zambezi Drainage Basin . . . . .	171
IV-2	Vegetation Zones (from Matthews 1983) . . . . .	172
IV-3	Soil Texture (from CSRC/FAO 1974) . . . . .	173
IV-4	Available Soil Water Capacity . . . . .	175
IV-5	Elevation (m above MSL) . . . . .	177
IV-6	Gradient (m) . . . . .	178
IV-7	Mean Annual and Seasonal Precipitation . . . . .	179
IV-8	Mean Annual and Seasonal Temperature . . . . .	181
IV-9	Mean Annual and Seasonal Net Irradiance . . . . .	182
IV-10	Mean Annual and Seasonal Potential ET . . . . .	184
IV-11	WBM-Calculated Mean Annual and Seasonal Soil Moisture . . . . .	209

IV-12	WBM-Calculated Mean Annual and Seasonal Evapotranspiration . . . . .	210
IV-13	WBM-Calculated Mean Annual and Seasonal Runoff . . . . .	211

## ABSTRACT

### MODELS OF MACRO-SCALE HYDROLOGY FOR USE IN GLOBAL CHANGE RESEARCH: TESTS ON TWO TROPICAL RIVER SYSTEMS

by

Charles Joseph Vörösmarty  
University of New Hampshire, May, 1991

The subject of this dissertation is the terrestrial water cycle and development of tools to study the issue of global hydrologic change. A rationale is developed to study the water cycle at regional and continental scales using macro-scale hydrology models coupled to Geographic Information Systems (GIS). A linked Water Balance/Water Transport Model (WBM/WTM) was constructed and tested as part of this research. The model was applied to two tropical river systems, the Amazon River in South America and the Zambezi River in southern Africa.

The WBM/WTM is a distributed parameter model, operating at  $0.5^\circ$  (latitude x longitude) spatial scale and with monthly timesteps. The WBM transforms spatially complex data on climate, vegetation, soils and topography into predictions of soil moisture, evapotranspiration and runoff. The WTM uses computed runoff, information on fluvial topology, linear transfer through river channels and a simple representation of floodplain storage to generate monthly discharge for any cell within a simulated catchment.

For the Amazon, WBM/WTM results were checked against established data sources and found to be in good agreement. The Zambezi simulation was more problematic. This study identified and corrected errors in the precipitation, potential evapotranspiration, and soil water capacity data sets, and demonstrated the importance of checking such calculations against reliable discharge data. Simulations with data from the Amazon and Zambezi River systems identified fluvial transport parameters which best matched observed discharge. Similar parameters captured the dynamics of river flow in these strikingly different river systems. This suggests that large tropical rivers may have convergent properties that can be modeled using simple algorithms.

This work produced a set of calibrated, macro-scale hydrology models for two large rivers prior to significant anthropogenic disturbance. Such simulations are prerequisites to the study of hydrologic change. The major impacts of such change, from shifting land use, climate change, and water resources management, can be simulated using macro-scale hydrology models. The dissertation offers a strategy to accomplish this goal.

## INTRODUCTION

The subject of this dissertation is the terrestrial water cycle and the use of models to analyze hydrology at the broad scale. This work is part of a larger and ongoing research effort with which I have been involved since 1986. That effort is aimed at understanding continental and global-scale biogeochemistry, including terrestrial nutrient cycling, carbon dioxide and trace gas exchange, and the transport of constituents through river networks. The overall study seeks to characterize nutrient and water cycling in an undisturbed condition and to quantify the resulting impacts of anthropogenic change. The hydrologic research reported upon here is a first step toward establishing an operational framework by which the dynamics of the atmosphere, water cycle and biosphere can be coupled.

It is widely recognized that humans have influenced the energy, water and biogeochemical dynamics of the planet, with often spectacular impacts at local and regional scales. The more localized phenomena, in turn, may produce compound, synergistic effects when viewed from the perspective of the entire Earth System. Our current understanding of global change at the broader scale is still in its infancy and much work remains to be done in understanding cumulative impacts.

The need for tools to analyze regional and continental-scale hydrology has guided progress on this

dissertation and resulted in the construction of a "macro-scale" hydrology model. In anticipation of eventual global coverage, the research presented here relies on a series of relatively simple models and data sets. It is meant to complement more sophisticated studies on a more localized scale which will examine the dynamics of land-atmosphere exchanges (e.g. Global Energy and Water Cycle Experiment, GEWEX; Anglo-Brazilian Amazonian Climate Observational Study, ABRACOS). These studies seek to integrate models, field experiments and remote sensing technology into the context of large drainage basins.

Owing to the scope of the problem, I have restricted the analysis to tropical river systems. The tropical region was chosen for several reasons. First, water is a dominant, yet often poorly-documented feature of this environment. The region is experiencing unprecedented rates of population growth and pressure for economic development. The rising expectations of the Third World poor will encumber increasing amounts of physical resources including water, and documenting the current and potential future status of tropical hydrology is important to the understanding of global change. Finally, the Tropics is a region in which my co-workers from the Institute for the Study of Earth, Oceans and Space (Durham, New Hampshire, USA), the Ecosystems Center of the Marine Biological Laboratory (Woods Hole, Massachusetts, USA) and the International Institute of



Applied Systems Analysis (Laxenburg, Austria) have made substantial progress in the past.

This dissertation considers two large drainage basins: the Amazon in South America and the Zambezi in southern Africa. Although both are drained by large tropical rivers, each has distinguishing attributes which provide a useful contrast against which to judge the transportability of the hydrology model. The Amazon is by far the world's largest river discharging approximately 20 percent of global runoff. In contrast, the Zambezi basin is much drier, with a mean specific discharge but 1/10th that of the Amazon. Along much of its length, the Zambezi is also regulated by impoundment which significantly changes the quantity and character of its discharge. Even though anthropogenic disturbance of the surrounding landscape is accelerating rapidly in Amazonia, in terms relative to the entire drainage basin the Zambezi's biota and hydrology have been more significantly transformed. In contrast to the Amazon River which has extensive, contiguous floodplains along much of its length, the Zambezi is punctuated by a series of distinct swamplands, incised channels and rapids.

Using the Amazon and Zambezi River systems, this dissertation will answer the following questions:

- 1). What are the characteristics of regional water balance in each of these two drainage basins? Namely, what are the relationships between precipitation,

evapotranspiration, soil moisture and runoff? How do these factors interact to define the patterns of riverine discharge characteristic of each drainage system?

2). How effective can simple, coupled models of water balance and horizontal transport be in characterizing these contrasting hydrologic settings? In particular, can such models be used in tandem with other tools for studying global change, such as the current generation of General Circulation Models (GCM's)?

3). How sensitive is model output to the quality of input data and to the choice of model parameters? Can similar parameters be used in simulating both the Amazon and Zambezi River systems, or are basin-specific parameters required?

To address these questions, I have constructed a tandem Water Balance/Water Transport Model (WBM/WTM) which processes information on long-term climatology and a series of biogeophysical inputs to predict mean monthly evapotranspiration, soil moisture and runoff at 0.5 degree (latitude x longitude) spatial resolution. The model is parameterized against a series of available discharge hydrographs for both the Amazon and Zambezi catchments.

The remainder of this dissertation is organized as a group of technical chapters and a set of concluding remarks. Chapter 2 provides a summary of some important concepts

which have guided my research. It first introduces the notion of global change and describes the emergence of Earth Systems Science as a new discipline. The chapter then summarizes key facets of the global water cycle and discusses its importance at the land surface. The chapter continues with a review of how humans alter the hydrologic cycle and presents a rationale for developing macro-scale hydrology models.

Chapter 3 presents a macro-scale hydrology model which is applied to South America and, in particular, the Amazon River system. Both model structure and input data sets are described in detail. Model calculations of water balance are compared to previous research and predictions of river flow are related to observed discharge hydrographs. A set of sensitivity tests are also offered to explore how the model behaves with respect to the turnover of surface water within river channels and to the temporary storage of water onto floodplains.

Chapter 4 gives a detailed description of the Zambezi River system. Key elements of its hydrologic cycle are described, with a focus given to the impact of humans on this and other tropical river systems. The anthropogenic activities include impoundment, land degradation, and climate change. The chapter also assembles the requisite data sets that will be used to produce a calibrated macro-scale model of the Zambezi catchment in Chapter 5.

The final technical section, Chapter 5, presents a macro-scale hydrology model for the Zambezi River catchment. Both water balance and fluvial transport are quantified. Based on model performance, an assessment is made of input data quality and uncertainty. The chapter continues by exploring the sensitivity of the model to various parameters which define river flow. As part of that analysis, a judgement is made as to the transportability of such parameters to other large tropical drainage basins.

Understanding the complexity of the natural water cycle, even without considering the impact of humans, presents formidable obstacles. Such complexity requires a multidisciplinary and collaborative effort. The chapters presented here reflect this emerging characteristic of Earth Systems Science. At the time of this writing, Chapters 3 and 4 have already appeared in press (Vörösmarty et. al. 1989; Vörösmarty and Moore 1991). Modified versions of both the Introduction and Chapter 5 are now being drafted, and these will be multi-authored as well. In each case, I have taken the lead on all technical aspects of the work and drafted the entire text.

Finally, the research presented in this dissertation is but a first and modest step toward understanding the ramifications of global change on the planet's water and biogeochemical cycles. Admittedly, the work is coarse in scale and the models are structurally simple. I hope,

nevertheless, that the work will serve as an important prototype study to guide future global change initiatives. I also hope that although the work can rightfully be considered basic research, it may at some later time provide necessary information to the policy-making community faced with enormous challenges in the coming decades.

## CHAPTER I

### HYDROLOGY AND THE CONCEPT OF GLOBAL CHANGE

#### Introduction

The hydrologic cycle for freshwater is a critical component of the Earth System. Its dynamics are complex, involving the solid, liquid and gaseous phases of water at and below the land surface and in the atmosphere (Figure I-1). Compared to the oceans, freshwater comprises an extremely small portion of the planet's total water supply (Table I-1). Surface water, subsurface storage and water locked in glacier and ice pack together make up no more than 3 percent of the global total. Atmospheric water, represents less than 1/1000 of a percent.

The terrestrial hydrologic cycle is active at a variety of time scales. The most rapid turnover, on the order of a few days, occurs in the atmosphere which transports water both vertically, to and from the land surface, and horizontally, over vast regions. Precipitation falls as either snow or rain. Rainfall that reaches the land surface has several potential fates. It can be intercepted by vegetation and re-evaporated, percolate into or through the root zone, be transformed into overland flow or pass to lower elevations through interflow. As snow, precipitation may be evaporated into the atmosphere or stored either

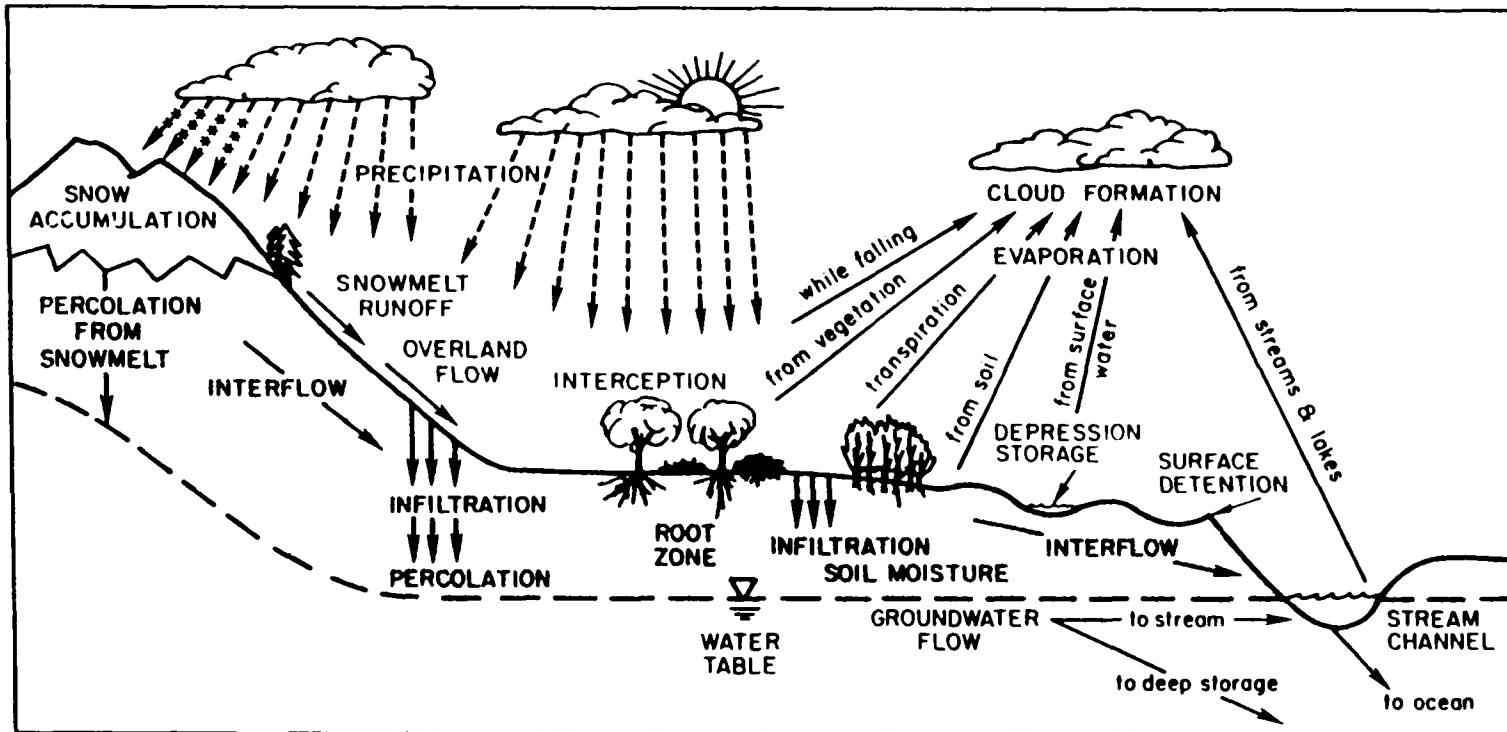


Fig. I-1. Key elements of the terrestrial water cycle.

TABLE I-1. Distribution of Global Water Pools (from Strahler and Strahler 1973).

Location	Surface Area (sq km)	Water Volume (sq km)	Percent of Total
Surface water			
Fresh-water lakes	860,000	125,000	0.009
Saline lakes and inland seas	700,000	104,000	0.008
Average in stream channels	----	1,250	0.0001
Substance water	130,000,000		
Soil moisture and intermediate- zone (vadose) water		67,000	0.005
Ground water within 0.8 km depth		4,170,000	0.31
Ground water, deep-lying		<u>4,170,000</u>	<u>0.31</u>
Total liquid water in land areas		8,637,000	0.635
Icecaps and glaciers	18,000,000	29,200,000	2.15
Atmosphere	510,000,000	13,000	0.001
World ocean	360,000,000	<u>1,322,000,000</u>	<u>97.2</u>
Totals (rounded)		1,360,000,000	100



seasonally or for extended periods of time in glaciers and ice pack. Upon melting the water liberated can serve as overland or interflow, recharge the soil or pass to groundwater pools. Soil water has seasonal dynamics associated not only with delivery of precipitation but also with the growth and vigor of terrestrial plants which transport this water back into the atmosphere through the process of evapotranspiration. Water as surface and subsurface runoff passes into streams and other open water bodies which flow to either internal basins or to the sea. During transit, water may be lost to the atmosphere through evaporation.

#### The Role of Water at the Earth's Surface

Freshwater serves many roles in the terrestrial biosphere and, on the global scale, its importance is disproportionate to its abundance. The cycling of water dominates the climate system and its availability at the land surface is of more or less immediate significance to the sustainability of terrestrial ecosystems and human society. The functions are diverse and encompass the physics, chemistry and biology of the Earth System.

#### Climatic Balances

The first role involves regulation of climate. Atmospheric vapor is an important greenhouse gas and cloud physics regulates the delivery of precipitation and radiation to the land surface. Snow and ice are not only

the dominant storage pools for freshwater but they as well regulate regional heat balance through storage, phase change and characteristically high albedo. Evaporation and transpiration by plants cool the earth's surface, and thereby regulate temperature. Evapotranspiration serves to transport huge quantities of water laterally across the Earth's surface, providing moisture to the atmosphere which can later fall as precipitation far from its original point of origin.

#### Biogeochemical Processing

Water also plays a central role in the biogeochemistry of the terrestrial biosphere. Water in the rooting zone is of obvious importance to primary production and, hence, CO<sub>2</sub> gas exchange and nutrient uptake by plants. It also controls the reciprocal process of decomposition that turns over carbon and nutrients. Water availability and its timing influence the river, wetland and coastal ecosystems into which runoff must pass. Soil moisture is likely to be the single most important control on the production of trace gases such as nitrous oxide and methane.

#### Weathering and Constituent Transport

The water cycle is intimately tied to the redistribution of materials from the landscape to the world's oceans. The denudation of the continents results from physical and chemical weathering with subsequent aqueous transport of particulate and dissolved species to

the oceans. In the long term, this loss of constituents is responsible for the current composition and density of seawater. Terrestrial ecosystems rely on water as a transport medium for a wide array of nutrient cycling processes. Since water is so mobile, these ecosystems also lose nutrients and carbon to varying degrees which depend on the particular vegetation, soil, topography and climate. Loss of phosphorus, nitrogen, and carbon are important to both donor (landscape) and recipient (aquatic) systems. Losses have obvious impacts on the landscape as standing stocks of critical plant nutrients may be depleted, especially when accelerated by activities which remove natural vegetative cover. Delivery of these materials to aquatic ecosystems can disrupt the normal capacity of river and lake ecosystems to process allochthonous inputs, resulting in eutrophication. The long-term transport of riverine nutrients may also regulate oceanic metabolism and have a truly global effect.

#### Habitat

Water provides habitat for both aquatic and terrestrial communities. Its availability and turnover directly control the ability of aquatic organisms to survive. Running water, lakes, and floodplains define unique and characteristic environments for specific plant, decomposer and animal communities. Water also furnishes habitat for landborne ecosystems, albeit indirectly. The distribution of

terrestrial ecosystems is strongly tied to climatic indices, particularly temperature and moisture availability.

Adequate soil water is essential not only for plants but as well for decomposing organisms that recycle nutrients.

#### Water Resources for Human Development

Our dependence on an adequate supply of water is clear. We depend on the hydrologic cycle for drinking water, irrigation, energy from hydropower, navigation, and waste assimilation. When quantity or quality fail to meet our needs, we institute engineering schemes to alleviate the undesirable effects. For floods we build impoundments and redirect river channels; for arid region agriculture we utilize water stored in reservoirs or pump from groundwater storage; unpotable water is processed in often elaborate water treatment facilities. Indeed, a major emphasis of the science of hydrology is devoted to optimizing water resources for the benefit of humans.

#### Anthropogenic Disturbance of the Hydrologic Cycle

Much of the globe's hydrology is now modified, and a pressing challenge is to develop quantitative understanding of how humans have disturbed the water cycle. In particular, consideration of engineering works, shifting landscape patterns and climate change will represent a significant step forward. Human activities have both purposeful and inadvertent impacts on the natural water cycle. I have conceptualized these disturbances into three

broad categories: Induced Climate Change, Water Resources Management Schemes, and Population/Land Use Change (Figure I-2). Each category is characterized by unique impacts, but there are as well synergistic interactions. A major scientific challenge thus presents itself to the Earth System Science community in seeking to understand the effects of anthropogenic change on the water cycle.

#### Climate Change

There is almost universal agreement within the scientific community that the global climate will inevitably change due to the introduction of radiatively important gases associated with economic development. Current debate now focuses on the detection of such change and on the distribution of regional impacts. In particular, it is believed that rising temperatures, the so-called greenhouse effect, will have an amplifying effect on terrestrial water balance. Thus, the patterns of wet and dry regions may shift, exposing the landscape to conditions outside the realm of the recent past and for which ecosystems and human societies may not be well-suited. Major limitations now exist in understanding the linkage between climate and hydrology.

Studies of climate change and surface runoff, both regionally and at finer scales, are beginning to appear in the literature. Climate change will have important effects on existing water management works, due to obsolescence of

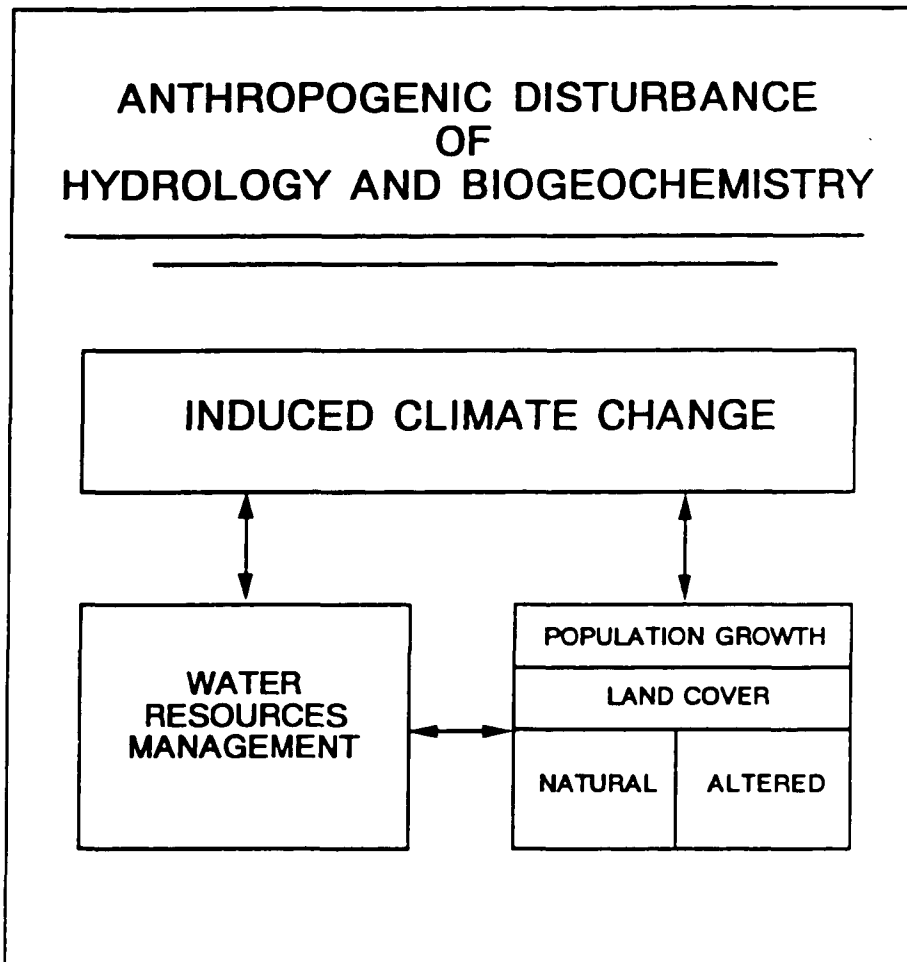


Fig. I-2. Major agents of anthropogenic change and their interactions.

hydrologic design data reflecting the climate of the recent past. Numerous studies have shown that the greatest change in surface hydrology will be in relatively dry areas, where runoff is defined by a precarious balance between precipitation and evapotranspiration. Linking computer simulations of climate and surface hydrology has proven particularly troublesome owing to large differences in spatial scale. There is also substantial disagreement among Global Circulation Model (GCM) configurations in predicting regional climate change impacts.

Climate change is likely to have profound effects on natural terrestrial ecosystems, altering their capacity to fix carbon, turn over nutrients and cycle water. Climate change may also influence the long-term distribution of plant communities. This could have major impacts on water cycling by the terrestrial biosphere. Differences in canopy structure, leaf area index, and rooting depths cause ecosystems to process water at differing rates. In addition, a carbon dioxide fertilization effect associated with the greenhouse phenomenon may improve plant water use efficiency, and at the drainage basin scale complicate our understanding of the more direct climate-induced temperature and precipitation effects. Changes in precipitation and temperature will also have effects on the distribution of human settlement and agricultural land. A changing climate

thus may become a powerful force defining the future mosaic of natural and altered landscapes.

#### Land Use Effects

The broad distribution of natural vegetation is established principally by climate, topography and edaphic factors. Over vast regions of the Earth, however, the current landscape is no longer determined by such factors. It is defined instead by widespread conversion of land to agriculture, grazing, commercial logging, controlled burning, thinning of woodlands for fuel wood and urbanization. Associated with these activities is a reduction in vegetative biomass.

Loss of biomass generally reduces the flux of water vapor to the atmosphere and simultaneously increases runoff. Two principle mechanisms are involved. The first is reduction in the hydraulically-active soil depth associated with removal of natural cover. A smaller pool of labile soil water means that evapotranspiration becomes more limited and runoff is favored in the overall water balance. Furthermore, a smaller soil moisture pool implies that less precipitation will be required to overcome any soil water deficits and, so, runoff will be generated more easily. The second mechanism is reduction of infiltration associated with disturbance of the soil. Vegetation and litter protect the soil surface from direct rainfall and maintain channels for subsequent infiltration. In less protected sites,



direct rainsplash clogs soil pores, reducing water entry into the soil and increasing stormflow runoff. In the case of overgrazing, outright compaction occurs. Afforestation normally has the opposite effect, increasing evapotranspiration at the expense of runoff.

The distribution of land cover is known to have important effects on local meteorology but may also hold potentially important feedbacks on global climate. In regions dominated by tropical rainforest the recycling of evaporation into precipitation is an important component of regional hydrology. Recent modeling experiments using GCMs for Amazonia show a dramatic weakening of the surficial water cycle associated with wholesale deforestation. The alteration is characterized by decreases in precipitation, evapotranspiration and runoff. To the extent that such land use change is pandemic, the regional impacts may accumulate as a global effect.

Land cover also influences the operation of water resources systems. Changes in land use can increase the erosion potential of the landscape and increase the siltation of reservoirs, thereby reducing their longevity. Land cover-induced changes in water balance may also create problems in the management of hydraulic engineering works. The timing or quantity of altered runoff may pass outside the domain of the calibration period by which operating rules were originally formulated. Increases in stormwater

runoff from land disturbance enhances the potential for flood damage, lowers water tables and decreases seasonal low flows, reducing well yields, exacerbating navigation problems and compromising instream wildlife habitat.

#### Water Resources Systems

The purposeful extraction, consumption and regulation of the world's freshwater resources is a prodigious, global phenomenon. Much of the world's freshwater discharge and many of the world's largest rivers are now regulated in some manner by humans. This regulation involves such activities as impoundment, interbasin transfers and consumptive use by industry and agriculture. Because water resource works are so widespread and diverse, their collective hydrologic impact, on even the regional scale will be difficult to quantify.

Reservoirs can dramatically alter regional water budgets and constituent transport through drainage basins. The hydrologic impact is achieved through a dampening of influent hydrographs and an enhancement of open-water evaporation. Massive irrigation schemes also alter regional water balances. In the US, for example, more than 50 percent of the water extracted from surface and ground waters for crop irrigation is consumed through evapotranspiration, and this represents, by far, the single largest consumptive loss for the nation. Throughout the southern High Plains region, Ogallala aquifer depletion is

unsustainable and water tables in some locations have dropped on the order of meters per year. Because of consumptive use and interbasin transfers, the Colorado River is reduced to a small stream by the time it crosses the US border with Mexico.

Water management has important ramifications on regional climate and land cover. In the Zambezi basin in southern Africa, for example, it has been estimated that in only one of its four major reservoirs, more than 20 percent of incoming river flow is lost to evaporation. The contemplated diversion of large boreal rivers by the Soviet Union for dryland irrigation was thought to have important consequences on freshwater inputs to the Arctic Ocean, where such inputs represent a relatively important contribution to an oceanic basin. Modeling studies suggest that such regulation could potentially alter the pattern of Arctic Ocean circulation and hence climate. The existence of adequate water resources, either natural or engineered, regulates human settlement patterns and makes often inhospitable climates useable. This in turn affects the distribution of natural and altered land cover.

#### Macro-Scale Hydrology Models

The drainage basin is a useful organizing concept by which to view the coupling of the Earth's water and chemical cycles. Numerous watershed studies have added significantly to our understanding of how landscapes process and transport

constituents, and how terrestrial ecosystems are affected by pollution. The inherent advantages of such studies should be realized as well at the global scale.

The rationale for developing continental-scale models of terrestrial hydrology is being articulated with increasing frequency. The motivations include defining the geographic distribution of land-atmosphere moisture exchange, fostering the effective management of water resources, and quantifying the impact of land use and global climate change on the water cycle. Water resources, and large river systems in particular, are often the catalyst for future economic growth. Because of their size, large river systems are often international, raising the specter of conflicting use and diplomatic impasse.

Suitably-scaled drainage basin models can assist the hydrologic community in interpreting Global Circulation Model predictions, by examining the spatial and temporal distributions of precipitation and latent heat flux with respect to surface water balance and river transport. In turn, such models would be of great value to the climate modeling community by providing an important constraint on GCM predictions. Theoretically, this could facilitate both the calibration and validation of the atmospheric models, materially improving our understanding of how the climate system functions and how climate change is likely to progress. Furthermore, a drainage basin model which links

terrestrial water balance and ecosystem nutrient cycling to fluvial transport and aquatic processing, would be a valuable scientific tool with which to address issues of global biogeochemical change.

Certain requirements must guide the development of macro-scale hydrology models. First, they must be of suitable scope and detail to capture both the spatial and seasonal dynamics of water on a broad scale. They must exploit the current generation of global biophysical datasets, including raster-based remote sensing data. Such models must also be tractable in terms of their required computing resources. To facilitate intercomparison of results and permit as wide a coverage as possible, modelers should strive to develop generic and transportable algorithms. Parameters should bear resemblance to actual physical entities and every effort should be made to minimize the number of such parameters.

Grid-based models for runoff generation and fluvial transport, organized at 0.5 degree (latitude x longitude) resolution and with monthly timesteps, represent a manageable first step. These models should initially remain simple and rely on widely-accepted methods of water balance accounting and runoff routing through drainage basins. In addition, the models and associated datasets should be organized in the context of a Geographic Information System (GIS) which can facilitate interactive database editing,

linkage to tabular and statistical data, and production of graphical output. With the growing power of computing systems and GIS technology, it is not unreasonable to set as an eventual goal that of global coverage. The first generation of such models operating at the continental scale are reported upon in this dissertation.

#### Summary

The terrestrial water cycle is a highly dynamic component of the Earth System. It is of great importance to the physics, chemistry, and biology of the planet, regulating climate, processing biologically active compounds, weathering and transporting constituents, providing habitat, and supplying water to humans for economic development. Humans have significantly altered the natural water cycle in three important ways: climate change, shifting land use and water resources management. There is a decided need for scientific tools by which to address these issues. The drainage basin is a useful organizing concept and forms the basis for constructing distributed parameter models of continental-scale hydrology. The first generation of such "macro-scale" hydrology models is represented by simple, grid-based algorithms (0.5 degree spatial resolution; monthly time steps) nested within a Geographic Information System.

## CHAPTER II

### CONTINENTAL-SCALE MODELS OF WATER BALANCE AND FLUVIAL TRANSPORT: AN APPLICATION TO SOUTH AMERICA

#### Introduction

The terrestrial water cycle is a key component of the Earth's climate and biogeochemistry. Associated with this cycle is a continuous exchange of water, energy and materials through the atmosphere, the landscape and inland aquatic ecosystems. Water also activates and is influenced by a myriad of biospheric processes including plant production, organic matter decay and gas exchange between terrestrial ecosystems and the lower troposphere. The availability of freshwater resources has obvious effects on human society as well. The hydrologic cycle is clearly important at local, regional, and global scales.

The impetus for studying the global water cycle has been articulated many times [International Geosphere-Biosphere Program (IGBP), 1988; National Aeronautics and Space Administration (NASA)/Earth System Sciences Committee (ESSC), 1988; Eagleson, 1986]. Of fundamental concern is the growing body of evidence implicating human activity as a major factor in global change. With the advent of requisite instrumentation and data base management capabilities, the scientific community is rapidly approaching a situation in

which the hydrologic cycle can be carefully monitored over vast regions. There is, however, a decided need for scientific tools which can aid researchers in analyzing the observational data sets to better understand the role of water in geosphere-biosphere dynamics.

The overall goal of the research reported here is to study major biogeochemical cycles at the global scale. It seeks to quantify rates of nutrient and carbon flux in terrestrial ecosystems and their exchanges among the landscape, inland aquatic ecosystems and the atmosphere [Moore et. al., 1989]. An important research activity is the development of models to aid in analyzing these phenomena (Figure II-1).

This paper describes the hydrologic component of a larger drainage basin model (DBM) which treats both water and constituent flux. The hydrologic component consists of a water balance model (WBM) and a water transport model (WTM) (Figure II-2). The spatial domain of each model is organized as a set of geographically-referenced cells superimposed on a  $0.5^{\circ} \times 0.5^{\circ}$  (latitude x longitude) grid. The WBM operates on independent grid cells and uses biogeophysical information to predict monthly soil moisture, evapotranspiration and runoff. The water balance calculations are linked to the terrestrial ecosystem model (TEM) and trace gas model (TGM) shown in Figure II-1 through



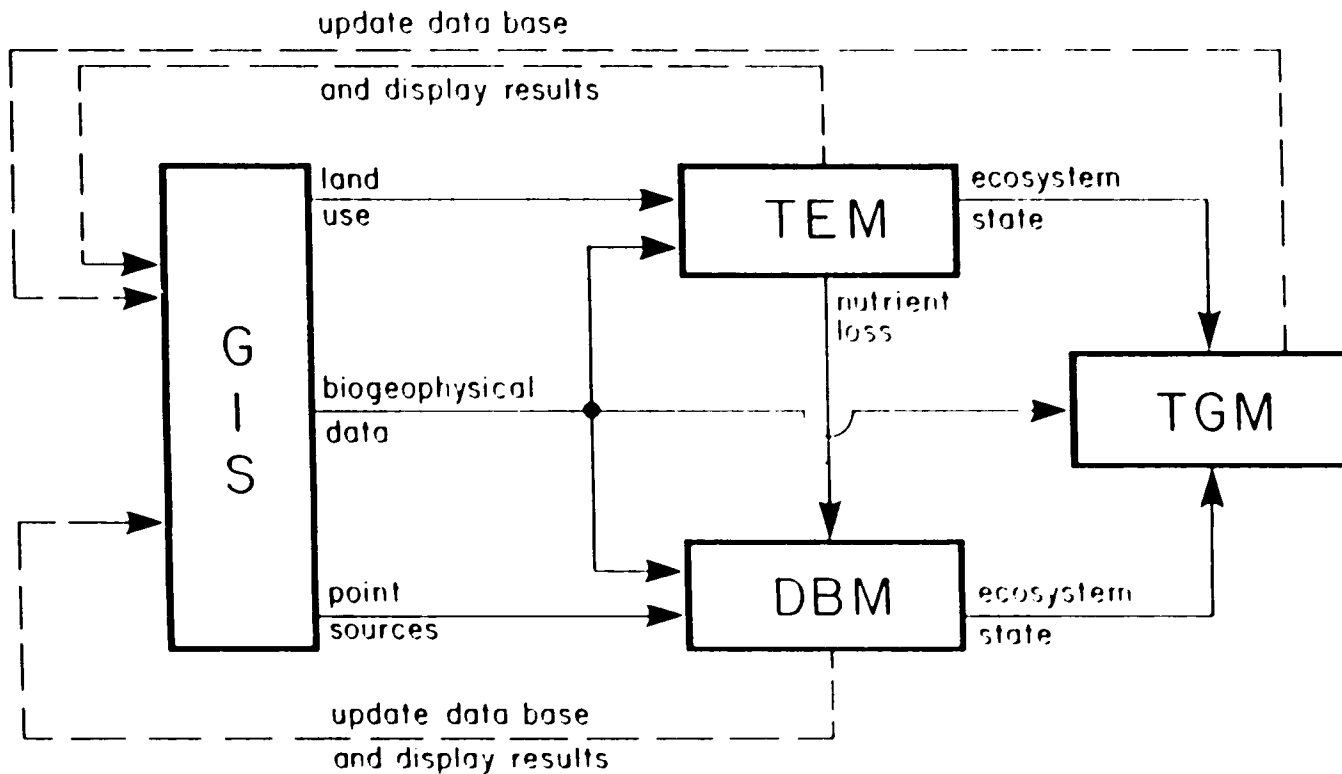


Fig. II-1. Modeling efforts in the study of global biogeochemical cycles. Information is organized in a geographic information system (GIS), which supports the data needs of a terrestrial ecosystem model (TEM), a drainage basin model (DBM), and a trace gas model (TGM), each organized at the  $0.5^\circ \times 0.5^\circ$  (latitude  $\times$  longitude) spatial scale. This paper describes the hydrologic components of DBM.

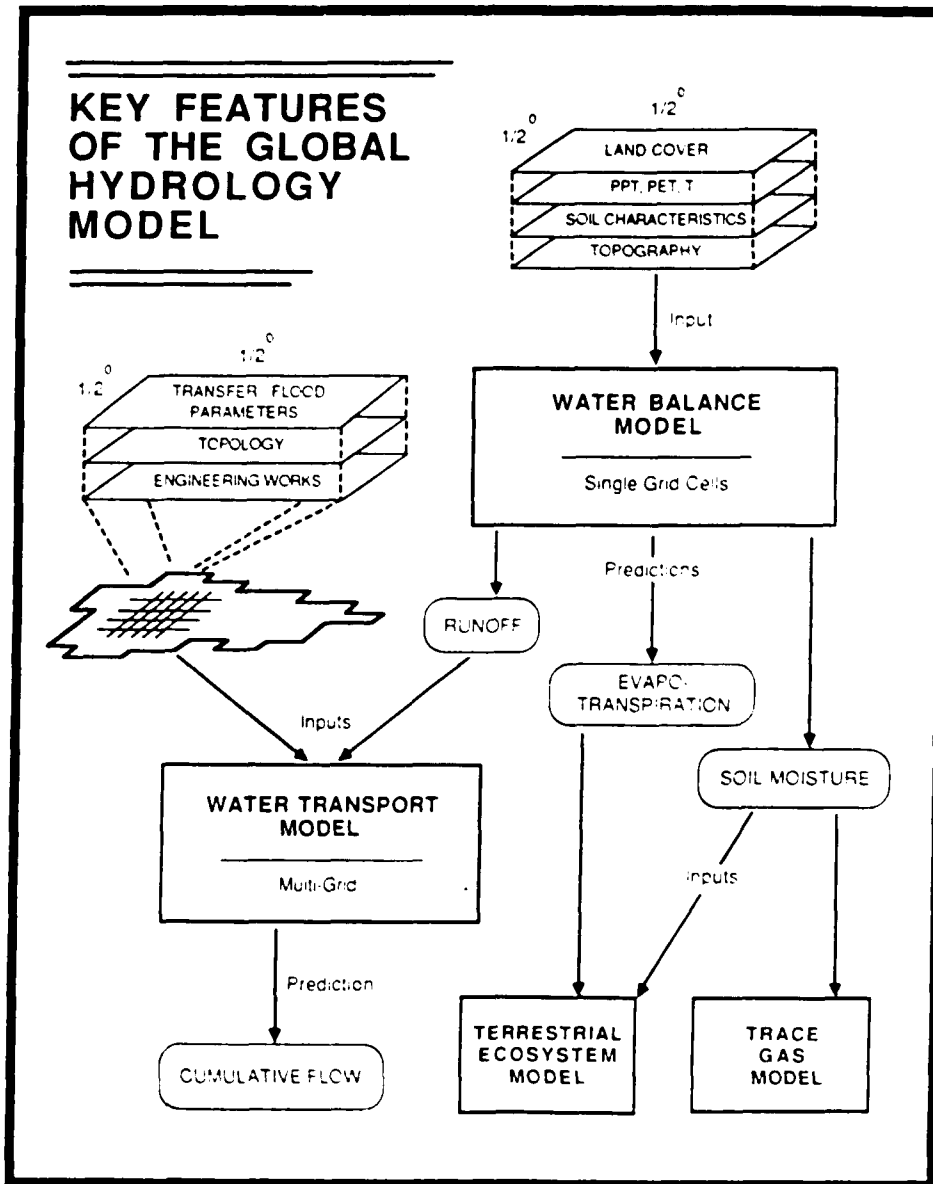


Fig. II-2. Structure of the global hydrologic model, showing the relationship between water balance and water transport models and a set of gridded data sets. The hydrologic model links to TEM and TGM through calculated evapotranspiration and soil moisture.

soil moisture and evapotranspiration. The WTM links single grid cells to define an integrated drainage basin topology. Discharge estimates are then made by routing WPM-derived runoff through simulated catchments.

Our work complements other regional and global studies of surface hydrology and material transport [Richey and Ribeiro, 1987; Vörösmarty et. al., 1986; Elder, 1985; Milliman and Meade, 1983; Stallard and Edmond, 1983; Meybeck, 1982; Giannessi et. al., 1981; United Nations, 1981; Brunskill et. al., 1975]. The methodology builds on earlier work using gridded climate and hydrologic models at a variety of spatial scales by Wiltshire et. al. [1986], Willmott et. al. [1985a], Schmidt [1981] and Cluis et. al. [1979].

The initial focus is South America, with particular emphasis on Amazonia. I choose this area for several reasons. Water flux is a dominant yet often poorly measured feature over much of the continent and refined estimates will be useful to a variety of scientific investigations. These include studies of biomass distribution and productivity (Raich et. al. 1991), the biogeochemistry of large tropical rivers [for example, Carbon in the Amazon River Experiment (CAMREX) (Brazilian-U.S. Consortium, J. Richey) and Proyecto Orinoco-Apure (POA) Orinoco (Ministerio del Ambiente y de los Recursos Naturales Renovables, Venezuela, A. Mejia)] and floodplain inundation as a

mediator of trace gas exchange [Quay et. al., 1988]. Although broad regions of the Amazonian rainforest remain undisturbed, they are increasingly subject to disruption [Fearnside, 1986]. Since the recycling of precipitable water through evapotranspiration is an important characteristic of basin hydrology [Salati and Vose, 1984], documenting its recent status will provide an important benchmark against which future anthropogenic disturbance and climate change can be assessed.

#### Model Development

To address scientific issues at the continental scale, terrestrial hydrologic models must characterize the dispersed nature of climate and hydrology over space and time while avoiding needless complexity. Although the science of hydrology, and hydrologic modeling in particular, is now quite sophisticated [Burgess, 1986; Singh, 1982], a continental-scale model requires prudent simplification [Dooge, 1986]. In the current context, simplification is required not only for reasonable computing time but also for developing a generic form applicable to a broad spectrum of systems across the globe. The model must also exploit the current generation of global data sets available in point, polygonal or gridded formats. To facilitate global coverage the model requires a minimal number of parameters for calibration.

### Water Balance Model: Structure

The WBM simulates grid cell level hydrology associated with long-term climate (Figure II-3). Inputs to the WBM include global- or continental-scale data sets covering precipitation, temperature, potential evapotranspiration, vegetation, soils and elevation. The WBM then predicts soil moisture (SM), evapotranspiration (ET) and runoff (RO) for each 0.5° grid cell in the simulated region. In the current study, independent water balance predictions are made for more than 5700 cells representing South America. The WBM component relies on techniques developed by Thornthwaite and Mather [1957] and subsequently modified as part of the current work.

The climatic variables are determined from long-term monthly averages for precipitation (PPT), temperature (T), and potential evapotranspiration (PET). In any month, rain and snow can occur simultaneously. The model is deterministic and employs a monthly time step. A dynamic steady state is achieved by applying monthly PPT, T and PET repeatedly over the year until the soil moisture, ET, runoff and snowmelt calculations for each successive twelve-month period converge to within an acceptable margin of difference (0.01%).

Soil moisture is determined from interactions among rainfall, snowmelt recharge and PET. During wet months (rain plus snowmelt in excess of PET), soil moisture can

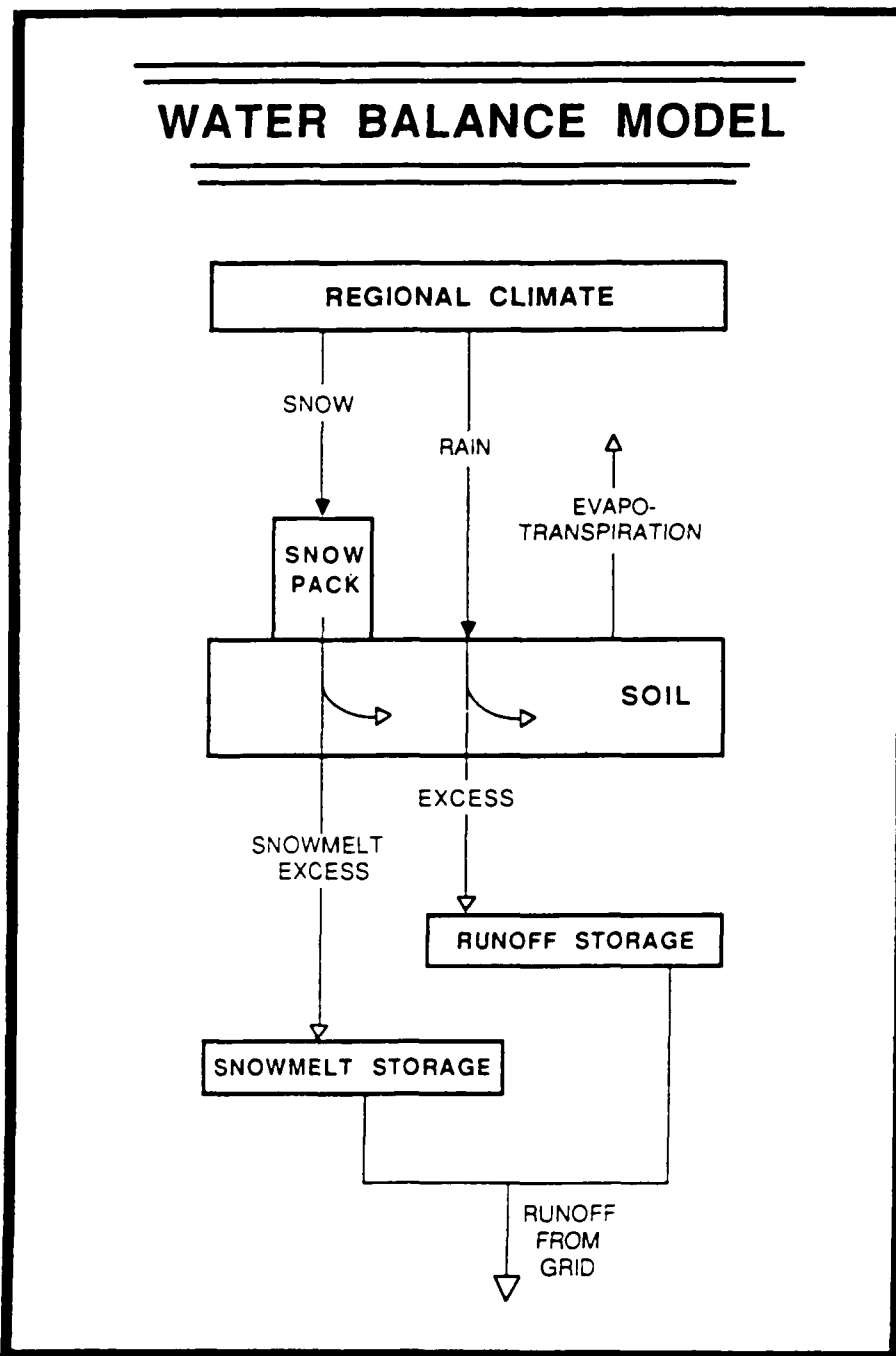


Fig. II-3. The water balance model showing pools and water transfers. Through a retention function for soil water, the model transforms precipitation and potential evapotranspiration into soil moisture, evapotranspiration and runoff. Closed triangles represent inputs; open triangles are flux determinations made by the model.

increase up to a maximum field capacity determined by soil texture and rooting depth. During dry periods (available water exceeded by PET), soil moisture becomes a function of potential water loss. Thus,

$$dSM/dt = (P_r + R_s - PET) \quad P_r + R_s \geq PET, \quad SM < FC \quad (1a)$$

$$dSM/dt = 0 \quad P_r + R_s \geq PET, \quad SM = FC \quad (1b)$$

$$dSM/dt = -a \quad SM \quad (PET - [P_r + R_s]) \quad P_r + R_s < PET \quad (1c)$$

where SM is soil moisture (millimeters),  $P_r$  is precipitation as rainfall (millimeters per month),  $R_s$  is snowmelt recharge (millimeters per month), PET is potential ET (millimeters per month), FC is soil field capacity (millimeters) and  $a$  is the slope of the moisture retention function described below. Calculations commence at the end of the wet season when it is assumed the soil is at field capacity. Soil water stocks are then depleted during the dry season in accordance with the moisture retention function. For each wet month, soil moisture is determined by incrementing antecedent values by the excess of available water over PET. This recharge may or may not be sufficient to bring the soil to field capacity at the end of the subsequent wet season.

As a soil dries it becomes increasingly difficult to remove moisture against increasing pore tension. For a particular soil, there is a linear relationship between  $\log$  SM and  $\Sigma [PET - (P_r + R_s)]$ , summed from the start of the dry season to the current month. The original tables offered by

Thorntwaite and Mather [1957] treated eleven field capacities in metric units. To calculate  $dSM/dt$  through (1c) for intermediate field capacities, the WBM defines a slope to the retention function:

$$a = \ln (FC)/(1.1282 FC)^{1.2756} \quad (2)$$

The numerator represents soil moisture (millimeters) with no net drying. The denominator is the accumulated potential water loss ( $\Sigma [PET - (P_r + R_s)]$ ) in millimeters at SM is 1.0 mm. With  $a$  determined the model can calculate  $dSM/dt$  as a function of soil dryness and update SM. Calculations for SM are similar to those used by Pastor and Post [1984].

The WBM calculates soil moisture to a maximum defined by the field capacity for a particular soil (i.e., moisture held in the soil drained by gravity). It makes no prediction of the degree of waterlogging beyond this capacity. Such a determination would require assignment of percolation rates to each soil type as well as a statistical distribution of rainfall duration and intensity over each month. Furthermore, the hydrology simulated in the current version of WBM is driven by pluvial processes alone; floodplain inundation is not explicitly considered.

Once soil moisture is determined evapotranspiration is calculated. Following Thorntwaite and Mather, ET is set equal to PET in wet months, when  $P_r + R_s \geq PET$ . During such times it is assumed that precipitation and any available



snowmelt are in sufficient abundance to satisfy all potential water demands of the resident vegetation. During dry seasons ( $P_r + R_s < PET$ ) the monthly average ET (in millimeters) is modified downward from its potential. The relevant equations are:

$$ET = PET \quad P_r + R_s \geq PET \quad (3a)$$

$$ET = P_r + R_s - dSM/dt \quad P_r + R_s < PET \quad (3b)$$

The WBM calculates runoff based on the availability of soil moisture. Whenever field capacity is attained, excess water is transferred to subsurface runoff pools for rain and snowmelt. From these storage pools, RO is generated as a linear function of the existing pool size. The transfer coefficients are set according to Thornthwaite and Mather [1957]. There is no contribution to the runoff storage pools when a moisture deficit exists in relation to field capacity; any available water recharges the soil. For rainfall runoff:

$$RO_r = 0.5 [ D_r + p (P_r + R_s - PET) ] \quad SM = FC, P_r + R_s \geq PET \quad (4a)$$

$$RO_r = 0.5 D_r \quad SM < FC \text{ or } P_r + R_s < PET \quad (4b)$$

where  $RO_r$  is rainfall-derived runoff (millimeters per month),  $D_r$  is rainfall-derived detention (storage) pool (millimeters) and  $p$  is the proportion of surplus water attributable to rain ( $P_r / [P_r + R_s]$ ).

Snowpack accumulates whenever mean monthly temperature is below  $-1.0^{\circ}\text{C}$ . Snowmelt occurs at or above  $-1.0^{\circ}\text{C}$ . Using snowmelt relationships developed by Willmott et. al. [1985a] and water budgets developed for fourteen ecosystem study sites [Univ. of New Hampshire/Marine Biological Laboratory, 1989], I developed a simple representation of snowpack behavior. At elevations of 500 m or less, the model removes the entire snowpack (plus any new snow) by the end of the first month of snowmelt. At elevations above 500 m, the melting process requires two months with half of the first month's snowpack retained until the second. Snowmelt is used first to recharge any soil moisture deficit. Any excess is then passed to a snowmelt storage pool for eventual runoff. By Thornthwaite and Mather [1957], sites at elevations of 500 m or less will lose 10% of this pool in the first month of snowmelt. In subsequent months, these sites will lose 50% per month. At higher elevations, sites will lose 10% in the first month, followed by 25% in the second month and 50% thereafter. For snowmelt at or below 500 m elevation:

$$RO_s = 0.1 (D_s + PK_s) \quad \text{month} = 1 \text{ of } T \geq -1.0^{\circ}\text{C} \quad (5a)$$

$$RO_s = 0.5 D_s \quad \text{month} > 1 \text{ of } T \geq -1.0^{\circ}\text{C} \quad (5b)$$

where  $RO_s$  is snowmelt-derived runoff (millimeters per month),  $D_s$  is snowmelt-derived detention (storage) pool (millimeters) and  $PK_s$  is snowpack (millimeters of water)

available after any required soil moisture recharge. For snowmelt above 500 m elevation:

$$RO_s = 0.1 (D_s + 0.5 PK_s) \quad \text{month} = 1 \text{ of } T \geq -1.0^\circ\text{C} \quad (6a)$$

$$RO_s = 0.25 (D_s + PK_s) \quad \text{month} = 2 \text{ of } T \geq -1.0^\circ\text{C} \quad (6b)$$

$$RO_s = 0.5 D_s \quad \text{month} > 2 \text{ of } T \geq -1.0^\circ\text{C} \quad (6c)$$

These equations are combined with the rainfall-derived runoff to yield the aggregate runoff (RO) from each grid cell. This RO is used as an input to the WTM.

#### Water Balance Model: Required Data

The WBM requires a number of geographically-referenced data sets which cover climatology, vegetation, soil texture and topography. This section identifies these data sources and the steps taken to prepare them for eventual use in the WBM.

Precipitation data were taken from the UNESCO Atlas of World Water Balance [Korzoun et. al., 1977]. Isohyets of mean total precipitation (millimeters per year) were digitized and subsequently gridded to the 0.5° scale using the ARC/INFO [Environmental Systems Research Institute Inc., Redlands, California] Geographical Information Systems (GIS) software. Monthly rain or snow was determined from site-specific histograms (showing annual percent precipitation) and two-dimensional interpolation [Akima, 1978]. The potential ET data set, also from Korzoun et. al. [1977], was developed in the same manner. The PET entries

are based on air temperature, radiation balance and moisture content of evaporating surfaces. Interception losses are not explicitly treated but are included as part of the PET estimates. At the continental scale, PPT and PET amount to 1679 and 1336 mm per year.

Snowmelt determinations required additional data sets for surface air temperature and elevation. Mean monthly temperature data were obtained from Willmott and Rowe [1986], recoded into 0.5° grid cells. I obtained elevation above mean sea level (msl) in 30-m vertical increments from a digital data set available through the National Center for Atmospheric Research (NCAR)/NAVY [1984]. The original data set was organized at the 10-min scale. I aggregated the "modal" elevation data into 0.5° grid cells.

Field capacity for each grid cell was determined as a function of soil texture and vegetation (Table II-1). Six soil texture classes were considered in conjunction with two broad categories of vegetative cover. First, I assigned a characteristic field capacity, as percent of total soil volume, to the six texture classes using data from Saxton et. al. [1986] representing soil moisture at 30-kPa water potential. I then established rooting depths for the various combinations of soil texture and vegetation using the assignment scheme given by Thornthwaite and Mather [1957]. The product of field capacity percentage and rooting depth defined field capacity in millimeters. Except

TABLE II-1. Relationships Linking Vegetation Class, Soil Texture, Rooting Depth and Moisture Capacities of Soil

Vegetation <sup>a</sup>	Sand	Sandy Loam	Silt Loam	Clay Loam	Clay	Lithosol
	<u>Root Depth, m</u>					
Forest	2.5	2.0	2.0	1.6	1.2	0.1
Grassland and shrubland	1.0	1.0	1.3	1.0	0.7	0.1
	<u>Field Capacity<sup>b</sup>, and Available Water Capacity (in Parentheses)<sup>c</sup>, mm of water</u>					
Forest	353.0 (196.0)	400.0 (218.0)	546.0 (282.0)	563.0 (243.0)	582.0 (153.0)	27.0 (14.0)
Grassland and shrubland	141.0 (78.0)	200.0 (109.0)	355.0 (183.0)	352.0 (152.0)	340.0 (89.0)	27.0 (14.0)

<sup>a</sup>WBM forests were assigned rooting depths for "mature forest" given by Thornthwaite and Mather [1957], WBM grasslands and shrublands were given rooting depths for "deep rooted crops."

<sup>b</sup>The field capacity values in mm were determined using the following values representing field capacity as a percentage of total soil volume: 14.1% (sand), 20.0 (sandy loam), 27.3 (silt loam), 35.2 (clay loam), 48.5 (clay). Field capacity was taken as moisture content at 30-kPa water potential. These values were taken from Saxton et al. [1986]. Lithosols were assigned a value of 27.3% and were assumed to have a rooting depth of 0.1 m for all vegetation classes.

<sup>c</sup>The available water capacities (field capacity minus wilting point) in millimeters were determined using the following values representing wilting point as a percentage of total soil volume: 6.3% (sand), 9.1 (sandy loam), 13.2 (silt loam), 20.0 (clay loam), 35.8 (clay). Wilting point was taken as moisture content at 1500-kPa water potential. These values were taken from Saxton et al. [1986]. Lithosols were assigned a value of 13.2% and were assumed to have a rooting depth of 0.1 m for all vegetation classes.

for lithosols (very rocky soils), specific values for the resulting FCs were therefore vegetation and texture dependent. Eleven potential field capacities were generated, from 27 to 582 mm of water.

A similar set of calculations was made for available water capacity (AWC), defined as field capacity minus wilting point. Because of its dependence on vegetation and soil characteristics, AWC also showed a broad numerical range, from 14 to 282 mm (Table II-1). These values represent an alternative to the use of a spatially uniform AWC field of 150 mm, evident in recent global climate modeling studies [Kellogg and Zhao, 1988].

The values presented in Table II-1 together with a series of geographically-referenced data sets were used to determine the distribution of FC and AWC across the continent. Soil texture for South America was derived from gridded 1:5,000,000 scale soil maps [Food and Agriculture Organization/Complex Systems Research Center (FAO/CSRC), 1974]. (The following FAO classifications were assigned to the various texture classes shown in Table II-1: "coarse" was assigned to sand, "medium" to silt loam, "fine" to clay, "coarse + medium" to sandy loam, "coarse + fine" to silt loam, "medium + fine" to clay loam, and "coarse + medium + fine" to silt loam.) Vegetative cover was from Matthews [1983], converted to 0.5° resolution. Table II-2 lists 14

TABLE II-2. Distribution of South American Ecosystems

Ecosystem	Area, 10 <sup>6</sup> km <sup>2</sup>
Forest	
Tropical evergreen forests	6.778
Tropical and subtropical drought-deciduous forests	1.488
Tropical and subtropical semi-deciduous broad-leaved forests	0.210
Subtropical evergreen forests	0.182
Temperate evergreen broad-leaved forests	0.017
Temperate mixed forests	0.014
Drought-deciduous woodlands	0.012
Total forest	8.700
Shrubland	
Xeric forests and woodlands	2.050
Xeric shrublands and scrub	1.338
Total shrubland	3.388
Grassland	
Savannas, 10-40% tree cover	1.909
Short grasslands, meadows, tropical alpine vegetation	1.115
Savannas, <10% tree cover	0.952
Tall grassland	0.458
Shrub savanna	<u>0.309</u>
Total grassland	4.743
Grand total	16.832

The ecosystem types listed were obtained from Matthews [1983] and classified into broad categories of vegetation in order to utilize information in Table 1 to distribute field and available water capacities over space. Areas given are corrected for latitude. Only those areas for which actual WBM calculations were made are tabulated. Totals may not add due to rounding.

broad ecosystem types and their associated areas. The dominant vegetation is forest (> 50% of all area) and in particular the tropical evergreen forest. Grasslands and savannas comprise approximately 30% of the continental landmass. Shrubland accounts for the remaining 20%. Ten field capacity classes are present ranging from 27 to 582 mm with an area-weighted mean of 394 mm. A map of the resulting field capacities is shown in Plate II-1. The distribution of available water capacity is shown in Plate II-2. The ten AWC classes range from 14 to 282 mm. The area-weighted mean for South America is 144 mm.

The spatial patterns of FC and AWC correlate well with the distribution of vegetation. Thus, forested areas with high capacities contrast sharply against lower-biomass regions having smaller values. Another dominant feature is the level of detail afforded by the 0.5° scale, a product of the original soil and vegetation data sets. These maps represent the most spatially-resolved estimates of FC and AWC currently available for South America.

#### Water Transport Model: Structure and Parameterization

The water transport model is a multigrid, dynamic model which computes discharge through each cell within a simulated drainage basin (Figure II-2). It combines runoff produced by WBM with information on network topology, fluvial transfer rates and the timing and extent of floodplain inundation. Discharge is predicted as a monthly



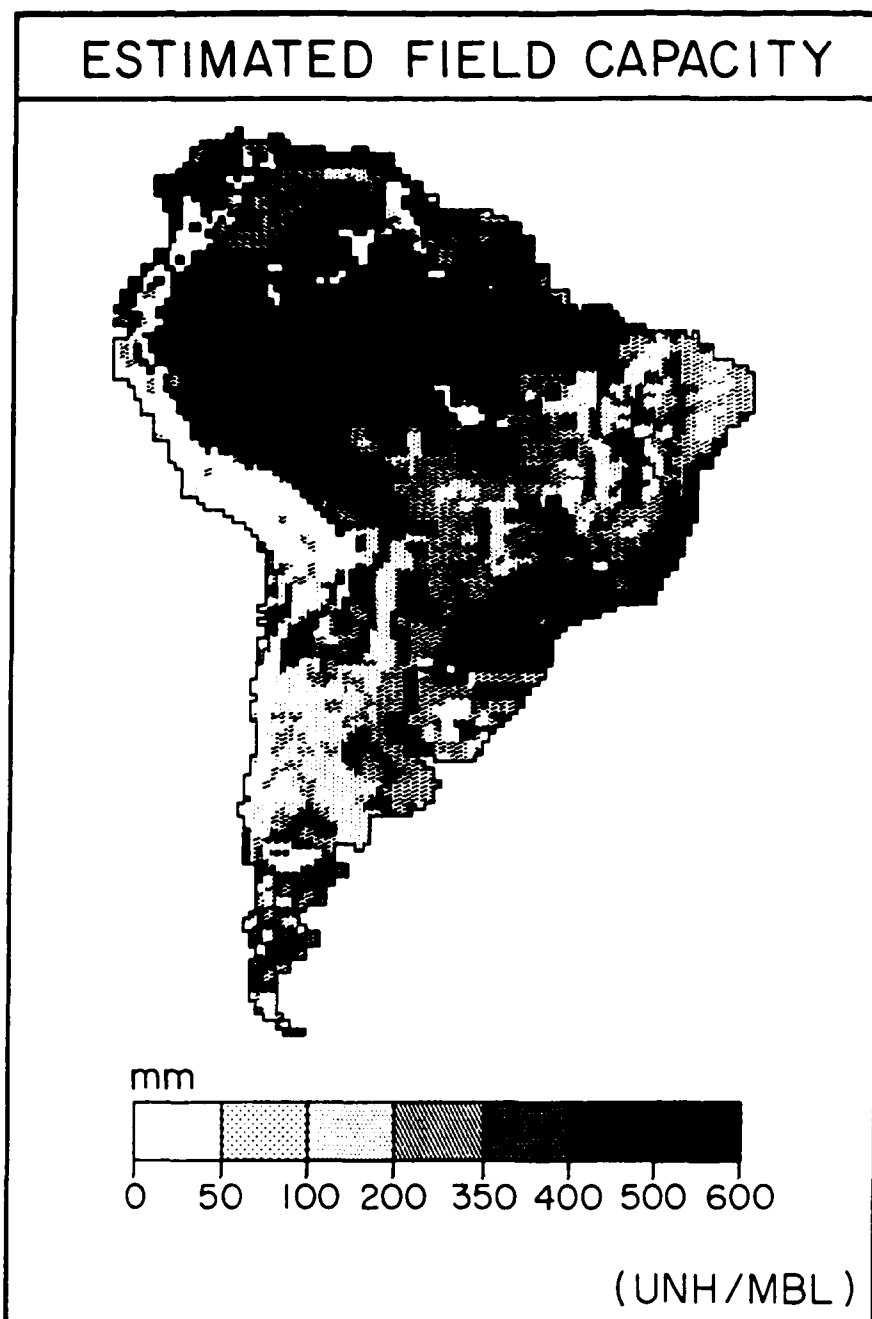


Plate II-1. Field capacities used by the water balance model at 0.5° spatial resolution. The capacities were generated using Table 1 and geographically-specific information on soils and vegetation. The areas represented by particular field capacities are 27 mm ( $1.9 \times 10^6$  km<sup>2</sup>), 141 ( $1.7 \times 10^6$ ), 200 ( $0.003 \times 10^6$ ), 340 ( $2.8 \times 10^6$ ), 352-355 ( $2.6 \times 10^6$ ), 546 ( $2.5 \times 10^6$ ), 563 ( $0.4 \times 10^6$ ), and 582 ( $4.9 \times 10^6$ ).

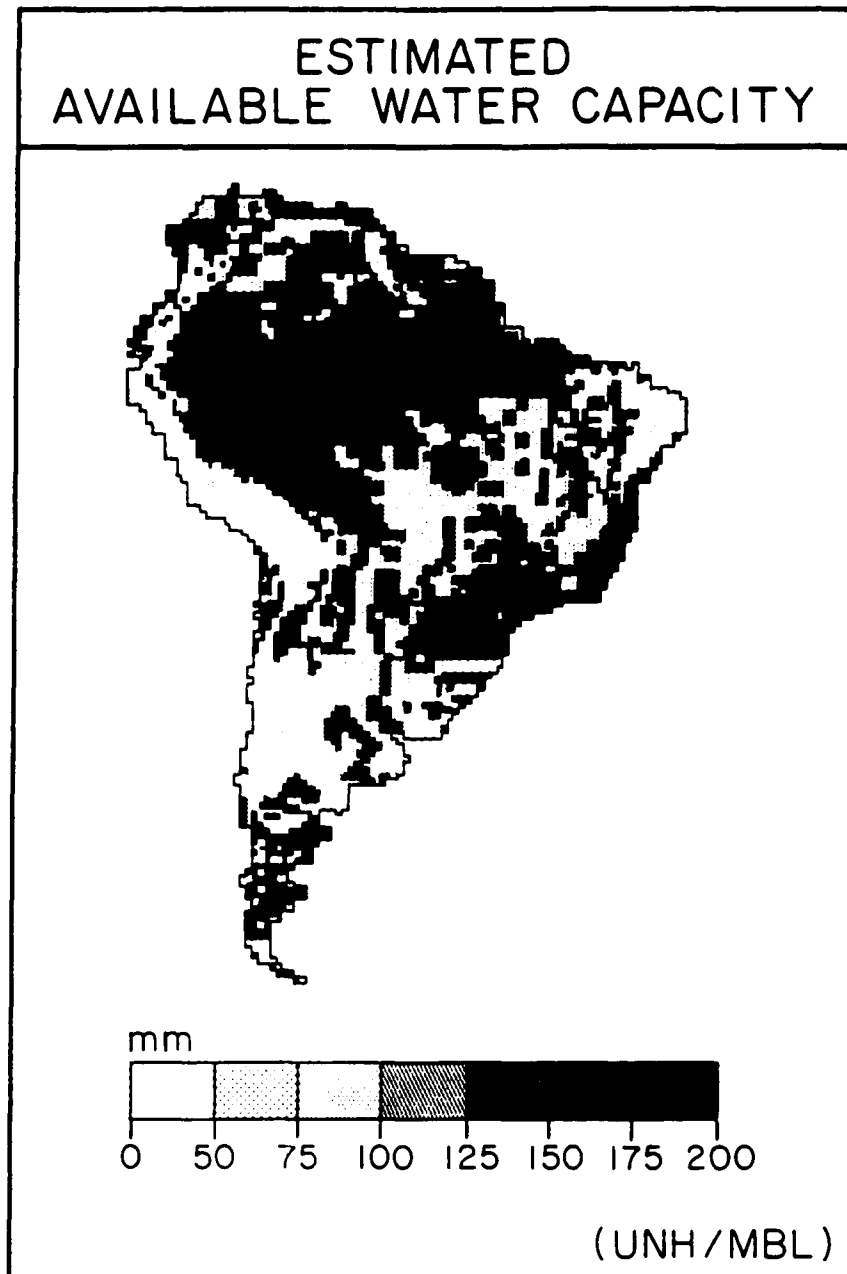


Plate II-2. Available water capacity (field capacity minus wilting point) computed by the water balance model at 0.5° spatial resolution. The values were generated using Table 1 and geographically-specific information on soils and vegetation. The areas represented by particular available water capacities are 14 mm ( $1.9 \times 10^6$  km<sup>2</sup>), 78 ( $1.7 \times 10^6$ ), 89 ( $2.8 \times 10^6$ ), 109 ( $0.003 \times 10^6$ ), 152 ( $0.4 \times 10^6$ ), 153 ( $4.9 \times 10^6$ ), 183 ( $1.9 \times 10^6$ ), 196 ( $0.3 \times 10^6$ ), 243 ( $0.4 \times 10^6$ ), and 282 ( $2.5 \times 10^6$ ). The mean area-weighted average is 144 mm.

mean. Because WBM-generated runoff drives the transport model, predicted discharges represent long-term climatic averages. Initial application of this model has been to the Amazon/Tocantins river system which represents nearly one-fifth of the world's freshwater discharge. The simulated Amazon Basin comprises 1936 grid cells ( $5.9 \times 10^6$  km<sup>2</sup>). The Tocantins River adds another 315 cells ( $0.96 \times 10^6$  km<sup>2</sup>).

Network topology was determined manually from a series of 1:1,000,000 Operational Navigation Charts [Defense Mapping Agency Aerospace Center (DMAAC), 1980, 1981, 1982, 1983, 1984, 1986] covering the Amazon/Tocantins system. For each 0.5° cell, a predominant direction of flow was determined by examining the discernible network of rivers and streams. With large rivers this afforded an unambiguous indicator of directionality. In grid cells representing small catchments, a predominant stream was sometimes absent. In these cases I relied on topographic features and elevational data reported on the DMAAC maps. Flow direction was therefore predicted less accurately for small rivers than for larger rivers. This effect was common in subcatchments of four or fewer grid cells (30% of such grid cells had less reliable directionality). A four-cell basin near the equator is approximately 12,000 km<sup>2</sup>, an area similar to that of a sixth-order stream [Leopold et. al.,

1964]. This represents the theoretical limit of WTM spatial resolution using a  $0.5^\circ$  grid structure.

Channel flow in the WTM is represented by a linear reservoir model [Huggins and Burney, 1982]. Each grid is considered a storage pool with a characteristic residence time ( $\bar{t}$ ). I assign a standard transfer coefficient,  $K$  ( $\bar{t}^{-1}$ ), to all cells and then modify this parameter based on geometric considerations. The standard is associated with rivers draining grid cells on the N-S or E-W axis. The  $K$  value is then lengthened or shortened depending on the geometry of influent and effluent streams. For example, a cell receiving influent from the southwest and with an exit at its northeast corner would have the standard  $K$  value multiplied by 0.7 to accommodate a longer residence in the grid cell. In the case of multiple tributaries, the residence time is weighted by mean annual flow. For grid cells lacking upstream inputs, the residence time is halved.

The WTM also predicts floodplain inundation independently of any WBM calculations. I have chosen flood parameters in WTM that have clear physical analogues. Floodplain exchanges take place whenever the monthly discharge exiting a grid cell exceeds a specified fraction of long-term mean annual flow. Above this fraction and with increasing discharge, inundation is simulated by apportioning the potential net increase in channel storage between the channel itself and its associated floodplain.

Floodplain storage increases until the time derivative of channel storage becomes negative. During flood recession, the potential net decrease in channel storage is accounted for by changes in channel and floodplain storage using the same ratios as for rising waters. These calculations attenuate the amplitude of rising flood waves and augment downstream discharge during periods of falling stage. For a single grid cell, the resulting flow and continuity equations are:

$$dS_c/dt = (\sum_1^n Q_u) - Q_d + Q_g + Q_f \quad (7a)$$

$$dS_f/dt = - Q_f \quad (7b)$$

$$Q_d = K S_c \quad (7c)$$

$$Q_g = A ( RO_r + RO_s )/1000. \quad (7d)$$

$$Q_f = - r_f [ (\sum_1^n Q_u) - Q_d + Q_g ] \quad Q_d \geq c_f Q_{dma} \quad (7e)$$

$$Q_f = 0 \quad Q_d < c_f Q_{dma} \quad (7f)$$

where  $S_c$  is channel storage in a grid cell during a month (cubic meters),  $S_f$  is floodplain storage (cubic meters),  $K$  is the downstream transfer coefficient ( $\text{month}^{-1}$ ),  $A$  is the area of the grid (square meters),  $n$  is the number of donor grid cells,  $Q_u$  is monthly upriver input,  $Q_d$  is discharge from cell exported downriver,  $Q_g$  is input from runoff generated within the grid cell,  $Q_f$  is exchange between channel and floodplain (plus denotes floodplain to channel), and  $Q_{dma}$  is the mean annual downstream discharge. All  $Q$  values are in cubic meters per month. The coefficient  $r_f$

determines the ratio ( $\geq 0.0$ ) of potential volume change that is assigned to floodplain storage and  $c_f$  is the flood initiation parameter, giving the proportion (0.0 to 1.0) of long-term mean annual flow required to invoke floodplain exchanges.

The established topology together with the flow and continuity equations (7a)-(7f) creates a system of linked differential equations. The system is solved for  $S_c$  and  $S_f$  using a fifth- to sixth-order Runge-Kutta integration technique [International Mathematical and Statistical Libraries (IMSL), Houston, Texas, 1982]. For the entire Amazon/Tocantins basin, 2251 cells are linked. The model applies monthly runoff values for each grid cell until a quasi-steady state solution emerges for the entire set of cells.

The linear transfer coefficient for channel flow,  $K$ , can be related to physically meaningful quantities and can assist in subsequent calibration. The continuity equation and the linear model are interrelated as follows:

$$Q_{dma} = V (WH) = 3.86 \times 10^{-7} K (WHLS) \quad (8)$$

where  $V$  is mean annual velocity (meters per second),  $W$  is channel width (meters),  $H$  is water height (meters),  $L$  is standard length of grid (meters), and  $S$  is a dimensionless expansion factor analogous to sinuosity. The constant is a time scaling factor. Equation (8) reduces to:

$$K = 2.59 \times 10^6 \text{ (V/LS)} \quad (9)$$

Velocity is predicted from  $Q_{dma}$  using relationships given by Leopold et. al. [1964, footnote to Table 7-21] for a wide spectrum of rivers. An aggregate relation was formulated:

$$\log V = 9.304 \times 10^{-2} \log Q_{dma} - 0.28515 \quad R^2 = 0.74 \quad (10)$$

Assigning a value of 55 km to L (standard cell length near the equator) permits solution for S as a function of K for particular flows. Figure II-4 shows these results. Three flow rates are considered, the mean for all grid cells plus high and low values which bracket the range of possible flow rates. If the length factor (S) is interpreted as a measure of sinuosity a range of candidate K values can be predicted. It is reasonable to conclude that transfer coefficients lower than about 5 (month<sup>-1</sup>) for low flows and 10-15 (month<sup>-1</sup>) for intermediate and large rivers yield length factors that are inappropriate [Richards, 1982]. Upper limits can also be defined. K values above 25 (month<sup>-1</sup>) for small rivers, 55 for intermediate rivers and 75 for large rivers yield length factors below 1, a condition that could only exist if the velocity prediction is in some way violated. If the velocity predictions are adhered to, there is then a wide theoretical range for K, on the order of 5-75. Because the model's performance will be determined

## TRANSFER COEFFICIENT ANALYSIS

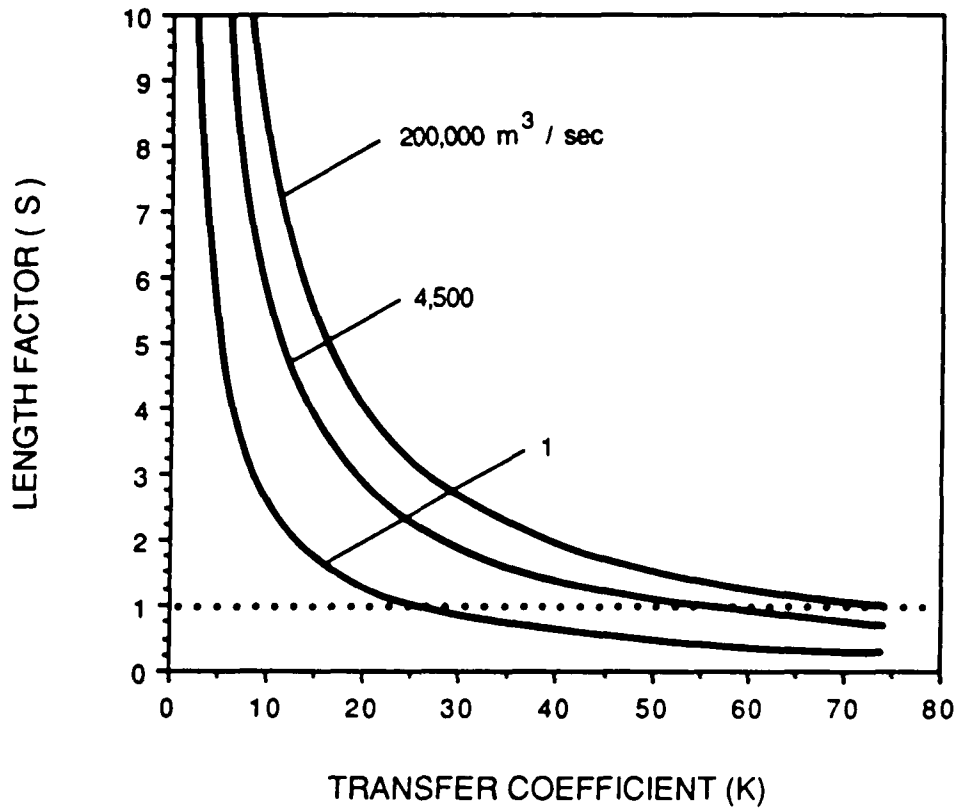


Fig. II-4. Relation of fluvial transfer coefficient,  $K$  ( $\text{month}^{-1}$ ), to a length scale,  $S$ , analogous to sinuosity. Curves bracket the range of flows encountered in this study and define reasonable choices for  $K$  in the Water Transport Model. The mean cell discharge is also shown.



most strongly by the mass of intermediate-flow grid cells a reasonable range is likely to be from 15 to 50.

The model was tuned using an unbiased estimator of performance relative to observed data. This index, modified from Willmott [1982] and Willmott et. al. [1985b] is:

$$d = 1 - \left( \frac{\sum_1^{12} |P_i - O_i|^y}{\sum_1^{12} (|P_i'| + |O_i'|)^y} \right) \quad (11a)$$

$$P_i' = P_i - O_m \quad (11b)$$

$$O_i' = O_i - O_m \quad (11c)$$

where  $d$  is the "index of agreement",  $i$  is the month,  $P_i$  is the  $i$ th model prediction,  $O_i$  is the corresponding observation,  $y$  is an exponent set to 1.0 based on discussion of Willmott et. al. [1985b], and  $O_m$  is the observed mean, in this case annual discharge. The  $d$  values calculated for each hydrograph were then combined to yield an aggregate measure of model performance. This measure was weighted to combine the effects of flow magnitude and duration of the discharge record. Because of the weighting factors,  $d$  values for large rivers and sites with long periods of record were favored.

To produce a best fit, WTM calculations were compared to observed discharge records [UNESCO, 1969, 1971, 1974, 1979, 1985] at six sampling stations. Discharge was expressed as a monthly mean for the period of record. (For Obidos on the mainstem Amazon, the discharge record prior to 1949 was deemed unreliable and therefore deleted from the

analysis.) Over 80 model runs were performed with various combinations of the standard channel transfer coefficient and flooding parameters. Minimum to maximum values for the standard  $K$ , the flood initiation parameter  $c_f$ , and the flooding ratio  $r_f$  were 12.5 to 50 ( $\text{month}^{-1}$ ), 0.6 - 1.4 and 0.0 - 1.0, respectively. Tests showed that the best model performance (weighted  $d = 0.823$ ) was afforded by the combination  $K = 20$ ,  $c_f = 0.9$  and  $r_f = 0.65$ . These parameters defined the standard scenario. A value for  $K$  of 20 (residence time of  $\approx 1.5$  day for a standard grid) corresponds to the expected values developed earlier. The flooding parameters combine to yield 6-7 months of inundation on the central Amazon. The fitted model indicates how well the combined WBM/WTM structure can reproduce the hydrographic features of the region. Time series data, rather than monthly climatic averages, would be required to test the predictive capacity of the calibration.

The WTM does not currently treat information about hydraulic alteration such as stream diversion or impoundment, although such effects are clearly dominant in other regions. The approach to modeling altered systems would be identical to that developed for unregulated river systems. Namely, an appropriate topology would be developed with mass balance and flow equations. The source/sink terms, however, would need to be modified to accommodate purposeful changes in water use and storage. The inclusion

of such information in any continental-scale model represents a formidable data management challenge.

### Results and Discussion

#### Water Balance Model: General Hydrologic Regimes in South America

The WBM made predictions on approximately 5750  $1/2^\circ$  grid cells in South America. A variety of climatic zones were represented. The bulk of the continent has a single wet ( $PPT + R_s \geq PET$ ) and dry ( $PPT + R_s < PET$ ) season each year. The dominant regime was one in which field capacity was attained during at least one month of the year ( $11.73 \times 10^6 \text{ km}^2$ ). Areas with snowfall,  $0.76 \times 10^6 \text{ km}^2$ , fell within this category. Field capacity was never attained on  $4.14 \times 10^6 \text{ km}^2$ . A significant subset of cells in this regime had persistent dryness for each month of the year ( $2.35 \times 10^6 \text{ km}^2$ ). Under such a condition, soil moisture and runoff were set equal to zero and all precipitation inputs, plus any snowmelt, were fully converted into evapotranspiration. Other climatic zones showed more complex behavior with multiple wet and dry seasons each year. Much smaller areas were represented:  $0.29 \times 10^6 \text{ km}^2$  (FC attained during two wet seasons),  $0.40 \times 10^6 \text{ km}^2$  (one wet season), and  $0.26 \times 10^6 \text{ km}^2$  (neither wet season).

For each grid cell, WBM computes the annual mean as well as subannual time series of SM, RO and ET. All such grid cell-level calculations, when geographically

referenced, define the continental-scale hydrology of South America. Figure II-5 shows examples of WBM inputs and resulting calculations for grid cells representing the two dominant hydrologic regimes of the continent.

One dominant regime has a single wet/dry season in which field capacity is attained. The representative grid cell is in the Amazon lowland forest (3.0°S, 60.0°W). The predominant soil texture is clay, the rooting depth is 1.2 m and FC is 582 mm of water. This site has a strong signal for seasonal precipitation with relatively uniform PET. The PPT exceeds PET in the single wet season which extends from November through May and is adequate to override any PET deficit incurred during the dry season from June through October. Soil moisture reflects this pattern of water availability. Drawdown begins in June and continues through October to a level 40% below FC. In November and December there is rapid recharge in response to surplus PPT. The maximum, which equals FC, occurs in January and SM remains at this level until the dry season once again begins. During the wet season, ET is equal to PET, and only during the dry season does it fall below the potential. The minimum ET is about 70% of PET. Runoff shows a strong seasonal pattern as well, with values ranging from near 0 to

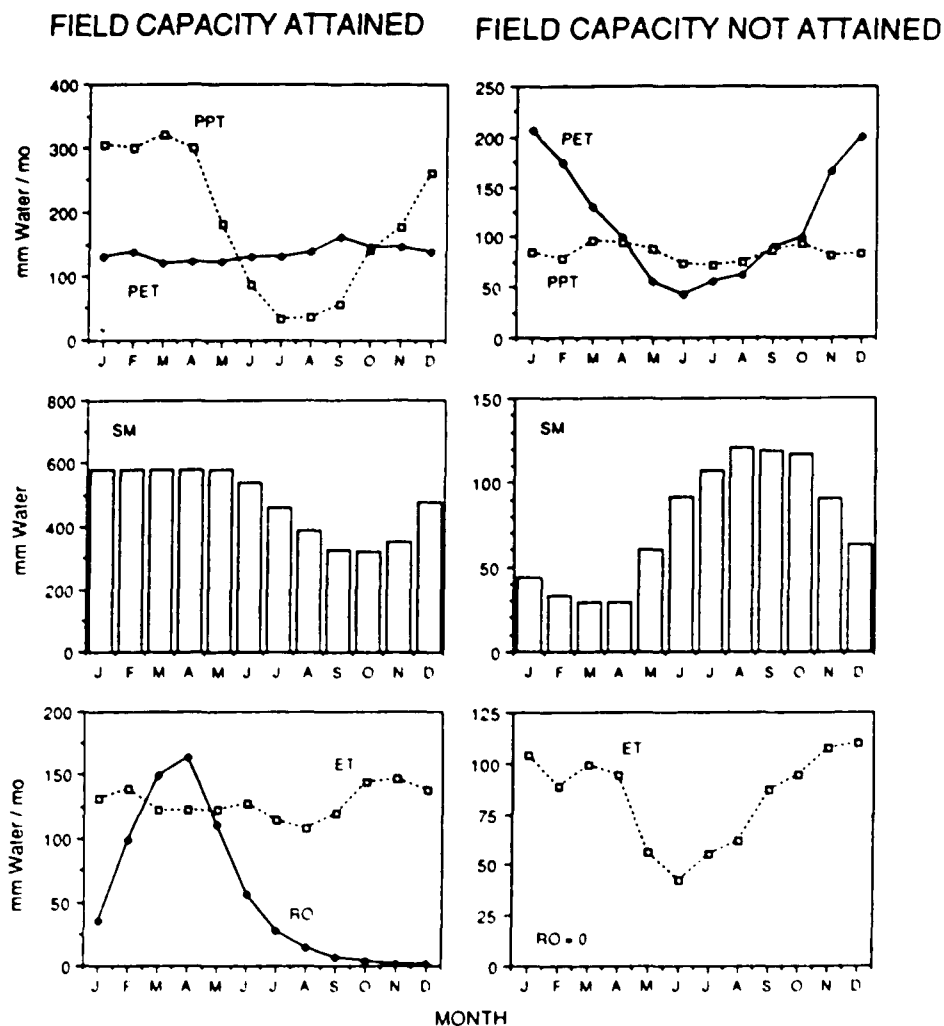


Fig. II-5. Water balance model calculations for representative  $0.5^\circ$  grid cells in South America. Each panel displays how the model transforms climatic variables into time series of soil moisture (millimeters), evapotranspiration (millimeters per month), and runoff (millimeters per month). Representative cells are from (Left) the Amazonian rainforest ( $2.0^\circ\text{S}$ ,  $60.0^\circ\text{W}$ ) and (Right) the Gran Chaco/Pampas region ( $33.0^\circ\text{S}$ ,  $58.0^\circ\text{W}$ ).

more than 170 mm/month. Although there is ample water surplus starting in January, RO continues to increase due to lags inherent in the linear storage pool. Runoff peaks in April and then decreases in response to smaller excess PPT over PET. Thereafter, RO decays exponentially until January when the soil is once again fully recharged.

A second major regime also has a single wet/dry season but field capacity is never attained. An example of this type of cell is located in the Gran Chaco/Pampas region (33.0°S, 58.0°W). The principal vegetation type is grassland having a 0.7 m rooting depth in a clay soil. The FC is 340 mm of water. This site represents a dry temperate climate in which PPT is relatively low and constant, and PET fluctuates in response to seasonal temperature and radiation. Although there is a distinct wet season from May through August total rainfall does not compensate for the effect of PET over the year and SM remains below FC. In fact, moisture stocks in the soil are always far below the 340 mm capacity, with a peak of only 120 mm. From its maximum in August, SM is drawn down to a minimum of 30 mm by April. Evapotranspiration is similarly limited by the lack of available water. The timing of ET follows PET but can only equal the potential during the four-month wet season. Thereafter, ET is limited. In fact, the ET is only 50% of potential in the particularly dry months of January and February. According to the Thornthwaite/Mather model no RO

is generated under such dry conditions. Obviously, there is storm runoff in the real world setting and a more complete version of the model would consider such an effect. Work by Rastetter et. al. 1991 seeks to improve this aspect of the WBM.

#### Water Balance Model: Detailed Calculations at the Continental Scale

Predictions are presented here for soil moisture, evapotranspiration and runoff in South America. Model results are organized at 0.5° spatial resolution and accommodate the effects of the numerous biogeophysical data sets detailed earlier. Results represent long-term or climatologically-averaged conditions. Figure II-6 is a map of the broad geographic regions referred to in the discussion that follows.

Soil Moisture. Predictions of soil moisture made by WBM are given in Plate II-3. Mean annual soil moisture for the entire continent is calculated as 284 millimeters, but there are substantial regional differences. The model indicates that mean annual soil moisture is highest in the Western and Eastern Amazon and the southeastern coast of Brazil, and lowest in the Gran Chaco, Pampas and Patagonian regions of Argentina, the Central Andes (with the Atacama Desert) and Eastern Brazil. In addition, the Northern and Patagonian Andes are areas of both high and low SM, owing to steep gradients in climate and soil type. Vast areas have

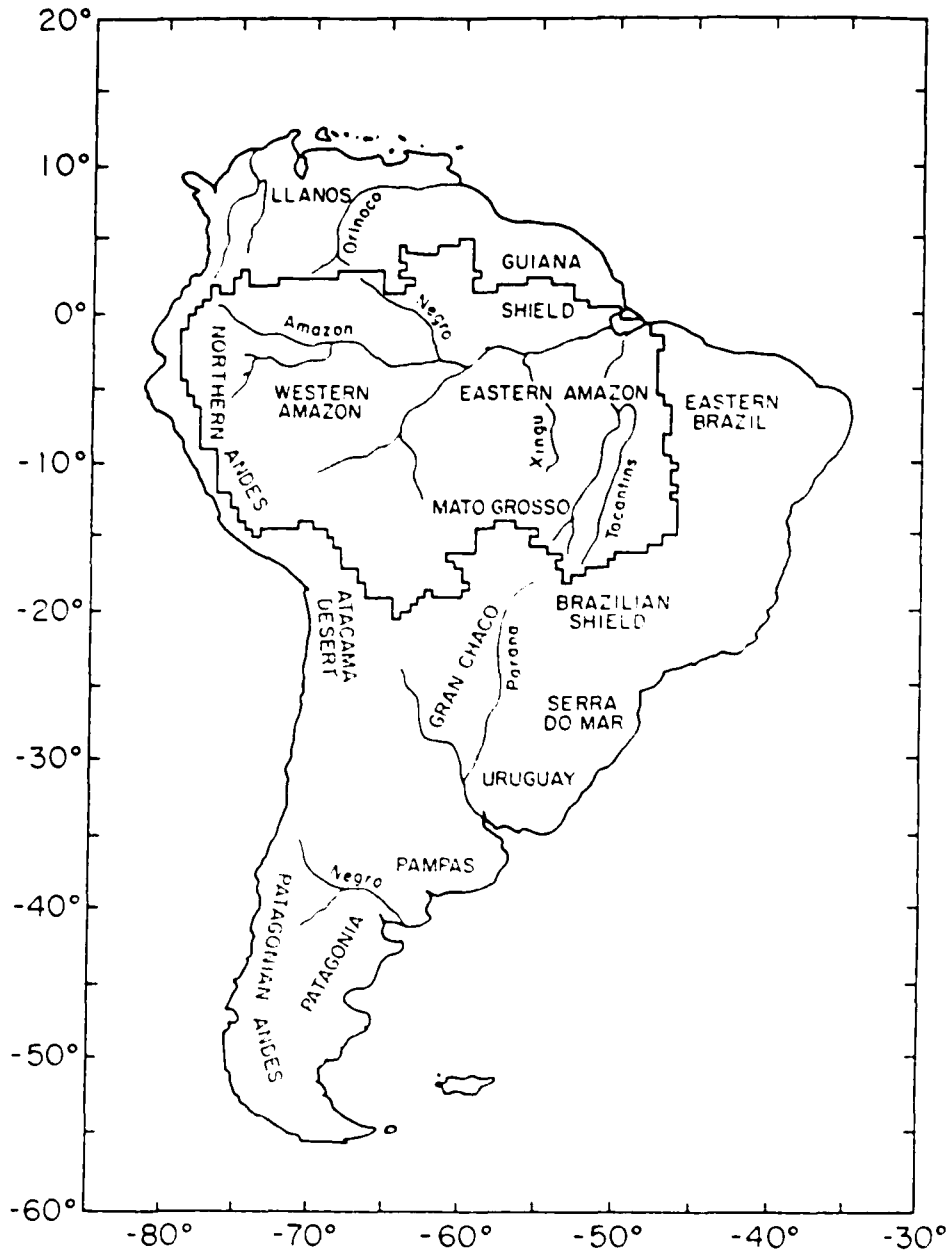


Fig. II-6. The major geographic regions of South America.



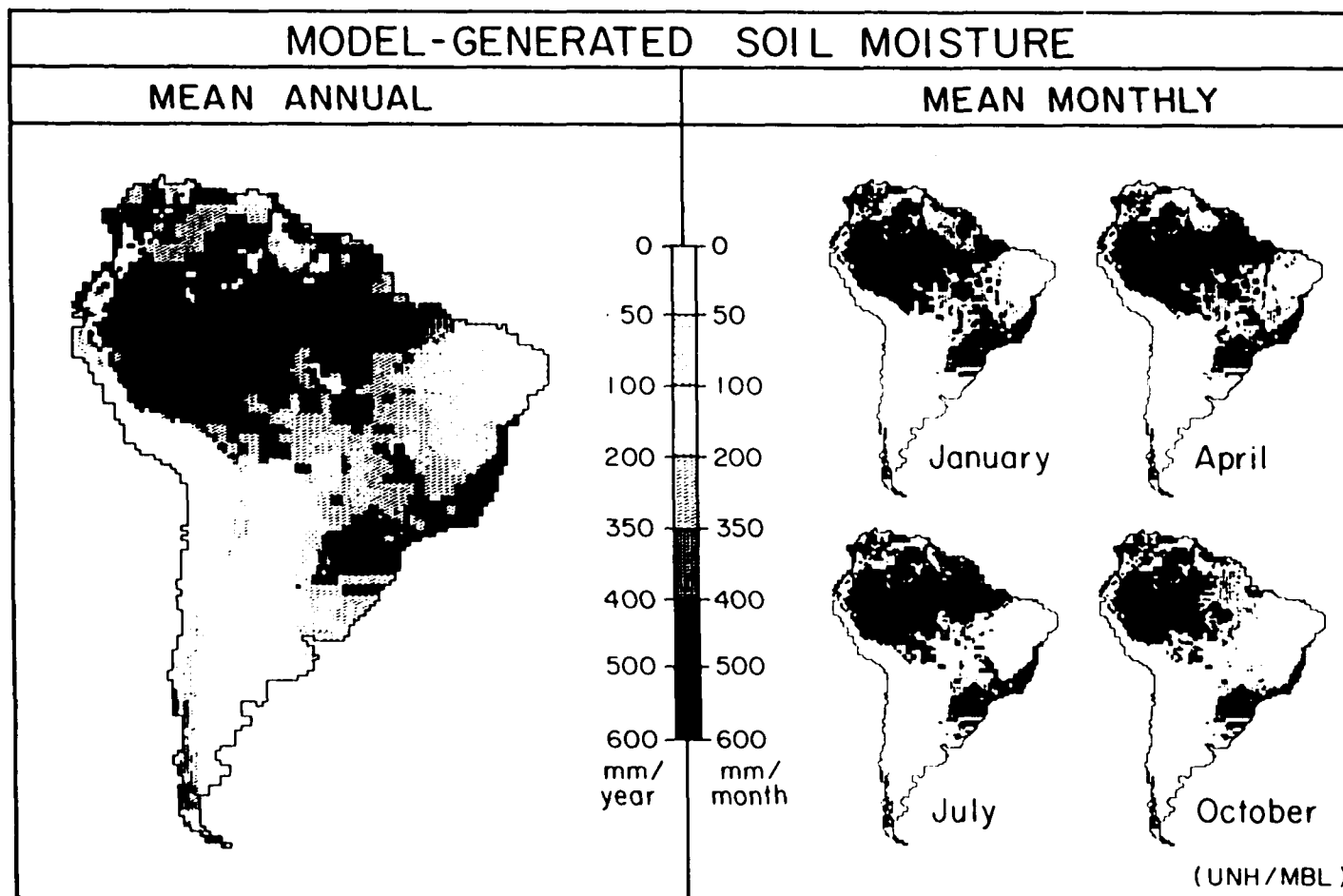


Plate II-3. Mean annual and monthly soil moisture predicted by the water balance model at  $1/2^\circ$  spatial resolution. Maximum values correspond to field capacities shown in Plate II-1. Predictions are independent of floodplain inundation.

moderate soil moisture. These zones are found over the Mato Grosso, the Brazilian Shield, the northern Guiana Shield and in the northern Llanos.

The WBM map for mean annual soil moisture follows the pattern of precipitation reported elsewhere [Korzoun et. al., 1977, Baumgartner and Reichel, 1975]. However, PPT alone is a poor predictor of SM in absolute terms (Figure II-7). The PPT dependency becomes more clear if the data are segregated by field capacity (Figure II-7). Each graph showing PPT and SM is characterized by three regions. The first is a low variability zone near the origin showing that with little PPT there is little resulting SM. Next is an intermediate zone characterized by higher variability. This zone has the greatest absolute range, suggesting that a variety of other biogeophysical factors are at play in determining mean moisture content. The third zone represents the effect of high precipitation which dampens the variability in SM which is held at or very near field capacity.

Estimates of soil water by WBM were compared to those of Willmott and Rowe [1986] after conversion to 0.5° cells. Willmott and Rowe express soil water from 0 mm above wilting point to 150 mm, an available water capacity applied uniformly to all grid cells. To permit meaningful comparison of the two data sets, I subtracted wilting point values (Table II-1) from WBM determinations of SM. The

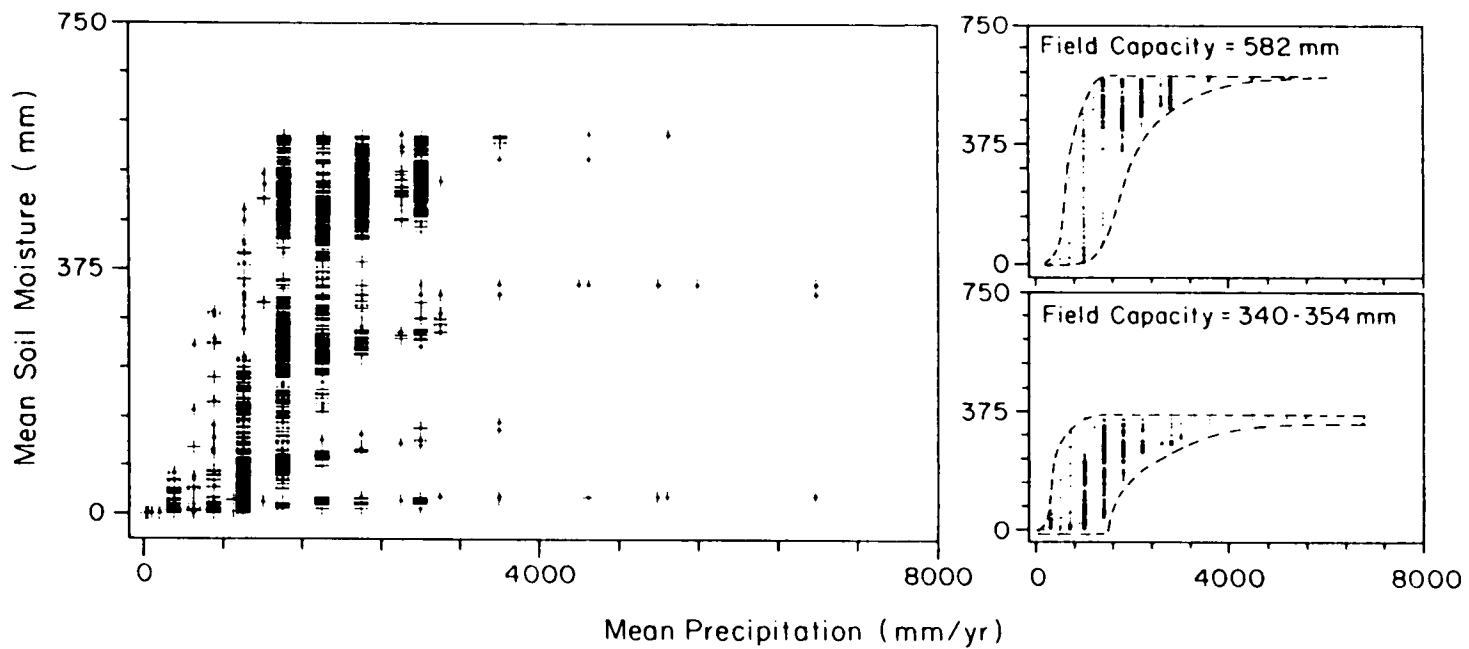


Fig. II-7. The relationship between precipitation (millimeters per year) and calculated mean annual soil moisture (millimeters) for grid cells of the South American continent. (Left) All field capacities, (Right) Representative classes.

Willmott and Rowe and modified WBM estimates are similar in terms of the spatial distribution of wet and dry soils but their absolute magnitudes often differ substantially. For the entire continent, the two data sets show, respectively, 79 and 35 mm of mean annual soil water. The distribution of numerical differences between the two data sets (Figure II-8) is unimodal and reflects the generally lower values determined using WBM. Only 34% of WBM grid cells have soil water values greater than those of Willmott and Rowe. These cells are evident where Willmott and Rowe predict relatively high soil water ( $\geq 75$  mm), generally forested areas with high rainfall and, in the case of WBM, available water capacities in excess of 150 millimeters (Table II-1). The majority of WBM predictions are lower than those of Willmott and Rowe in drier areas ( $< 75$  mm soil water). This reflects not only differences in PPT and PET data fields but also the ability of the Thornthwaite and Mather model to draw soil moisture stocks below wilting point.

The seasonal pattern of soil moisture is summarized using four representative months (Plate II-3). For much of the continent, moisture values are surprisingly stable. This constancy is associated with broad regions of moderate to high mean annual SM, namely, the Western Amazon basin, much of the southeastern Brazilian Shield and portions of the Northern and Patagonian Andes. Over much of this area, soils are at or near field capacity throughout the year.

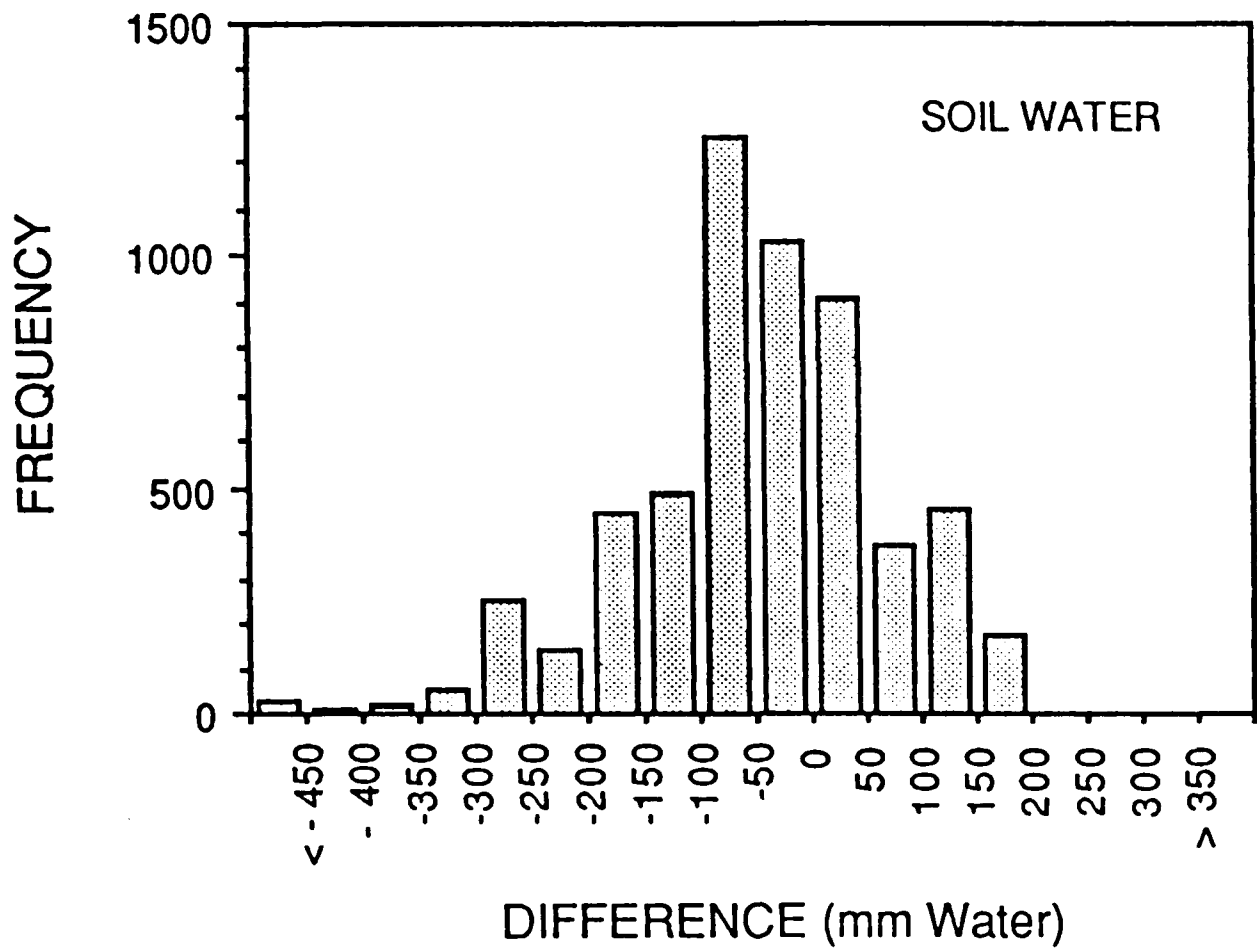


Fig. II-8. Correspondence between soil moisture estimates made by the water balance model and Willmott and Rowe [1986]. Each difference value (millimeters) is computed as WBM value minus Willmott and Rowe value.

Relatively dry and stable areas are the Gran Chaco Plains, the Pampas and the central Andes. Areas within the Northern Andes have persistently low SM because of the limited 27 mm field capacity of lithosols.

More dynamic soil conditions dominate much of Eastern Brazil, the Guiana Shield, the Eastern Amazon and the Mato Grosso. For most of these regions April is the wettest month and relatively dry areas are found only in extreme Eastern Brazil, the fringe of the Gran Chaco and the northern Guiana Shield. By July, the area of drying soils expands and major portions of the Amazon, Brazilian Shield and Mato Grosso show net depletion. Predictions for October indicate an expansion and intensification of the drying zone that influences most of these regions. By January each region has a net increase in soil water and the extent of dry zones diminishes dramatically. In contrast, the timing of such changes in soil moisture is offset by approximately three months for the Guiana Shield, due to changes in the position of the Intertropical Convergence Zone. In areas where the variations in calculated SM are substantial the seasonal pattern is correlated with the seasonality of precipitation [Korzoun et. al., 1977].

Evapotranspiration. WBM determinations of mean annual ET and its fluctuation over the year are shown in Plate II-4. The broad pattern of ET is influenced by the distribution and timing of precipitation, potential ET and

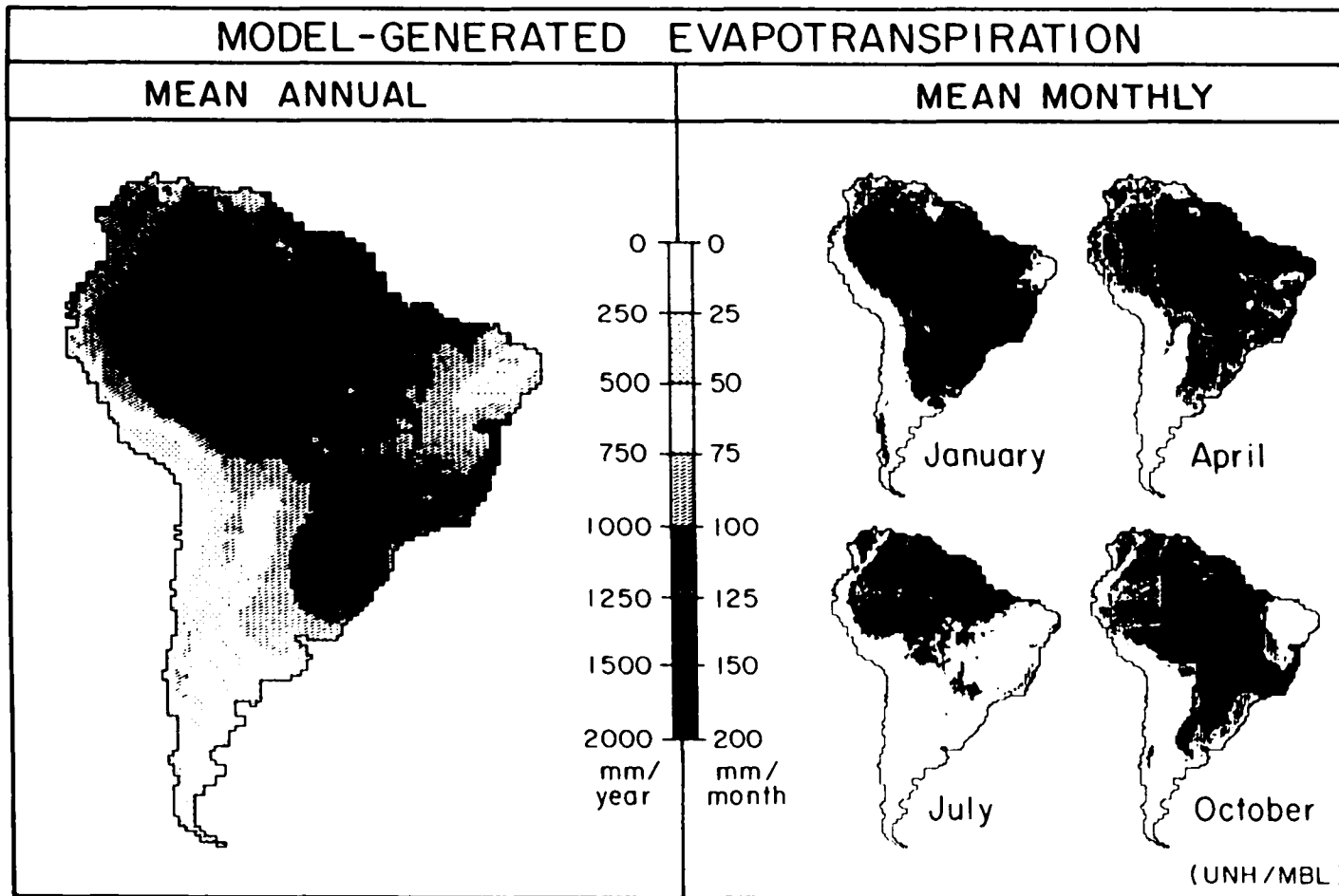


Plate II-4. Mean annual and monthly evapotranspiration predicted by the Water Balance Model at 0.5° resolution.

buffering capacity of the soil moisture pool. On a continental scale, mean ET was predicted by WBM to be 1059 mm/yr or approximately 80% of potential ET.

Because of surplus PPT, large sections of the continent have predicted ET values only modestly reduced from PET. The best example of this is the Western Amazon where ample rainfall fully satisfies (within the bounds of map resolution) the PET demand. Other areas where this is true are the Northern Andes, portions of the Patagonian Andes, the Guiana Shield, the Llanos region of Venezuela and the coastal region from Eastern Brazil to Uruguay. The southernmost tip of the continent has a wet climate and almost completely satisfies the modest potential ET demands driven by a cold climate.

Mean annual ET is substantially reduced from PET in areas where PPT is limited and the dry season(s) dominates. Predictions for Eastern Brazil, the Pampas, and the Atacama Desert therefore all show this effect. The Guiana Shield, the Mato Grosso and the Brazilian Shield are locations of more moderate rainfall (relative to PET) and therefore the PET is altered less drastically. In these areas, ET is neither unlimited by ample rainfall nor severely constrained by its scarcity.

The calculated geographical distribution of mean annual ET suggests that it is strongly related to PPT. Figure II-9 shows the predicted fraction of PET that emerges as ET



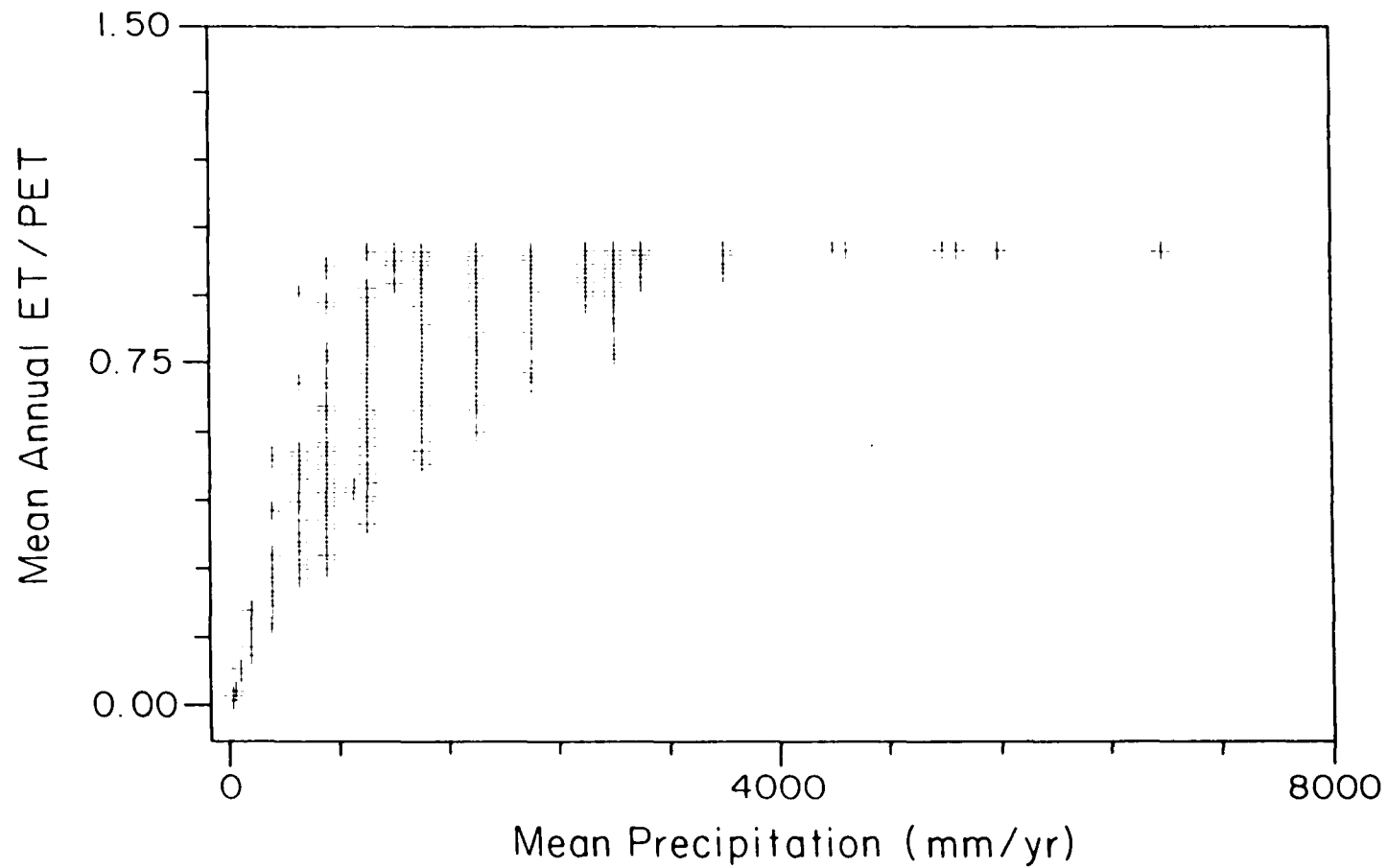


Fig. II-9. The relationship between precipitation and computed evapotranspiration for grid cells of the South American continent. The abscissa is precipitation; the ordinate is the fraction of potential ET that is computed to actually be lost from the soil as evapotranspiration. Potential ET, actual ET and precipitation are in millimeters of water per year.

expressed as a function of PPT for all South American grid cells. The plot provides a check on the ability of WBM to calculate reasonable ET estimates over a broad range of climatology. As expected, ET is strongly controlled by PPT in both very dry and very wet grid cells. The high variance in ET/PET for cells with intermediate PPT is due to the influence of wet and dry season timing and soil water retention.

WBM predictions of ET can be compared to the Korzoun et. al. [1977] and Willmott and Rowe [1986] data sets. Overall, the three data sets are comparable in magnitude (computed ET ranged from 880 to 1060 millimeters per year) and the spatial distributions match best in areas of low ET. The spatial patterns match more poorly in regions of moderate to high ET. Although the spatial distributions of ET are most similar between WBM and Korzoun et. al., ET for South America is predicted to be higher with WBM (Figure II-10). The mean ET for the entire continent given by Korzoun et. al. is 882 mm/yr, compared to 1059 mm/yr for WBM. The bulk of the differences between the two data sets ranges from -200 to +600 mm/yr (WBM minus value of Korzoun et. al.). The differences show no systematic pattern in relation to the magnitude of ET. A comparison of WBM calculations to those made by Willmott and Rowe yields a different picture (Figure II-10). The disparity is now nearly unimodal, with WBM showing systematically higher

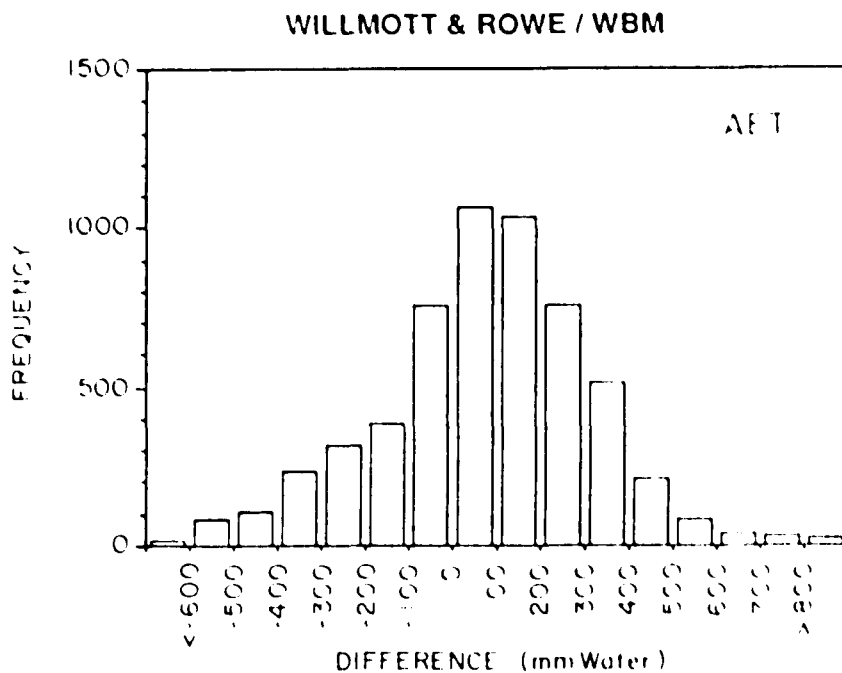
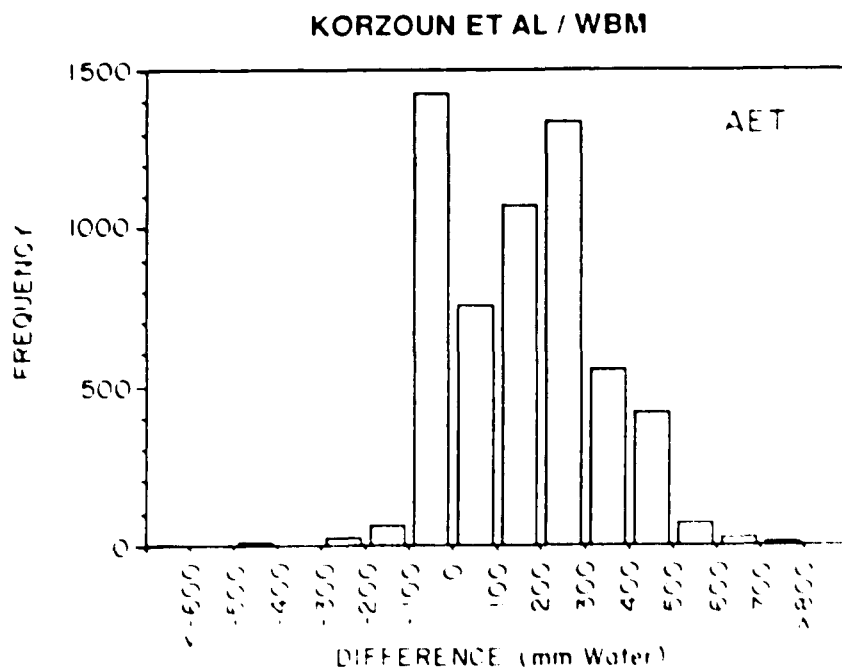


Fig. II-10. Correspondence between evapotranspiration determined by the water balance model, (Top) Korzoun et al. [1977] and (Bottom) Willmott and Rowe [1986]. Each difference value (millimeters per year) is computed as WBM value minus Willmott and Rowe value and as WBM value minus Korzoun et al. value.

estimates of ET. The mean ET predicted by Willmott and Rowe is 997 mm/yr, falling between WBM and Korzoun et. al. predictions. The range of disparity is greater than in the previous comparison, mainly from -600 to +600 millimeters per year (WBM minus Willmott and Rowe value) although the mean difference is only +62 mm/yr. As in the previous comparison, differences in the WBM/Willmott and Rowe contrast were not clearly related to the magnitude of ET.

The disparities among the three data sets are difficult to trace and are a complex function of the manner in which soils and climatology interact in each study, and any interpolation of ground-based data. Nonetheless, WBM compares favorably with these established data sets. On a continental basis, WBM estimates for mean annual ET fall within 20% and 6% of estimates of Korzoun et. al. and Willmott and Rowe, respectively.

The temporal distribution of ET over the continent was also analyzed (Plate II-4). There are two major contiguous zones with nearly constant ET: the northernmost Andes/Western Amazon/Orinoco region for high ET and Patagonia/Pampas/Atacama Desert region for low ET. These extremes reflect the availability of PPT in these areas. In persistently wet zones PET is nearly unlimited and ET is high; in very dry areas soil water retention limits ET. The remainder of South America displays distinct seasonal patterns. Examples are the Eastern Amazon, the Guiana

Shield, Eastern Brazil, the Brazilian Shield and the Gran Chaco. These are areas in which there is a strong seasonality of PPT. With the exception of Eastern Brazil and the Gran Chaco (which show peak ET in summer and fall), the more seasonal areas display highest ET in the winter and spring.

Runoff. Continental runoff for South America (Plate II-5) was computed to be 619 mm/yr, representing 37% of total precipitation. Mean annual RO is spatially correlated to continental PPT. Thus, areas within the Amazon and Orinoco catchments, the Serra do Mar, and the Northern and Patagonian Andes, show high annual RO. The regions contributing least RO encompass Eastern Brazil, the Pampas and Gran Chaco Plain in Argentina, and the Atacama Desert. Large areas of the continent ( $5.65 \times 10^6 \text{ km}^2$ ) show less than 100 mm/yr RO. Intermediate values are apparent in the Guiana and Brazilian Shields, the Mato Grosso and the northern Llanos, regions which have a relative balance between PPT and PET. These areas correspond to those with intermediate SM shown in Plate II-3.

A strong relationship exists between PPT and computed mean annual RO for South American grid cells (Figure II-11). The distribution of points begins near the origin, passes through a zone of increased variability and finally ends as a nearly straight line with slope close to 1. At low values of PPT, little RO is generated since most PPT is

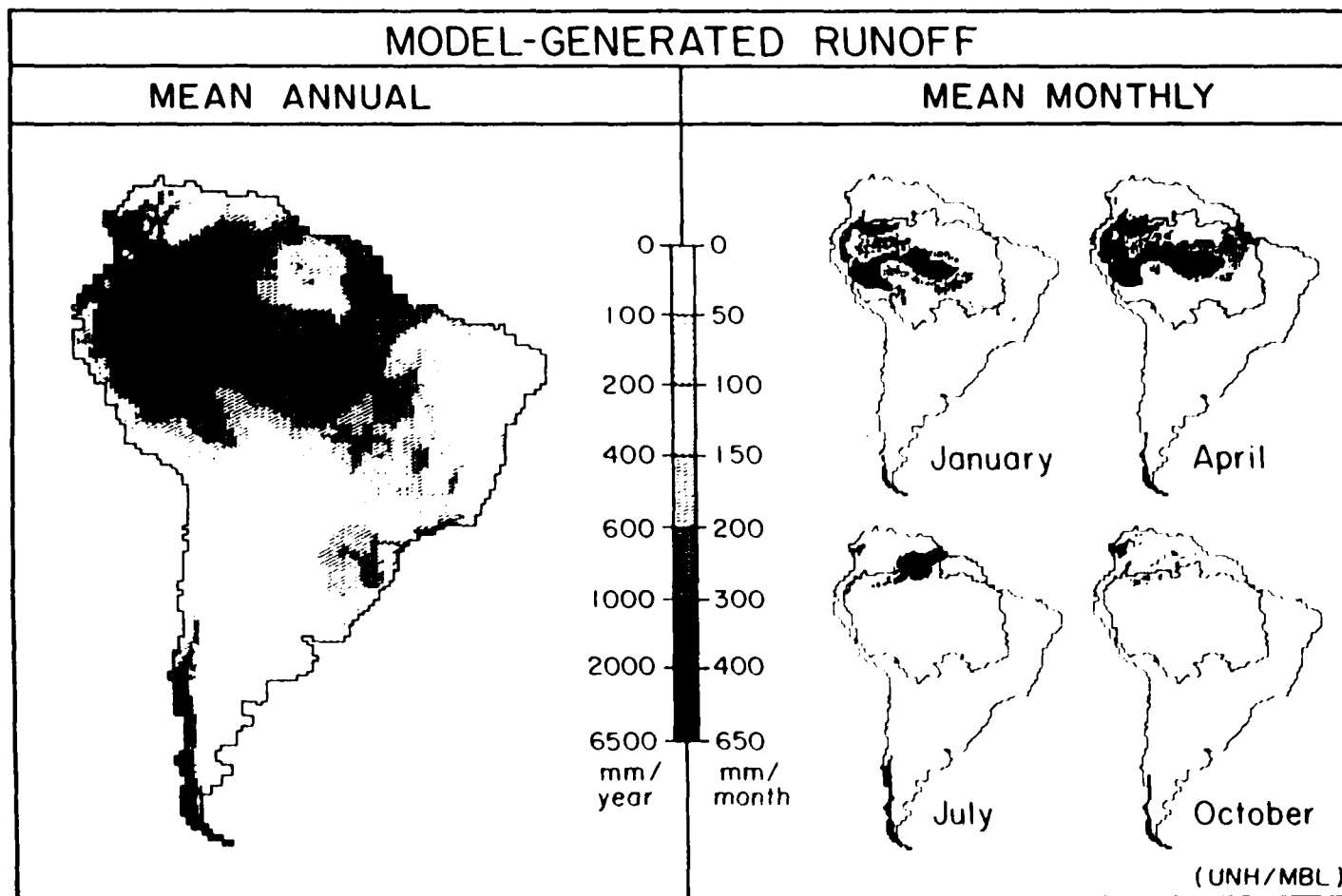


Plate II-5. Mean annual and monthly runoff predicted by the Water Balance Model at 0.5° resolution. The Amazon /Tocantins drainage basin is outlined.

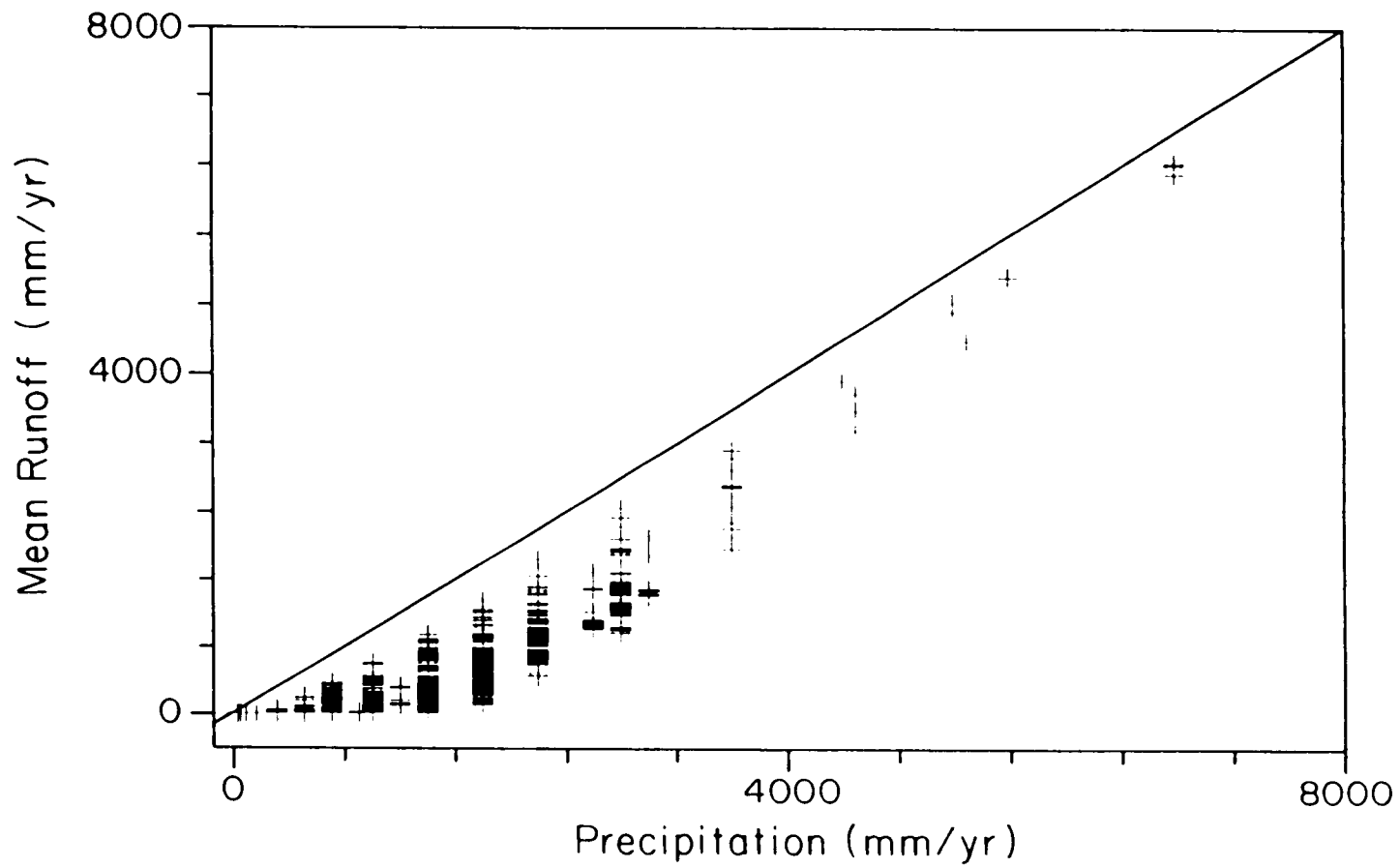


Fig. II-11. The relationship between precipitation and model-derived runoff for grid cells of the South American continent. All values are in millimeters per year.

conveyed to soil moisture recharge and ET. At intermediate levels, there is a more variable response associated with more variable ET and SM dynamics, which in turn determine the availability of surplus water. At the highest PPT values, soil moisture approaches field capacity and increases in PPT result in linear increases in RO since ET and soil storage are near their maximum. This same finding is reported for South America using a climate model [Dickinson and Henderson-Sellers, 1988] and has been observed at the local scale [FAO/United Nations Development Program (UNDP), 1968; Likens et. al., 1977; Havel and Bligh, 1982].

I compared runoff generated by WBM to an observational data set from Korzoun et. al. [1977], based on contoured data from 236 hydrographic monitoring stations having a range of 4 to 63 years of record. The correspondence is extremely close, both in terms of spatial pattern and magnitude. For the continent as a whole, WBM runoff is slightly lower than that of Korzoun et. al. Areas of high RO correlate best; namely the Amazon basin, the Patagonian and Northern Andes and the Serra do Mar. WBM predicts a slightly larger area with sparse RO for the Gran Chaco, Pampas, portions of the Northern Andes, Patagonia and Eastern Brazil. Regions of intermediate RO, such as those within and immediately surrounding the Brazilian and Guiana Shields, show significantly greater spatial detail with WBM.



The data in Figure II-12 further demonstrate a close correspondence between the two data sets. The frequency plot shows that the disparity (WBM minus values of Korzoun et. al.) has a unimodal distribution centered about the 0 to -200 millimeters per year class with the bulk of the differences lying within +/- 600 mm/yr. For the continent as a whole, the mean disparity is -73 mm/yr or 11% of the observed continental runoff (692 mm/yr). In grid cells reported by Korzoun et. al. to have  $\leq 1000$  mm/yr RO, WBM calculates slightly lower RO values relative to the observational data. The effect can be traced to assumptions regarding the absence of storm flow in WBM for drier regions. In wetter areas ( $> 1000$  mm/yr RO), differences between the two data sets are centered more closely about zero.

The seasonal pattern of RO was calculated by WBM (Plate II-5). A striking feature of the maps is the relative constancy of RO for major portions of the continent over the year. These areas are dry and include Eastern Brazil, the Gran Chaco, the central Andes, Pampas and Patagonia. Another area of relative stability is the wet Patagonian Andes which shows only slight seasonality, being driest in the early part of the year and wettest in July due to low PET demands associated with the southern hemisphere winter. Seasonal RO dynamics are most complex in the equatorial

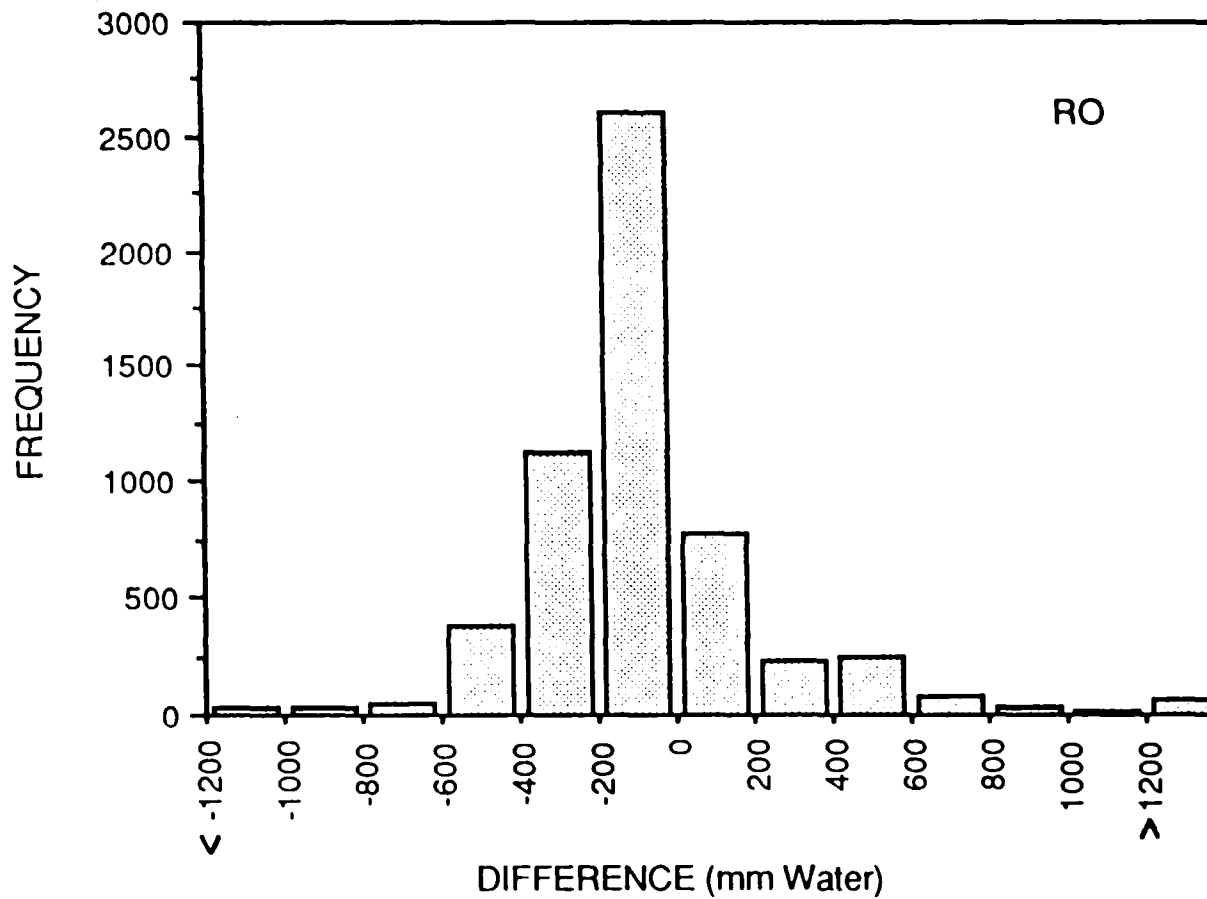


Fig. II-12. Correspondence between runoff estimates made by the water balance model and Korzoun et al. [1977]. Each difference value (millimeters per year) is computed as WBM value minus Korzoun et al. value.

zone, from about 10°N to 20°S. Only in the northernmost Llanos region does RO appear relatively constant.

Water Balance Model: Amazon/Tocantins Drainage Basin

The dominant runoff-producing region is the Amazon/Tocantins drainage system. The combined basin had a mean annual RO of 1.01 m, with 1.08 m in the Amazon basin, and 0.56 m in the Tocantins. The value of 1.01 m/yr compares favorably with other hydrologic studies as reported by Salati [1985]. Runoff values for the entire basin, based on a variety of methods, fall within the range of 0.7 to 1.25 m/yr. WBM-generated runoff, expressed as an annual mean for the combined basin, corresponds to a net discharge to the ocean of 224,000 m<sup>3</sup>/s. The Amazon itself contributes 207,000 m<sup>3</sup>/s and the Tocantins 17,000 m<sup>3</sup>/s.

Precipitation entering the Amazon/Tocantins region delivers 2.26 m of water on an annual basis. Predicted ET accounts for 1.24 m. Fifty-five percent of the precipitation delivered to the simulated Amazon/Tocantins Basin thus emerges as ET and 45% as RO. These percentages are nearly identical for the basins considered separately. WBM predictions agree with other regional analyses. For example, Salati [1985] cites a series of estimates showing ET/RO ratios from roughly 50/50 to 70/30. Salati's basinwide estimate is 54/46, nearly identical to that found in this study.

The temporal pattern of RO reflects a shifting mosaic of source areas that is important in defining the pattern of fluvial transport. Throughout much of the region, the early part of the year shows significant RO ( $> 50$  mm/month). January and April are the wettest months and a decided movement northward in runoff-producing regions is apparent. By July, the runoff-generating zone moves northward and only the most northern areas of the basin contribute any significant RO. By October, the majority of the basin is relatively dry and fails to generate significant runoff. Only the far western area is active. These patterns agree well with observed patterns of monthly RO given elsewhere [Korzoun et. al., 1977; UNESCO, 1969, 1971, 1974, 1979, 1985]. The WBM determinations also correlate well with the climatology of the region [Salati, 1985; Salati and Marques, 1984].

#### Water Transport Model: Amazon/Tocantins River

The WTM computed discharge hydrographs for each of the 2251 grid cells of the Amazon/Tocantins river system. Results are summarized in this section using site-specific data. I first compare model performance to a set of observed hydrographs, go on to discuss the seasonality of discharge in major tributaries and the mainstem, and finally perform a sensitivity analysis to explore the nature of computed channel flow and the importance of floodplain inundation.

Comparison to Observed Hydrographs. Because there are few reliable discharge estimates for the Amazon/Tocantins River system it is difficult to assess fully the accuracy of the WTM. Model results were compared initially to ten discharge hydrographs compiled from UNESCO [1969, 1971, 1974, 1979, 1985] using the parameterization described earlier. Four of the sites were located in the Andes where sharp climatic gradients and complex drainage patterns restricted the effectiveness of the transport model. Two of the Andean sites were associated with rivers that drained catchments much smaller than the size of a single  $0.5^\circ$  grid cell. The transport model thus performed poorly in these areas (average unweighted  $d = 0.57$ ; equation (11)). In contrast, the remaining six sites represent larger basins with more clearly defined routing and, generally, longer periods of record. These showed improved model performance ( $d = 0.76$ ).

On a mean annual basis, calculated discharges for the Obidos, Araguaia, Porto Nacional, Itupiranga, Xingu and Madeira sites were, respectively, within 1, 3, 6, 18, 28 and 33% of the corresponding observed discharges (Figure II-13). Predictions for the timing of subannual discharge corresponded well with observation for all sites. However, slight disparities in this timing and in the overall magnitude of discharge, can result in relatively large errors in absolute terms. The above sites, respectively,

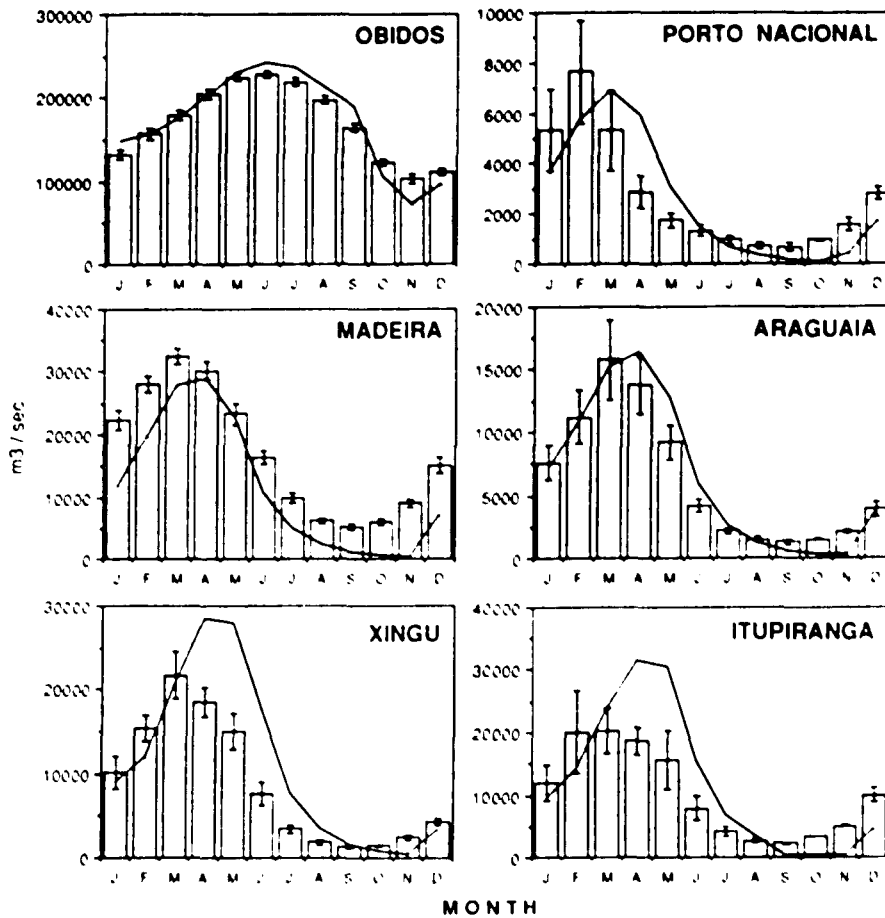


Fig. II-13. Modeled and observed discharge hydrographs for selected sites in the Amazon and Tocantins River system. Model predictions (lines) represent the best aggregate fit of the fluvial transfer and flooding coefficients. Observed data (bars) are from UNESCO [1969, 1971, 1974, 1979, 1985] for the following periods of record: Obidos (1969, 1971-1978), Madeira (1968-1979), Xingu (1977-1979), Porto Nacional (1976-1979), Araguaia (1976-1979), Itupiranga (1976-1979). The first three sites are in the Amazon Basin; the latter three are in the Tocantins.

showed mean average error (MAE) values of 13550, 1120, 1110, 5370, 4040 and 5620 m<sup>3</sup>/s. Mean average error is defined as:

$$MAE = N^{-1} \sum_{i=1}^n | P_i - O_i | \quad (12)$$

where N is the number of observations, P<sub>i</sub> is model prediction for month i, O<sub>i</sub> is corresponding observed discharge Willmott [1982]. For all sites, there is a tendency for the WTM to underestimate during periods of low flow, an effect linked in part to the WBM protocol restricting storm flow during the dry season. The quality of simulated discharges made for the period of higher flow is more variable.

Overall, the Obidos site performs best, with both the timing and magnitude of flow closely following the observed hydrograph. The hydrograph generated for the Araguaia site also matches observation, although a slight lag in peak flow is apparent. The timing of calculated flows at the Madeira site corresponds well to observation although the overall magnitude of the modeled discharge is low. The shape of WTM hydrographs for the remaining sites -- Xingu, Itupiranga and Porto Nacional -- are less precise, but considering the short period of record [1976-1979], comparisons may be misleading. The largest disparity between WTM and observed discharges is associated with peak flow. For Porto Nacional, this merely represents a timing issue. In the

case of Xingu and Itupiranga, the disparity also reflects overestimates in calculated annual discharge.

Such "errors" can be corrected by judicious choice of parameters in the water balance model, the transport model or both. Lacking a comprehensive basin-wide data base, no recalibration was attempted. Further, the modeling analysis is based on long-term climatic conditions with natural vegetation; observed hydrographs may be influenced by ongoing changes in land use [Gentry and Lopez-Parodi, 1980]. The results presented therefore represent the inherent resolution of our coupled WBM/WTM algorithm and limitations in the associated data sets. Nonetheless, WBM/WTM provides an excellent prediction of observed monthly discharges at major sampling stations in the Amazon/Tocantins River system. (For the six hydrographs I found a highly significant relationship, with slope  $\approx 1$ , between observed and calculated monthly discharge:  $\text{calc (m}^3/\text{s)} = 1.045 \text{ obs} + 1519.8$  ( $r^2 = 0.99$  ;  $n = 72$  ;  $p \ll 0.001$ ).)

Qualitative comparisons were made using normalized hydrographs and corresponding observations found in the work by Korzoun et. al. [1977] (Figure II-14). There was considerable difficulty in determining the specific location of the observed time series, and there was no information on the period of record nor on the magnitude of flow. As best I could determine, the sites are associated with relatively small catchments with 30 to 600  $\text{m}^3/\text{s}$  mean annual flow.



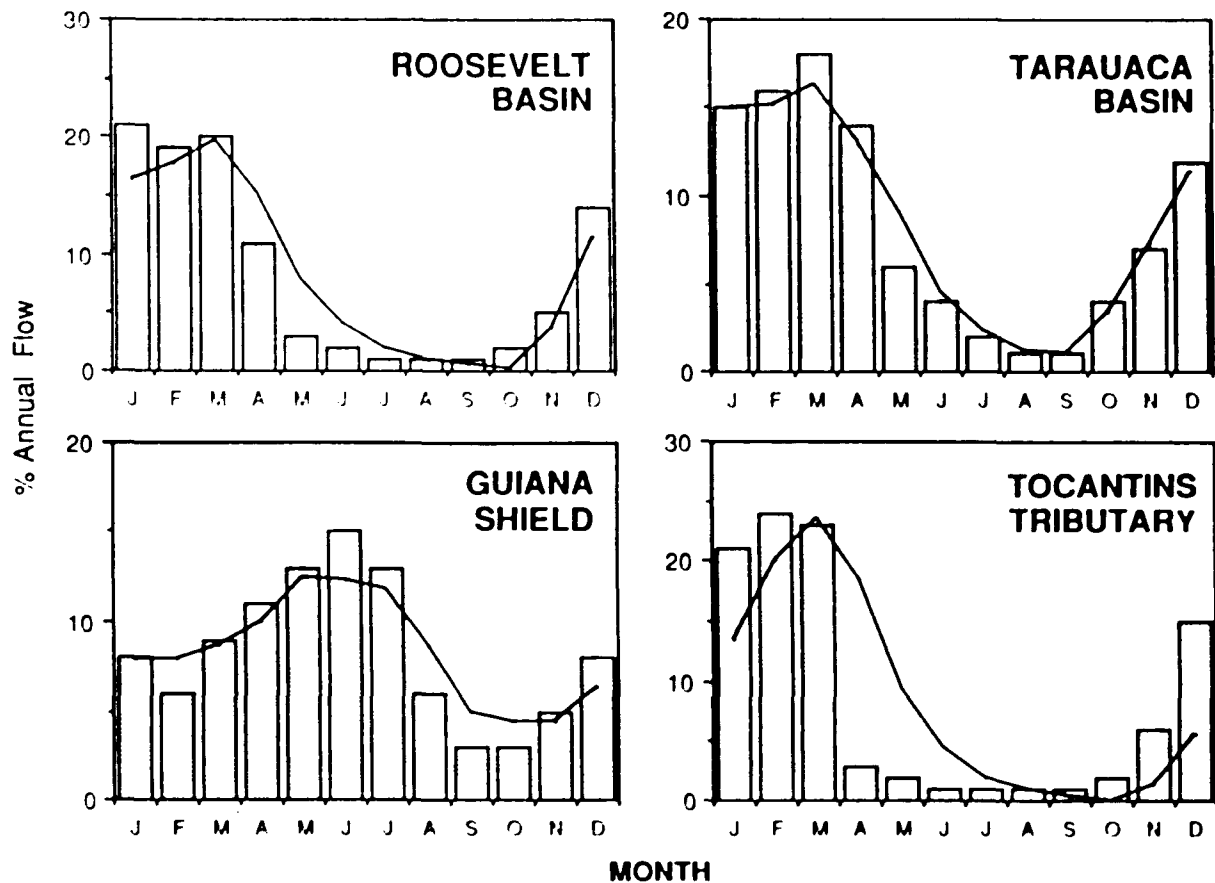


Fig. II-14. Normalized discharge hydrographs comparing WTM calculations (lines) to observations (bars) at selected sites within the Amazon and Tocantins drainage basin. Model estimates represent the best aggregate fit of the fluvial transfer and flooding coefficients. Observed data are from Korzoun et al. [1977]. Except for the Tocantins tributary, all hydrographs are in the Amazon Basin proper.

Despite these limitations on the comparison, there is good agreement between model results and observed patterns of discharge.

Model-generated discharge hydrographs at eleven mainstem Amazon and two Tocantins locations are presented, along with estimated discharges for the mouth of each system (Table II-3). Upriver sites represent the locations of major confluences and include flows derived from the named tributaries. When corrected for tributary effects, the calculated mainstem hydrographs for Ica, Negro, and Obidos correspond closely to hydrographs presented by Richey et. al. [1986] for 1982-1984.

Model estimates for monthly and mean annual flow on thirteen major tributaries of the Amazon River are summarized in Table II-4. For each tributary strong seasonal patterns are apparent, related to both the mosaic of WBM-generated RO and transport of this RO within the river network. For both northern and southern tributaries there is a west to east movement in the timing of peak and low flows which correspond to inputs from WBM. The northern tributaries show this effect most clearly with a 2-3 month lag from western to eastern sites. The southern tributaries act more in unison, with peak and low flows displaced by only 1-2 months.

The tributary dynamics suggest that a flood wave will appear in the western portion of the mainstem and progress

TABLE II-3. Model-Generated Discharges for the Mainstem Amazon and Tocantins

		Flow Rate, ( $10^3 \text{ m}^3/\text{sec}$ )												
Confluence Site Name	Grid Cell <sup>a</sup> (Latitude/Longitude)	Jan.	Feb.	March	April	May	June	July	Aug.	Sept.	Oct.	Nov.	Dec.	Annual Mean
<u>Amazon River</u>														
Napo	3.5°S/73.0°W	40.3	46.8	57.4	67.5	69.1	48.3	26.7	13.5	10.5	17.1	31.1	36.4	38.7
Javari	4.5°S/70.0°W	46.1	49.8	57.6	68.2	76.7	73.8	46.0	23.9	16.0	18.0	32.5	42.3	45.9
Ica	3.5°S/68.0°W	57.7	62.2	66.8	76.0	86.6	90.9	77.3	41.6	24.8	23.4	38.4	52.3	58.2
Japura	3.5°S/65.0°W	85.0	95.8	104.7	111.0	120.1	127.4	122.3	88.6	47.0	35.5	53.3	78.3	89.1
Purus	4.0°S/61.5°W	101.0	112.3	128.4	141.5	145.7	143.6	137.3	127.7	72.9	44.1	49.4	87.5	107.6
Negro	3.5°S/60.0°W	123.1	133.4	149.7	166.7	175.1	178.5	175.8	172.5	123.9	74.0	66.4	103.7	136.9
Madeira	3.5°S/59.0°W	150.9	167.5	193.0	220.4	234.4	230.6	208.7	187.9	142.2	80.3	68.5	116.4	166.7
Trombetas (Obidos)	2.0°S/56.0°W	148.2	155.9	174.9	203.1	230.0	241.2	235.7	213.0	189.6	105.0	71.7	96.4	172.1
Tapajos	2.5°S/55.0°W	159.4	173.0	195.3	230.5	261.0	271.1	253.3	227.5	199.2	116.6	76.5	99.6	188.6
Xingu	2.0°S/52.5°W	154.7	180.5	198.4	237.8	278.7	298.6	283.9	255.9	224.0	151.1	86.5	87.0	203.1
Mouth	0.5°N/50.0°W	126.1	177.1	186.3	201.3	236.6	275.6	296.9	288.5	262.5	227.0	118.8	82.4	206.6
<u>Tocantins River</u>														
Araguaia/ Itacaiuna	5.5°S/49.5°W	9.3	14.2	23.9	31.4	30.4	15.4	6.8	3.4	0.4	0.3	0.3	4.4	11.7
Mouth	0.5°S/48.5°W	7.3	14.2	18.2	28.7	38.7	40.5	32.6	14.5	6.1	2.5	1.0	1.0	17.1

Discharges are calculated below the confluence of the named tributary.

<sup>a</sup>Latitude/longitude values refer to southwest corner of grid cell.

TABLE 11-4. Model-Generated Discharges for Major Amazon River Tributaries

Name	Grid Cell <sup>a</sup> (Latitude, <sup>o</sup> S/ Longitude, <sup>o</sup> W)	Flow Rate, 10 <sup>3</sup> m <sup>3</sup> /s												Annual Mean
		Jan.	Feb.	March	April	May	June	July	Aug.	Sept.	Oct.	Nov.	Dec.	
<u>Northern Tributaries</u>														
Napo	3.5/73.5	8.1	7.7	9.1	10.2	10.8	10.2	7.7	4.3	3.2	4.0	7.1	7.9	7.5
Ica	3.0/68.5	10.2	10.4	10.0	10.3	11.0	11.1	10.5	7.4	4.9	5.1	7.7	8.6	8.9
Japura	2.0/66.5	16.8	17.8	16.7	16.8	19.0	20.4	17.3	11.2	7.3	9.1	12.5	13.9	15.0
Negro	3.0/61.0	23.8	26.0	27.9	28.9	29.9	32.8	36.5	39.5	28.2	24.2	20.4	22.2	28.4
Trombetas	1.5/56.5	0.1	0.0	0.1	1.2	2.6	3.2	3.5	2.6	1.3	0.6	0.3	0.1	1.3
<u>Southern Tributaries</u>														
Marañon	5.0/74.5	18.8	23.1	28.5	32.3	28.9	16.4	8.8	4.4	3.9	7.2	12.6	15.6	16.7
Ucayali	5.5/74.5	15.2	19.1	23.6	25.4	21.1	9.8	4.5	2.1	2.3	5.2	10.8	12.6	12.6
Javari	4.5/71.0	5.1	4.8	5.5	5.5	4.7	2.5	1.6	1.2	1.8	2.5	3.7	4.7	3.6
Jurua	3.0/66.0	11.2	14.2	17.2	18.7	18.3	12.8	5.8	2.7	1.6	2.8	6.6	9.3	10.1
Purus	4.5/62.0	15.9	20.6	25.9	29.3	27.5	18.4	8.1	3.6	1.6	0.8	3.5	12.7	14.0
Madeira	4.0/59.5	26.7	35.2	44.7	54.2	56.6	47.4	24.4	10.5	4.5	1.9	3.3	16.2	27.1
Tapajós	3.0/55.5	14.6	19.9	27.6	34.9	36.0	28.3	12.3	5.4	2.4	1.3	2.3	9.7	16.2
Xingu	2.5/52.5	8.4	11.1	18.6	28.4	31.6	24.1	10.6	4.6	2.0	0.9	0.5	2.6	12.0

Discharges are calculated at the mouth of each tributary and prior to entering the mainstream.

<sup>a</sup>Latitude/longitude values refer to southwest corner of grid cell.

eastward over the year. The model simulates this effect (Table II-3) and shows that there is a distinct lag between peak flows as the flood wave travels eastward from May (Napo, Javari) to July (Mouth). Low flows originate in September in the west, and the basin mouth shows minimum discharge in December.

Mainstem/Tributary Interactions. I explored in more detail the impact of modeled tributary inputs on the behavior of the mainstem Amazon, and estimated the degree to which the main river can buffer tributary inputs. Table II-5 shows a longitudinal profile of discharge variability at a series of mainstem sites and contrasts this with influent variability. The months of maximum flow and the proportion of mainstem flow attributed to each tributary are also shown.

There is a general tendency for the Amazon River to decrease its subannual variability (measured by  $V^m$ ) from the westernmost site to the Madeira confluence, where there is a sharp reversal in the dampening trend. The tributaries show no clear longitudinal pattern of variability over the same region. In all but one case, the mainstem has greater variability than its tributaries, from both the north and south. Downstream of the Madeira to its mouth, the Amazon maintains a consistent degree of seasonal oscillation and there is no apparent additional dampening of the flood wave.

TABLE II-5. Influence of Tributary Inputs on the Behavior of the Mainstem Amazon River.

Site Name <sup>a</sup>	$V^M$	$V^T$	Flow Proportion <sup>b</sup> , %
Napo	1.51 (May) <sup>c</sup>	1.01 (May)	19
Javari	1.32 (May)	1.19 (April)	8
Ica	1.16 (June)	0.70 (June)	15
Japura	1.03 (June)	0.87 (June)	17
Purus	0.94 (May)	2.04 (April)	13
Negro	0.82 (June)	0.67 (Aug.)	21
Madeira	1.00 (May)	2.01 (May)	16
Trombetas (Obidos)	0.98 (June)	2.69 (July)	1
Tapajos	1.03 (June)	2.14 (May)	9
Xingu	1.04 (June)	2.59 (May)	6
Mouth	1.04 (July)	----	---

$V^M$  is the variation in mainstem discharge over the year ( $V^M = (Q_{max} - Q_{min})/Q$ ) at each site.  $V^T$  is same as  $V^M$  but for tributary.

<sup>a</sup>Refers to confluence site on mainstem for  $V^M$ ; to mouth of tributary for  $V^T$ .

<sup>b</sup>Calculated as  $Q_{trib}/Q_{main}$ , where mainstem flow includes  $Q_{trib}$ .

<sup>c</sup>Month of peak discharge.

However, the mainstem is consistently less variable than its tributaries and dampens well the input signals.

Calculated tributary inputs are important in determining the timing of the peak flows on the mainstem Amazon. From the Napo to Japura sites there is an orderly progression downstream of the peak flood wave in May and June and the timing coincides with that of tributary inputs which are sizable fractions of the overall mainstem flow. From the Purus to Madeira sites, flood wave timing is more variable and is shifted either forward or backward in time depending on the behavior of the tributary inputs. For example, at the Purus site the mainstem peaks in May, one month earlier than at the adjacent upriver site, in apparent response to an early peak in tributary discharge during April. Downriver of the Madeira, tributary inputs are relatively small and the mainstem flood wave propagates independently. The time of highest discharge shifts forward from May to July in the mainstem reach from the Madeira to the mouth.

The mainstem Amazon is therefore most influenced by the behavior of its tributaries in the western portion of the basin. The tributaries control the timing of the mainstem flood wave and the mainstem does not appear to dampen its tributary signals in its upstream reaches. In contrast, the river downstream of the Madeira confluence is stable,

dampens variability in its tributary inflows and is unaffected by the timing of these inputs.

Sensitivity to Transfer and Flooding Parameters. I examined the sensitivity of the fluvial model to variations in the linear transfer coefficient (K) and the parameters defining floodplain inundation ( $c_f, r_f$ ) given in equation (7). The analysis sought to identify reasonable rates of water turnover and the importance of wetland flooding in the Amazon River system.

For experiments involving the transfer coefficient I examined the resulting flow at Obidos when K was varied from 12.5 to 75 ( $\text{month}^{-1}$ ), with  $c_f$  set to 1.0 and  $r_f$  to 0.75 (Figure II-15). The effect of the transfer coefficient is to regulate both the timing and amplitude of the discharge wave. Starting with K at 75 there is a significant overestimate of high flow, an early maximum in April and a minimum in September. With decreasing K values (from 37.5 to 25) the peak diminishes and is offset forward in time. Low flows are preserved but occur later in the year. For K = 12.5, the shape of the hydrograph is clearly inappropriate. A range of  $12.5 < K < 75$  appears to offer reasonable results and is in agreement with the theoretical range developed earlier.

Experiments testing the importance of wetland flooding are also shown in Figure II-15. The first scenarios involve  $c_f$ , which initiates floodplain inundation. The graph shows



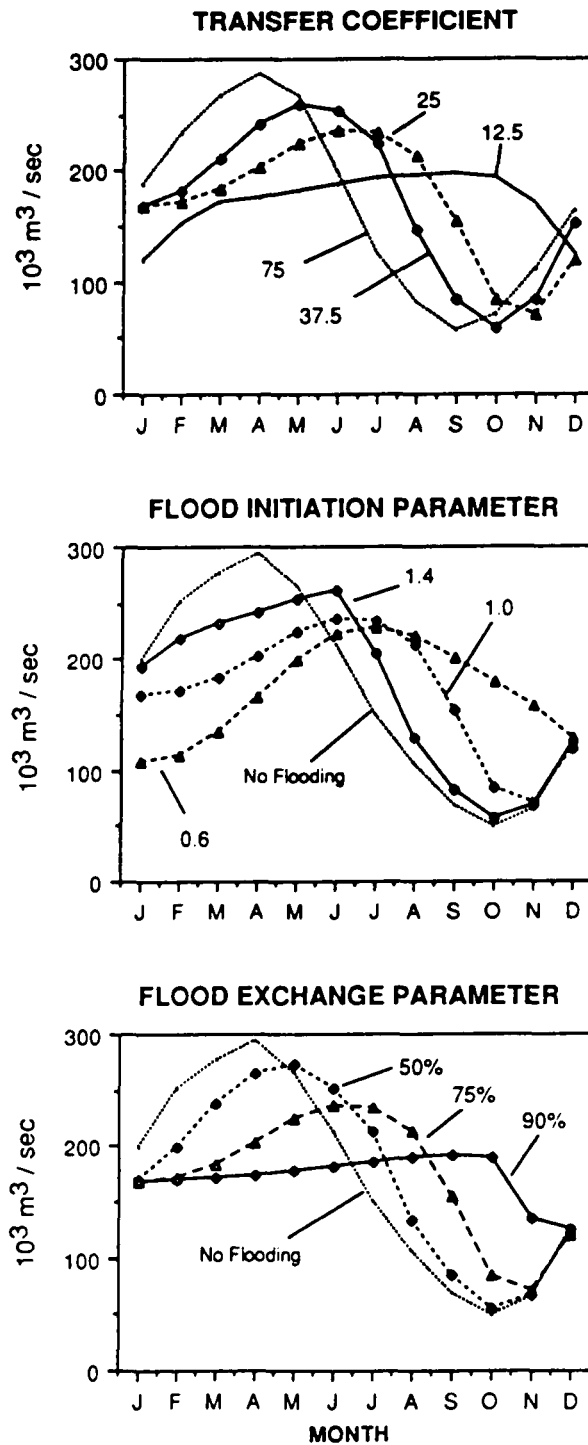


Fig. II-15. Model results showing the effect of variation in the fluvial transfer coefficient ( $K$ ), the flood initiation ( $c_f$ ), and the flooding exchange parameter ( $r_f$ ) on the discharge hydrograph at Obidos.

the effect of limiting the flood cycle. The case of no flooding gives a smooth, nearly sinusoidal curve with a range from 50,000 to 300,000 m<sup>3</sup>/s. By selectively varying the proportion of mean annual flow at which flooding can occur, the hydrograph can be dampened and altered in its timing. A minimum amount of flooding occurs with  $C_f = 1.4$ . Nonetheless, peak discharge is both delayed and decreased in magnitude. Lowering the flooding criterion to 1.0 and 0.6 achieves the same effect on peak flows but also enhances and delays low flows. A similar effect is shown for experiments involving the flooding exchange parameter,  $r_f$ . Increasing the proportion of volume change attributable to floodplain inundation dampens and shifts the hydrograph forward in time. Clearly, the model Amazon River is highly sensitive to the effects of floodplain storage. It is a critical component of the river's hydrology.

It has been estimated that there are approximately 100,000 km<sup>2</sup> of Amazonian floodplains [Goulding, 1985], up to 100 km wide [Rzóska, 1978]. On average these are inundated for 6 months each year although a range of 2 to 10 months has been reported depending on topography and river level fluctuations [Melack and Lesack, 1988; Goulding, 1985; Herrera, 1985; Pires and Prance, 1985; Adis, 1984; Junk and Howard-Williams, 1984]. WTM determined a 6- to 7-month floodplain inundation over the central Amazon. Considering the impact of flood exchanges on the discharge of channel

water and the fact that floodplain inundation is likely to regulate unique and intense metabolic activity [Richey, 1983; Elder, 1985; Fisher, 1986; Melack and Lesack, 1986; Harriss et. al., 1988], a realistic treatment of this effect in regional biogeochemical studies, especially in the context of ongoing land use conversion, is critical.

#### Future Research Needs

Despite their simplicity, the WBM and WTM together can characterize water dynamics over large areas of landscape with high spatial and temporal resolution. Although these results are encouraging, there are numerous opportunities to refine and expand the current effort. For instance, the water balance component would clearly benefit from a more refined treatment of storm flow runoff and water ponding in soils. The transport model could be refined to include more sophisticated flow dynamics and a more realistic assignment of flow and flood parameters over space. The combined WBM/WTM simulation now operates at dynamic steady state and requires reformulation to consider transient phenomena. The impact of important episodic events (for example, the El Niño/Southern Oscillation) on the terrestrial water balance and ecosystem dynamics could then be more effectively evaluated. A real-time model also might more readily be checked against data sets collected for specific times and at finer temporal scales. The major limitation in

developing such a model is the lack of input data of sufficient quality, scope and spatial resolution.

The WBM/WTM is a relatively simple computational device that can be used to study the impact of land use and climate change on surface hydrology and, in turn, terrestrial nutrient cycling and trace gas exchange. It is easy to envision an initial series of tests in which one can apply independently-derived climate and land cover fields available from maps, digital data sets and/or General Circulation Model (GCM) studies to explore resultant model behaviors. Since the WBM/WTM is gridded and organized into modules, with suitable refinement it could eventually be incorporated into a GCM context to simulate atmosphere/landscape coupling and quantify more directly the impact of climatic feedbacks on landscape hydrology and nutrient biogeochemistry.

The use of parameters derived from remote sensing in conjunction with models such as WBM/WTM has the potential to provide a comprehensive view of the Earth's hydrology [Johnson, 1986; Goodison, 1985]. For example, use of satellite-borne passive microwave in conjunction with visible and infrared sensors like the Advanced Very High Resolution Radiometer (AVHRR) can give an index of vegetation state, soil moisture and water cycling potentials at spatial scales comparable to that used in this study [Tucker et. al., 1986; Choudhury, 1988; Choudhury and Golus,

1988]. Active microwave imagery has been used recently to determine the duration and extent of wetland inundation [Imhoff et. al., 1987; Hoffer et. al., 1986]. High-resolution global data sets for digital topography and channel routing are also feasible using radar altimetry [NASA/Topographic Science Working Group, 1988] and would augment existing global data sets with coarse vertical resolution [NCAR/NAVY, 1984]. The unique and complementary suite of sensors proposed as part of NASA's Earth Observing System (EOS) will provide an unprecedented opportunity to study surface hydrology at the continental scale. Models of continental-scale water balance and transport will be an integral part of this initiative [NASA/EOS, 1984 and supplements].

The hydrologic model reported here will be expanded to include the dynamics of carbon, major nutrients and sediments. It will serve as a semimechanistic tool by which to study the transport of materials from the continents to the world's oceans and help refine current estimates of riverine flux. The model will provide much needed insight into the linkages between climate and fluvial dynamics in large river systems. The enhanced model will provide a mechanism to quantify the impact of climate or land use change on water and material flux in major river systems of the globe.

### Summary and Conclusions

Water is one of the dominant factors regulating the biogeochemistry of the planet. Gaining an understanding of the linkages between the global hydrologic cycle and the global cycles of carbon, nitrogen and other life-supporting elements is a prerequisite to quantifying the impact of climate and land use change on the Earth's biota. A continental-scale hydrologic model was constructed and applied to South America with emphasis on the Amazonian region. The hydrologic model consists of two components: a Water Balance Model and a Water Transport Model (WBM/WTM). The combined model creates a set of high-resolution data sets for soil moisture, evapotranspiration, runoff, river discharge and floodplain inundation. The work described in this chapter is a first step toward eventual global coverage.

The WBM predicts monthly and annual soil moisture, evapotranspiration and runoff for more than 5700 grid cells ( $0.5^\circ$  by  $0.5^\circ$ , latitude by longitude) which constitute South America. A set of global data bases covering precipitation, potential ET, temperature, soil texture, vegetation and topography is used in conjunction with the model to characterize the surface hydrology of diverse landscapes and climate. The data define conditions of long-term, average climate. The WBM calculates the most spatially-resolved estimates of terrestrial water cycle components currently

available for South America. The distribution and timing of WBM-calculated soil moisture, evapotranspiration and runoff were found to be highly dependent on precipitation. The patterns predicted by the model for the continent compare well with existing data sets, although absolute magnitudes differ, at times substantially [cf. Korzoun et. al., 1977; Willmott and Rowe, 1986].

The WTM was applied to the Amazon/Tocantins River system. The model relies on runoff from single grid cells calculated by WBM, river network topology and simultaneous solution of flow and mass balance equations. There are linear transfers of discharge between grid cells and a simple representation of wetland flooding. Scenario experiments using WTM showed that the linear transfer coefficients producing the most reasonable discharge hydrographs were well within the range predicted from geomorphologic principles (average cell turnover of  $\approx 1.5$  days). Parameters defining floodplain exchanges which gave the best results also were supported by accounts given in the literature (6-7 months of flooding in the mainstem Amazon). In the model, channel turnover and floodplain inundation combine to produce a pattern in which the upper reaches of the mainstem Amazon are greatly influenced by tributary inputs. In contrast, the lower mainstem river shows propagation of a distinct flood wave and demonstrates a significant capacity to dampen influent signals.

The fluvial discharge and routing components successfully determined the timing and magnitude of discharge for a set of observed hydrographs in the selected basin. Flow at a major downstream site on the Amazon (Obidos) followed the observed interannual pattern, and the calculated annual mean flow was within 1% of observation. Other sites showed disparities from 3 to 33%, with higher values indicating an ill-defined water balance. The record of observed discharge provides an important check against model performance for both fluvial transport and water balance. Unfortunately, the observational data set for the Amazon/Tocantins is sparse. Without a global network of well-instrumented rivers, an accurate geography of the terrestrial water cycle will be difficult to establish.

While the long-term objectives of this research extend beyond the water cycle, hydrologic information is essential for modeling continental and global-scale distributions of primary production, decomposition, trace gas exchange with the atmosphere and nutrient export to coastal ecosystems. Ultimately, these models will allow the scientific community to explore the issue of global change, in terms of both climate and land use. For example, they can be used to address questions such as, "What will be the impact of an average 3°C warming on evapotranspiration, river discharge, primary production and trace gas exchanges for the global



land mass?" These questions assume growing urgency as sustained increases in atmospheric CO<sub>2</sub>, methane and other trace gases foreshadow a global climate well outside the bounds of recent geologic history.

## CHAPTER III

### MODELING BASIN-SCALE HYDROLOGY IN SUPPORT OF PHYSICAL CLIMATE AND GLOBAL BIOGEOCHEMICAL STUDIES: AN EXAMPLE USING THE ZAMBEZI RIVER

#### Introduction

The rationale for developing regional-scale models of terrestrial hydrology has been elucidated many times [e.g. Moore et. al., 1989; Committee on Global Change, 1988; Becker & Nemec, 1987; Eagleson, 1986; Dooge, 1986]. The motivations include defining the geographic distribution of land-atmosphere moisture exchange, fostering the effective management of water resources, and quantifying the impact of land use and global climate change on the water cycle.

Water also plays a pivotal role in the biogeochemistry of the terrestrial biosphere. Water in the rooting zone is of obvious importance to primary production and, hence, CO<sub>2</sub> gas exchange and nutrient uptake by plants. It also controls the activity of decomposing organisms that turn over carbon and nutrients. Water availability and its timing influence the river, wetland and coastal ecosystems into which runoff must pass. Fluvial networks transport from the landscape the products of erosion, chemical weathering and biotic nutrient cycling and may thereby regulate the long-term productivity of the world's oceans. Furthermore, soil water is likely to be the single most

important control on the production of trace gases such as nitrous oxide and methane.

The drainage basin is a useful organizing concept with which to view the coupling of the Earth's water and chemical cycles. Numerous watershed studies have added significantly to our understanding of how landscapes process and transport constituents, and how terrestrial ecosystems are affected by pollution (Swank and Crossley, 1988; Correll, 1986; Likens et. al., 1977). The inherent advantages of such studies should be realized as well at the global scale. Recent estimates of global riverine flux for various constituents (e.g. Milliman and Meade, 1983; Meybeck, 1982, 1976; van Bennekom and Salomons, 1981) are essentially compilations of existing basin-scale data sets. Although these studies represent impressive benchmarks, they are limited in their ability to predict future change. A suitably-scaled drainage basin model, linking terrestrial water balance and ecosystem nutrient cycling to fluvial transport and aquatic processing, would be a valuable scientific tool with which to address issues of global change.

A simple model for nitrogen transport in the Mississippi River drainage system was offered by Gildea et. al. (1986) and Vörösmarty et. al. (1986). Estimates of water and nutrient flux were organized at the level of the subregional drainage basin. Although the model was able to clearly show increases in nutrient flux due to human

activity, its rather coarse spatial scale and predetermined hydrology limited its predictive capability. Significant enhancements are possible using finer spatial scales and coupled atmosphere/land surface hydrology simulations. To this end, the recent proposal for tandem field, modeling and remote sensing experiments for the Mississippi River as part of the Global Energy and Water Cycle Experiment (GEWEX) -- a joint World Meteorological Organization and International Association of Hydrological Sciences initiative -- will provide critical water cycle parameters for regional biogeochemical studies (Chahine 1989).

Recent modeling experiments by Vörösmarty et. al. (1989) demonstrated the potential for employing grid-based hydrologic simulations in the Amazon drainage basin. These models were developed as part of a larger research effort to study continental-scale biogeochemistry, including terrestrial nutrient cycling, CO<sub>2</sub> and trace gas exchange, and transport of constituents through river networks. The hydrologic research sets a framework in which to couple physical climate models to the global biogeochemical subsystem. A key facet of the overall study is to quantify the impact of humans by contrasting pre-disturbance and contemporary conditions. In anticipation of eventual global coverage, which necessarily must consider data-poor regions, the water and nutrient cycling models are simple in structure and modest in their input requirements.

Much of the globe's hydrology is now modified, and a pressing challenge is to develop a quantitative understanding of how humans have disturbed the water cycle. In particular, the consideration of engineering works, shifting landscape patterns and climate change represents a significant step forward. A key research question surrounds the transportability of regional-scale hydrologic models like those developed for the relatively undisturbed Amazon.

This paper examines the feasibility of applying a linked water balance and fluvial transport model, developed initially for the Amazon/Tocantins, to another large tropical river, the Zambezi in southern Africa. The Zambezi River has numerous attributes which distinguish it from the Amazon and thereby make it an attractive choice for model testing. In contrast to Amazonia, the Zambezi basin is much drier, with a mean runoff of  $0.08\text{m yr}^{-1}$  (UNEP, 1986; Borchert and Kempe, 1985; Balon and Coche, 1974), compared to  $1.01\text{ m/yr}^{-1}$  (Vörösmarty et. al., 1989). Throughout much of its length, the Zambezi is also regulated by impoundment. In addition, anthropogenic disturbance in the surrounding landscape is relatively widespread and has significantly defined the character of the region's biota and hydrology. Research on the Amazon River (Richey et. al., 1989; Vörösmarty et. al., 1989; Melack and Lesack, 1988) has demonstrated the importance of wetland/channel interactions in defining discharge and nutrient regimes. In contrast to

the Amazon River which has extensive, contiguous floodplains along much of its length, the Zambezi is punctuated by a series of distinct swamplands.

In this exploration, I set forth a modeling strategy to treat landscape/hydrology interactions for the full Zambezi catchment, describe key hydrological phenomena operating in the basin, and assemble a coherent data set in support of the proposed modeling effort. In addition to its scientific objectives, this chapter, hopefully, will complement other work dealing with the rational development of resources in the region. These include studies on energy resource optimization (Gandolfi and Salewicz, 1990; Gilbert Commonwealth International, 1987; Hosier, 1986; Bhagavan, 1985), irrigation (Kiele, 1982), fisheries (Bernacsek and Lopes, 1984; Kenmuir, 1982; Machena and Fair, 1986) and wildlife (Mwenya and Kaweche, 1982).

#### Site Description

The Zambezi is the fourth largest drainage basin in Africa and the largest with discharge to the Indian Ocean (Lewis and Berry, 1988). The basin can be considered to consist of three sections: the Upper Zambezi, from the headwaters to Livingstone near Victoria Falls; the Middle from Livingstone to Cahora Bassa Dam; and, the Lower, from Cahora Bassa to the river's mouth (Figure III-1). The Upper Basin drains a large area in the Central African Plateau and intercepts numerous swamps before making its descent toward

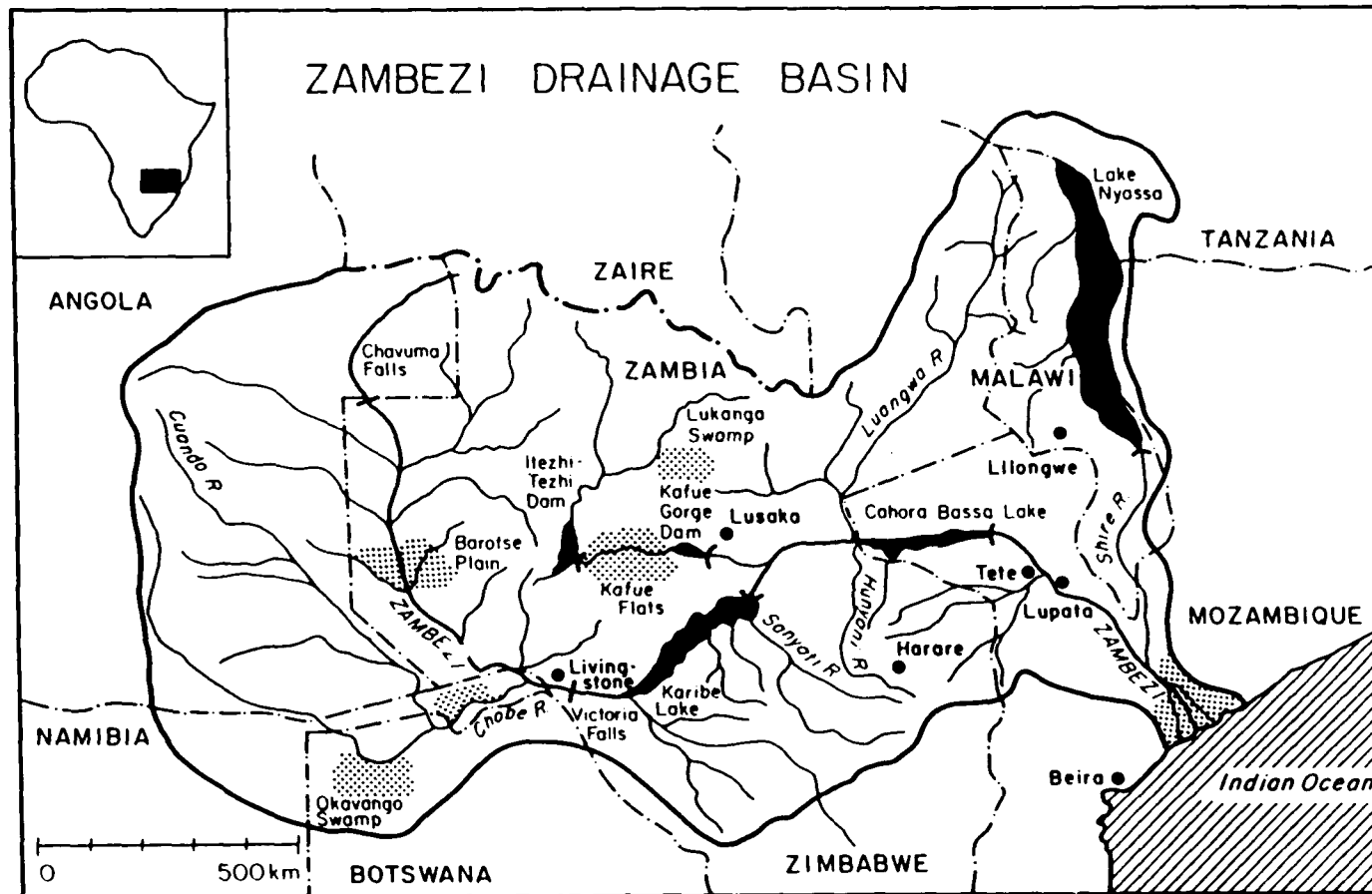


Fig. III-1. Map of the Zambezi River system.

the coast, through a series of mountain ranges. Its area has been estimated to range from 1.2 to 1.4 million km<sup>2</sup> (Table III-1), depending on whether certain arid drainage basins in the western part of the basin, with ephemeral discharge into the Zambezi proper, are included.

The basin lies fully within the Tropics between 10° and 20°S, encompassing humid, semi-arid and arid regions dominated by seasonal rainfall patterns associated with the Inter-tropical Convergence Zone (Korzoun et. al., 1977). The peak rainy season is during the southern hemisphere summer; the winter months are dry (Figure III-2). There is a gradual decrease in precipitation, from more than 1200 mm yr<sup>-1</sup> in the North to 600 mm yr<sup>-1</sup> in the South. The catchment's natural vegetation has alternatively been described as drought deciduous woodland (Matthews, 1983); as steppe, woodland and savanna (both moist and dry) (Balek, 1977); and, in the Upper Zambezi evergreen and semi-deciduous forests and woodlands, bushlands, scrubland and grassland (Sharma and Nyumbu, 1985).

The Zambezi is an important international river. It drains large portions of Zambia, Angola, Malawi, Mozambique and Zimbabwe, and less prominently, areas of Botswana, Namibia and Tanzania. Twenty million people inhabit the catchment (UNEP, 1986). The basin states are experiencing unprecedented rates of population growth with only marginal, or declining per capita agricultural production, rising



TABLE III-1. Drainage Areas Reported for the Zambezi River System

Location	Area(km <sup>2</sup> )	Reference
Chavuma Falls	75,967	Balek (1977)
Above Chobe River	360,505 <sup>a</sup>	Balek (1977)
Livingstone (Victoria Falls)	320,000	Pinay (1988)
	365,822 <sup>a</sup>	Balek (1977)
	480,000	Bolton (1984)
	501,760	Sharma and Nyumbu (1985)
	507,000	Santa Clara (1988), Reeve and Edmonds (1966)
Below Kafue River	684,058 <sup>a</sup>	Balek (1977)
Below Luangwa River	851,475 <sup>a</sup>	Balek (1977)
Upstream of Kariba	409,600	Pinay (1988)
	492,000 <sup>b</sup>	Reeve and Edmonds (1966)
	650,000	Bolton (1984)
	663,800	Santa Clara (1988), Reeve and Edmonds (1966)
	684,000	Begg (1973)
Cahora Bass Rapids	1,000,000	Bolton (1984)
	1,118,000	Santa Clara (1988), Pinay (1988)
	1,180,000	Pinay (1988)
Mouth	1,190,000	Balon and Coche (1974)
	1,220,000	This study
	1,300,000	Bolton (1983)
	1,400,000	Pinay (1988)
Kafue Mouth	155,000	Balek (1977), Obrdlik et al. (1989), Bolton (1983), Pinay (1988), Nepham and Nepham (1987)
Kafue (@ Itzhi-Tezhi)	106,200	Pinay (1988)
Sanyati Mouth	43,500	Pinay (1988)
Luangwa Mouth	142,000	Bolton (1983)
	148,000	Balek (1977), Pinay (1988)
Munyani Mouth	23,900	Pinay (1988)
Shire Mouth	115,000	Pinay (1988)

<sup>a</sup> Excludes Chobe subcatchment which = 871,000 km<sup>2</sup> with the W. Kalahari

<sup>b</sup> Explicitly stated that estimate excludes Kwando subcatchment which = 172,000 km<sup>2</sup>

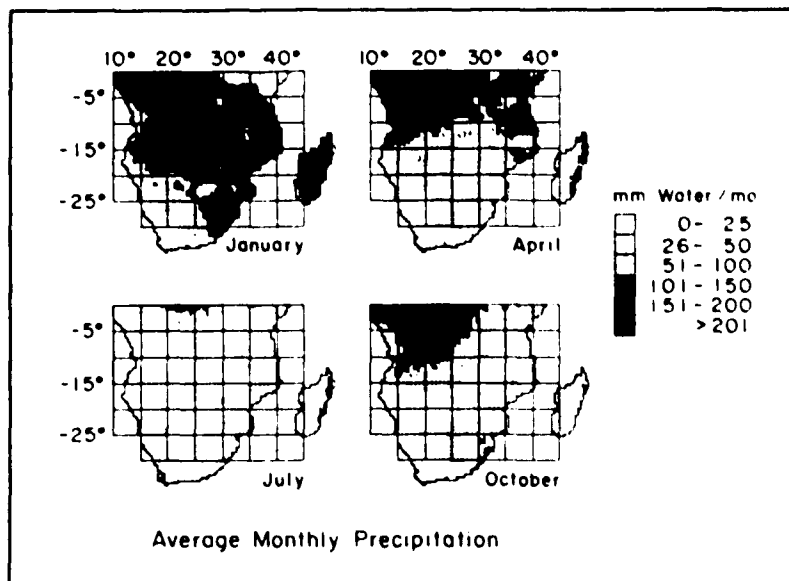
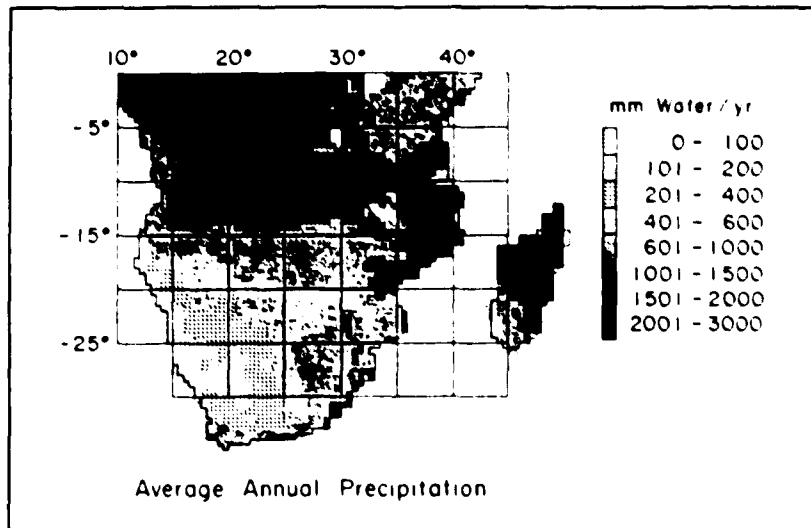


Fig. III-2. Precipitation patterns in the Zambezi basin. (Top) Annual; (Bottom) Selected months.

pressures on grazing land and deforestation from fuelwood collection (Lewis and Berry, 1988). For this reason, much of the present landscape is characterized by a mosaic of grazing, agricultural and natural lands. Although there has been no definitive appraisal of land cover for the basin as a whole, it appears that the most active land use is in the Middle and Lower Basins (Leenaers, 1989). Owing to its arid/semi-arid nature, there is a great deal of variability in precipitation and hence susceptibility to drought (Yair and Lavee, 1985; Lewis and Berry, 1988).

#### Catchment-scale Hydrologic Models

From the standpoint of developing a catchment hydrology model, the Zambezi River offers many challenges. An adequately-scaled model must first accommodate strong spatial gradients in climate, progressing from relatively wet conditions in the North to drier zones in the South. It must appropriately simulate the seasonality of natural river discharge which is strongly dependent on the march of the Inter-tropical Convergence Zone (ITCZ) across the basin. Land-based phenomena must also be addressed. These include the interception of discharge by swamps and other wetlands; the passage of river water through numerous high relief rapids; and the regulation of streamflow by impoundment. Finally, a desirable model should necessarily have the capacity to analyze altered land use and potential changes in regional climate.

### Brief Overview of Models

The proposed catchment-scale model is organized as a set of interacting algorithms and data planes (Figure III-3). These represent a distributed parameter scheme, operating at a gridded spatial scale of  $0.5^\circ \times 0.5^\circ$  (latitude x longitude) and a time step of one month. The drainage basin is represented by 409 single grid cells, forming a topological network shown in Figure III-4. Its simulated area is 1.22 million  $\text{km}^2$ . The algorithms for computing runoff and the horizontal transport of water are called the Water Balance (WBM) and Water Transport Models (WTM), respectively. Although important first steps, these models are admittedly coarse. There is substantial opportunity to refine the models using remotely-sensed global data sets, such as those envisioned to emerge in the 1990's from NASA's proposed Earth Observing System (NASA/EOS 1984 and supplements).

The WBM is a single-grid algorithm which transforms biogeophysical information into estimates of monthly soil moisture (mm), evapotranspiration ( $\text{mm month}^{-1}$ ) and runoff ( $\text{mm month}^{-1}$ ). The input data sets for climate include information on monthly precipitation ( $\text{mm month}^{-1}$ ), mean temperature ( $^\circ\text{C}$ ), cloud cover (% of daylight hours) and global irradiance ( $\text{cal cm}^{-2}\text{day}^{-1}$ ). From temperature, irradiance and/or cloud cover a monthly potential evapotranspiration (PET) can be calculated using one of a

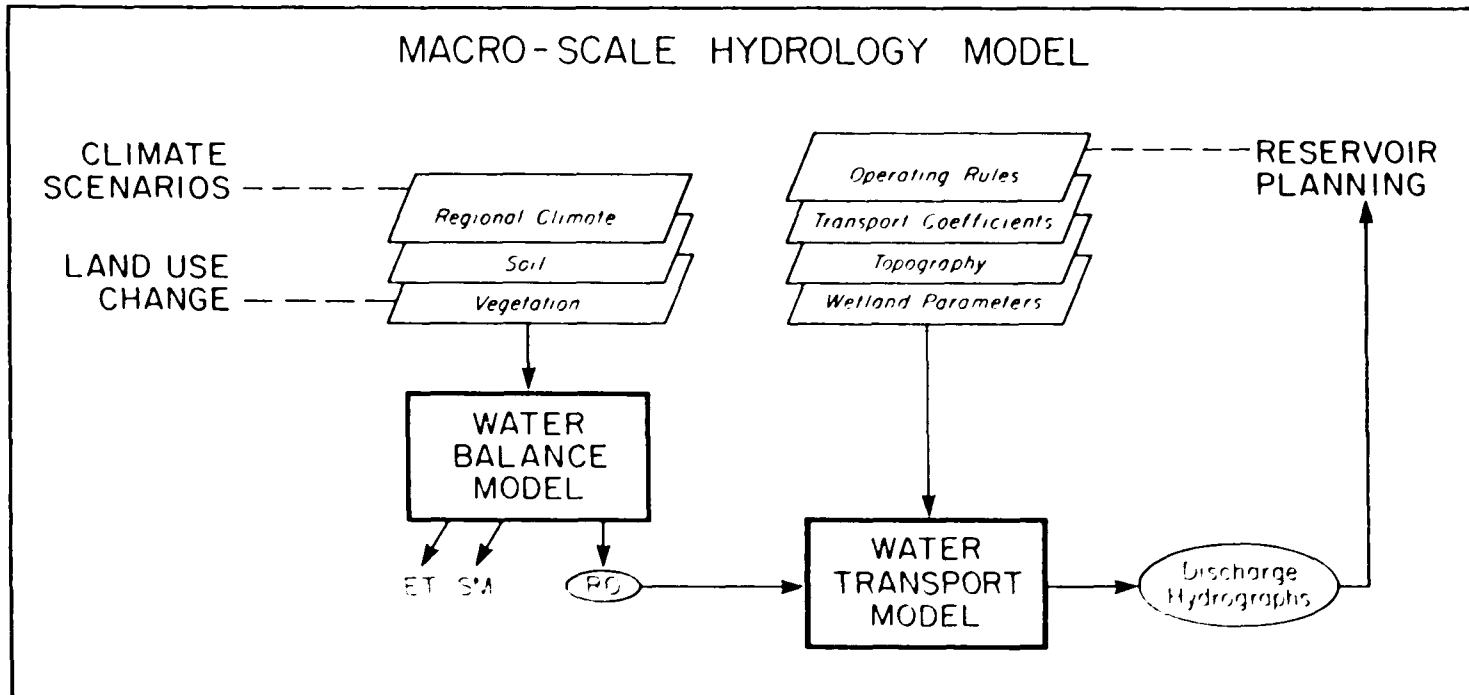


Fig. III-3. Overall organization of the catchment modeling analysis. (ET = evapotranspiration, SM = soil moisture, RO = runoff).

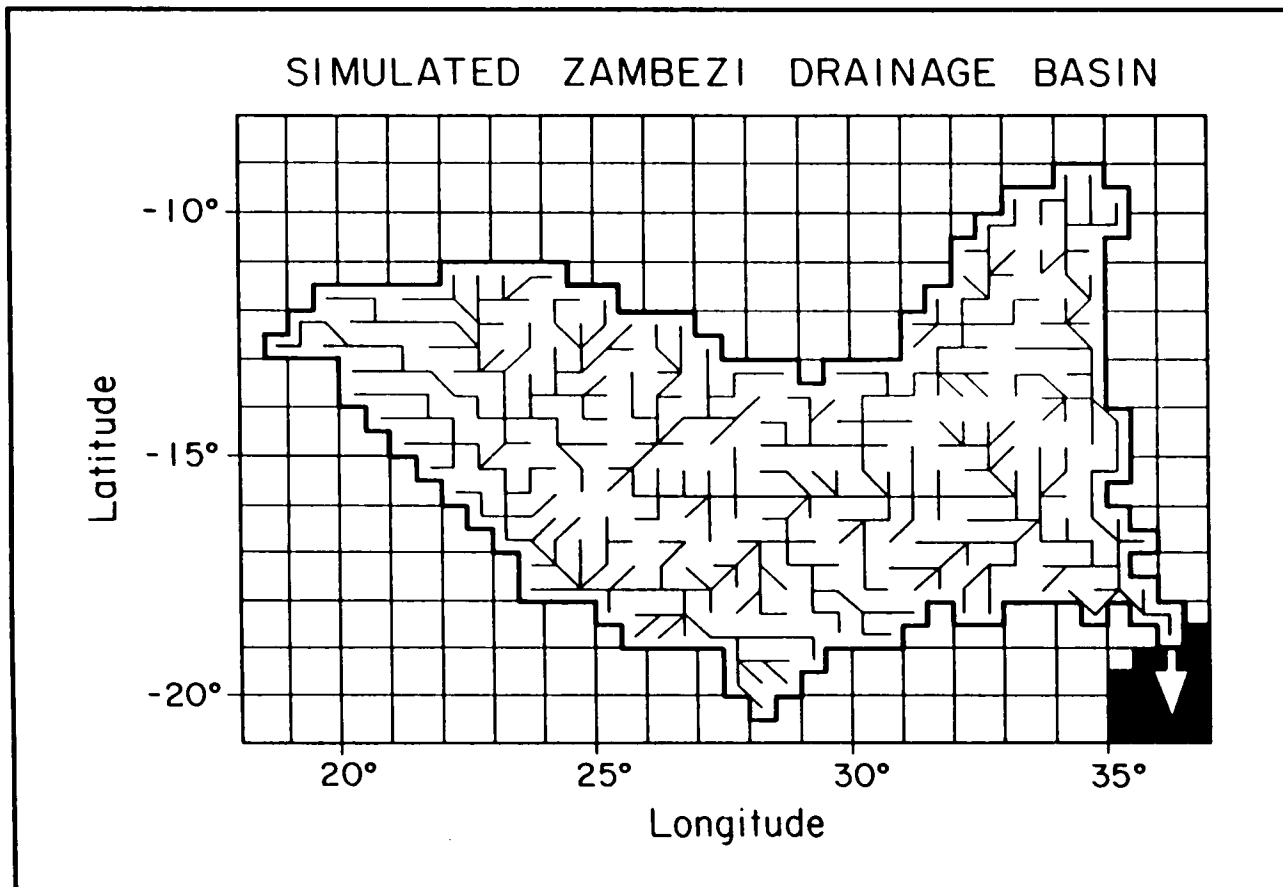


Fig. III-4. Simulated topology of the Zambezi River system at 0.5 x 0.5 degree (latitude x longitude) spatial resolution. The direction of flow associated with this network was based on a series of Operational Navigation Charts (DMAAC, various years).

variety of methods as detailed in Appendix A. Data for soil texture, coupled to vegetation-dependent rooting depths, define an active pool of soil water which is tracked over time. From this pool of soil moisture, evapotranspiration and runoff are derived.

Calculated runoff forms the link between the Water Balance and Water Transport Models. This runoff and an additional series of spatially-referenced data sets serve as inputs to the WTM. Specifically, these data include the rate of water turnover in each grid cell, the occurrence and extent of floodplains or swamps and reservoir characteristics. Runoff from WBM is routed through the transport algorithm which links the 409 grid cells into a series of simultaneous differential equations representing channel flow, wetland inundation and evaporation from the water surface. The model determines annual discharge and monthly hydrographs for any cell located within the simulated basin.

From a standard reference condition which represents the long-term average for climate, natural land cover and unregulated river flow, a series of scenario analyses can be performed on the linked WBM/WTM configuration. One scenario can represent the contemporary state of land cover and reservoir operation. Other scenarios invoke various potential changes in the region's land use, its climate as well as combinations of the two. The impacts of these

changes on the water balance (i.e. soil moisture, evapotranspiration and runoff) as well as channel discharge and wetland inundation then could be documented. The influence of altered climate and land use are evoked first through changes the region's water balance and later through the transport of water within the river network. An important alteration to the natural flow regime is the operation of impoundments. The proposed modeling strategy should not only establish how historic reservoir operation has affected the river system, but indicate how the future river flow regime may influence the impoundments.

#### Water Balance Model

Supporting Data and Technical Considerations. It is clear that development of a catchment-scale model represents a formidable data management task. Since the modeling approach outlined below is dependent on a series of data layers, or 'data planes', inaccuracies within any of the contributing data sets are capable of producing sequential error that could compromise the overall quality of the analysis. However, it is our belief that with due caution distributed parameter models can be developed which represent the quantitative hydrology of complex drainage basins like the Zambezi.

Table III-2 lists the required data that will be used by the basin-scale model in the context of a Geographic Information System (GIS). It is difficult to judge the



TABLE III-2. Required Datasets for Water Balance Model

Data Plane	Current Source(s)
Soil Texture	FAO/CSRC (1974)
Land Cover	FAO/UNESCO (1977) <sup>a</sup> Mathews (1983) White (1983) Olson et al. (1983)
Precipitation	Legates and Willmott (1989) Willmott and Rowe (1986)
Temperature	Legates and Willmott (1989) Willmott and Rowe (1986)
Cloud Cover	Hahn et al. (1988)

<sup>a</sup>Derived from map text.

overall quality of the numerous data sets. However, taken together, they represent the best and most current information at the regional scale that could be employed in such a study. Soil texture is derived from FAO/CSRC (1974) soil maps digitized at the 10-km horizontal scale and maintained in the Global Environmental Monitoring System (GEMS) data archive (Leenaers, 1989). It can also be extracted from a 0.5° version of this data set maintained at the Institute for the Study of Earth, Oceans and Space, University of New Hampshire. The best data set for natural land cover is likely to be White's (1983) vegetation maps of Africa, also available through the GEMS data archive, at a relatively fine (10-km) spatial scale. The data set of Olson et. al. (1983) similarly treats both natural and managed ecosystems but is only available at the 1° scale. A data set by Matthews (1983) gives broad vegetation classes at the 1° spatial scale. Leenaers (1989) demonstrated that it is possible to use the written material (FAO/UNESCO, 1977) accompanying the FAO soils maps to identify candidate areas for agriculture based on soil type and phase. Precipitation and temperature fields have been developed from a network of meteorological stations distributed within the basin (Legates & Willmott, 1989; Willmott & Rowe, 1986). The information on precipitation may be biased due to the relatively sparse series of stations, the episodic nature of precipitation in such a semi-arid basin, and rain gauge

sampling problems (Yair & Lavee, 1985; Mather & Ambroziak, 1986).

The issue of climatic data quality was examined briefly by comparing meteorological station data from the Kafue Basin with data extracted from the Willmott and Rowe (1986) database at 15.0° S and 27.5°E (Figure III-5). There is excellent correspondence among the temperature and precipitation timeseries. The cloud cover data set from Hahn et. al. (1988) also matches well data for irradiance at this particular station. Calculated potential evapotranspiration can be compared to pan measurements. Figure III-6 shows PET estimates using a variety of methods detailed in Appendix A. There is considerable disparity among the various techniques but it appears that the method of Jensen and Haise (1963), relying on a combination of temperature and surface radiation, offers the most promising approach of those tested. The method also appears to work well in the humid tropics (Vörösmarty, unpublished data).

The first phase of model calibration is to establish a baseline regional water balance under climatically-averaged conditions and without appreciable human disturbance. As demonstrated in the next section, water balance calculations on single grid cells are the result of numerous interactions among vegetation, climate and soils data sets. Defined for entire drainage basins, the water balance is also influenced by the flooding of wetlands with an attendant loss of water

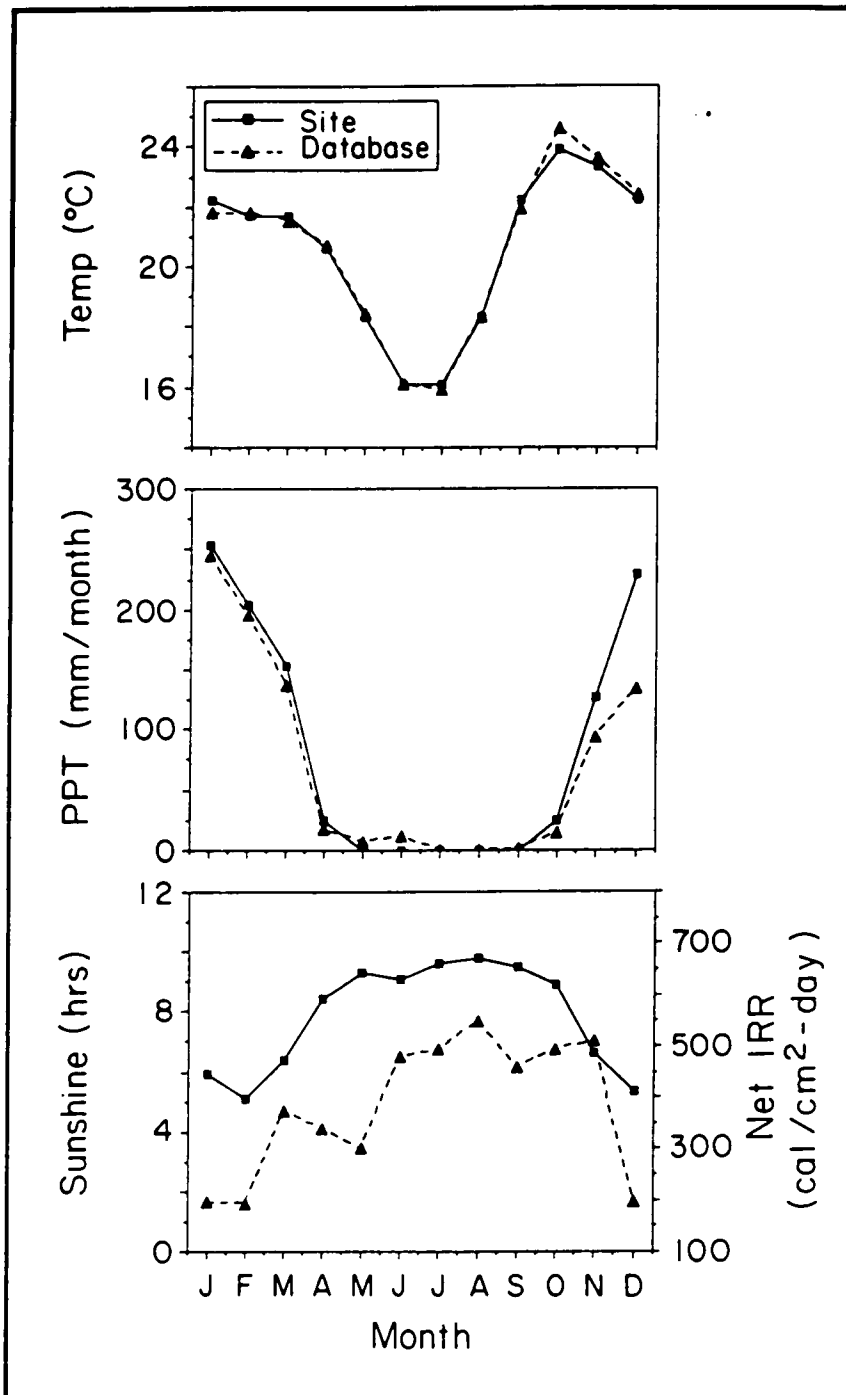


Fig. III-5. Comparison of site-specific and continental-scale data sets for air temperature, precipitation, and irradiance (sunshine) for a grid cell located in the Kafue basin. See text for data sources.

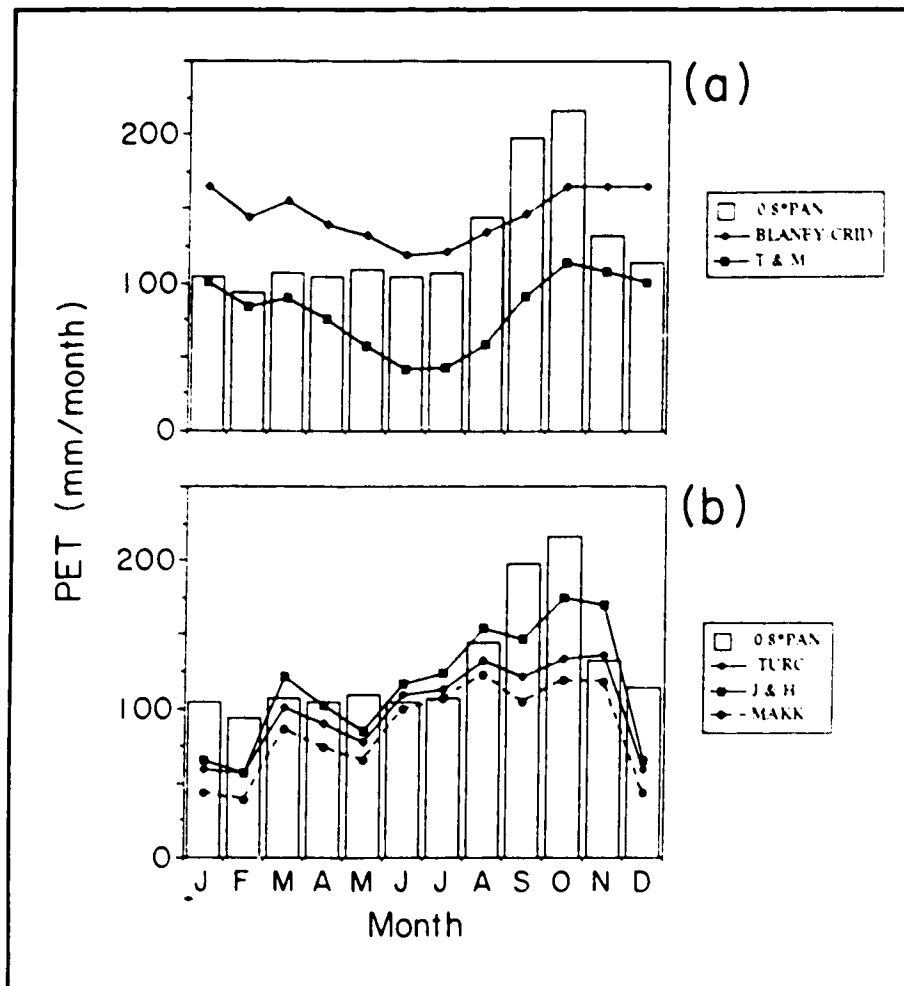


Fig. III-6. Alternative calculation schemes for determining potential evapotranspiration. The bars represent 80% of pan evapotranspiration for a site in the Kafue sub-basin reported in FAO/UNDP (1968). (Top) Temperature-based methods; (Bottom) Temperature / radiation - based methods. (BLANEY - CRID = Blaney and Criddle (1962); T & M = Thornthwaite and Mather (1957); TURC = Turc (1961); J & H = Jensen and Haise (1963); MAKK = Makkink (1957)).

through evapotranspiration. Swamp and floodplain losses are simulated using PET from the water balance model and information on duration of flooding. Reservoir systems also alter discharge regimes and transfer significant amounts of water to the atmosphere.

It is assumed initially that the climate forcings and all other geographically-specific datasets are correct. A pre-disturbance condition is defined by specifying natural vegetation from the datasets described above and by the absence of impoundments. The model for the contemporary setting is calibrated by altering the "natural" water holding capacity of soils in each subcatchment for which adequate discharge information exists. An initial water holding capacity is defined by rooting depth of vegetation and soil texture. The values range from 27mm to 582 mm (Vörösmarty et. al. 1989). Altered capacities are associated with removal of natural vegetative cover and influence runoff potential. The contemporary setting is also affected by the basin's reservoirs. Information on mean annual flows from Table III-3 can be used to establish subregional checks on the runoff determinations. Ancillary information such as rainfall/runoff correlations (FAO/UNDP, 1968) can also assist in determining regional water balance. The inferred level of land clearing can be validated with information on population density and settlement patterns

TABLE III-3. Observed Mean Annual Discharges

Location	Discharge (m <sup>3</sup> /s)	MAINSTEM Years of Record	Reference
Chavuma Falls	554 <sup>a</sup>	NA	Balek (1977)
	754 <sup>a</sup>	1946-64	Balek (1977)
	761	NA	UNEP (1986)
Below Chobe River: Livingstone	1237 <sup>a</sup>	NA	Balek (1977)
	1374	1928-61	Balek (1977)
	901-1111	1926-51	Plinston (1981)
	1237 <sup>a</sup>	NA	Balek (1977)
	1273	NA	Sharma and Nyumbu (1985)
	1323	1974-85	CAPCO (unpublished data, 1988)
	1332	1925-83	Borchert and Kempe (1985)
	1345	NA	Obrodik et al. (1989)
1348	1974-79	Plinston (1981)	
1564	1950-79	Plinston (1981)	
Below Kafue River	1914 <sup>a</sup>	NA	Balek (1977)
Below Luanwa River	2500 <sup>a</sup>	NA	Balek (1977)
Upstream of Kariba	1364	1974-80	Plinston (1981)
	1451	1974-88	Reeve and Idrook (1966)
	1490	NA	Borchert and Kempe (1985)
	1585	NA	UNEP (1986), Reeve and Idrook (1966)
	1633	1974-79	Plinston (1981)
Cabora Bassa	1874	1951-79	Plinston (1981)
	2695	NA	UNEP (1986)
	3001	NA	Hall et al. (1976)
Lupata Mouth	3349	1931-64	CAPCO (unpublished data, 1988)
	7135	NA	Amptogbe (1980)
	3171	NA	UNEP (1986), Borchert and Kempe (1985)
Sanyati Mouth	118	NA	Pinay (1988)
Tlozeu Mouth	288	1934-39, 1951-61	FAC/UNDP (1968)
		1953-64	
	374 <sup>a</sup>	1974-39, 1951-61	CAPCO (unpublished data, 1988)
	386	NA	Mepham and Mepham (1987)
	392	1954-64	FAC/UNDP (1968)
Export from Kafue Flats	282	NA	Mepham and Mepham (1987)
Kafue Mouth or Gorge	283	1925-64	FAC/UNDP (1968), Bolton (1987)
	319 <sup>a</sup>	1974-77	CAPCO (unpublished data, 1988)
	32	NA	Pinay (1988)
	331	NA	Obrodik et al. (1989)
	392	1974-74	FAC/UNDP (1968)
	41	NA	Balek (1977)
Luanwa Mouth	411	NA	Obrodik et al. (1989), Pinay (1988)
	436 <sup>a</sup>	NA	Balek (1977)
	424-678	1931-78	Bolton (1987) (using various sources)
Nonyani Mouth	44	NA	Pinay (1988)
Shute Mouth	476	NA	UNEP (1986)

<sup>a</sup>Known to be a poor database (Bolton, 1987).

<sup>b</sup>Data is essentially that found in FAC/UNDP (1968) with extensions for the years listed.

which could be superimposed onto the existing land cover maps using GIS techniques.

The foregoing discussion suggests that limitations in the current generation of data sets will restrict validation of the model. A basin-scale model, calibrated as described, can, however, be used to explore the general response of water balance to alterations in land use and climate. Global climate modelers have experienced similar limitations for many years, but by securing a careful understanding of the limitations of their models, they have explored the potential impacts of global climate change in response to the widespread release of radiatively important gases. An important product of our research strategy will be identification of critical gaps in our knowledge about the hydrology of the Zambezi River and other similar drainage systems.

The Algorithm. The WBM is organized to simulate grid cell hydrology under long-term or altered climate (Figure III-3). Inputs to the model include regional or continental-scale data sets covering precipitation, temperature, vegetation and soils. The WBM then predicts soil moisture (SM), evapotranspiration (ET) and runoff (RO) for each 0.5° grid cell in the simulated region. In the proposed study, independent water balance predictions will be made for more than 400 cells representing the Zambezi drainage basin. The WBM component relies on techniques



developed by Thornthwaite and Mather (1957) and subsequently modified by Vörösmarty et. al. (1989). The WBM is deterministic and employs a monthly time step. A dynamic steady state is achieved by applying monthly PPT, T and PET repeatedly over the year until the soil moisture, ET and runoff calculations for each successive twelve-month period converge to within an acceptable margin of difference (0.01%).

Soil moisture is determined from interactions among rainfall and potential ET. During wet months (rain in excess of PET), soil moisture can increase up to a maximum field capacity determined by soil texture and rooting depth. During dry periods (available water exceeded by PET), soil moisture becomes a function of potential water loss. Thus,

$$dSM/dt = (P_r - PET) \quad P_r \geq PET, SM < FC \quad (1a)$$

$$dSM/dt = 0 \quad P_r \geq PET, SM = FC \quad (1b)$$

$$dSM/dt = -aSM(PET - P_r) \quad P_r < PET \quad (1c)$$

where SM is soil moisture (millimeters),  $P_r$  is precipitation as rainfall (millimeters per month), PET is potential ET (millimeters per month), FC is soil field capacity (millimeters) and  $a$  is the slope of the moisture retention function described below. Calculations commence at the end of the wet season when it is assumed the soil is at field capacity. Soil water stocks are then depleted during the dry season in accordance with the moisture retention

function. For each wet month, soil moisture is determined by incrementing antecedent values by the excess of available water over PET. This recharge may or may not be sufficient to bring the soil to field capacity at the end of the subsequent wet season.

As a soil dries it becomes increasingly difficult to remove moisture against increasing pore tension. For a particular soil, there is a linear relationship between  $\log SM$  and  $\Sigma (PET - P_r)$ , summed from the start of the dry season to the current month. The original tables offered by Thornthwaite and Mather (1957) treated eleven field capacities in metric units. To calculate  $dSM/dt$  through (1c) for intermediate field capacities, the WBM defines a slope to the retention function:

$$\underline{a} = \ln (FC) / (1.1282 FC)^{1.2756} \quad (2)$$

The numerator represents soil moisture (millimeters) with no net drying. The denominator is the accumulated potential water loss ( $\Sigma\{PET - P_r\}$ ) in millimeters at  $SM = 1.0$  mm. With  $\underline{a}$  determined the model can calculate  $dSM/dt$  as a function of soil dryness and update  $SM$ .

The WBM calculates soil moisture to a maximum defined by the field capacity for a particular soil (i.e. moisture held in the soil drained by gravity). It makes no prediction of the degree of waterlogging beyond this capacity. Such a determination would require assignment of

percolation rates to each soil type as well as a statistical distribution of rainfall duration and intensity over each month. Further, the hydrology simulated in the current version of WBM is driven by pluvial processes alone; floodplain inundation is not explicitly considered. The current WBM using Thornthwaite and Mather's (1957) and Dunne and Leopold's (1978) technique is unrestricted in depleting soil water below wilting point. In a wet region like the Amazon, this does not appreciably affect water balance calculations. In more arid regions, however, a modification may be necessary. This would involve specifying an available water capacity (water holding capacity minus wilting point) and modifying the nature of the retention function. More accurate scaling from daily to monthly timesteps may also be required to avoid temporal aggregation bias (Rastetter et. al., 1990).

Once soil moisture is determined evapotranspiration is calculated. Following Thornthwaite and Mather, ET is set equal to PET in wet months, when  $P_r \geq PET$ . During such times it is assumed that precipitation is in sufficient abundance to satisfy all potential water demands of the resident vegetation. During dry seasons ( $P_r < PET$ ) the monthly average ET (in millimeters) is modified downward from its potential. The relevant equations are:

$$ET = PET \qquad P_r \geq PET \qquad (3a)$$

$$ET = P_r - dSM/dt \qquad P_r < PET \qquad (3b)$$

The WBM determines runoff based on the availability of soil moisture. Whenever field capacity is attained, excess water is transferred to subsurface runoff pools. From these storage pools, RO is generated as a linear function of the existing pool size. There is no new contribution to the runoff storage pools when a moisture deficit exists in relation to field capacity; any available water recharges the soil. For rainfall detention and runoff:

$$dD_r/dt = (P_r - PET) - \beta D_r \quad SM = FC, \quad P_r \geq PET \quad (4a)$$

$$dD_r/dt = -\beta D_r \quad SM < FC \text{ or } P_r < PET \quad (4b)$$

$$RO_r = \beta D_r \quad (4c)$$

where  $RO_r$  is rainfall-derived runoff (millimeters per month),  $\beta$  is a linear transfer coefficient and  $D_r$  is rainfall-derived detention (storage) pool (millimeters). The  $RO_r$  term from each grid cell is later passed to the WTM for subsequent downstream routing.

#### Water Transport Model

Supporting Data and Technical Considerations. For the transport model to calculate realistic discharge hydrographs, an adequate record of measured river flows must be assembled. Of significant concern in this regard is the paucity of reliable discharge records in the Zambezi basin. Bolton (1983) reviewed discharge records and hydrologic analyses in the Zambezi and concluded that there are

numerous irregularities. There is also a wide spectrum in the quality of the findings from the individual analyses. Prior to 1955, there were only two sites with rated level gages, and indicative of the general state of affairs in collecting discharge data in remote areas was the situation at Chavuma, where data were routinely carried 50 miles by bicycle to the nearest telegraph station for relay (Reeve and Edmonds, 1966). Discharge data is now more abundant, but for relatively shorter periods of record. The Global Runoff Data Center (Koblenz, GDR) lists holdings for numerous gaging stations within the Zambezi, but most have a relatively short (3-5 year) period of coverage. In addition, there are national yearbooks which could conceivably give station data dating from 1956, but the quality of the data sets is unknown at this time.

Table III-3 is a compilation of annual discharge data from a variety of sources available to the author at the time of writing. In some cases the data replicate themselves and merely reflect use of the same original data source. It is also apparent that for specific sites, a wide range of discharge estimates is offered, a product of differences in methodology, years sampled, etc. Data from Itezhi Tezhi, Kafue Gorge and Livingstone (CAPCO unpublished data, 1988) and from Lupata (Dos Santos, 1968) have been used routinely in reservoir management and this proposed

work should also rely strongly on these records (Figure III-7).

The important role of floodplains and swamps in the functional hydrology of the Zambezi deserves special attention. Figure III-8 shows grid cells in which wetlands are a dominant landscape feature capable of modifying channel discharges. These were identified by inspection of the Operational Navigation Charts and the occurrence of wetland soils in the FAO/CSRC (1974) soils database. Table III-4 summarizes some key attributes of these wetlands, including area, evapotranspiration, and the occurrence and timing of inundation. Although there is disagreement on the exact magnitude of their role in regional water balance, their primary impact is as a sink for runoff and as an attenuator of downstream floodwaves. These wetlands intercept runoff, often generated at great distances, distribute this water over large areas and, through evapotranspiration, subsequently translocate it out of the basin and into the atmosphere.

Atmospheric losses for individual wetlands appear modest but on the catchment scale they may serve collectively as significant sinks for riverine water. A water balance estimated by Balek (1977) for two major swamps in the Kafue sub-basin, the Kafue Flats and Lukanga Swamps, showed modest losses of 4 and 8% of influent, respectively. In contrast, calculations presented by Mephram and Mephram (1987) for the

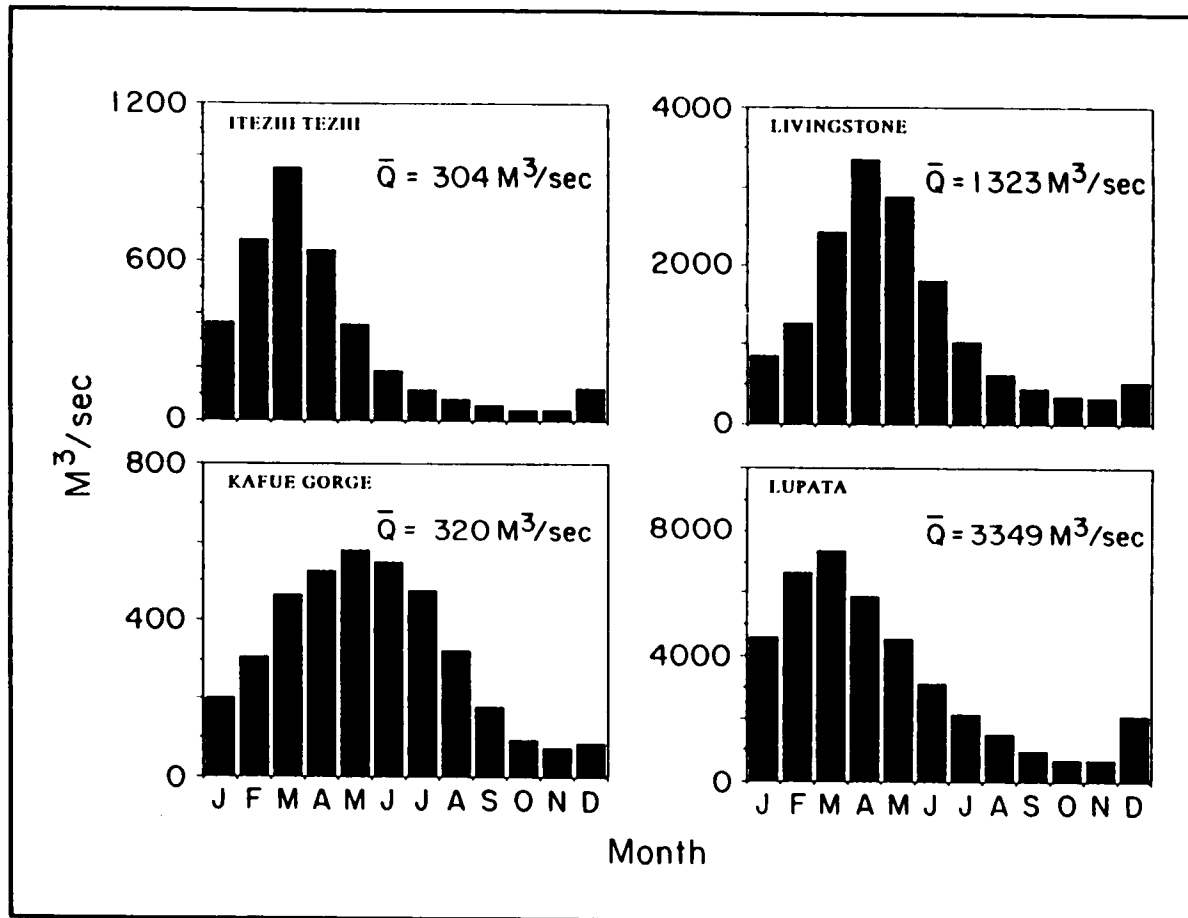


Fig. III-7. Long-term discharge hydrographs from four sites in the Zambezi drainage basin with relatively reliable data quality. Data are from the Central African Power Corporation (unpublished data, 1988) and apply to pre-impoundment conditions.

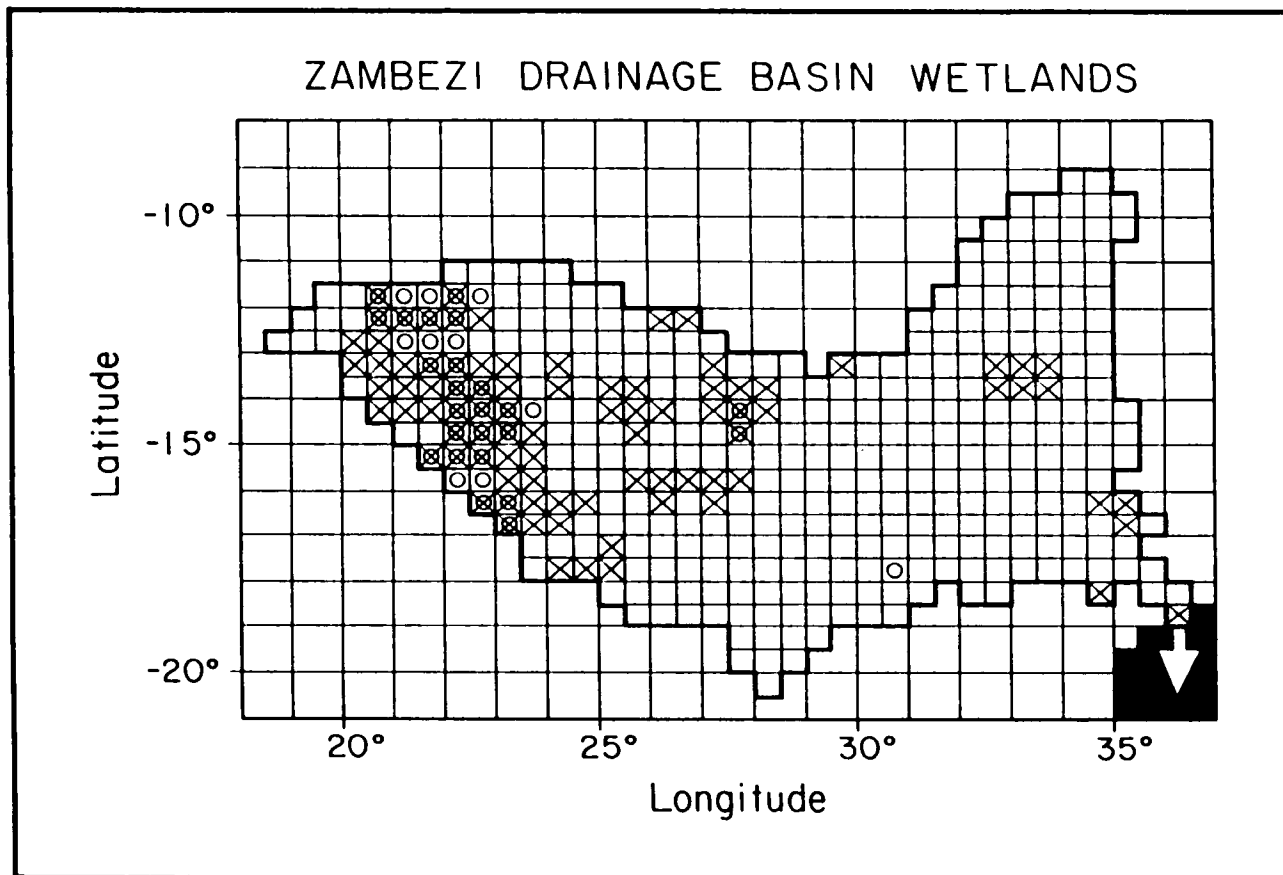


Fig. III-8. Grid cell locations having appreciable areas of wetland. The "X" markings represent the occurrence of swamps and/or floodplains identified from Operational Navigation Charts (DMAAC, various years). The cells with circles are locations having wetland soils determined from FAO/CSRC (1974). The wetlands within each cell do not necessarily fill the entire area of the grid.



TABLE III-4. Wetlands in the Zambezi River System

WETLAND	AREA (km <sup>2</sup> )	ET	COMMENT
Kafue Flats	5400 (l) 7000 (i) 5650 (b,k) 2600 (c) 1215 permanent (b) 5680 in wet year(j) 3650 in dry year(j) 2430 seasonal(j)	0.3 m/y seasonally flooded areas (j) 1.0 m/y permanently flooded areas (j) 1.8-1.9 km <sup>3</sup> /y (b,i,j,k)	Flood starts in December, peak in Feb/March in west, peak in April/May in east (i) Peak in April; dry in Sept (b) Average peak volume 10.5 km <sup>3</sup> (i)
Lukanga Swamps	2500-2600 (b,c,d,j) 2100 permanent (b) 1295 Lukanga floodwater (j) 1295 Kafue floodwater(j)	1.7 km <sup>3</sup> /yr (e) 0.5 km <sup>3</sup> /yr from Kafue (j) 0.5 km <sup>3</sup> /yr from Lukanga(j)	0.5-0.6 km <sup>3</sup> /yr spillover from Kafue (c,j) 0.5-0.6 km <sup>3</sup> /yr spillover from tributaries (j) 7.4 km <sup>3</sup> (b), 8.4 km <sup>3</sup> (j) storage volume
Busanga Swamps	1000 (permanent) (b)		
Mpetamoto to Kafue Rail Bridge			Rainy season floodplain inundation (j)
Barotse Swamps	7700(b) 7500(g)	"Huge"(e)	Stores 8-9 km <sup>3</sup> (e,f,g,h) in normal flood;17 km <sup>3</sup> (h) in high flood Flood starts November, peak April, recession May-Oct (b) December-June flood (h) January-May flood @ Senanga (e)
Chobe Swamps	2500 (g)		Zambezi water backs up Chobe and flood south side (g)
Mana Pools			Not regularly flooded, but waterlogged (a)
Shire Swamps			Wet December-July; peak flood May (b)
Lower Zambezi			Does not flood each year (m)floodplains8 km wide floodpain w/ rapid flows (b)

Footnotes: (a) du Toit (1983) (b) Mepham and Mepham (1987) (c) Balek (1977) (d) Seagrief (1962) (e) Sharma and Nyumbu (1985)  
(f) Nugent (1988) (g) Santa Clara (1988) (h) Reeve and Edmonds (1966) (i) Obrdlik et al (1989) (j) FAO/UNDP (1968)  
(k) Pinay (1988) (l) White (1973) (m) Bolton (1983); reference unclear but probably refers to Lower Zambezi

entire Kafue subcatchment showed a loss of 25-30% due to evaporation on open water surfaces and flats. The authors' own calculations using data from FAO/UNDP (1968), with supplements from CAPCO (unpublished data, 1988), support the contention that swampland water loss is tied to the occurrence of wet and dry conditions. Losses amounting to 24% of influent through the Kafue flats were calculated for the dry water year of 1965; in a wet year (1952) net gains of 38% were tabulated due to local runoff. For the entire Zambezi basin, it has been calculated (UNEP 1986) that approximately 2/3 of all water that is at one time in rivers fails to reach the Indian Ocean because of such losses. An accurate modeling analysis should correct for this phenomenon and account for the fact that most wetlands are only periodically flooded. Such capabilities are particularly important in addressing climate change issues.

The impact of temporary water storage through a large wetland can have dramatic effects on the shape of the emergent hydrograph. For example, Figure III-7 shows the upriver hydrograph at Itezhi Tezhi, clearly transformed by the influence of the Kafue flats. There is a strong dampening and delay in discharge due to passage through the swamp at Kafue Gorge. With passage through the comparably-sized Barotse Flats there are similar effects, though less dramatic (Figure III-9). In addition, Table III-4 demonstrates that the various large wetlands of the

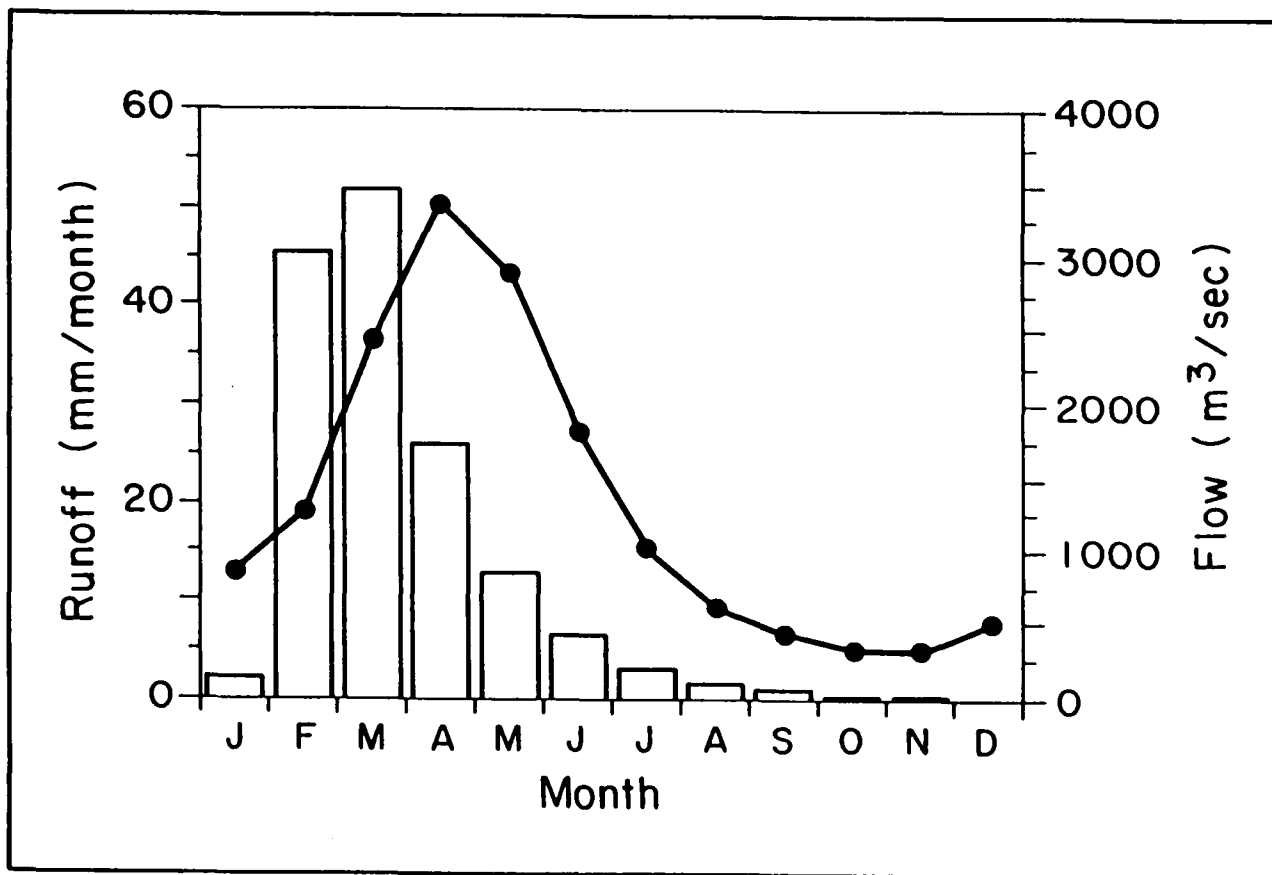


Fig. III-9. Inferred floodwave attenuation on the Upper Zambezi. Each bar represents runoff calculated by WBM for a typical grid cell located upstream of Livingstone, at -13.5 latitude and 23.0 longitude. The line represents average pre-disturbance discharge at Livingstone.

Zambezi do not necessarily act in unison, with some wetlands apparently flooding regularly each year and others only intermittently. It is unclear, therefore, from cursory analysis how active the wetlands are in regulating the water balance of the catchment. The linked WBM/WTM, accounting for the numerous local conditions given in Table III-4, will be used to make a more quantitative assessment of the phenomenon for the entire basin.

As a final note on the impact of wetlands, large expanses, especially in northern regions of the Central African Plains, are riddled with low-lying dambos. These are treeless swamps fed by rainfall and surface runoff which serve to delay the movement of water out of the catchment (Mephram and Mephram, 1987; Balek, 1977; FAO/UNDP, 1968). There are no reliable catchment-wide estimates of the areal extent nor of the precise distribution of these dambos. Evidence for their influence may emerge as anomalous subcatchments in the water balance modeling. For the suspect subcatchments, obvious numerical inconsistencies between computed and empirical runoff estimates (Table III-3) can be cross-checked against data on dambos offered by Balek (1977) and FAO/UNDP (1968).

The Algorithm. The Water Transport Model is a multigrid, dynamic model which computes discharge through each cell of the simulated drainage basin. It combines runoff produced by WBM with information on network topology,

fluvial transfer rates and the timing and extent of floodplain inundation. Discharge is predicted as a monthly mean. Because WBM-generated runoff drives the transport model, predicted discharges initially represent those under climatically-averaged conditions.

Network topology (Figure III-4) was determined from a series of 1:1,000,000 Operational Navigation Charts (DMAAC, various years) covering the Zambezi system. For each  $0.5^\circ$  cell, a predominant direction of flow was determined by examining the discernible network of rivers and streams. With large rivers this afforded an unambiguous indication of directionality. In grid cells draining small areas, a predominant stream was sometimes absent. In these cases the DMAAC maps were consulted for topographic features and elevation. Flow direction was therefore predicted less accurately for small rivers than for larger rivers. Vorosmarty et. al. (1989) found for the Amazon drainage basin that this effect was common in subcatchments of four or fewer grid cells, and represented the inherent resolution of such a gridded structure.

Channel flow in the WTM is represented by a linear reservoir model. Each grid is considered a storage pool with a characteristic residence time ( $t$ ). A standard transfer coefficient,  $K$  ( $t^{-1}$ ), must be assigned to all cells and then modified on the basis of geometric considerations. The standard is associated with rivers draining grid cells

on the N-S or E-W axis. The K value is then lengthened or shortened depending on the geometry of influent and effluent streams. For example, a cell receiving influent from the southwest and with an exit at its northeast corner would have the standard K value multiplied by 0.7 to accommodate a longer residence in the grid cell. In the case of multiple tributaries, the residence time is weighted by mean annual flow. For grid cells lacking upstream inputs, the residence time is halved. Previous work (Vorösmarty et. al., 1989) identified a theoretical range from 15 to 50 month<sup>-1</sup>, with best results (at least for the Amazon and Tocantins Rivers) afforded by a K value of 20 month<sup>-1</sup> applied to each cell. A similar approach initially can be taken for the Zambezi. Discharge coefficients may also be dependent on topographic gradient, mean annual flowrate or the combination of the two and such a dependency should also be explored as part of the proposed work. Data for the Kafue (FAO/UNDP, 1968) linking hydraulic gradient, discharge and mean reach velocity could be used in this context. Time of travel estimates for floodwaves given in Table III-5, although sketchy, provide tentative calibration targets.

The WTM also predicts floodplain inundation. Flood parameters in WTM have clear physical analogues. Floodplain and swamp exchanges take place whenever the monthly discharge exiting a grid cell exceeds a specified fraction of long-term mean annual flow. Above this fraction and with

TABLE III-5. Floodwave Translation

RIVER REACH	# of CELLS	TIME REQUIRED	REFERENCE
Chavuma to Livingstone	14	1-3 months 3-5 weeks 31 days	Balek (1977) Santa Clara (1988) Sharma and Nyumbu (1985)
Barotse Plains	6	6 weeks 3-5 weeks 19 days	Nugent (1988) Reeve and Edmonds (1966) Sharma and Nyumbu (1985)
Senanga to Sesheke	4	2 days	Sharma and Nyumbu (1985)
Chobe Swamps	1	10 days	Sharma and Nyumbu (1985)
Katima to Livingstone	3	10-12 days	Reeve and Edmonds (1966)
Kafue Flats	4	60 days	FAO/UNDP (1968), CAPCO (unpublished data, 1988)
Livingstone to Kariba Gorge	6	80-90 days 5 days	Mephram and Mephram (1987) Nugent (1988)
Kariba to Ocean	21	12 days	Begg (1973)

\*Refers to 0.5° grid cells.

increasing discharge, inundation is simulated by apportioning the potential net increase in water storage between the channel and its associated floodplain. Floodplain storage increases until the time derivative of grid cell water storage becomes negative. During flood recession, the potential net decrease in grid cell storage is accounted for by changes in channel and floodplain storage using the same ratios as for rising waters. These calculations attenuate the amplitude of rising flood waves and augment downstream discharge during periods of falling stage. For a single grid cell, the resulting flow and continuity equations are:

$$dS_c/dt = (\sum_1^n Q_u) - Q_d + Q_g + Q_f \quad (5a)$$

$$dS_f/dt = -Q_f - A_s(PET - P_r) / 1000. \quad S_f \geq 0 \quad (5b)$$

$$Q_d = KS_c \quad (5c)$$

$$Q_g = A(RO_r) / 1000. \quad (5d)$$

$$Q_f = -r_f[(\sum_1^n Q_u) - Q_d + Q_g] \quad Q_d \geq c_f Q_{dma} \quad (5e)$$

$$Q_f = 0 \quad Q_d < c_f Q_{dma} \quad (5f)$$

where  $S_c$  is channel storage in a grid cell during a month ( $m^3$ ),  $S_f$  is floodplain storage ( $m^3$ ),  $K$  is the downstream transfer coefficient ( $month^{-1}$ ),  $A$  is the area of the grid ( $m^2$ ),  $A_s$  is the area in swamps ( $m^2$ ),  $n$  is the number of donor grid cells,  $Q_u$  is monthly upriver input,  $Q_d$  is discharge from cell exported downriver,  $Q_g$  is input from runoff



generated within the grid cell,  $Q_f$  is exchange between channel and floodplain (plus denotes floodplain to channel), and  $Q_{dms}$  is the mean annual downstream discharge. All  $Q$  values are in cubic meters per month. The coefficient  $r_f$  determines the ratio (0.0 to 1.0) of potential volume change that is assigned to floodplain storage and  $c_f$  is the flood initiation parameter, giving the proportion ( $\geq 0.0$ ) of long-term mean annual flow required to invoke floodplain exchanges. Due to potentially significant evaporative losses in the wetlands of the Zambezi (Table III-4), PET terms, calculated by the Water Balance Model, can be included in equation (5b). The computed atmospheric transfers can be compared to the Table III-4 values. The WTM treatment of wetlands is a simplified version of the models outlined by Minderhoud (1978), Sutcliffe and Parks (1989), Hutchinson and Midgley (1973), and White (1973).

The established topology together with the flow and continuity equations (5a)-(5f) creates a system of linked differential equations. The system is solved for  $S_c$  and  $S_f$  using a fifth- to sixth-order Runge-Kutta integration technique (International Mathematical and Statistical Libraries [IMSL], Houston, Texas). For the entire Zambezi basin, 409 cells are linked. The model applies monthly runoff values for each grid cell until a quasi-steady state solution emerges for the entire set of cells.

The WBM/WTM is parameterized by varying the water holding capacities of soil, the runoff transfer coefficient  $\beta$  and combinations of  $K$ ,  $r_f$ , and  $c_f$ . The parameterization is aided by an unbiased estimator of model performance relative to observed data. This index, modified from Willmott (1982) and Willmott et. al. (1985) is:

$$d = 1 - \frac{\sum_1^{12} |P_i - O_i|^y}{\sum_1^{12} (|P_i'| + |O_i'|)^y} \quad (6a)$$

$$P_i' = P_i - O_m \quad (6b)$$

$$O_i' = O_i - O_m \quad (6c)$$

where  $d$  is the "index of agreement",  $i$  is the month,  $P_i$  is the  $i$ th model prediction,  $O_i$  is the corresponding observation,  $y$  is an exponent set to 1.0 based on discussion of Willmott et. al. (1985), and  $O_m$  is the observed mean, in this case annual discharge. The  $d$  values calculated for each hydrograph are then weighted to combine the effects of flow magnitude and duration of the discharge record. Because of the weighting factors,  $d$  values for large rivers and sites with long periods of record are favored.

To produce a best fit, WTM calculations are compared to observed discharge records and those scenarios which maximize the  $d$  statistic are favored. Due to limitations in the available data, it is unlikely that a pre-disturbance scenario (i.e. natural vegetation and no impoundments) can be calibrated with absolute accuracy. However, the contemporary setting (i.e. extensive land use and

impoundments) can use this parameterization scheme. Two model runs need to be made. The first establishes water balance calculations using the more plentiful mean annual discharge data (Table III-3). A second considers subannual discharge hydrographs. As discussed earlier, the most reliable hydrographs are for the Kafue River at Itezhi Tezhi and Kafue Gorge, and the Zambezi at Livingstone and Lupata. Other data sources with shorter periods of record can be consulted, but are given less weighting in the calibration procedure.

#### Anthropogenic Disturbance: An Important Component of the Terrestrial Water Cycle

The following sections describe three important alterations of the hydrologic cycle in the Zambezi catchment and modeling strategies to address those issues. To varying degrees, many of the world's drainage basins are or will soon be affected by such phenomena, making the Zambezi an important test region for the development of global hydrology models. The first section below considers the influence of large impoundments on discharge patterns. The second treats water balance effects caused by land use change and degradation. Finally, there is a consideration of climate change. Although it is seldom perceived by planners in the Zambezi region as a critical basin-scale issue, the evidence presented below suggests that it is likely to become a concern of significant and well-founded urgency in the coming decades.

### Impoundment

Reservoirs can dramatically alter regional water budgets and constituent transport through drainage basins. The hydrologic impact is achieved through a dampening of influent hydrographs, open-water evaporation, and, if the water is used for irrigation, enhanced evapotranspiration. Constituent transport is altered as riverborne nutrients and sediments enter a lentic environment with slower hydraulic turnover and more quiescent conditions. The emplacement of reservoirs in river networks disrupts a normal continuum of physical, chemical and biotic processes which link free-flowing streams of varying size (Vannote et. al., 1980). The disruption establishes serial discontinuities in this continuum as ecosystems readjust to changing conditions (Ward and Stanford, 1983).

Major dams in the Zambezi basin are located on the mainstem at Kariba and Cahora Bassa as well as in the Kafue basin at Itezhi Tezhi and Kafue Gorge. The Itezhi Tezhi facility is designed as a water storage reservoir; the remainder produce electricity. Because of their importance to the regional economy these impoundments will likely remain a key factor defining the basin's hydrology for decades.

A complete understanding of the quantitative differences under free-flowing and impounded river settings does not now exist for the Zambezi River. A retrospective

analysis of basin-scale hydrology prior to impoundment contrasted against post-impoundment conditions can lend insight into the role that river regulation has had on downstream processes such as flow velocity, wetland flooding, and, in turn, material transport. I focus here on the hydrological aspects of this question.

There is significant controversy surrounding the specific manner in which downstream flow historically has been altered by these impoundments. Based on reservoir dimensions and inflows, the potential for changes in downstream discharge is substantial. For example, the total live capacity of Lake Kariba approaches an entire year's inflow (Bolton, 1983), and more than 20% of the annual inflow is typically lost through evaporation (Central African Power Corporation, 1985). Nonetheless, Attwell (1970), Guy (1981) and du Toit (1983) fail to concur on post-operational impacts. They found, respectively, that withdrawals from Kariba have produced more constant seasonal flows, more accentuation of flow differences and the persistence of a more or less natural regime.

Despite such uncertainties, numerous downstream impacts have been attributed to the operation of these facilities. Direct impacts on humans include the displacement of nearly 100,000 people as a consequence of the Kariba and Cahora Bassa projects (Bolton, 1983; Davies et. al., 1975), generally to areas with less fertile soils (J. R. Barnes,

Institute of Cultural Affairs, Zimbabwe; personal communication). There as well have been reports of an enhancement in parasitic disease vectors (van der Lingen, 1973). Other detrimental effects include the scouring of river channels (Atwell, 1970), choking of channels by infestant weeds (Davies, 1979; van der Lingen, 1973), loss of wildlife habitat due to altered floodplain inundation (Atwell, 1970), depletion of forage on floodplains from dessication and overgrazing (Davies, 1979; Begg, 1973) and loss of instream and wetland fisheries (Obrdlik et. al., 1989; Minderhoud, 1978; Davies et. al., 1975). There were unexpected releases of toxic  $H_2S$  following reservoir filling (Davies et. al., 1975; van der Lingen, 1973) and fears of excessive  $H_2S$  production with increased floodplain inundation (White, 1973). Changes in constituent transport can be far-reaching as trapped sediment can no longer nourish the coastal delta, resulting in significant dieback of mangrove ecosystems (Davies, 1979; Davies et. al., 1975) and enhanced saltwater intrusion detrimental to coastal fisheries (Davies, 1979).

Table III-6 is a summary of relevant information on the major impoundments that can be used in the basin-scale model. The volumetric specifications are used to define a single control volume for each impoundment. The control volume is defined as the total reservoir capacity minus the "dead volume". The resulting "live volume" fluctuates in

TABLE III-6. Characteristics of Major Impoundments

RESERVOIR	LAT	LN	MAXIMUM	DEAD	SURFACE	CATCHMENT	ANNUAL	FIRST	FIRST
			CAPACITY	VOLUME	AREA	AREA	FLOW	YEAR	YEAR
			(km <sup>3</sup> )	(km <sup>3</sup> )	(km <sup>2</sup> )	(km <sup>2</sup> )	(m <sup>3</sup> /y)	CONST <sup>a</sup>	OPER <sup>a</sup>
Kariba	+17°	28°	18.1 <sup>a</sup>	116.0 <sup>a</sup>	5200 <sup>a</sup>	650,000 <sup>a</sup>	1640 <sup>a</sup>	1955	1958
Tabora Bassa	+16.0°	34°	12.1 <sup>b</sup>	12.5 <sup>b</sup>	2100 <sup>b,c</sup>	1,000,000 <sup>b</sup>	2661 <sup>b</sup> -3000 <sup>b</sup>	1969	1974
Mbezi Tezhi	+16.0°	35°	0.14 <sup>d</sup>	0.7 <sup>d</sup>	120 <sup>d</sup>	105,000 <sup>d</sup>	317 <sup>d</sup>	1973	1976
Kafue Gorge	+16.0°	28.0°	0.04 <sup>e</sup>	0.14 <sup>e</sup>	800 <sup>e</sup>	150,000 <sup>e</sup>	317 <sup>e</sup>	1967	1970

RESERVOIR	MEAN WITHDRAWAL RATES (m <sup>3</sup> /sec)												ANNUAL
	JAN	FEB	MAR	APR	MAY	JUN	JUL	AUG	SEP	OCT	NOV	DEC	
Kariba <sup>a</sup>	1441 (-17)	196 (-)	27 (-)	2441 (-)	2468 (111)	3219 (93)	3282 (87)	396 (111)	856 (146)	904 (16)	1093 (116)	1087 (-39)	1431 (192)
Tabora Bassa <sup>f,g</sup>	1354 (-)	2014 (-)	1244 (-)	481 (-)	3331 (12)	3498 (11)	3487 (8)	1749 (174)	1883 (147)	2723 (117)	2515 (24)	3427 (-4)	2199 (191)
Mbezi Tezhi <sup>h</sup>	121 (-17)	4 (-)	8 (-)	47 (-)	400 (11)	2 (9)	355 (11)	275 (11)	200 (16)	27 (1)	207 (16)	200 (-3)	108 (192)
Kafue Gorge <sup>i</sup>	219 (-17)	28 (-)	48 (-)	124 (-)	552 (11)	522 (9)	456 (11)	349 (11)	218 (146)	176 (16)	161 (116)	177 (-3)	337 (192)

a - Pinay (1986)  
 b - Hall et al. (1986)  
 c - Davies et al. (1985)  
 d - Obrdlík et al. (1984)  
 e - CAPCO, unpublished data, for 1962-198  
 f - Withdrawals from Pinay (1986), for 1974-1988  
 g - Gross ET from Tezhi (2003) corrected for precipitation by C. van der Wal (1989)  
 h - Withdrawals from Mbezi (2003) under average conditions from Rajaratnam and Abu-Zeid (1982); ET from Institute of

response to upstream inflows and reservoir withdrawals. Inflows are calculated by the WTM upstream of the impoundments. Reservoir effluents are simulated by implanting discharge forcing functions within the simulated river network. The withdrawal values represent long-term means compiled by CAPCO (unpublished data) from monthly time series. Evaporation is expressed in the Table as a net depth of water (monthly precipitation minus pan evaporation) and together with surface area define total volume loss. Although surface area is given in the Table as a constant, it is in reality a function of stage or reservoir volume, and more sophisticated area/volume relationships (Bolton, 1983) may need to be employed to accurately estimate evaporation.

WBM/WTM discharge scenarios associated with land use and climate change (see below) will have obvious value to an appraisal of reservoir storage and release strategies. Standard operating strategies may be inappropriate under shifting patterns of land use and climate. Since the WBM/WTM provides basinwide flow estimates, it offers the potential to uncover potentially important downstream impacts that may result from operating decisions made at upstream facilities. This knowledge can aid in optimizing the collective operation of the major Zambezi reservoirs.



### Land Degradation

In addition to the potentially catastrophic impacts of erosion on agricultural productivity and sediment transport, the disruption of regional water balance can be an important consequence of land degradation in rapidly developing catchments like the Zambezi. Reduction of natural cover through lumbering, fuelwood removal, grazing or clearing for agriculture fosters rapid runoff. This, in turn, increases the potential for flood damage (Elwell, 1983; du Toit, 1985). It also lowers the water table and decreases seasonal low flows (Lewis and Berry, 1988; Elwell, 1985), reducing well yields (Elwell, 1983), exacerbating navigation problems and compromising instream wildlife habitat. The phenomenon is widely recognized in arid and humid areas, both temperate and tropical (Whitlow, 1987; Havel and Bligh, 1982; Pearce et. al., 1980; Krecek and Zeleny, 1980; Yates, 1972; Blackie, 1972; Swank and Helvey, 1970; Sopper and Lynch, 1970). Understanding the impacts of such change will be important not only to the development of management strategies for the river's large impoundments but also in helping to understand the impact of humans on catchment-scale hydrodynamics more generally.

Two principle mechanisms must be modeled. The first is reduction in the hydraulically-active soil depth associated with removal of natural cover. This removal can be thought of as a general reduction in overall biomass due to biotic

impoverishment. In disturbed semi-arid grasslands, reduction in the mean depth of active soil also may result from increased heterogeneity, specifically bare soil interspersed with invasive shrubs (Schlesinger et. al., 1990). A smaller pool of labile soil water means that evapotranspiration becomes more limited and runoff is favored in the overall water balance. Furthermore, a smaller soil moisture pool implies that less precipitation will be required to overcome any soil water deficits and, so, runoff will be generated more easily. Figure III-10 shows a simple experiment using the Water Balance Model to explore how sensitive this effect might be in the Zambezi region. The site chosen is in the Kafue Basin at 15°S and 27.5°E, assumed to have climate data identical to that presented in Figure III-5. The landscape is characterized by a grassland on clay loam. The soil water holding capacity is 352 mm. Deviations from this standard (water capacity inflator = 1.00) are given on the horizontal axis; associated annual runoffs are on the vertical axis. Proportional decreases in the water holding capacity are associated with decreases in biomass. Runoff increases sharply with decreases in holding capacity. It is reasonable to conclude that the water balance of the region is highly sensitive to changes in land use from this mechanism alone.

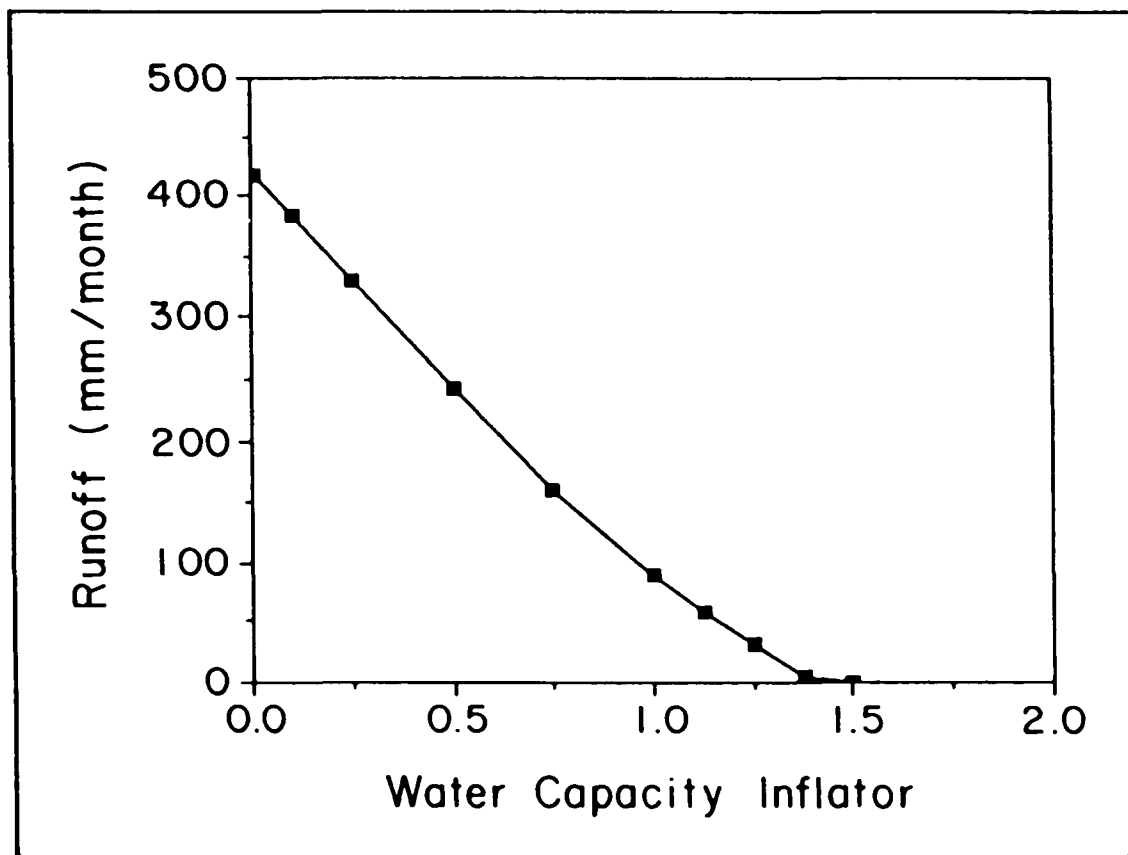


Fig. III-10. Water balance model sensitivity to changes in the water holding capacity of soils. Reduction in the water capacity inflator is associated with reduction in natural cover. (Nominal capacity = 1.0).

The second mechanism is reduction of infiltration associated with disturbance of the soil. Vegetation and litter protect the soil surface from direct rainfall impact and maintain channels for subsequent infiltration (du Toit, 1985). In less protected sites, direct rainsplash clogs soil pores reducing water entry into the soil and increasing stormflow runoff. Arid and semi-arid areas having little vegetative cover are naturally prone to this clogging as well as chemical reactions which create a "crusting" phenomenon (Yair and Lavee, 1985). Such crusting may induce long-lived effects, especially when the landscape is prevented from recovering. In the case of overgrazing, outright compaction occurs (Whitlow, 1987). These effects are well-known, but are difficult to quantify and separate from the impacts of reducing the hydraulically-active soil layer described above.

To further complicate matters, land use change is not always associated with increases in catchment runoff. There appears to be a threshold which must be attained before such changes are invoked. In a temperate zone forest studied by Plamondon and Ouellet (1980) a 30% removal of cover through clearcutting produced no discernable increase in catchment runoff. A comparative study by Oyebande (1988) on tropical forests and woodlands yielded a similar finding. Furthermore, such changes may be reversible through either regrowth to a natural system (Shiklomanov and Krestovsky,

1988; Swank and Helvey, 1970) or by proper land use management and conservation techniques (Walling, 1987).

For the Zambezi and its neighboring basins, altered land use has the potential to greatly modify existing surface hydrology and there is ample evidence to show that it has already produced widespread change. Elwell (1983) cites studies on overgrazed or bare-fallowed plots with 4-5% slopes which have eight-fold to thirteen-fold increases in runoff compared to full vegetative cover. Similar order-of-magnitude increases are reported by Elwell and Stocking (1973) and Barnes and Franklin (1970). duToit (1985) analyzed the phenomenon in the Sabi catchment of Zimbabwe and found that increases in annual stormflow runoff were statistically independent of changes in rainfall and were instead associated with large-scale reductions in woodland area. Whitlow (1987) cites extensive evidence linking the impoverishment of African ecosystems (from grazing, fuelwood collection and landscape burning) to associated increases in stormflow, decreases in soil moisture and lowering of water tables. On land which normally experiences  $300 \text{ mm yr}^{-1}$  runoff and is subject to clearfelling in the Kafue subcatchment, average increases of  $500 \text{ mm yr}^{-1}$  have been tabulated (FAO/UNDP, 1968). Campbell and Child (1971) reconstructed historical (pre-1900) patterns of land use change in Botswana and concluded that the destruction of veld, with concomitant invasion of woody

plants, was associated with heavy overgrazing and the drying of perennial surface waters. These biogeophysical changes were not assignable to changes in rainfall.

Owing to the site-specific nature of these varied landscape effects, runoff must be simulated using a combined field-scale and grid-cell modeling approach. The basin-scale estimates of land use change will be coupled to field-scale algorithms (e.g. SMODERP, Technical University of Prague; ANSWERS, US Environmental Protection Agency) to calculate spatial patterns of enhanced runoff. The models first require an estimate of land use intensity through the basin. Digitized vegetation maps can be examined in conjunction with information on soils, land suitability and topography to identify likely areas of contemporary settlement. This exercise can also validate the water balance tuning discussed above. Such predictions of land use distribution can then be compared to country-wide maps for verification. A series of scenarios can then be generated to extrapolate current trends in land settlement.

The field scale models operate on single rainfall events and require detailed information about slope, soils, vegetative cover, and rainfall. Given the characteristics of typical precipitation events (Balek, 1977) a series of tests can be performed to predict storm runoff losses from different types of fields. The field settings are determined from likely combinations of cropping practices,

slope, soil type, etc. For areas where there is adequate fine-resolution map coverage, relationships could be developed linking local conditions to those represented by the 0.5° database. Average topographic gradient, vegetation, land use, soils and climate would be considered. These relationships would then be extrapolated to areas without adequate data. In the catchment-scale model, a proportion of grid cell precipitation will be passed directly to a storm runoff variable and routed downstream with the standard runoff calculated by the current version of WBM.

#### Climate Change

A growing and convincing body of scientific evidence points to eventual warming of the Earth's surface due to the greenhouse effect, with an amplifying effect on continental hydrology (Dickinson and Henderson-Sellers, 1988; Kellogg and Zhao, 1988; Hansen et. al., 1988a, b; Hansen and Lebedeff, 1987; Mitchell et. al., 1987; Manabe and Wetherald, 1986). Soil wetness, boundary layer vapor flux, precipitation patterns and intensity, cloud distribution and variability in runoff and snowmelt are likely to be modified. Terrestrial and aquatic ecosystems are sensitive to these transformations, and the patterns of nutrient, carbon and trace gas exchange may be modified over large areas. This will require a broad perspective, and these

changes cannot be understood without a direct consideration of continental-scale hydrology.

Not only is the direction of climate change important, but its associated degree of variability as well (US National Academy of Sciences, 1977). Accompanying global warming will be an increased frequency of extreme events including drought and flooding. Arid and semi-arid regions are particularly sensitive, as the coefficient of variation in runoff increases with decreasing precipitation (Walling, 1984; Yair and Lavee, 1985). Nemec and Schaake (1982) and Klemas (1985) have reviewed the response of sample drainage basins to simple climate change scenarios and found that runoff, particularly under dry conditions, is most highly sensitive to changes in precipitation. They also demonstrated that to accommodate these changes in runoff, substantial alteration of the design capacity of reservoir systems would be required. A formidable challenge will thus present itself to the water resources community in the coming decades.

Significant climate variation is already a natural and important component of the Zambezi region's hydrology. East Africa has experienced recent episodes of increased variability in precipitation from the 1960's to 1970's (Lewis and Berry, 1988). From 1924-46, lower flowrates were associated with lower variability in contrast to the years 1947-83 when there were higher flows and higher variability



(Borchert and Kempe, 1985). The year 1958 was particularly noteworthy at the Kariba Dam site, as the highest discharges on record (and well outside the design criteria) surpassed the ability of the dam to regulate the river, causing considerable damage to the construction works (Santa Clara, 1988).

The influence of future climate change on water budgets in the Zambezi basin will be difficult to quantify. There is no concerted scientific effort to study the problem at the catchment scale and any quantitative information will likely come from coarse-scale global climate simulations. For southern Africa, there is considerable disagreement in predictions made by the current generation of General Circulation Models (GCM's) for soil moisture, evapotranspiration and runoff. These disparities arise from differential treatment of atmospheric and boundary layer physics, initial conditions and spatial resolution, in both the horizontal and vertical dimensions (Mitchell et. al., 1987; Kellogg and Zhao, 1988). Predictions made by such models for shifts in regional climate must therefore be viewed with appropriate caution.

To explore the potential impacts of climate change on the Zambezi basin a series of sample General Circulation Model predictions under a 2x increase in CO<sub>2</sub> can be considered. Results from four GCM configurations simulating the impact on precipitation are summarized in Table III-7,

TABLE III-7. Simulated Impact of 2x CO<sub>2</sub> on Precipitation in the Zambezi Basin.

MODEL	June to August $\Delta$ (mm/day <sup>-1</sup> ) <sup>a</sup>		December to February $\Delta$ (mm/day <sup>-1</sup> ) <sup>a</sup>	
	WEST	EAST	WEST	EAST
Washington & Meehl (1984)	0 to -1	0 to +1	+1 to +2	0 to -3
Mitchell et al (1987) 11 layer model	0 to -1	0 to +1	0 to -3	0 to -3
Mitchell et al (1987) 5 layer model	0 to -1	0 to +1	0 to +4	0 to +4
Mitchell (1983)	0 to -1	0 to +1	0 to +2	0 to +2

<sup>a</sup> Precipitation rate relative to current climate.

with increases or decreases benchmarked to the current climate. All models converge in predicting reduced precipitation in the western portion of the Zambezi and an increase of similar magnitude in the East during the Southern Hemisphere winter. For the period December through February there is less agreement, in terms of both the magnitude and direction of change; moreover, the models generally develop steep gradients in the precipitation anomalies. Such uncertainties are noteworthy given that much of the annual precipitation falls within this period. Further, these results are associated with a 1-4° rise in temperature across the basin from CO<sub>2</sub> alone (Washington and Meehl, 1984; Mitchell, 1983). Such results must be considered conservative in light of the fact that other greenhouse gases such as methane and N<sub>2</sub>O will accelerate the warming, potentially leading to significant impacts in the early part of next century.

Superimposed on these direct climatic disturbances are indirect effects from changes in land cover. These arise as the natural plant community adjusts to a new climate or as patterns of land settlement and agricultural technology are modified. The impacts of land use described in the preceding section showed that with a decrease in vegetative cover, increases in runoff are likely to occur. This finding, however, assumes no climatic feedback, which in all likelihood does exist, especially where land use change

is extensive. Work by Salati (1985) in the Amazon has demonstrated that approximately 50% of the precipitation falling on that drainage basin is actively recycled by the natural tropical forest. Extensive deforestation is feared to result in catastrophic alteration of regional hydrology and global weather patterns. Any widespread impoverishment of ecosystems in the Zambezi may similarly create a feedback on climate that could alter the patterns of precipitation and runoff. Observations by J. R. Barnes (Institute of Cultural Affairs, Zimbabwe; personal communication) confirm such effects locally in deforested areas of eastern Africa.

It is difficult to isolate the impact of climate change in basins which have experienced widespread alteration of vegetative cover. A demonstration of this is afforded by considering the possible mechanisms by which runoff yield from the Upper Zambezi has increased since the late 1940's, from approximately  $1000 \text{ m}^3 \text{ s}^{-1}$  to  $1500 \text{ m}^3 \text{ s}^{-1}$  at Livingstone (CAPCO, unpublished data, 1988). Borchert and Kempe (1985) attribute this rise to precipitation changes alone, whereas Plinston (1981) assigns but 30% of the increase to persistent climatic change. In contrast, Bolton (1983) concluded that there has been no systematic change in precipitation and attributed increased runoff to the intensification of land use in the drainage basin. Mephram and Mephram (1987) report extensive burning of the upper catchment, and this also may be an effect. The situation

remains fundamentally unresolved (Santa Clara, 1988). A similar rise, to a near doubling of early-1900 values occurred in the Kafue basin (Mephram and Mephram, 1987; FAO/UNDP, 1968).

In the face of such difficult scientific issues, it is sensible to begin with a straightforward analysis using the WBM/WTM algorithm, coupled to a finite series of scenario tests. Such an approach is directed at more clearly defining the bounds on the hydrologic system response to climate change. Since the proposed suite of hydrology models is grid-based, results from ongoing GCM studies can easily be incorporated into a regional context. The construction of such a coupled model will make an important contribution to both the regional analysis at hand and the ongoing development of global General Circulation Models (Becker and Nemec, 1987). Such a modeling exercise will be used to document possible limits to the changes that climate can elicit on the Zambezi. In addition, it will generate estimates of riverine discharge which, when compared to observed hydrographs, provide a useful constraint on GCM model predictions of contemporary regional water balance.

#### Summary and Conclusions

This paper has developed a rationale for studying the hydrology of the Zambezi River system at the catchment scale. A strategy has also been developed for implementing computer models of the major hydrologic processes operating

within the basin. A coherent data set for calibrating the models has also been assembled. The algorithms consist of a Water Balance (WBM) and a Water Transport (WTM). These models transform complex patterns of regional climatology into estimates of soil water, evapotranspiration, runoff, and discharge through rivers of various size. These models are also dependent on the characteristics of the terrestrial surface, principally soil texture and land cover.

Human activity is an important agent defining the contemporary hydrologic cycle. I have documented the potential impacts of impoundment, land use change and climate change on the Zambezi and found that they can be substantial. A full analysis will require construction and parameterization of a simulation for the entire catchment. An important design consideration for the numerous impoundments in the Zambezi requires an understanding of the seasonal variation in discharge, in particular how it might respond to climate and land use change. Thus, in addition to addressing basic scientific issues, the research described here will aid in developing management support tools in the context of a large international drainage basin, whose member nations are experiencing unprecedented rates of population growth and impoverishment of land resources.

Although a model of such scope would have enormous potential to advance our state of knowledge about the

hydrology of the Zambezi, and support the activities of the water management community, it necessarily will suffer without adequate supporting data. Of particular importance is the absence of long-term and accurate flow records. This restricts and effectively precludes validation of these models. The model, which now operates under a steady-state climate, would be substantially improved with a real-time capability. Retrospective timeseries of regional climate and land use should be assembled in order to understand recent changes in basin dynamics. Future changes in runoff could be addressed with a properly-mounted initiative incorporating remote sensing, field and literature-based data.

The hydrologic components of such a model are of particular value to the climate modeling community. Although current General Circulation Models can converge in defining the broad features of climate (for example, precipitation across latitude), they produce more substantial differences at the regional scale (Gutowski et. al., 1989; Grotch, 1988). To help overcome this limitation, finer-scale Limited Area Models (LAM's) are now being developed, nested within larger GCM's which provide the required initial and lateral boundary conditions (Giorgi, 1989). A necessary first step is to determine contemporary hydrologic budgets. These budgets are determined by accounting for precipitation inputs, soil water dynamics,

evaporative losses and runoff. Runoff, after conversion into cumulative discharge, is the only output variable for which reliable data potentially exist to validate GCM predictions. However, a global, geographically-based system that permits co-registration of observed and GCM output data sets is currently lacking.

To fulfill this need, a Global Hydrology Archive and Analysis System (GHAAS) system is currently being developed at the Institute for the Study of Earth, Oceans and Space of the University of New Hampshire. The GHAAS will maintain data on discharge, flow regulation, meteorology, topology and constituent loads. The GHAAS is grid-based with 0.5° spatial resolution. It organizes clusters of grid cells into simulated catchments which topologically resemble actual drainage basins. The GHAAS also organizes biogeophysical data sets for global change studies (Moore et. al., 1989). It thus has ready access to a suite of global landscape parameters useful to basin hydrology modeling, such as land cover, soils, elevation, population, urban centers, and nutrient stocks. The system maintains data sets from both ground-based studies as well as from remote sensing data and modeling experiments. Such an integrated information system, coupled to regional models, will be a critical determinant of our ability to identify and understand the dynamics of global change in the coming decades.



## CHAPTER IV

### FURTHER TESTS OF A MACRO-SCALE HYDROLOGY MODEL IN TROPICAL RIVER SYSTEMS

#### Introduction

The purpose of this paper is to test the ability of a macro-scale hydrology model, originally developed for the Amazon/Tocantins River, to simulate water balance and fluvial transport in another the large tropical river, the Zambezi located in southern Africa. Earlier work by Vörösmarty et. al. (1989) presented a distributed parameter model which calculated key elements of the terrestrial water balance (soil moisture, evapotranspiration and runoff) for the South American continent. The study also demonstrated that a simple fluvial transport model could convert the spatial and temporal dynamics of computed runoff into monthly discharge hydrographs that compared favorably with observed river flow.

Discharge was computed in the original set of experiments on the Amazon River using a uniform parameterization for the entire basin. Three parameters were used: a linear transfer coefficient representing instream flow; a factor initiating floodplain inundation; and, the proportion of channel flow conveyed to floodplain inundation. An optimal set of coefficients was identified using sensitivity analysis. In this paper I will test the

effectiveness of uniformly applying fluvial transport parameters in another tropical river system. I will also document whether the optimal set of coefficients for the Amazon bears any resemblance to that identified for the Zambezi.

The Zambezi catchment affords an extreme test of the original parameterization, and thereby offers an excellent opportunity to judge the general utility of the model in analyzing large tropical river systems. Although the Zambezi is today a highly impounded river, this paper will report on a model and data sets which simulate the drainage basin in a pre-disturbed state. I do this to facilitate comparison with earlier work on the essentially unregulated Amazon/Tocantins River system.

The remainder of the paper is organized into three sections. In the first I offer a brief site description of the Zambezi River catchment. I then go on to describe the general features of the model and recent improvements since the previous analysis of South America. Finally, I discuss a series of parameter and model performance tests. In that last section, I present a set of calibrated models that can be used for global change studies and describe the surface hydrology of the simulated basin.

#### Site Description and Biophysical Data Sets

Consideration of the Zambezi River drainage system (Figure IV-1) provides a useful contrast to previous work on

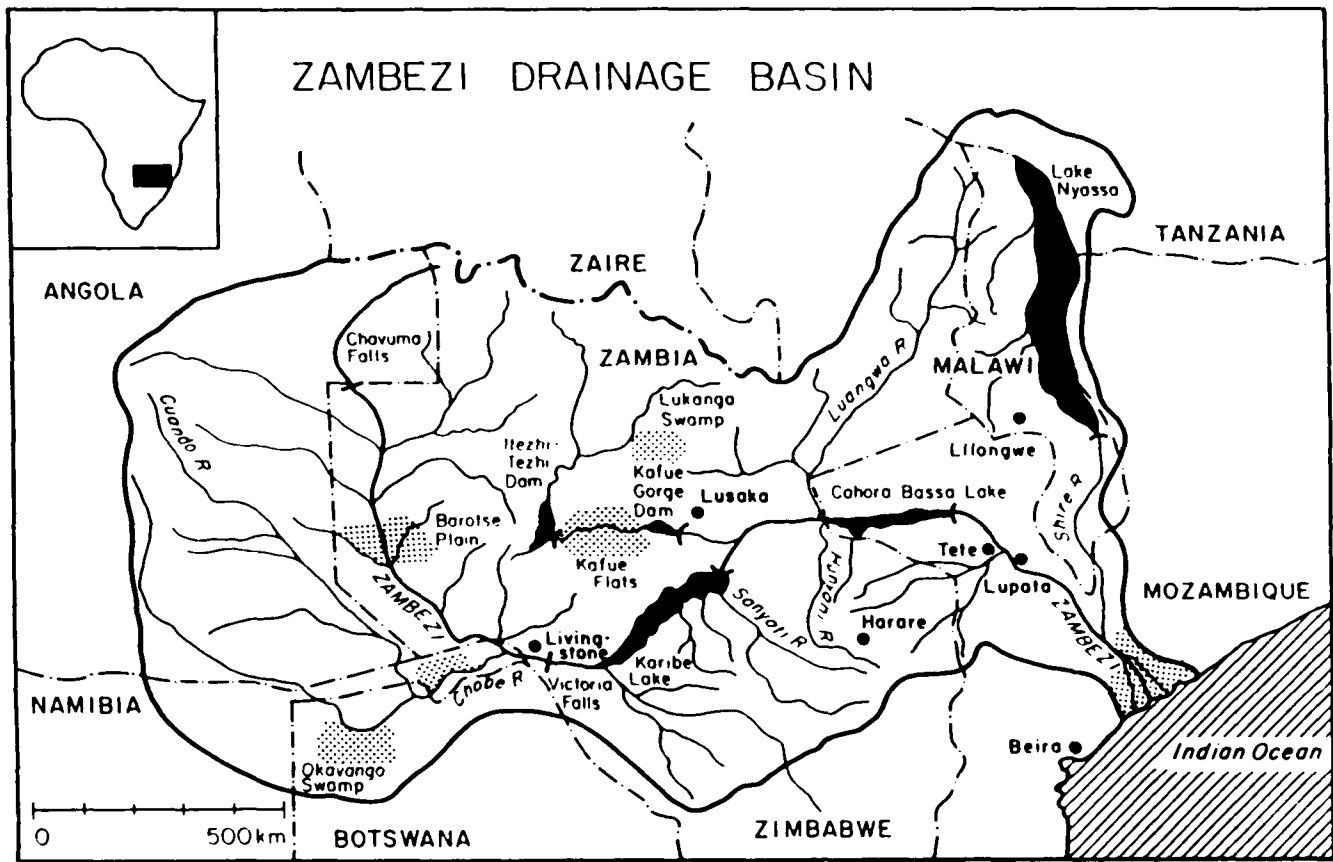


Fig. IV-1. Key features of the Zambezi River drainage system.

the Amazon. Although both are large tropical rivers, enormous differences are apparent in their key biophysical attributes including climate, vegetation and topography. The Zambezi is much drier than the Amazon. It yields less than 100 mm/yr runoff compared to almost 1000 mm/yr. In numerous reaches the Zambezi has an incised channel leading to the formation of waterfalls and rapids. In contrast, the mainstem Amazon shows a progressive reduction in gradient in the seaward direction (Sioli 1984, Rzóska 1978), and an extensive and well-developed floodplain system. Floodplains are relatively restricted along the mainstem Zambezi, although numerous dispersed wetlands are reported, especially in the northwest.

For the purposes of defining an accurate water balance, the Zambezi drainage system was divided into a series of subbasins. The subcatchments were determined by the availability of adequate mean annual or monthly discharge data. There is generally good correspondence among observed and simulated cumulative areas using cells arranged on a 0.5 degree (latitude x longitude) grid (Table IV-1). The largest disparities relate to whether relatively dry seasonal rivers in the western portion of the basin are included, and the simulated catchment (Figure IV-2) does not explicitly account for these. More than 400 grid cells constitute the Zambezi basin simulated in this study.

TABLE IV-1. Cumulative Drainage Area for Subcatchments of the Zambezi River System.

Location	Observed Area (km <sup>2</sup> )	Simulated Area (km <sup>2</sup> )	Reference for observed data
<u>Mainstream</u>	75,967	72,589	Balek (1977)
Chavuma Falls			
Livingstone	320,000	368,700	Reeve and Edmonds (1966)
(Victoria Falls)	to		Balek(1977), Bolton(1984)
	507,000		Sharma and Nyumbu (1985)
			Pinay(1988), Santa Clara
			(1988)
Upstream of Kariba	409,600	480,235	Reeve and Edmonds (1966),
	to		Begg(1973), Bolton (1984),
	684,000		Pinay(1988), Santa Clara
			(1988)
Cahora Bassa Rapids	1,000,000	916,683	Bolton (1984), Pinay (1988)
	to		Santa Clara (1988)
	1,180,000		
Lupeta	-NA-	1,044,400	-NA-
Mouth	1,119,000	1,218,290	Balon and Coche (1974),
	to		Bolton (1983), Pinay (1988)
	1,400,000		
<u>Tributaries</u>			
Kafue Mouth	155,000	143,588	Balek (1977), Bolton (1983),
			Pinay (1988), Mephram and Mephram (1987), Obrdlik et al. (1989)
Kafue at Itezhi-	106,200	93,019	Pinay (1988)
Tezhi			
Sanyati Mouth	43,500	38,205	Pinay (1988)
Luangwa Mouth	142,000	159,612	Balek (1977), Bolton (1983),
	to		Pinay (1988)
	148,000		
Hunyani Mouth	23,900	23,664	Pinay (1988)
Shire Mouth	115,000	138,644 <sup>a</sup>	Pinay (1988)

<sup>a</sup>Includes Lake Nyasa

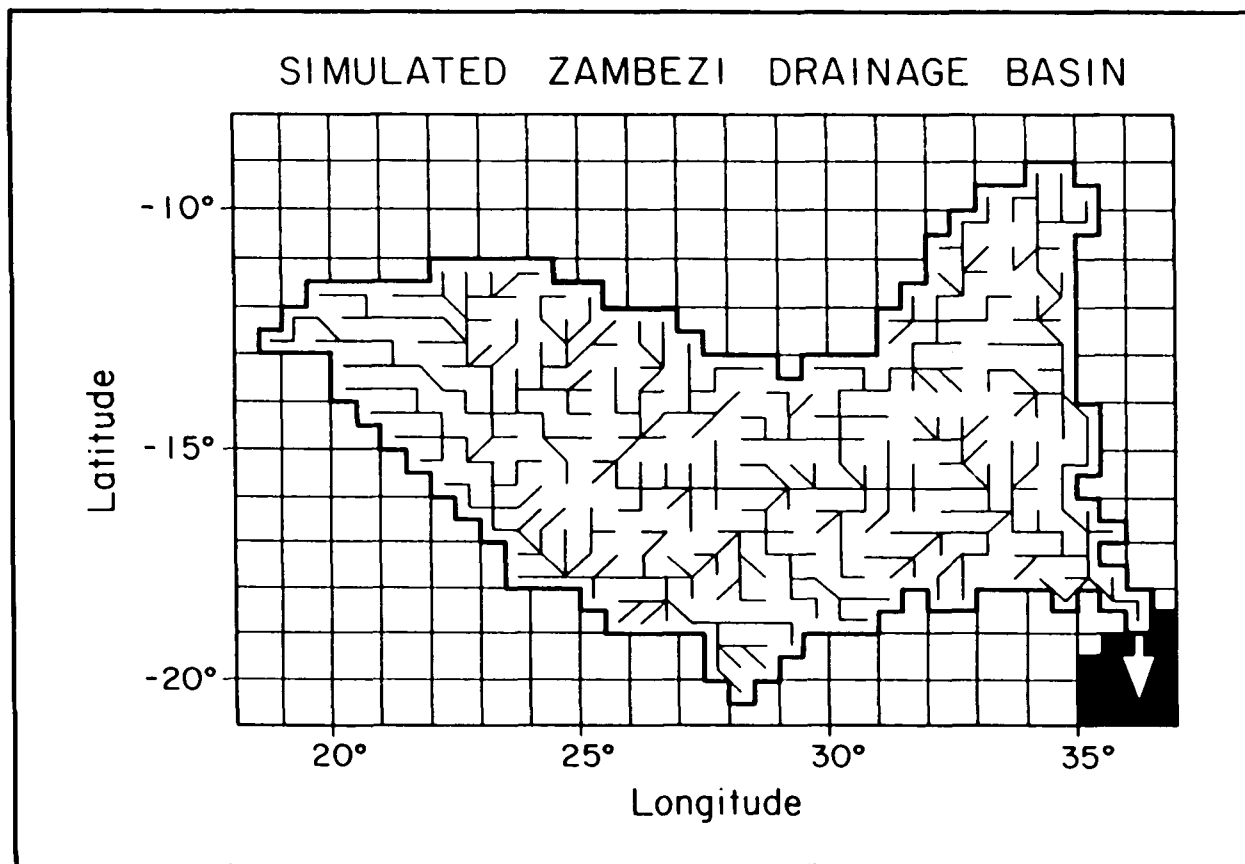


Fig. IV-2. Simulated topology of the Zambezi River system at 0.5 degree (latitude x longitude) spatial resolution. Flow directions were determined from Operational Navigation Charts (DMAAC, various years).

The key biophysical attributes of each of the 12 subbasins are given in Table IV-2. The subbasins have been classified by drainage basin "order". In the Table, a subcatchment of order two or higher represents an interbasin area, that is, a contributing area between the major upstream influent and major downstream effluent plus any intervening tributaries. It should be emphasized that subbasin order is based solely on the availability of discharge data and not on any geomorphological principles. The subbasins are shown in Plate IV-1.

The dominant vegetation throughout virtually the entire Zambezi region is tropical/subtropical deciduous woodland, although grassland, savanna, and forest are also present (Matthews 1983) (Plate IV-2). The vegetation is distributed across a variety of soil textures, including sands, loams, clay and lithosol (Plate IV-3). Updating information given in Vörösmarty et. al. (1989), I calculated mean rooting depth and available water capacity (field capacity minus wilting point) for each grid cell based on soils and land cover (Table IV-3). Mean depth in the subbasins varies between 0.87 and 1.52 m. Mean subbasin water capacity is between 106 and 197 mm, but exceeds 200 mm in certain locations (Plate IV-4). The overall capacity is smaller than that noted for the Amazon (Vörösmarty et. al. 1989), predominantly due to the absence of appreciable areas of tropical rainforest.

TABLE IV-2. Biophysical Attributes of the 12 Subbasins of the Zambezi River System. The basin names refer to those given in Plate 1.

Sub-Basin Name	Area <sup>a</sup> (1000 km <sup>2</sup> )	Dominant <sup>a</sup> Vegetation	Dominant <sup>b</sup> Soil Texture	Rooting Depth <sup>c</sup> (m)	Available <sup>c</sup> Water (mm)	Elevation <sup>d</sup> (m above MSL)	Gradient <sup>e</sup> (m)
<b>1st Order</b>							
Chavuma Falls	72.6	W	S	1.50	195	1198	59
Ithezhi-Tezhi	93.0	W	Cl	1.00	129	1195	43
Sanyati	38.2	W	S (Li)	0.96	124	1110	122
Huangwa	159.6	W	Cl(Li)	0.82	106	1143	165
Hunyani	23.7	W	L(Li)(S)	0.98	127	1018	209
Shire	138.6	W	Cl(C) (Li)	0.87	112	908	291
<b>2nd Order</b>							
Livingstone	296.1	W	S	1.52	197	1127	39
Kafue Gorge	47.6	W ( G )	Cl	0.98	126	1089	90
<b>3rd Order</b>							
Kariba	111.5	W ( SS )	S	1.17	151	1001	127
<b>4th Order</b>							
Cahora Bassa	74.4	W	S ( Sl )	0.87	113	744	205
<b>5th Order</b>							
Lupeta	127.6	W ( S )	Sl ( Cl )	1.30	168	821	196
<b>6th Order</b>							
Zambezi Mouth	35.3	SS	Cl ( C )	1.26	162	216	103

For Vegetation: W = Tropical/Subtropical Deciduous Woodland; G = Short Grassland, Meadow; S = Savanna, 10-40% woody cover; SS = Savanna, Shrub Cover; F = Tropical/Subtropical Evergreen Forest

For Soil Texture: S = Sand; C = Clay; Cl = Clay loam; Li = Lithosol; L = Loam; Sl = Sandy loam

<sup>a</sup> Matthews(1983)

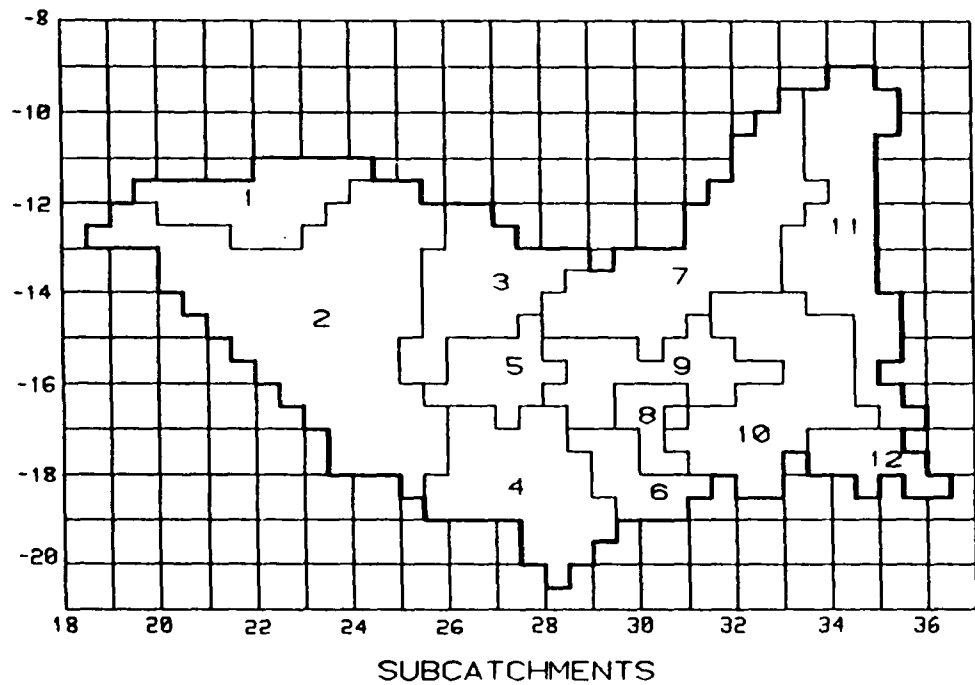
<sup>b</sup> FAO/CSRC(1974)

<sup>c</sup> Lookup function from Raich et al (1991)

<sup>d</sup> NCAR/NAVY (1984)

<sup>e</sup> Computed from elevation of nearest neighbors using 0.5 degree cells





- 1 Chavuma Falls
- 2 Livingstone
- 3 Ithezhi-Tezhi
- 4 Kariba Input
- 5 Kafue
- 6 Sanyati
- 7 Huangwa
- 8 Hunyani
- 9 Cahora Bassa
- 10 Lupata
- 11 Shire
- 12 Mouth

PLATE IV-1.

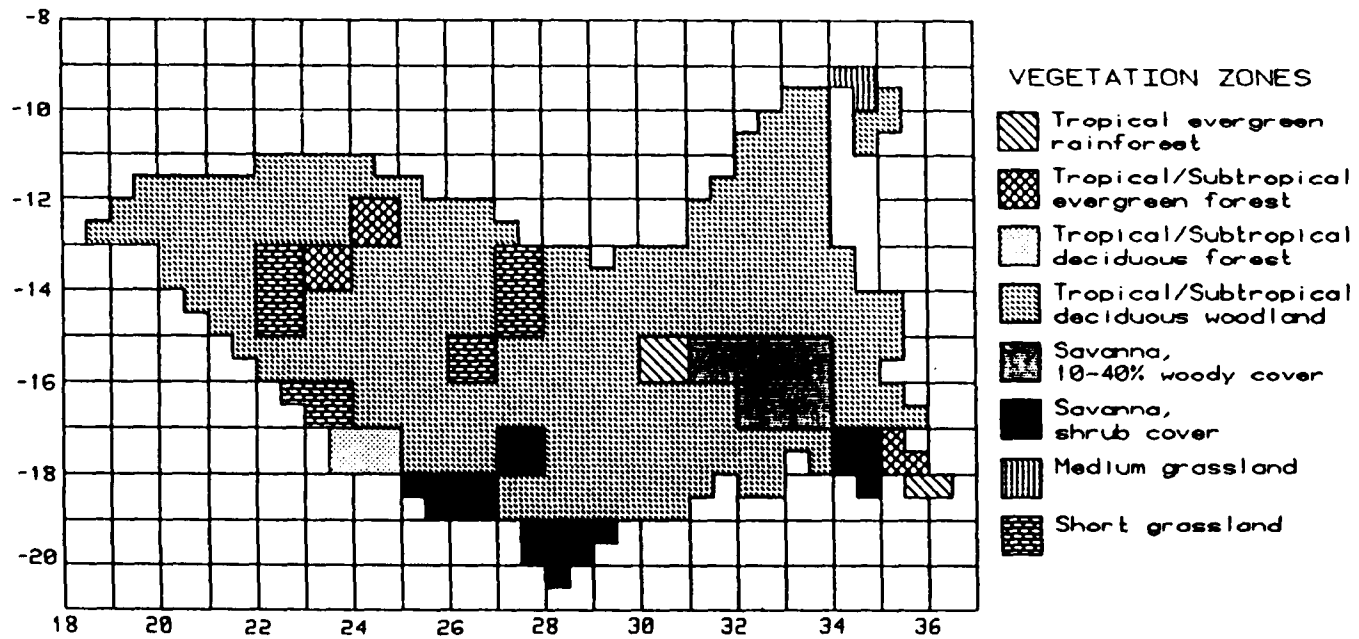


PLATE IV-2.

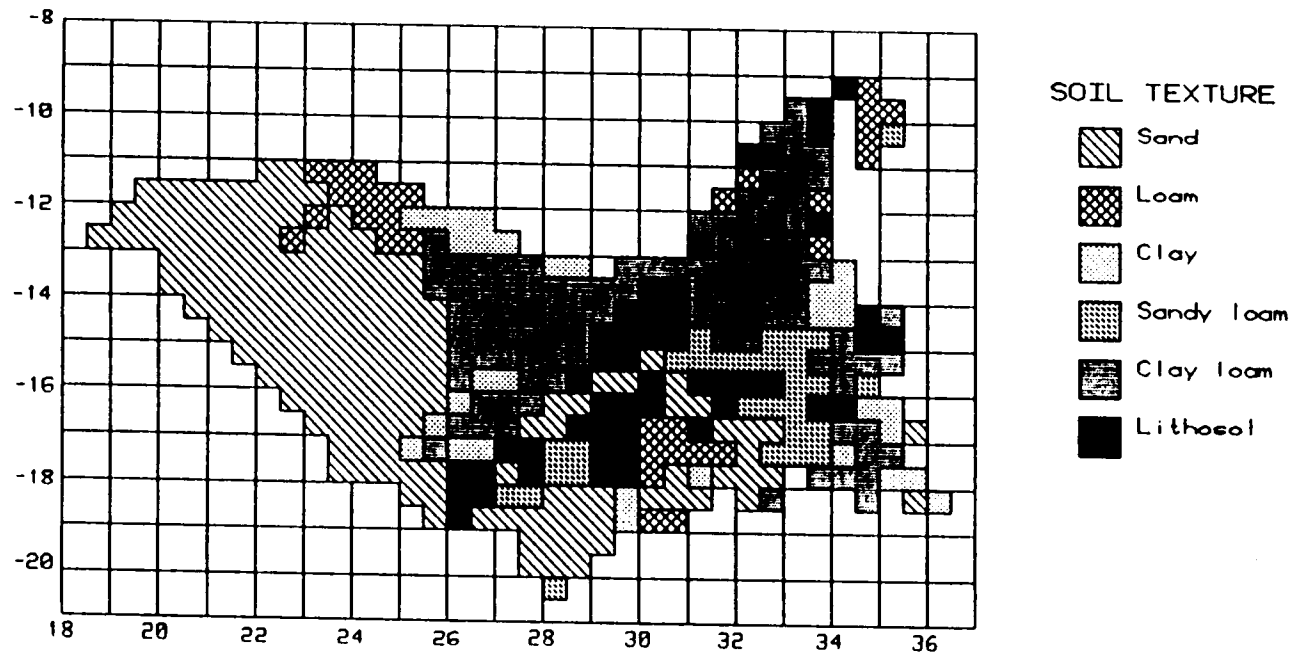


PLATE IV-3.

TABLE IV-3. Relationships Linking Vegetation Class, Soil Texture, Rooting Depth and Moisture Capacities of Soil

Vegetation	Sand	Sandy Loam	Silt Loam	Clay Loam	Clay	Lithosol
<u>Root Depth, m</u>						
Forest	2.50	2.00	2.00	1.60	1.17	0.1
Shrub/Savanna	1.50	1.67	1.50	1.00	0.67	0.1
Grassland	1.00	1.00	1.25	1.00	0.67	0.1
<u>Field Capacity, mm of water<sup>a</sup></u>						
Forest	525	500	580	512	410	29
Shrub/Savanna	315	418	435	320	235	29
Grassland	210	250	363	320	235	29
<u>Available Water Capacity, mm of water<sup>b</sup></u>						
Forest	325	260	260	208	152	13
Shrub/Savanna	195	217	195	130	87	13
Grassland	130	130	163	130	87	13

<sup>a</sup>Determined from percentage of total soil volume from Ratliff et. al. (1983): Sand (21%); Sandy-Loam (25%); Silt-Loam (29%); Clay-Loam (32%); Clay (35%); Lithosol (29%)

<sup>b</sup>Determined from Ratliff et. al. (1983) such that the difference between field capacity and permanent wilting point is 13%.

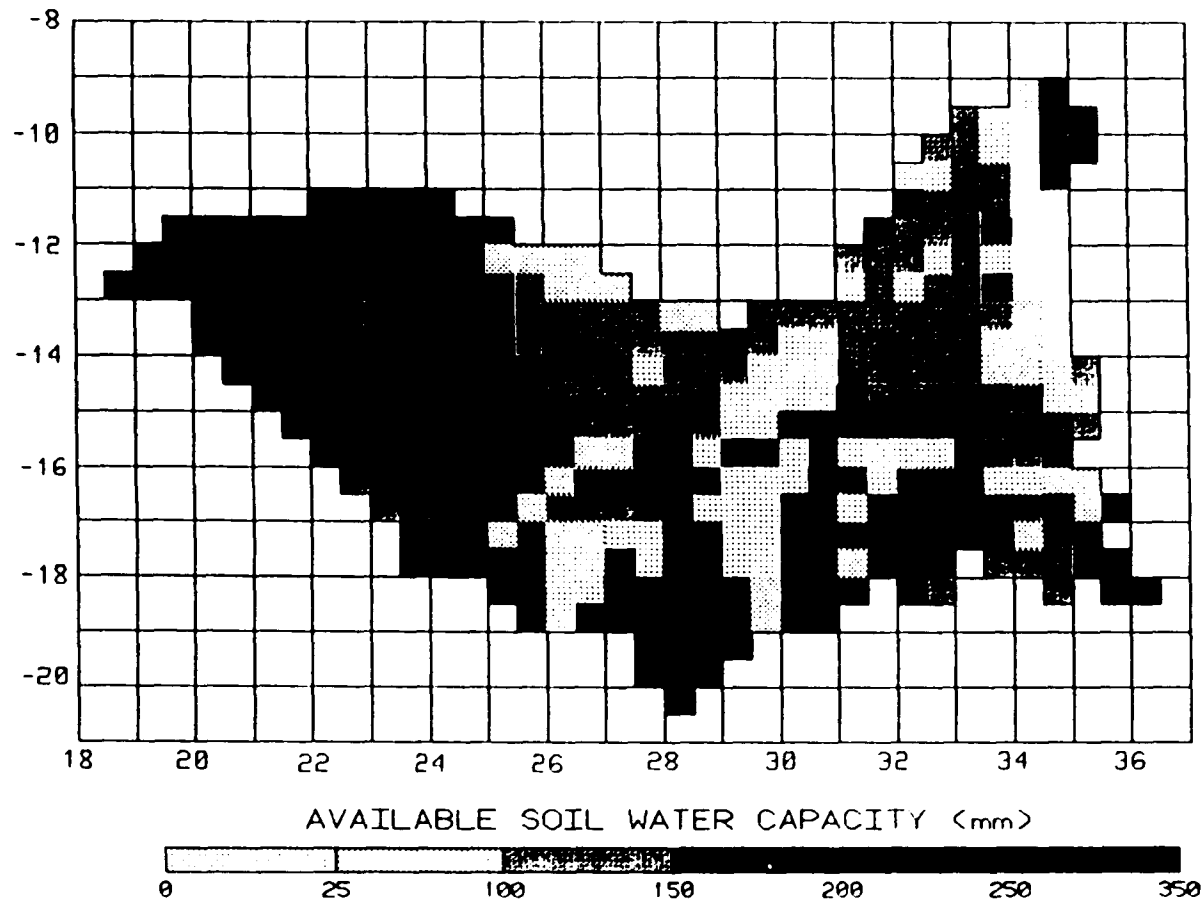


PLATE IV-4.

As evidenced by the progression of mean basin elevation (/gradient) in Plates IV-5 and IV-6 from Chavuma Falls (1198 m/59 m) to Livingstone (1127/39) to Kariba Input (1001/127) to Cahora Bassa (744/205) to Lupata (821/196) to the Zambezi Mouth (216/103), there is a broad region of drainage off the relatively flat Central African Plateau before the river begins its descent to the sea. This descent is marked by passage through a more mountainous zone downstream of the Kariba site.

Gridded 0.5 x 0.5 degree data sets were used to characterize climate dynamics at monthly intervals. Plate IV-7 shows mean annual precipitation and its seasonal distribution, as given by Legates and Willmott (1989). There is a strong gradient in mean annual rainfall with high values in the North and low values in the South, associated with the position of the drainage basin at the fringe of the Intertropical Convergence Zone. There are strong seasonal gradients as well. The movement of the Convergence Zone across the Zambezi is apparent, with a southward trend starting in October, a peak in January and a movement northward by April. According to this data set, maximum rates of rainfall in January can exceed 225 mm/month. In contrast, July is among the driest months with less than 25 mm/month precipitation throughout the entire basin.

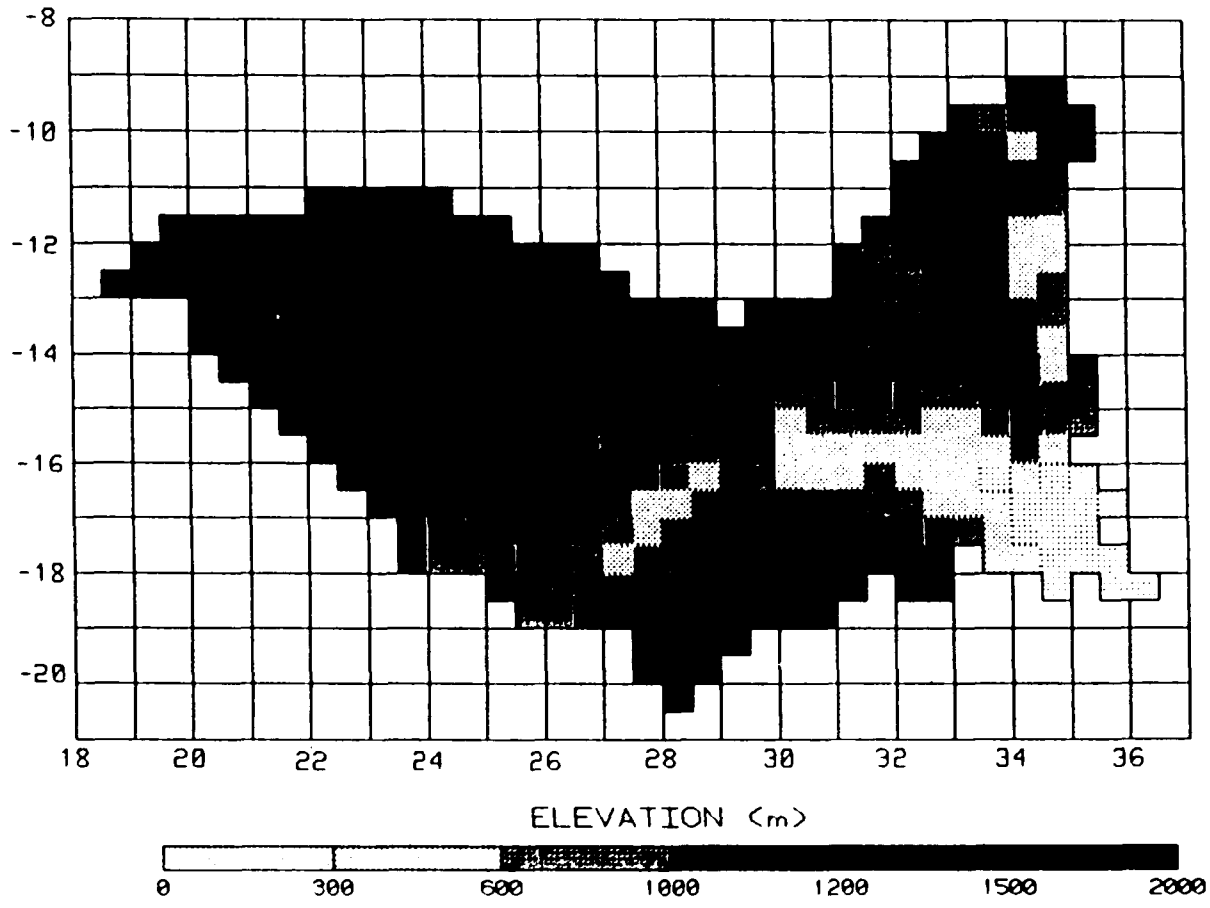


PLATE IV-5.

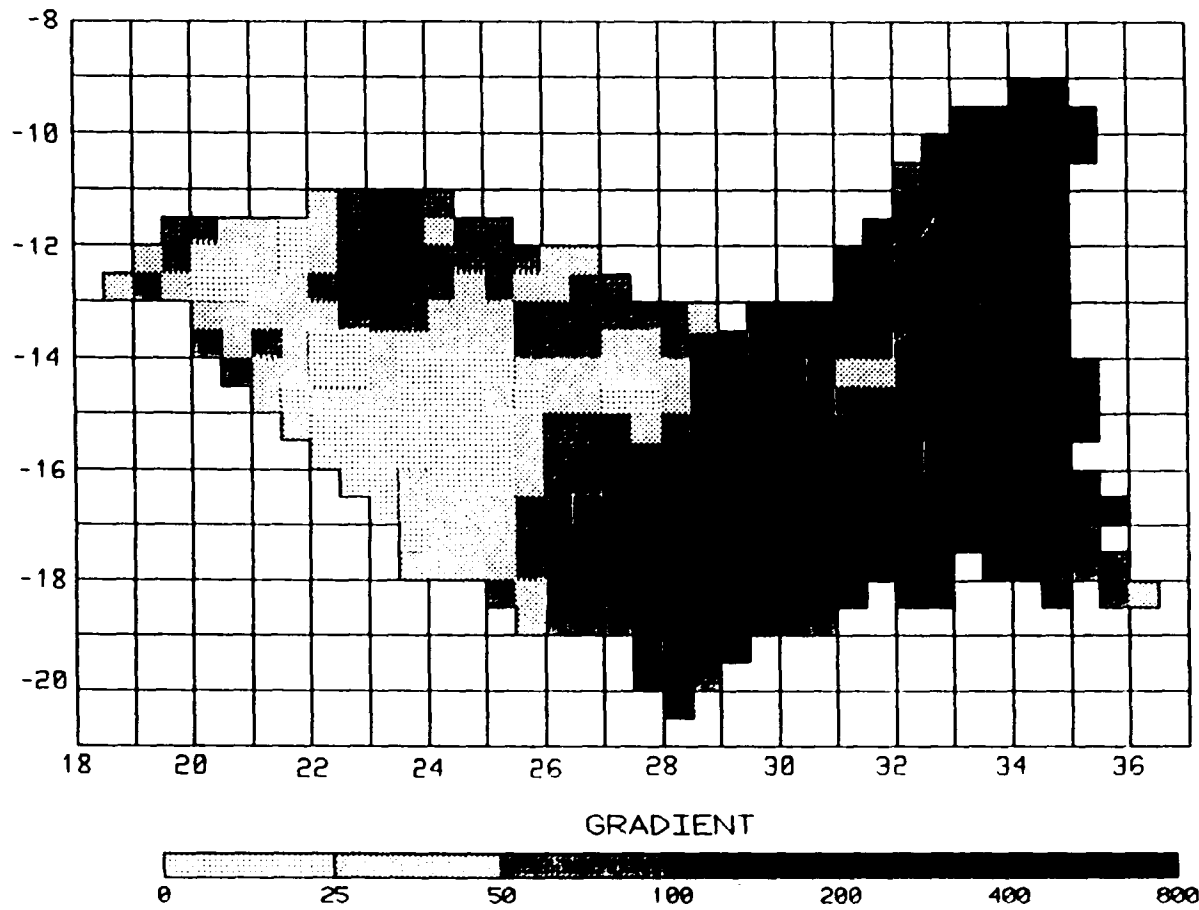


PLATE IV-6.



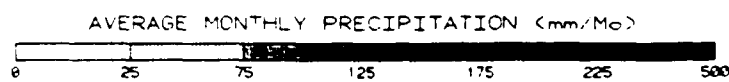
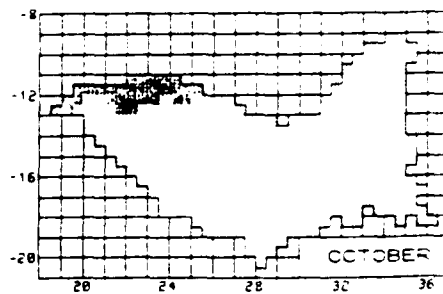
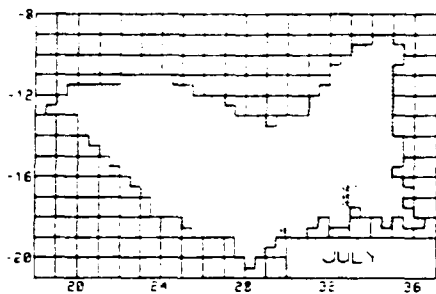
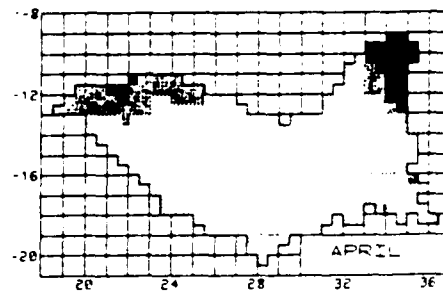
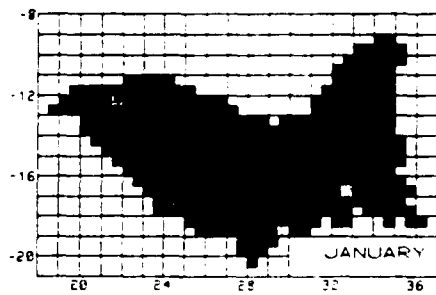
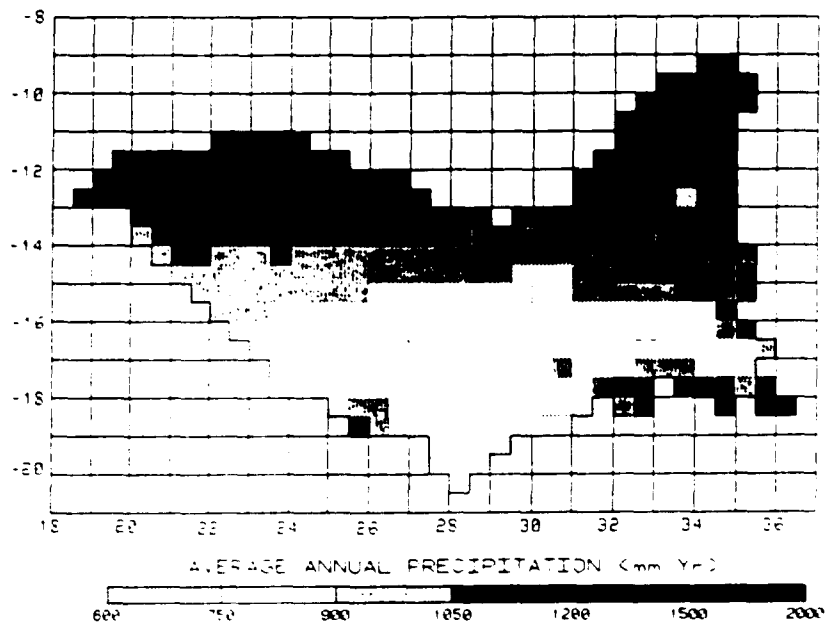


PLATE IV-7.

The distributions of temperature (Legates and Willmott 1989) (Plate IV-8) and net solar irradiance (Vörösmarty, unpublished data) (Plate IV-9) are used to determine monthly potential evapotranspiration (PET). There is an interesting North-South trend in mean annual temperature. Highest temperatures are along an East-West band in the mid-section of the basin. These are flanked by lower temperatures to the North, where cloud cover limits radiation, and to the South, where increasing distance from the equator becomes a key factor. A seasonal oscillation of more than 10° C characterizes much of the basin with coldest temperatures in July. Warmest temperatures occur in October rather than in January because of increased cloudiness during the rainy season.

Values for net solar irradiance were calculated from the formula of Black (1956):

$$I = I_t (0.803 - 0.340 C_1 - 0.458 C_1^2) \quad (1)$$

where  $I$  = net solar irradiance ( $\text{cal cm}^{-2} \text{ day}^{-1}$ ) for a grid cell,  $I_t$  is incoming solar radiation at the top of the atmosphere ( $\text{cal cm}^{-2} \text{ day}^{-1}$ ), and  $C_1$  = mean monthly cloudiness as a decimal fraction. Cloudiness was determined from the global data set of Hahn et. al. (1988), interpolated to 0.5 degree spatial resolution. An increase of annual net irradiance is present in the southward direction, reflecting the general pattern of cloudiness and

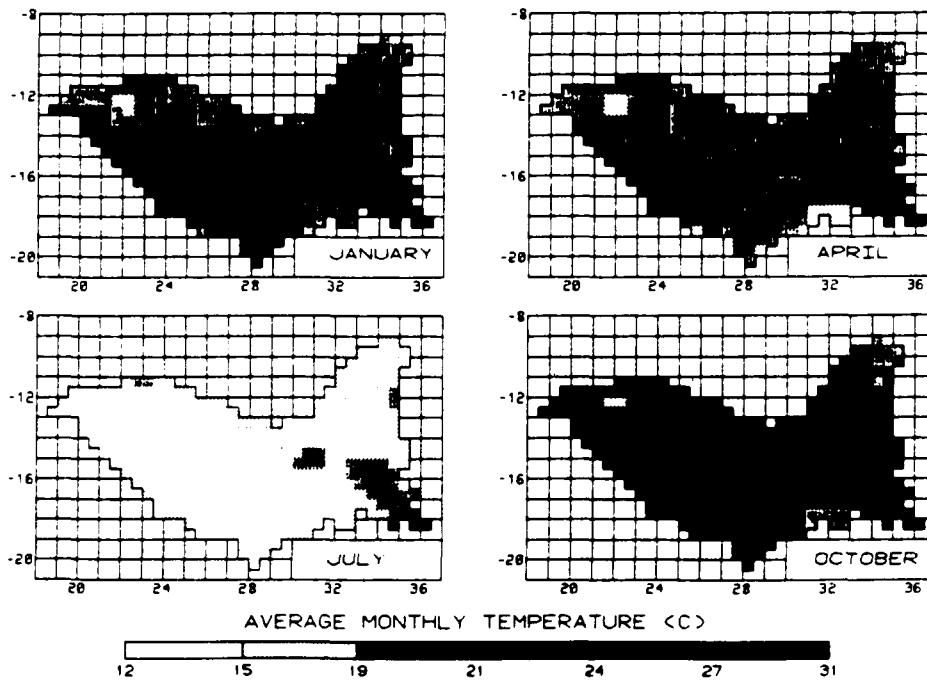
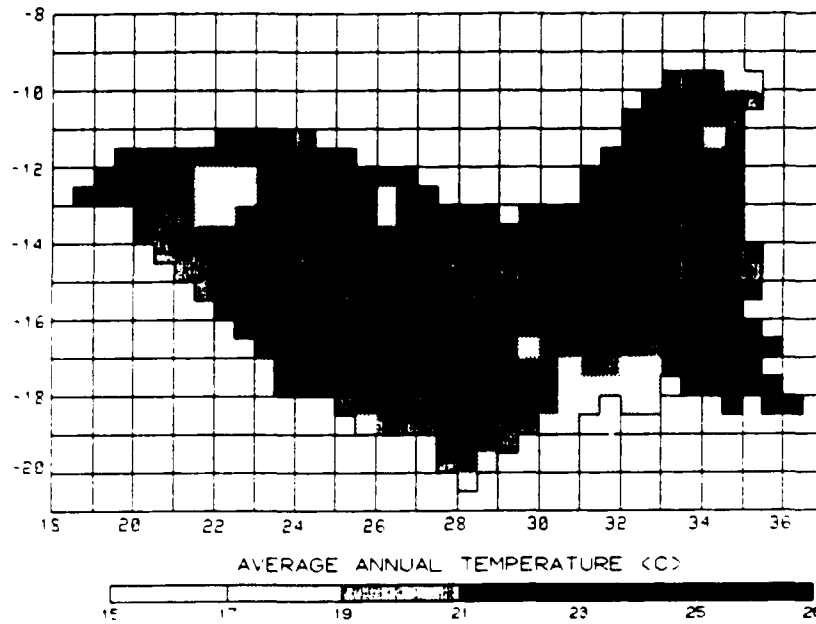


PLATE IV-8.

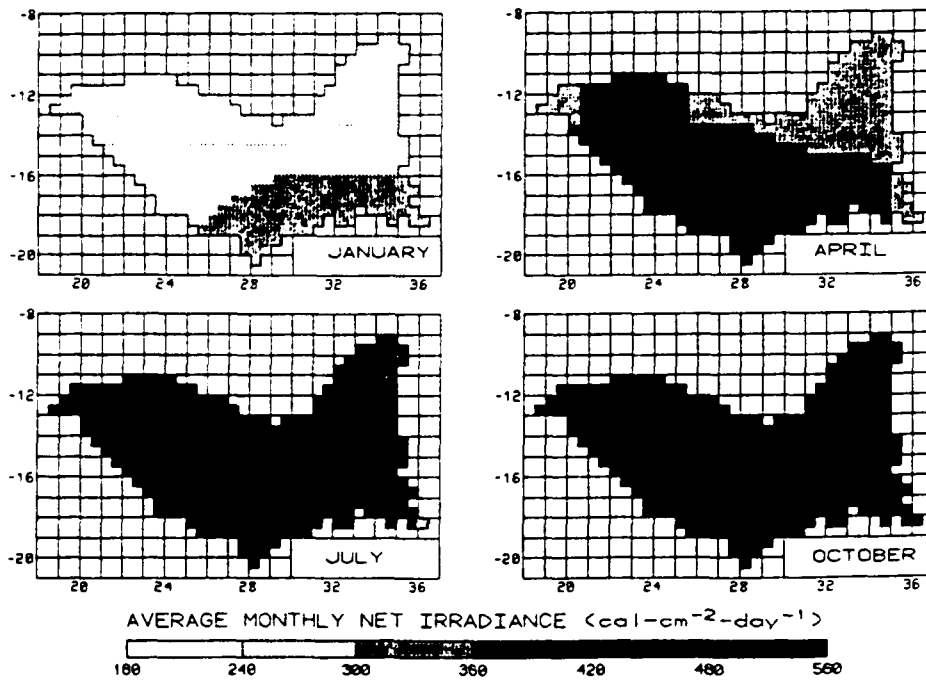
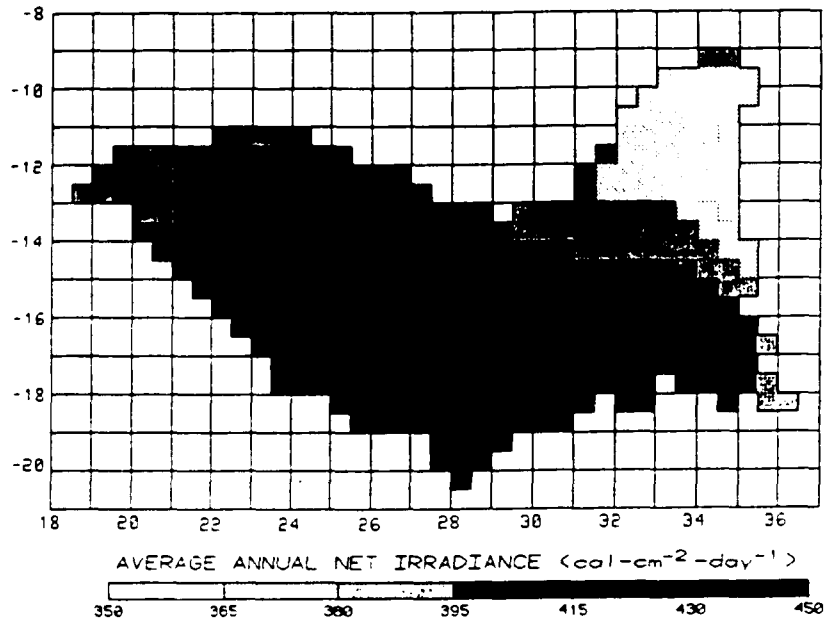


PLATE IV-9.

rainfall within the basin. The seasonal pattern of net irradiance also mirrors the movement of clouds across the basin during the rainy season, and is thus lowest during January and highest in July and October.

Potential evapotranspiration was calculated using the method of Jensen and Haise (1963). The formula was analyzed in Vörösmarty and Moore (1991), Allen (1990), and McGuinness and Bordne (1972) and was shown to be suitable over a broad geographic range. It is a simple representation based on net solar radiation and temperature:

$$PET = 1.6742 \times 10^{-2} I D (0.014 [(1.8T) + 32] - 0.37) \quad (2)$$

where PET is in mm/month, T is mean monthly temperature (°C) and D is the number of days in a month. The first constant converts from irradiance (I) to equivalent depth of water. The spatial patterns of PET (Plate IV-10) are complex, reflecting variations in both the temperature and radiation. The middle sections of the Zambezi are characterized by relatively high mean annual values. Flanking zones to the North and South are limited by excessive cloud cover and lower temperatures, respectively. Seasonally, PET for the entire basin is lowest during the peak January rainy season and greatest during the October period when clouds are generally absent and temperatures are rising.

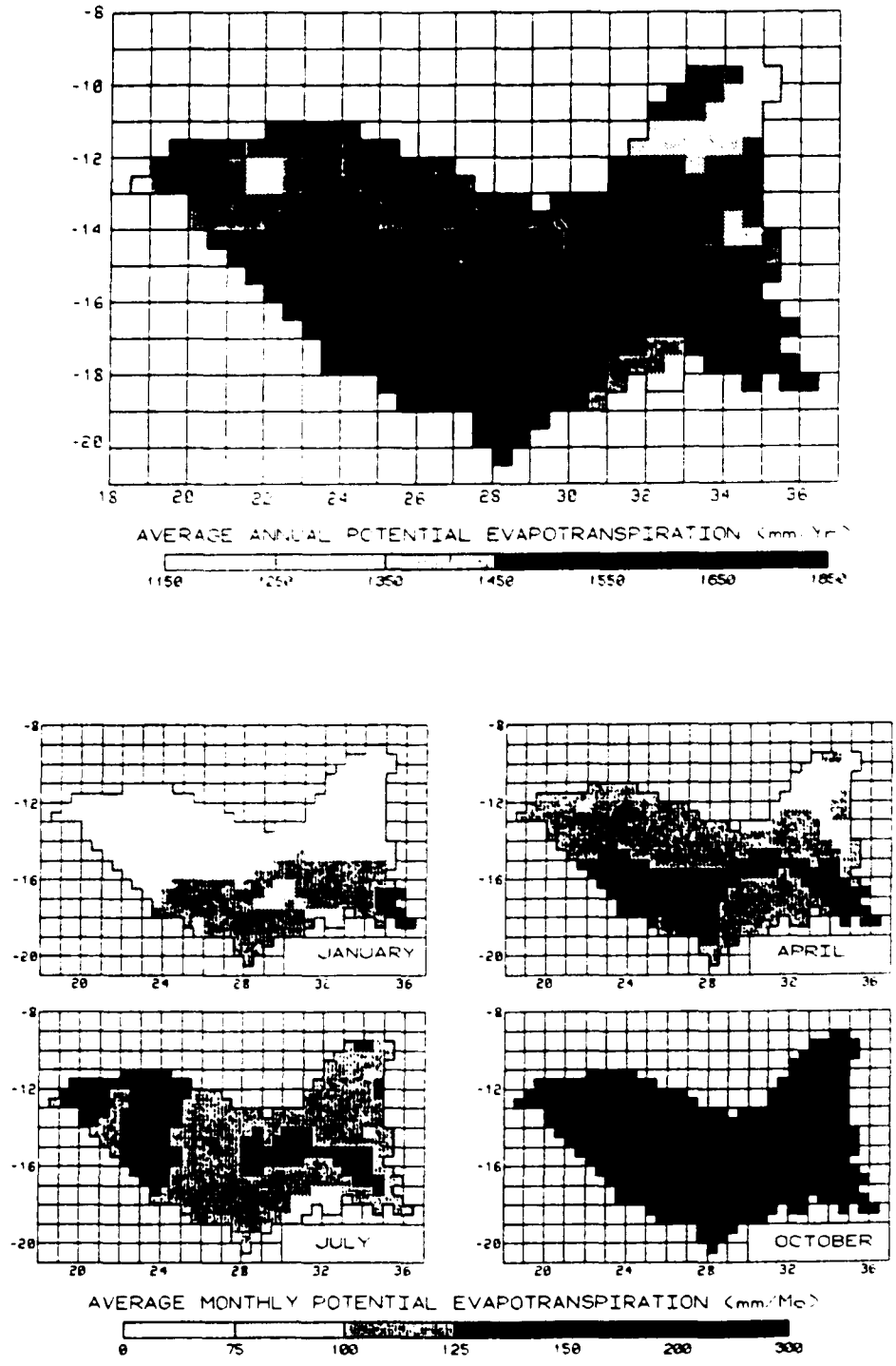


PLATE IV-10.

### Model Description

The Water Balance/Water Transport Model (WBM/WTM) is a distributed parameter model operating at regional to continental scales (Figure IV-3). It represents a two-level modeling approach, simulating both vertical and horizontal water fluxes (Becker and Nemec 1987). The WBM/WTM is a linked algorithm that first calculates key elements of the terrestrial water budget. The fluvial transport algorithm then integrates the predicted spatial and temporal patterns of runoff and converts these into discharge hydrographs for any cell within a simulated drainage basin. The next two sections detail the two algorithms.

#### Water Balance Model

The WBM relies on the many biophysical data sets described above. It converts grid cell-based data on regional precipitation, temperature, radiation, vegetation and soils into predictions of soil moisture (SM), evapotranspiration (ET) and runoff (RO) at monthly timesteps. The WBM is based on techniques developed by Thornthwaite and Mather (1957) and subsequently modified by Vörösmarty et. al. (1989) and Rastetter et. al. (1991).

Soil moisture is determined from interactions among rainfall and PET. Vörösmarty and Moore (1991) presented three domains in which soil moisture calculations are made: rain in excess of PET but soil moisture (SM) less than water holding capacity; rain in excess of PET but SM equal to

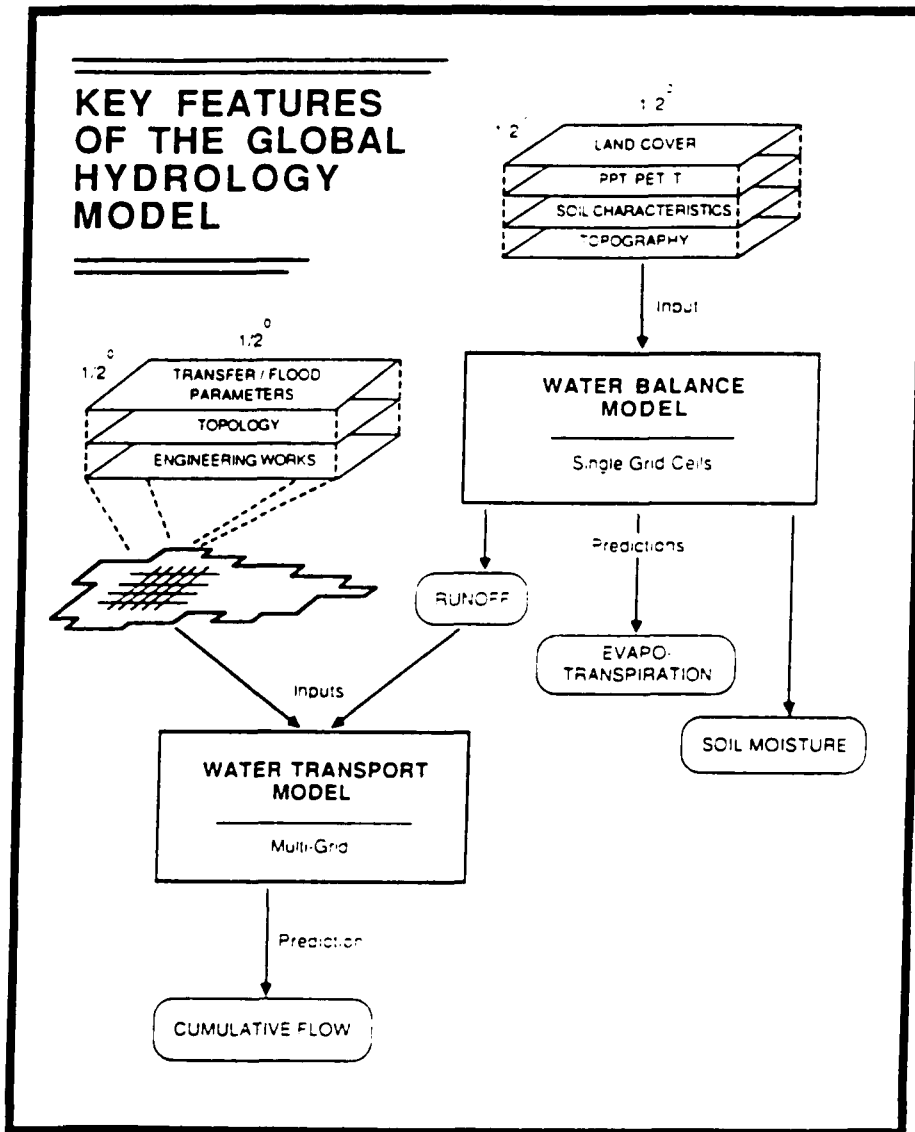


Fig. IV-3. Structure of the global hydrologic model, showing the relationship between the Water Balance and Water Transport Models and a set of gridded data sets.



capacity; and rainfall exceeded by PET. A single function combining these three contingencies is derived and tested in Rastetter et. al. (1991). The method corrects for bias in soil wetting and drying as a consequence of using monthly timesteps to simulate what in reality occurs at much finer time scales. The aggregated equation to predict the change in soil moisture over a month is:

$$dSM/dt = D [p \bar{R} \{g(SM) + [1-g(SM)] e^{-\bar{PET}/\bar{R}} - e^{-\bar{PET} \cdot (AWC+SM)/\bar{R}}\} - \bar{PET} g(M)] \quad (3a)$$

$$p = 1 - e^{-uR} \quad (3b)$$

$$\bar{R} = R / (D p) \quad (3c)$$

$$g(SM) = \frac{ET - R}{PET - R} = \frac{(1 + e^{-5.0(SM/AWC)})}{(1 + e^{-5.0})} \quad (3d)$$

where SM is soil moisture (mm), p is the probability of having a rainy day within a particular month,  $\bar{R}$  is average daily rainfall for rainy days (mm/day),  $\bar{PET}$  is average daily potential ET (mm/day), g(SM) is a soil drying function representing the proportion of residual potential ET that actually passes from the soil as ET (i.e. when both are corrected for immediate rainfall loss), AWC is available water capacity (mm) (i.e. field capacity minus wilting point), u is a coefficient set to 0.005 from Rastetter et.

al. (1991),  $R$  is monthly rainfall (mm/month), and  $D$  is again the number of days in the month.

The differential equation for soil moisture (3a) is integrated using a fifth- to sixth-order Runge-Kutta algorithm (International Mathematical and Statistical Libraries, Houston, Texas, USA, 1982), and calculations progress until a quasi-steady state is achieved over the year. Once soil moisture is determined, the remaining elements of the water balance can be computed. Thus,

$$ET = \min[PET, (R - dSM/dt)] \quad (4)$$

where  $ET$  is computed evapotranspiration (mm/month).

Runoff is generated by the WBM based on rainfall, computed  $ET$ , and the status of soil moisture within each grid cell. Excess water is defined as the difference between rainfall and the sum of  $ET$  and the change in soil water over the month. In practice, contributions to this pool are active when there is no soil moisture deficit relative to  $AWC$ , since surplus rainfall would otherwise be required to recharge the soil. From this storage pool, runoff is generated as a linear function of pool size. For rainfall detention and runoff:

$$dD_r / dt = (R - ET - dSM/dt) - \beta D_r \quad (5a)$$

$$RO = \beta D_r \quad (5b)$$

where  $D_r$  is rainfall-derived detention (storage) pool (mm),  $B$  is a linear transfer coefficient ( $\text{mon}^{-1}$ ) set equal to 0.5 from Thornthwaite and Mather (1957) and Vörösmarty et. al. (1989),  $RO$  is rainfall-derived runoff (mm/mon). For Lake Nyasa grid cells  $RO$  was defined as simply the difference between monthly rainfall and PET, with no detention pools entering into the calculations.

#### Water Transport Model

Fluvial transport is simulated using a multi-cell, dynamic model that computes discharge through each cell of the simulated drainage basin. It combines runoff produced by WBM with information on network topology, fluvial transfer rates and the timing and extent of floodplain inundation. The network topology shown in Figure IV-2 was determined from a series of 1 : 1,000,000 Operational Navigation Charts (DMAAC, various years). Channel flow in the WTM is determined from a linear reservoir model, and discharge is predicted as a monthly mean. Each grid is considered a storage pool with a characteristic residence time ( $t$ ). A standard transfer coefficient,  $K$  ( $t^{-1}$ ), is assigned to all cells and then modified on the basis of geometric considerations. The standard  $K$  is associated with drainage across a cell in the N-S or E-W axis. The  $K$  is then lengthened or shortened depending on the location of influents and effluents.

The WTM also predicts temporary floodplain storage. Floodplain and swamp exchanges take place whenever the monthly discharge exiting a grid cell exceeds a specified fraction of long-term mean annual flow. Above this fraction and with increasing discharge, inundation is simulated by apportioning the potential net increase in water storage between the channel and its associated floodplain. Floodplain storage increases until the time derivative of grid cell water storage becomes negative. During flood recession, the potential net decrease in grid cell storage is accounted for by changes in channel and floodplain storage using the same ratios as for rising waters. These calculations attenuate the amplitude of rising flood waves and augment downstream discharge during periods of falling stage. For a single grid cell, the resulting flow and continuity equations are:

$$dS_c / dt = \left( \sum_1^n Q_u \right) - Q_d + Q_g + Q_f \quad (6a)$$

$$dS_f / dt = -Q_f \quad (6b)$$

$$Q_d = K S_c \quad (6c)$$

$$Q_g = A (RO) / 1000. \quad (6d)$$

$$Q_f = -r_f \left[ \left( \sum_1^n Q_u \right) - Q_d + Q_g \right] \quad Q_d \geq c_f Q_{dma} \quad (6e)$$

$$Q_f = 0$$

$$Q_d < c_f Q_{dma} \text{ or}$$

where  $S_c$  is channel storage in a grid cell during a month ( $m^3$ ),  $S_f$  is floodplain storage ( $m^3$ ),  $K$  is the downstream transfer coefficient (month<sup>-1</sup>),  $A$  is the area of the grid cell ( $m^2$ ),  $n$  is the number of donor grid cells,  $Q_u$  is monthly upriver input,  $Q_d$  is monthly discharge from the cell,  $Q_g$  is input from runoff generated within the grid,  $Q_e$  is exchange between channel and floodplain (+ denotes floodplain to channel), and  $Q_{dma}$  is the mean annual downstream discharge. All  $Q$  values are in  $m^3$  per month. The coefficient  $c_f$  is the flood initiation parameter, giving the proportion (0.0 to 1.0) of  $Q_{dma}$  required to invoke floodplain exchanges. When active,  $r_f$  determines the ratio (0.0 to 1.0) of potential volume change assigned to floodplain storage.

The established topology (Figure IV-2) together with the flow and continuity equations (6a-6f) creates a system of linked differential equations. The system is solved for  $S_c$  and  $S_f$  using the same fifth- to sixth-order Runge-Kutta integration routine as for the WBM. The model applies monthly runoff values from each of 409 grid cells of the Zambezi catchment until a quasi-steady state solution emerges for the entire set of cells.

### Model Performance Tests

Model performance tests were used in calibrating both the WBM and the combined WBM/WTM models. An unbiased estimator of model performance relative to observed data is given by Willmott (1982) and Willmott et. al. (1985):

$$d = 1 - \left\{ \frac{\sum_1^{\text{obs}} |P_i - O_i|^y}{\sum_1^{\text{obs}} (|P'_i| + |O'_i|)^y} \right\} \quad (7a)$$

$$P'_i = P_i - O_m \quad (7b)$$

$$O'_i = O_i - O_m \quad (7c)$$

where  $d$  is the "index of agreement,"  $\text{obs}$  is the total number of stations,  $P_i$  is the  $i$ th model prediction,  $O_i$  is the corresponding observation,  $y$  is an exponent set to 1.0 based on discussion in Willmott et. al. (1985), and  $O_m$  is the observed mean.

The data were pooled in two ways. In the first, 13 stations will be used to develop an aggregate Water Balance Model parameterization based on mean annual flow (i.e.  $\text{obs} = 13$ ;  $O_m$  is the mean of the 13 sites). Table IV-4 gives the observed mean annual flow at the selected subcatchments. To the extent possible, the data were screened to reduce the effect of the large Kariba, Itzhi-Tezhi, Kafue Gorge, and Cahora Bassa impoundments.

TABLE IV-4. Mean Annual Discharge for Selected Subcatchments of the Zambezi.

LOCATION	MEAN ANN DISCHARGE (m3/sec)	YRS of RECORD	REFERENCE
<b><u>MAINSTEM</u></b>			
Chavuma Falls	761	- NA -	UNEP (1986)
Livingstone	1323 <sup>a</sup>	1924-85	CAPCO (unpublished data, 1988)
Upstream of Kariba	1633	1924-79	Plinston (1981)
Cabora Bassa	2848	- NA -	UNEP (1986), Hall et al. (1976)
Lupata	3349 <sup>a</sup>	1930-65	CAPCO (unpublished data, 1988)
Mouth	3171	- NA -	UNEP (1986), Borchert and Kempe (1985)
<b><u>TRIBUTARIES</u></b>			
Sanyati Mouth	108	- NA -	Pinay (1988)
Kafue @ Itezhi-Tezhi	304 <sup>a</sup>	1924-39/ 50-70	CAPCO (unpublished data, 1988)
Export from Kafue Flats	282	- NA -	Mephram and Mephram (1987)
Kafue Mouth	320 <sup>a</sup>	1924-70	CAPCO (unpublished data, 1988)
Luangwa Mouth	530	1925-70	Bolton (1983)
Hunyani Mouth	44	- NA -	Pinay (1988)
Shire Mouth	476	- NA -	UNEP (1986)

<sup>a</sup> Also gives monthly discharges

\*\*\*\*\*  
Criteria used for assembling the above table:

Entries assembled from Table III of Vörösmarty and Moore (1991). The data set of Balek (1977) was deemed poor by Bolton (1983) after careful analysis, and so was omitted from this analysis. For the mouth of the Zambezi, data from Ambroggi (1980) were discredited by Borchert and Kempe (1985) and this information was also omitted. When multiple entries were encountered, and the author was unable to determine the quality of the data, a simple mean was taken.

The index of agreement (d) and % error values were also used to parameterize channel flow dynamics using discharge hydrographs at Livingstone, Itezhi-Tezhi and Lupata. (The hydrograph at Kafue was not included in the analysis due to significant local alteration by the adjacent Kafue Flats). In these cases obs = 12;  $Q_m$  is mean annual flow at each site. A weighting of these d values will be used to obtain an aggregate measure of model performance. The weighing is based on flowrate and number of years of record such that:

$$d_{wt} = \frac{\sum_{\text{sites}} d_j (Q_{dmaj}) (Y_j)}{\sum_{\text{sites}} (Q_{dmaj}) (Y_j)} \quad 18$$

where  $d_{wt}$  is the weighted index of agreement for the scenario, sites is the total number of station hydrographs,  $d_j$  is site j's index of agreement,  $Q_{dmaj}$  is site j's mean annual discharge, and  $Y_j$  is the number of years of record for site j.

A % error estimate was also formulated:

$$\%ERR = 100 \left[ \frac{\sum_{\text{obs}} (|P_i - O_i| / |O_i|)}{\text{obs}} \right] \quad 19$$

A similar weighting was given to the % error calculation as for the index of agreement.



## Results and Discussion

### Preliminary Calibration -- Water Balance

The first and most obvious requirement of a calibrated basin-scale model is to predict the overall water balance. The WBM, in conjunction with the data sets described earlier, was unable to compute reasonable water balance estimates. There was a systematic and substantial overestimate of mean annual runoff (Figure IV-4). For the basin as a whole, runoff was in error by nearly 200%. The degree of disparity emphasizes the fact that runoff in such relatively dry regions is determined by a precarious balance between precipitation and evapotranspiration that is difficult to quantify. Given the success of the model in South America, I assumed that the problem was not linked to the algorithm per se, but instead to intrinsic errors in the input data fields.

It is not known specifically which data sets may have singly or in combination produced the bias. For the climatic data two possibilities exist: a). the nominal precipitation was systematically overestimated or b). the nominal potential ET fields were systematically underestimated. In addition, underestimating the effective available water capacity of soils can cause significant errors in water balance. A smaller hydraulically active zone restricts soil-derived evapotranspiration, facilitates soil recharge during wet periods and enhances runoff.

## MEAN ANNUAL RUNOFF

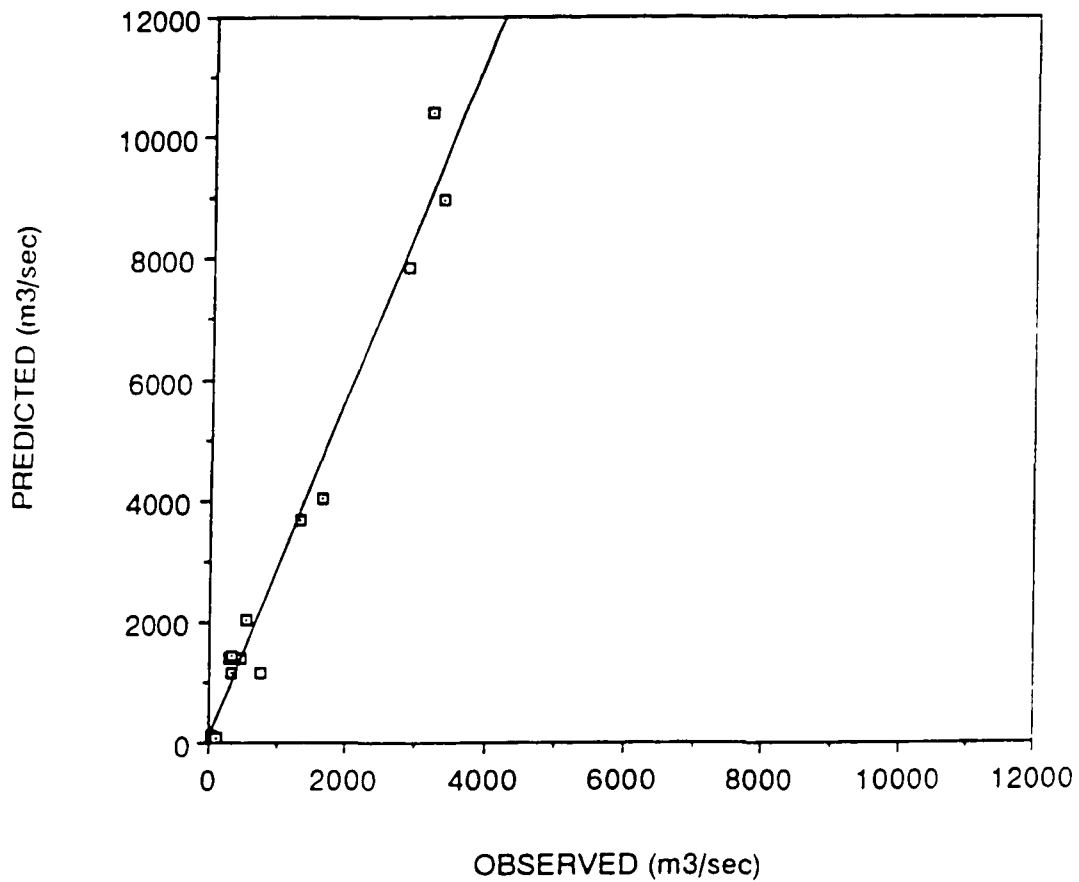


Fig. IV-4. Model performance using WBM and existing biophysical data sets. Predictions systematically overestimate observed discharge. The relationship depicted is :  $\text{pred} = 2.837 \text{ obs} + 55.31$ ,  $r^2 = 0.97$ . Observed data for mean annual discharge are from Table IV-4.

Willmott and Robeson (1990) describe the phenomenon in which interpolated climatological fields are under or overestimated based on the richness of the contributing station data. Systematic overestimates in precipitation normally occur when the station data are sparse, as in the Zambezi region (Legates and Willmott 1990). Further, overestimates are likely to occur in transition zones where gradients in precipitation are strong (C.J. Willmott, personal communication). The Zambezi basin, at the fringe of the Intertropical Convergence Zone, may suffer from this effect.

An underestimate of the effective evapotranspiration may also have contributed to errors in the regional water budget. Numerous factors may be involved, both natural and anthropogenic. For example, there has been a sustained expansion of irrigated agriculture in the region (van der Leeden et. al. 1990, van den Wall Bake 1986, Pinay 1988) which would serve to retard the passage of water off the landscape and direct it instead to the atmosphere. There are also numerous small reservoirs (Ward 1980, van der Wall Bake 1986, Pinay 1988), which would have a similar effect. Large areas, especially in the northern regions of the Central African Plains, are punctuated by low-lying dambos, or swampy, treeless basins where rainwater and runoff collect and subsequently evaporate (Mephram and Mephram 1987, Balek 1977, FAO/UNDP 1968). The role of deep-rooted

phreatophytes in the region is of unknown importance. Dunne and Leopold (1978) cite rates of water loss amounting to  $0.02 \text{ m}^3/\text{sec}\text{-km}^2$  for the southwestern USA. Assuming similar rates in the Zambezi, less than 15% of its drainage area would be required to lose an equivalent of its mean annual discharge to the Indian Ocean through this mechanism. In the more arid regions alluvial consumption of discharge (Yair and Lavee 1985, Thomsen and Schumann 1968) may further serve to reduce effective runoff from the landscape.

Great uncertainty surrounds the character of the hydraulically active root zone. Plate IV-2 gives a very broad overview of ecosystem types, and the assumed rooting depths show a relatively small range (Table IV-2). The functions relating ecosystem type to rooting depth are based essentially on general data provided by Thornthwaite and Mather (1957) and the general ecological literature. Certain ecosystems are known to have more extensive root systems than those assumed in the current study (Geiske et. al. 1990, Reichle 1981, FAO/CSRC 1974), but how these systematically influence available water capacity derived from a relatively crude land cover data set cannot now be assessed.

Further uncertainties prevail in defining the hydraulically active soil water capacity. The current WBM uses "available water capacity" defined as the difference between field capacity and permanent wilting point. This

essentially reflects assumptions made by the climate and climate modeling community (e.g. Willmott et. al. 1985, Serafani and Mintz 1990, Kellogg and Zhao 1988). However, numerous studies (Rastetter et. al. 1991, Vörösmarty et. al. 1989, Pastor and Post 1984, Dunne and Leopold 1978, Thornthwaite and Mather 1957) have calculated water budgets in which soil water is drawn well below the wilting point, increasing the apparent hydraulically active zone. Such increases can essentially double the active zone in relation to available water capacity (Table IV-3 and Vörösmarty et. al. 1989) and correspondingly decrease runoff.

I formulated a preliminary calibration of the water balance by applying adjustment factors to the precipitation, potential ET and water capacity fields. Each adjustment (1.00 = nominal data set value) was applied uniformly across all grid cells of the basin and over all simulated months. The factors that produced the best fit were 0.73 for precipitation, 1.65 for potential ET and 3.00 for the available water capacity. Figure IV-5 gives the resulting plot of observed and predicted discharge for the precipitation-corrected scenario. Similar plots were obtained for the potential ET and water capacity adjustments, and in each case the slope was close to 1.00. Intercepts were on the order of 100 m<sup>3</sup>/sec, so that a small systematic bias remains with each adjustment. The index of agreement for each of the adjustments were 0.881, 0.879 and

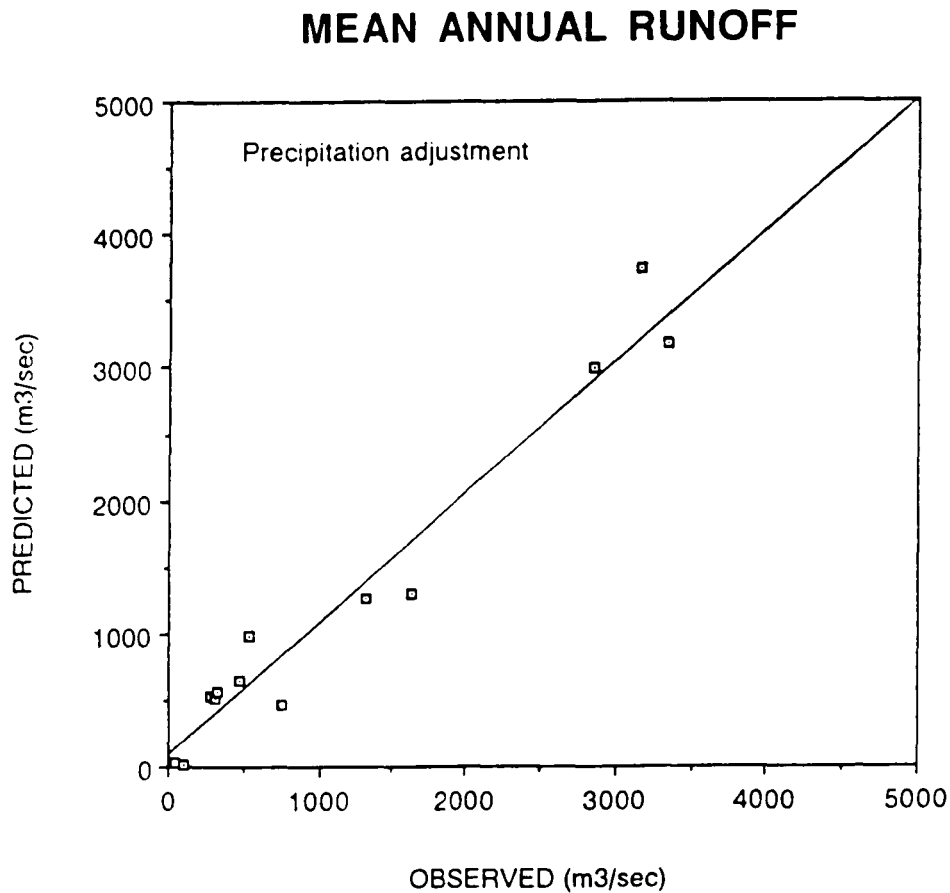


Fig. IV-5. Best model performance for mean annual runoff using WBM and adjusted precipitation ( $\text{pred} = 1.00 \text{ obs} + 79.9$ ;  $r^2 = 0.95$ ). Corrections were applied uniformly to all grids throughout the basin. Similar results were obtained for adjusted evapotranspiration ( $\text{pred} = 1.02 \text{ obs} + 97.3$ ;  $r^2 = 0.95$ ), and soil water capacity ( $\text{pred} = 1.03 \text{ obs} + 90.9$ ;  $r^2 = 0.88$ ). The adjustment factors for precipitation, ET and water capacity were, respectively, 0.73, 1.65 and 3.00 times the nominal discharge value for each variable. Observed data for mean annual discharge are from Table IV-4.

0.808 for the rainfall, ET and water capacity calibrations, respectively. With corrected rainfall predicted mean annual runoff varied between 5% and 91% of observed values. With adjusted ET and water capacity the ranges were 2 to 94% and 2 to 129%, respectively. Largest errors were associated with the smallest observed discharge values. In contrast, the six stations used in calibrating the Amazon River system had errors only varied from 1 to 33 %.

#### Preliminary Calibration -- Fluvial Transport

With the annual water balance so adjusted a series of preliminary parameter tests exploring the seasonal dynamics of river flow were performed. As for the Amazon/Tocantins system, I tested whether basin-wide  $K$ ,  $c_f$ , and  $r_f$  values could adequately simulate river dynamics over the year. Three sets of experiments were analyzed, corresponding to the three water budget adjustments (i.e. rainfall, ET or water capacity). Eighty four scenarios were run for each adjusted water balance, testing  $K$  values from 12.5 to 50.0,  $c_f$  values from 0.6 to 1.4, and  $r_f$  values from 0.0 to 1.00. Model performance was judged on the basis of monthly, long-term discharge records at Livingstone, Itezhi-Tezhi, and Lupata.

Model performance as measured by the weighted  $d$  statistic varied between 0.08 and 0.76 for all scenarios tested. In comparison to the best parameter sets for the Amazon/Tocantins River system (Table IV-5), those for the

TABLE IV-5. Amazon/Tocantins River Model Performance Tests  
(after Vorosmarty et al. 1989).

K	$C_f$	$R_f$	Index of Agreement, $d_{wt}$	Mean % Error
20.0	0.9	0.65	0.823	16
25.0	0.9	0.75	0.819	15
20.0	0.8	0.65	0.815	16
25.0	1.0	0.75	0.799	17
20.0	1.0	0.65	0.793	18



Zambezi simulation (Table IV-6) explained less of the within-year variability. The best  $d_{wt}$  statistics ranged from 0.70 to 0.76 from the Zambezi vs 0.79 to 0.82 from the Amazon; mean percent error was approximately 50-60% vs <20%.

These experiments would suggest that, in general, the Zambezi has a higher turnover of surface water (K values up to 50) than the Amazon/Tocantins and less prominent seasonal floodplain storage ( $c_f$ , routinely over 1.0). The Zambezi results also show that depending on how the annual water balance is adjusted, ambiguous parameter choices may emerge. For example, when potential ET is adjusted, a top performing parameter set shows a K value of 12.5, indicating an unexpectedly sluggish river. As shown later, these ambiguities disappear when more accurate water balances are imposed at the subbasin scale. Indeed, the conclusion that the Zambezi has a relatively rapid turnover of surface water will also be called into question.

Model performance can also be assessed by comparing monthly observed discharges to those computed by the WBM/WTM. Figure IV-6 shows such a plot for the best-performing parameter set associated with adjusted precipitation. The plot is representative of results obtained using the other adjustments. In each case there is general agreement between observed and predicted values but a slope > 1.00 and an intercept below zero suggest that the predictions are systematically in error. There is also

TABLE IV-6. Zambezi River Model Performance Tests, Based on Preliminary Water Balance Adjustment

K	C <sub>f</sub>	R <sub>f</sub>	Index of Agreement, d <sub>wt</sub>	Mean % Error
<u>Precipitation Adjustment</u>				
37.5	1.4	0.75	0.735	60
37.5	1.2	0.75	0.725	60
30.0	1.1	0.65	0.717	60
25.0	1.4	0.50	0.716	60
30.0	1.0	0.65	0.714	60
<u>Potential ET Adjustment</u>				
37.5	1.4	0.75	0.712	65
37.5	1.2	0.75	0.708	64
50.0	1.0	0.75	0.701	64
12.5	-NA-	0.0	0.701	56
30.0	1.1	0.65	0.699	64
<u>Water Capacity Adjustment</u>				
50.0	1.4	0.75	0.762	54
25.0	1.4	0.50	0.754	52
25.0	1.4	0.25	0.753	52
25.0	1.2	0.25	0.752	52
37.5	1.4	0.50	0.751	54

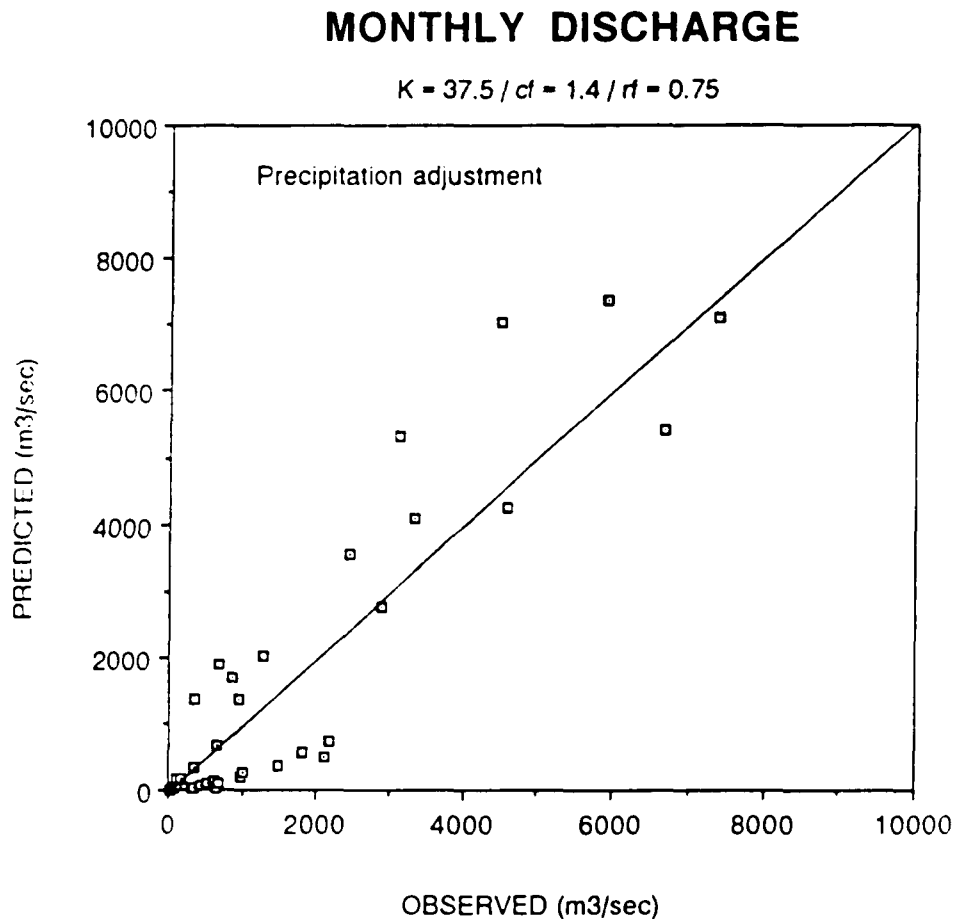


Fig. IV-6. Best model performance for monthly discharge using linked WBM/WTM, adjusted precipitation and observed data from the Livingstone, Itezhi-Tezhi and Lupata sites. Adjustments were applied uniformly to the entire basin. Results for precipitation adjustment are shown (pred = 1.07 obs - 115.8;  $r^2 = 0.83$ ). Similar results were obtained for adjustment of evapotranspiration (pred = 1.11 obs - 104.1;  $r^2 = 0.81$ ), and soil water capacity (pred = 1.11 obs - 283.1;  $r^2 = 0.84$ ). The adjustment factors for precipitation, ET and water capacity were, respectively, 0.73, 1.65 and 3.00 times the nominal value for each variable. See text for parameter definitions.

substantial scatter throughout the domain of observed flows. The computed timeseries for the Livingstone, Itezhi-Tezhi and Lupata sites are given in Figures IV-7a-c. The general character of the discharge is captured by each of the adjusted models. However, high flows are generally overestimated and low flows underestimated. Substantial opportunity for improving the calibration is apparent. This would involve correcting both the timing of flow, and as in the case of Itezhi-Tezhi, residual water balance errors.

#### Enhanced Parameterization -- Water Balance

I investigated the sensitivity of the fluvial transport model to errors in water balance by selectively adjusting the precipitation, ET and water capacity fields by subbasin. The calibration proceeded incrementally until observed and predicted mean annual runoff for each subcatchment agreed to within 2%. Water balance on eleven subcatchments were adjusted; two subcatchments were omitted from the adjustment procedure because they would have yielded negative runoff. The aggregate index of agreement (% error) for the precipitation, ET and water capacity adjustments were 0.967 (4.5%), 0.968 (3.9%), and 0.969 (3.7%), respectively. These indices were based on thirteen sites, allowing comparison to the basin-wide adjustments reported earlier. For the entire basin, 97 mm of runoff were generated, representing less than 15% of incident precipitation for any of the adjustment scenarios.

## MONTHLY DISCHARGE

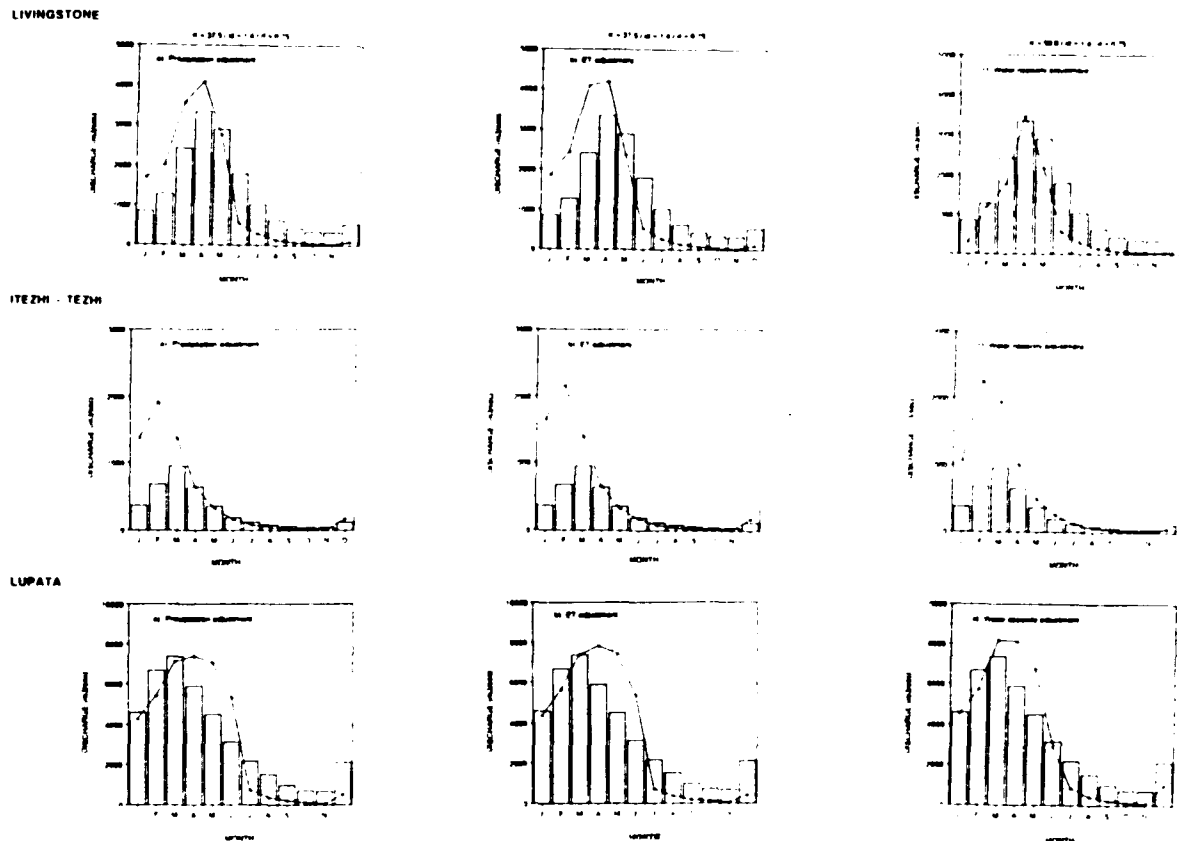


Fig. IV-7. Monthly timeseries predicted by linked WBM/WTM and adjusted biophysical data sets at three discharge monitoring stations. Adjustments were applied uniformly to the entire basin for: a). precipitation , b). evapotranspiration, and c). soil water capacity. The adjustment factors for precipitation, ET and water capacity were, respectively, 0.73, 1.65 and 3.00 times the nominal value for each variable. Bars denote observed flows; lines are WBM/WTM-computed. See text for parameter definitions.

The dynamic distribution of corrected water balance components is given in Plates IV-11, IV-12 and IV-13, showing results from the corrected precipitation scenario. Mean annual soil moisture shows no regular pattern, although in general terms mimics the available water capacity (Plate IV-4). Its magnitude is for lower than AWC reflecting limitations imposed by a distinct wet/dry seasonality. This seasonality is apparent as January-April maxima close to AWC and July-October minima with as little as 0-20 mm of soil moisture throughout much of the basin.

Computed ET also shows a complex distribution that scarcely resembles the PET distribution (Plate IV-10). The overall magnitude is much smaller than PET and the patchiness reflects the variability of soil water. Coupled with the availability of rainfall, January ET values are nearly identical to those for PET. For the remainder of the year, however, seasonal ET is much smaller than the potential and shows greatest limitation in July and October when rainfall and soil water are lowest.

Finally, mean annual runoff shows a rich pattern spatially. Highest values, as expected, are in the North. Relatively high values are also apparent, in the middle and southern sections of the catchments. These areas benefit from relatively shallow rooting zones which favor runoff. Sub-annual dynamics are very strong, and maximum runoff occurs in January in tandem with maximum rain. Minimum

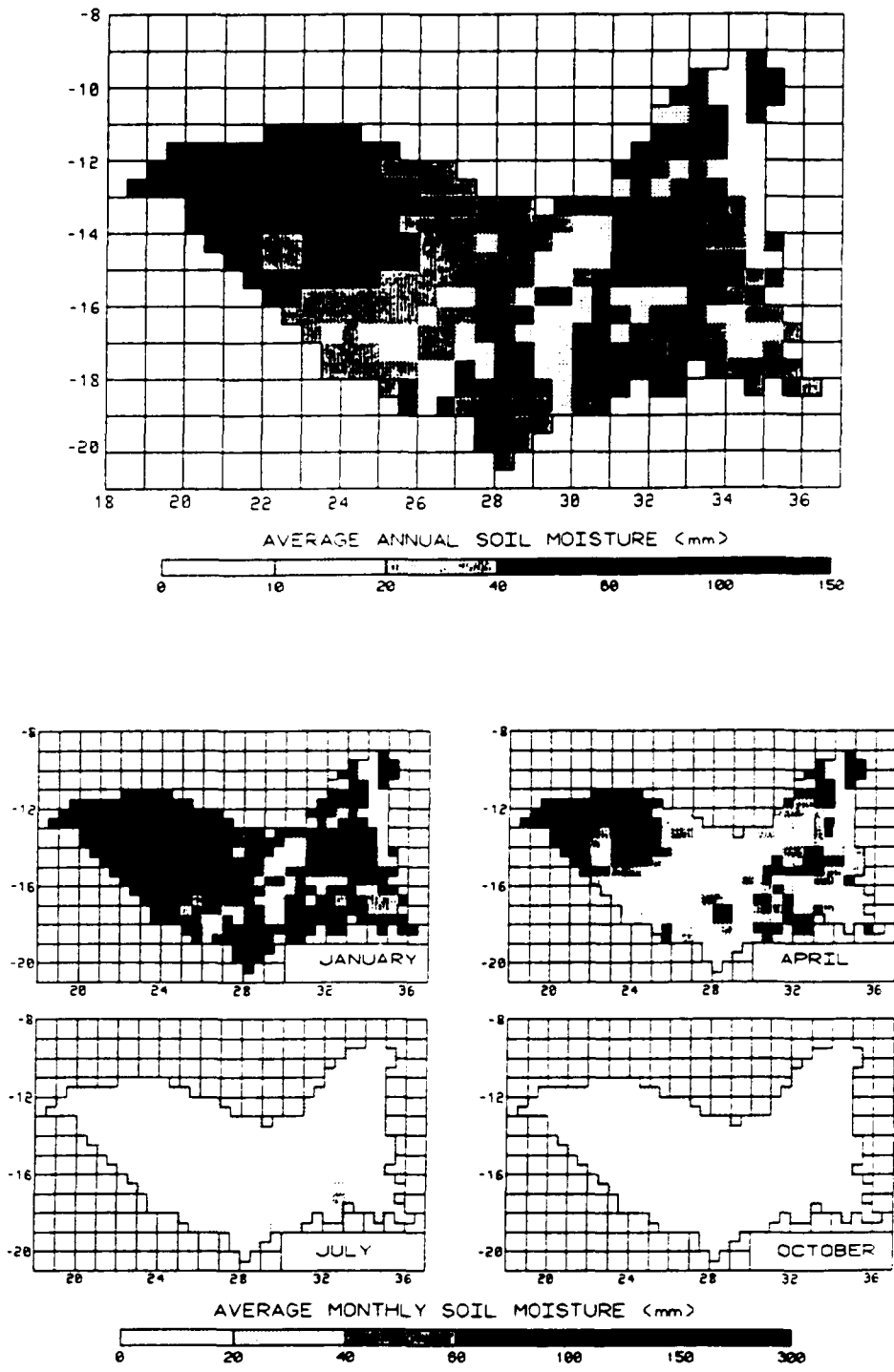


PLATE IV-11.

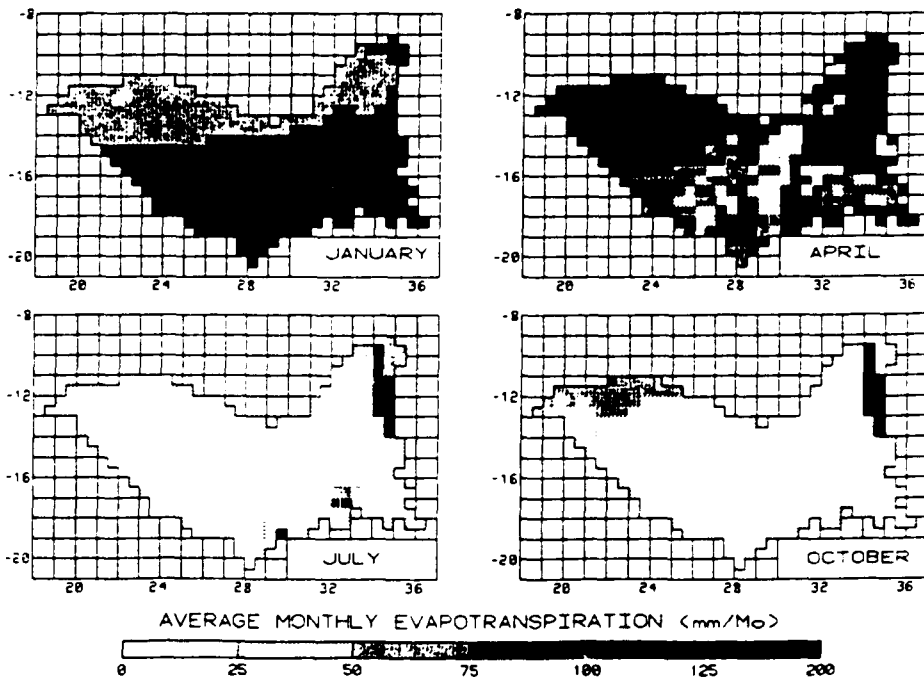
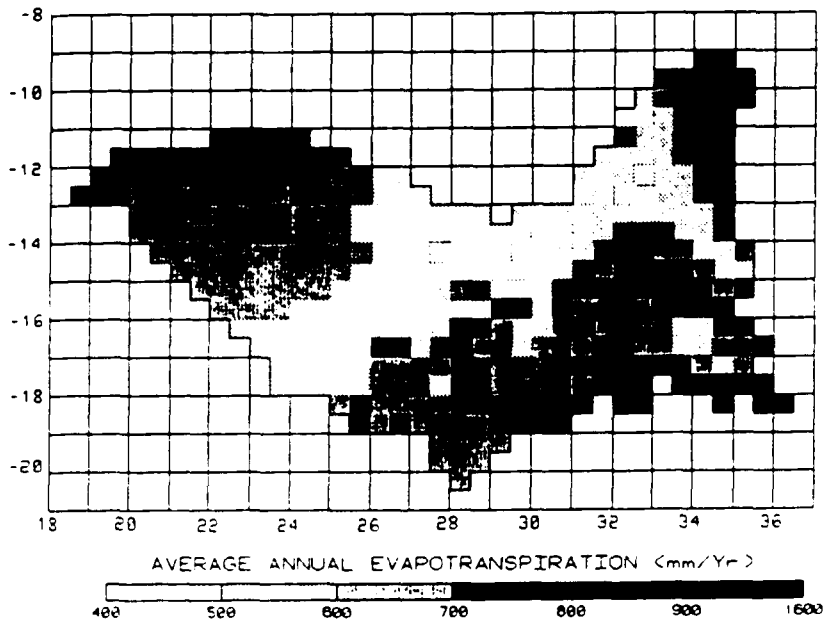


PLATE IV-12.



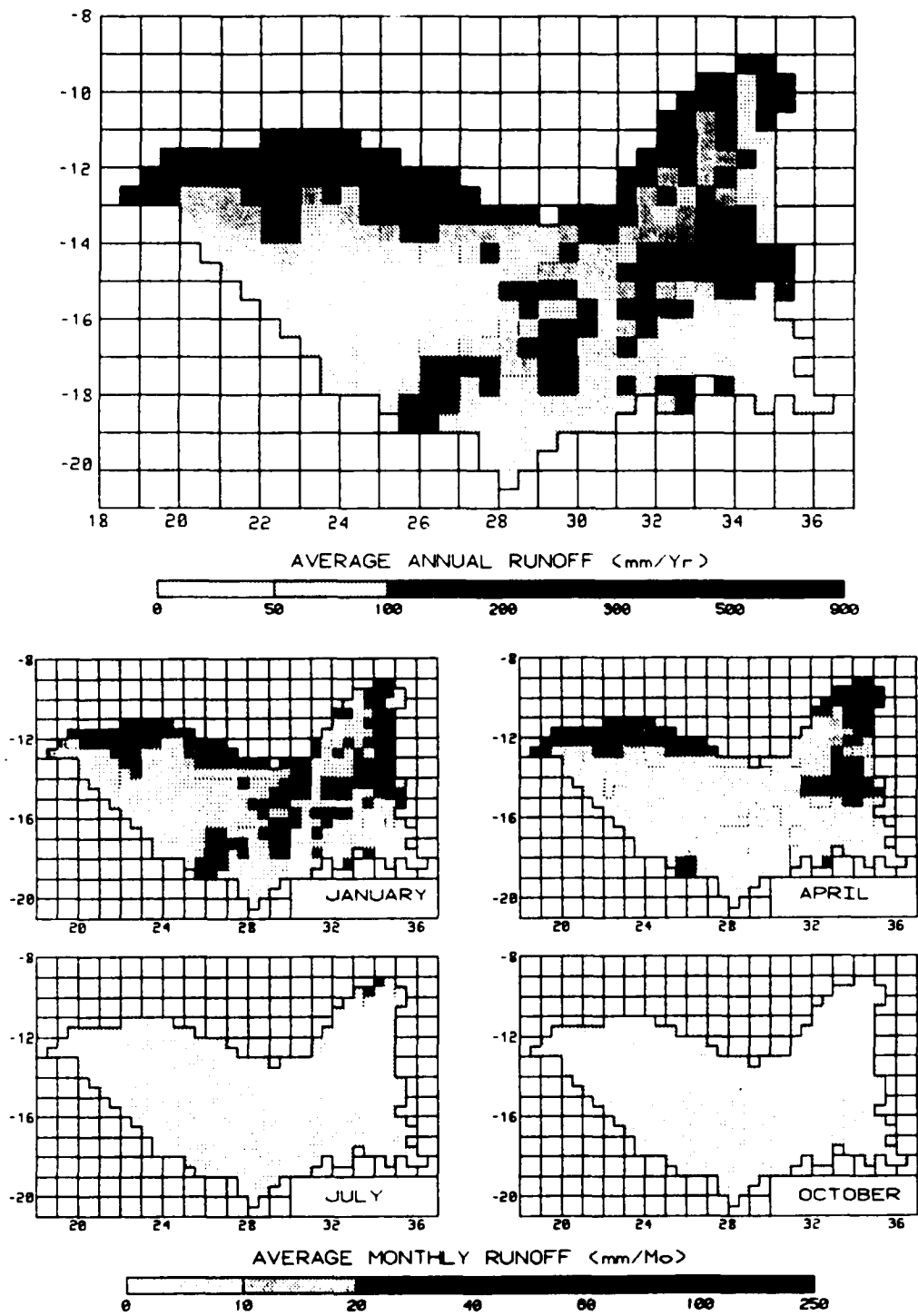


PLATE IV-13.

values occur in July and October when rainfall is low. Many areas are persistently poor runoff generators, and these regions have relatively deep root zones and correspondingly high water capacities.

Tables IV-7 through IV-9 give the subcatchment-specific adjustment factors and resulting water balances under each scenario. The Tables show immediately the variability in calibration factors needed to correctly predict mean annual runoff. Adjustments varied from 0.625 to 1.030 for precipitation, from 0.95 to 2.08 for potential ET and from 0.50 to 14.5 for available water capacity. The tables also show large spatial gradients in the climate and resulting runoff fields. Runoff varies from subbasin to subbasin, from less than 10 to more than 300 mm/yr. In the driest subbasins runoff represents only 1% of precipitation; in wet subbasins the values can approach 30%. This variability highlights the challenge in relying upon continental and global-scale data sets and undoubtedly contributed to the residual errors when uniform correction factors were applied to the entire basin.

For all of the adjustment factors, there was no discernible spatial pattern in how the correction factors were distributed. Furthermore, there was no apparent correlation with any of the biophysical factors given in Table IV-2. It is also difficult to imagine how each of these factors alone could be responsible for the water

TABLE IV-7. Water budgets with precipitation inputs adjusted by subbasin. All other inputs are assigned default values. The basin names refer to those given in Plate IV-1.

Sub-Basin Name	Precipitation Factor	Precipitation (mm/yr)	Potential ET (mm/yr)	Estimated ET (mm/yr)	Runoff (mm/yr)
<b>1st Order</b>					
Chavuma Falls	0.850	1126	1414	802	324
Ithezhi-Tezhi	0.625	671	1461	570	101
Sanyati	1.025	823	1518	735	87
Huangwa	0.625	644	1463	543	101
Hunyani	0.800	699	1519	642	58
Shire	0.800	973	1413	868	105
<b>2nd Order</b>					
Livingstone	0.690	713	1544	653	61
Kafue Gorge	0.700	592	1632	577	15
<b>3rd Order</b>					
Kariba Input	1.030	765	1626	691	75
<b>4th Order</b>					
Cahora Bassa	0.940	797	1688	670	127
<b>5th Order</b>					
Lupata	0.860	819	1575	724	95

TABLE IV-8. Water budgets with potential ET adjusted by subbasin. All other inputs are assigned default values. The basin names refer to those given in Plate IV-1.

Sub-Basin Name	Potential ET Factor	Precipitation (mm/yr)	Potential ET (mm/yr)	Estimated ET (mm/yr)	Runoff (mm/yr)
<b>1st Order</b>					
Chavuma Falls	1.35	1325	1909	993	332
Ithezhi-Tezhi	2.08	1073	3039	970	103
Sanyati	0.95	802	1442	713	90
Huangwa	2.01	1030	2941	927	104
Hunyani	1.37	874	2081	816	58
Shire	1.31	1216	1851	1111	105
<b>2nd Order</b>					
Livingstone	1.80	1033	2780	973	60
Kafue Gorge	1.65	846	2693	834	12
<b>3rd Order</b>					
Kariba Input	0.95	743	1545	668	75
<b>4th Order</b>					
Cahora Bassa	1.15	848	1942	735	113
<b>5th Order</b>					
Lupata	1.20	952	1889	839	113

TABLE IV-9. Water budgets with available water capacities adjusted by subbasin. All other inputs are assigned default values. The basin names refer to those given in Plate IV-1.

Sub-Basin Name	Water Capacity Factor	Precipitation (mm/yr)	Potential ET (mm/yr)	Estimated ET (mm/yr)	Runoff (mm/yr)
<b>1st Order</b>					
Chavuma Falls	1.95	1325	1414	997	327
Ithezhi-Tezhi	4.60	1073	1461	971	102
Sanyati	0.87	802	1518	717	86
Huangwa	6.00	1030	1463	927	103
Hunyani	13.50	874	1519	817	57
Shire	14.50	1216	1413	1109	107
<b>2nd Order</b>					
Livingstone	2.85	1033	1544	976	58
Kafue Gorge	3.00	846	1632	838	8
<b>3rd Order</b>					
Kariba Input	0.50	743	1626	647	97
<b>4th Order</b>					
Cahora Bassa	4.00	848	1688	757	90
<b>5th Order</b>					
Lupata	1.50	952	1575	831	121

balance inequities, given the rather large adjustment factors required in some of the subbasins. This suggests that there are random errors in either the flow data or the numerous input data planes that will be impossible to trace with any accuracy. As discussed by Band (1991), distributed parameter models must utilize numerous geographically-specific data sets that are often derived from disparate sources of variable quality and map scale. Errors may arise both from the individual data sets or from their conjunction. This is especially true when gradients in the input data are strong.

#### Enhanced Parameterization -- Fluvial Transport

After securing the refined subbasin-specific water balances, I proceeded to simulate river transport in a further set of experiments. For these tests, I recognized that applying floodplain dynamics universally did not faithfully reflect the situation in the Zambezi River. I therefore applied floodplain storage only to grid cells (Figure IV-8) in which floodplains/wetlands could be identified from soil type or observation of DMAAC Navigation Charts (Vorosmarty and Moore 1991). The same set of 84 scenarios were run as before. Within each scenario, the K, c, and r, parameters were applied uniformly, but now with selective floodplain inundation. The experiments were repeated three times, corresponding to the precipitation,

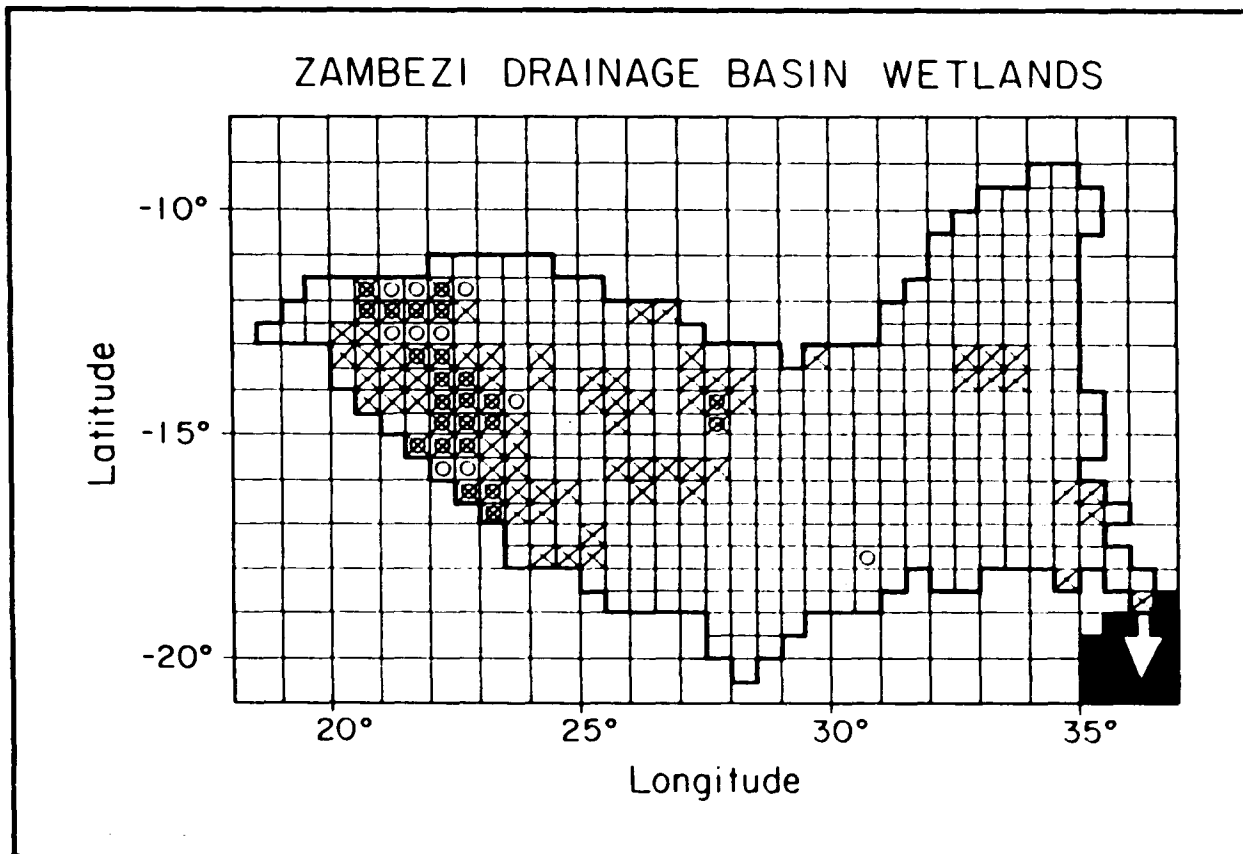


Fig. IV-8. Grid cells having appreciable areas of wetland. The 'X' markings represent swamps and/or floodplains identified from Operational Navigation Charts (DMAAC, various yers). The cells with circles have wetland soils determined from FAO/CSRC (1974). The wetlands within each cell do not necessarily fill the entire grid.

potential ET and water capacity adjustments at the subbasin scale.

In all scenarios tested, the weighted  $d$  statistic varied over a much smaller range (0.42 to 0.82) than for the preliminary calibration. The parameter sets which best matched observed monthly discharges at Livingstone, Itezhi-Tezhi and Lupata (Table IV-10) had weighted indices of agreement ( $d_{wt}$ ) ranging from 0.80 to nearly 0.82. There is substantial improvement over the previous set of experiments in which basin-wide adjustment factors were applied (Table IV-6), and the new parameterizations now rival those from the Amazon/Tocantins analysis (Table IV-5). Although mean percent errors still approach 50 percent, these are predominantly associated with low flows and are of small absolute magnitude. Figure IV-9 shows aggregate model performance based on observed and predicted monthly discharge for the adjusted precipitation scenario. Higher  $r^2$  values for all scenarios (0.93 to 0.95) indicate reduced scatter (c.f. Figure IV-6). However, negative intercepts (-283 to -167) and slopes  $> 1.00$  (1.12 to 1.18) still indicate systematic underestimates at low flows and overestimates at high flows. This same characteristic was noted for the Amazon using the WBM/WTM (Vörösmarty et. al. 1989) and by Richey et. al. (1989) using a Muskingum model,



TABLE IV-10. Zambezi River Model Performance Tests, Based on Refined Water Balance Adjustment and Selective Floodplain Inundation

K	$C_f$	$R_f$	Index of Agreement, $d_{vt}$	Mean % Error
<u>Precipitation Adjustment</u>				
25.0	0.6	0.75	0.817	45
25.0	0.8	0.75	0.814	45
25.0	0.7	0.75	0.813	46
20.0	0.6	0.65	0.810	45
25.0	0.9	0.75	0.809	47
<u>Potential ET Adjustment</u>				
25.0	0.6	0.75	0.811	47
25.0	0.7	0.75	0.805	47
25.0	0.8	0.75	0.801	48
30.0	1.1	0.85	0.800	50
20.0	0.6	0.65	0.799	47
<u>Water Capacity Adjustment</u>				
25.0	1.4	0.75	0.816	46
25.0	0.9	0.65	0.816	44
25.0	1.2	0.75	0.816	45
30.0	0.9	0.75	0.814	45
20.0	1.1	0.65	0.812	45

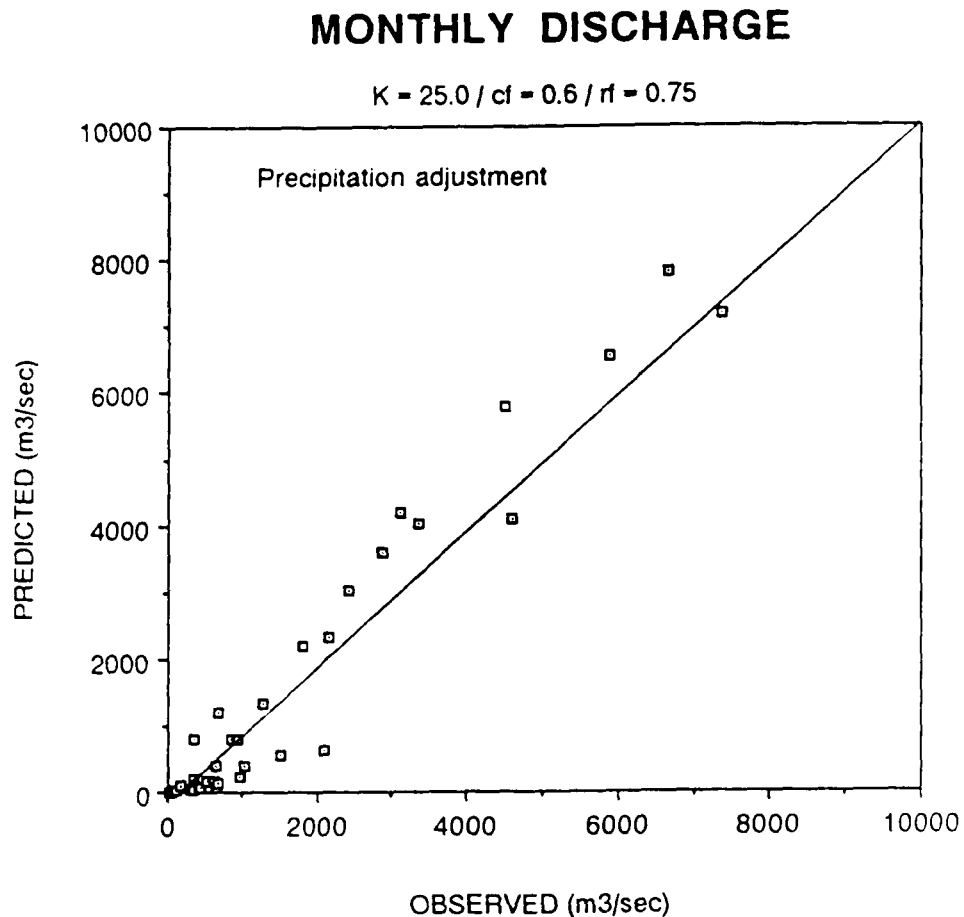


Fig. IV-9. Best model performance for monthly discharge using linked WBM/WTM, adjusted precipitation and observed data from the Livingstone, Itezhi-Tezhi and Lupata sites. Adjustments were applied at the subbasin level. Results shown are for precipitation adjustment ( $\text{pred} = 1.12 \text{ obs} - 167.3$ ;  $r^2 = 0.94$ ). Similar results were obtained for adjusted evapotranspiration ( $\text{pred} = 1.18 \text{ obs} - 283.4$ ;  $r^2 = 0.95$ ) and soil water capacity ( $\text{pred} = 1.15 \text{ obs} - 239.0$ ;  $r^2 = 0.93$ ). Adjustment factors are given in Tables IV-7 through IV-9. See text for parameter definitions.

and may be an inherent limitation of such linear models. Despite these residual disparities, the time series for each of the adjusted scenarios reasonably matches the observed discharge record at all sites tested on the Zambezi (Figure IV-10a-c).

The parameters which conveyed best model performance (Table IV-10) are now similar to those of the original Amazonian analysis (Table IV-5). The five best parameter sets on the Zambezi show K values between 20 and 30, similar to the 20 to 25 range tabulated for the Amazon and within the theoretical range predicted by Vörösmarty et. al. (1989). Furthermore, for both the PPT and PET-adjusted scenarios, the flood initiation parameter ( $c_f$ ) is, in nearly all cases, below 1.0 and the flooding ratio ( $r_f$ ) is between 0.65 and 0.85. The best Amazonian analogues varied between 0.8 and 1.0 and between 0.65 to 0.75 for  $c_f$  and  $r_f$ , respectively. For adjusted precipitation, one of the top five parameter sets for the Zambezi ( $K = 25$ ,  $c_f = 0.9$ ,  $r_f = 0.75$ ) appeared as well among the preferred parameter sets for the Amazon.

The scenarios in which the available water capacity was adjusted showed a similarly small range in K values (20 to 30), but convey a different picture of floodplain inundation. Initiation of flooding appears delayed ( $c_f$  from 0.9 to 1.4), although once flooding occurs, flooding ratios are similar to those of the other scenarios. The available

## MONTHLY DISCHARGE

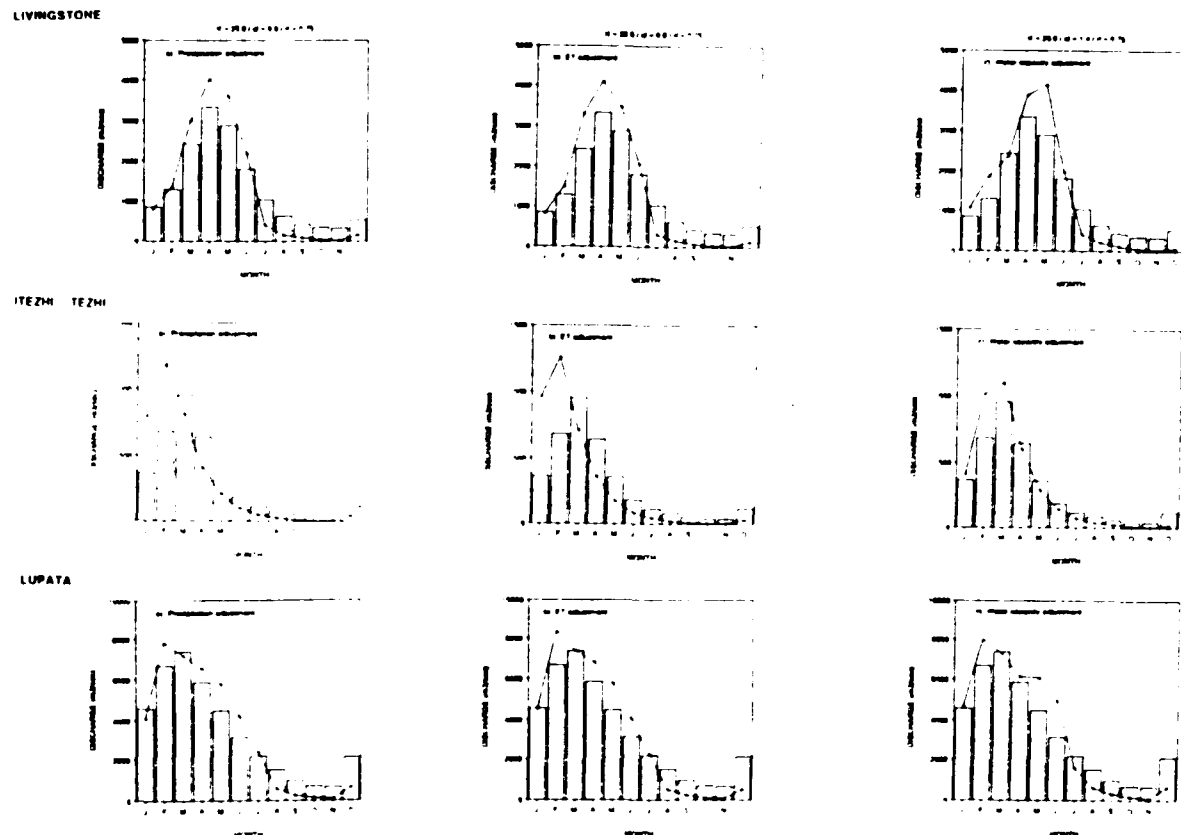


Fig. IV-10. Monthly timeseries predicted by linked WBM/WTM and adjusted biophysical data sets at three discharge monitoring stations. Adjustments were applied at the subbasin level for: a). precipitation , b). evapotranspiration, and c). soil water capacity. Adjustment factors are given in Tables VI through VIII. Bars denote observed flows; lines are WBM/WTM-computed. See text for parameter definitions.

water capacity adjustments appear to have an inordinate effect on the fluvial dynamics. Larger available water capacities serve to delay the generation of runoff and therefore retard the passage of runoff through the drainage basin. This in a sense mimics floodplain inundation and the fluvial transport parameters would need to minimize the apparent degree of flooding to best match observed discharges. In light of the consistent results from the precipitation and ET scenarios, and the rather large water capacity corrections required (Table IV-9), it appears that less confidence should be placed in the results of this final scenario.

From these tests, it is reasonable to conclude that K values from 20 to 30,  $c_f$  from 0.6 to 1.0, and  $r_f$  from 0.65 to 0.85 can adequately simulate flow dynamics in both the Amazon and Zambezi River systems. The fluvial transport parameters were cast to resemble parameters with clear physical analogues. Demonstrating a fairly narrow range in both river systems is an important finding since it suggests that the dynamics of such large river systems may have convergent properties. A survey of additional river systems may yield relationships similar to those of Leopold et. al. (1964) linking flow velocity, river geometry, slope, and discharge.

To the degree that the Zambezi and Amazon/Tocantins Rivers represent large tropical river systems, the parameter

sets identified as part of this study may apply generally to the Tropics. This hypothesis assumes that errors in water balance are minimized and selective floodplain inundation can be ascertained. Obviously, more tests are required, but the capacity of similar parameters to successfully capture the dynamics of river flow in disparate river systems like the Amazon and the Zambezi is encouraging. Identifying universal parameter sets is also important because global assessments will require simulation of poorly-studied tropical rivers in which flow data are often incomplete or non-existent. Finally, it would be interesting to explore the degree to which such parameter sets can successfully simulate rivers in other regions of the globe.

#### Summary and Conclusions

In this paper I have presented a simple water balance and fluvial transport model, together with a series of biophysical data sets, for the Zambezi River system in southeastern Africa. The model was used to examine key features of the catchment's surface hydrology including soil moisture, evapotranspiration, landscape runoff and river discharge. It was also used to identify key dynamic attributes of tropical river systems that may be widely applicable.

Observed river discharge was used to check water balance calculations. Unadjusted WBM calculations did not agree with direct measurements of regional runoff. Three

sources of error were identified, and each was associated with a primary, geographically-referenced input data set. The data sets represented precipitation, potential evapotranspiration and available water capacity. The problems encountered in defining an accurate water budget highlight the difficulty in correctly characterizing even the most basic of climatic and biophysical variables in the Tropics. There is no substitute for accurate observed discharge when making such water balance estimates.

An accurate water balance also affects inferences about the dynamics of river flow. I found that in cases where runoff was poorly defined, a wide array of parameters (for surface water flux and floodplain inundation) could explain observed patterns of monthly river discharge in the Zambezi River. With improvements in the water budget and clearly identified areas of floodplain inundation, the range of optimal parameter sets was more constrained. Furthermore, these parameters bore a clear resemblance to those used for the Amazon/Tocantins River system. Time series of predicted flow showed a reasonable correspondence to observed data in both the Zambezi and Amazon basins.

Although the WBM/WTM operates successfully at the coarse scale, the dynamics of many smaller basin features cannot be captured. For example, swamps which have a dramatic local effect on both the timing of flows and evaporative losses were not explicitly treated in this

analysis. Detailed information on volume, surface area, influent and effluent hydrographs would be required for each large swamp in the basin, but such data is not necessarily available (Vörösmarty and Moore 1991). In addition, the distribution of small impoundments and dispersed irrigation throughout the basin makes a fully comprehensive analysis impossible.

The strength of the current macro-scale model instead lies in assessing the impact of global change. Human activity is, and will continue to be, an important factor in the terrestrial water cycle, through global climate change, shifting land use and the operation of water resources systems. This study has presented a calibrated model representing long-term climatic conditions, natural land cover and unregulated river flows. From this reference condition, a series of scenario analyses can be performed. Since the WBM/WTM is a distributed parameter model, scenarios could be cast which imbed the various disturbances within the simulated drainage basin. For climate change, inputs from the current generation of General Circulation Models (GCM's) could be gridded to 0.5 degree spatial scale and analyzed in the context of the WBM/WTM, for example under a 2X CO<sub>2</sub> atmosphere. For land use effects, contemporary and potential future distributions of agricultural and urban landscapes could be mapped and the resulting water balance and river flow alterations noted.



For water resources management, key reservoir attributes and operating rules could be applied to specific grid locations to determine the historic and future impacts of river regulation.

Such experiments must increasingly rely on automated data storage and retrieval systems, especially as we seek global coverage. To fulfill this need, a Global Hydrology Archive and Analysis System (GHAAS) is currently being developed at the Institute for the Study of Earth, Oceans, and Space at the University of New Hampshire (USA). The GHAAS will maintain data on discharge, flow regulation, climatology, water quality and river topology. It will also be linked to a Geographic Information System and thereby have the potential to import, create, and modify a suite of geographically-referenced biophysical data sets. The system will maintain information from ground-based stations as well as remote sensing data and modeling experiments. Such an integrated information system, coupled to macro-scale hydrology models like the WBM/WTM, will serve as a critical component in our quest to understand the dynamics of global change in the coming decades.

## CONCLUSIONS

As described earlier, there is a critical need for tools to analyze regional and continental-scale hydrology in light of the growing challenges presented by global change. The research described in this dissertation has resulted in the construction of one such tool, a macro-scale hydrology model (WBM/WTM). My work has demonstrated that a relatively simple construct, linking water balance and fluvial transport models to extant biophysical data sets, can faithfully characterize the surface hydrology of tropical regions. The Amazon/Tocantins River in South America and the Zambezi River in Southern Africa were studied.

In this dissertation, I set forth a modeling strategy to analyze landscape/hydrology interactions, assembled a coherent set of data for use in the simulation studies, and constructed and tested the proposed model. Using the model, I was able to quantify, with high spatial and temporal resolution, key components of the terrestrial water balance on two continents. These components related to soil moisture, evapotranspiration, and runoff.

Results from the Amazon River water balance simulation compared favorably to existing data sources depicting the spatial pattern of water cycle components. The results were further checked against river flow records. In the case of

the Zambezi River system, however, large errors in regional runoff were tabulated using the Water Balance Model and existing biophysical data sets. Three sources of error were identified, representing the precipitation, potential evapotranspiration and available water capacity data inputs. With suitable adjustment these results rivalled those of the Amazon. I went on to use the model to produce a set of discharge hydrographs that adequately reflected observed timeseries in both rivers.

The WBM/WTM was found to be sensitive to the quality of input data and to the choice of fluvial parameters. An accurate accounting of water balance was found to be critical in simulating river dynamics. Another important finding was that numerically similar parameters could be used to predict fluvial dynamics in the strikingly different Amazon and Zambezi River systems.

The modeling described in this study should be viewed as a first and modest step --the Amazon and Zambezi River systems were analyzed solely from the standpoint of long-term climatology, minimal land use change and the absence of any major water engineering works. Of course there are few remaining river systems that are spared the impacts of such anthropogenic disturbance. With a demonstrated capability of the WBM/WTM, the focus can now shift to the issue of global hydrologic change. The set of relevant questions is of course enormous. Among these are a

calibrated WBM/WTM in its current form:

- 1). What are the potential impacts of induced climate change on water balance components and on the horizontal flux of water?
- 2). How has the operation of large-scale engineering works (e.g. large impoundments, irrigation schemes, interbasin transfers) altered regional water balance and the nature of river flow?
- 3). What are the potential consequences of widespread land use change on water balance and the horizontal flux of water?
- 4). Induced climate change, water engineering works, and shifting land use hold potentially enormous impacts on the water cycle. How do these agents of anthropogenic change influence the transport and processing of biogeochemical constituents?

The first question can be addressed using the WBM/WTM in tandem with global circulation modeling (GCM) results. The numerical experiments will use climatic forcing functions from a series of GCM's to drive the WBM/WTM and to generate predictions of runoff and discharge hydrographs under a contemporary climate. These predictions will be compared to the surface hydrology quantified by the calibrated WBM/WTM using interpolated, gridded data sets

derived from land-based meteorological stations. Output from each of the GCMs under a 2X CO<sub>2</sub> climate, for instance, can then be used in the context of the WBM/WTM to predict the potential impact of climate change on large drainage basins. The analysis would result in a documentation of GCM performance in determining hydrologically-meaningful variables in the contemporary setting. It would also document the range of potential future impacts of climate change.

The second question requires a retrospective analysis of basin-scale hydrology prior to impoundment, contrasted against post-impoundment conditions. The experiments seek to elucidate the role that river regulation has had on downstream processes such as flow velocity and wetland flooding. In the Zambezi catchment, for example, the WBM/WTM can be used to define a natural surface hydrology, a pre-impoundment situation with altered land use, and the current situation with land use plus the operation of four major impoundments on the mainstem and its tributaries. Both regional water balance and discharge hydrographs could be analyzed in the context of the various land use and hydrologic settings.

The third question could be addressed by exercising particular GCM configurations (i.e. National Center for Atmospheric Research, Boulder Colorado USA; Meteorological Office, Bracknell UK; University of Maryland, College Park,

Maryland USA). These have already been used to analyze changes in precipitation and evapotranspiration due to widespread deforestation in the Amazon. The WBM/WTM will use GCM-generated precipitation, cloud cover and temperature data to produce the first assessment of how deforestation might influence the discharge hydrograph of the Amazon River. The nature of the hydrograph, including the timing of the floodwave and extent of floodplain inundation will be examined.

Finally, this research has demonstrated that the drainage basin is a useful organizing concept, even at regional and continental scales. As a catchment-scale model, the WBM/WTM holds significant potential for addressing issues of regional biogeochemistry, beyond simply predicting elements of the terrestrial water cycle. As humans have dramatically altered the terrestrial water cycle, so too have they accelerated the loss of organic and inorganic constituents from the landscape to the world's oceans. A suitably-cast model, linking water balance, ecosystem nutrient cycling, fluvial transport, and aquatic processing could provide an important new tool for assessing the cumulative impact of humans on the terrestrial biosphere. The WBM/WTM is an important step towards this goal.

## REFERENCES

- Adis, J., Seasonal igapó-forests of Central Amazonian blackwater rivers and their terrestrial arthropod fauna, In: Sioli, H. (ed.), The Amazon: Limnology and Landscape Ecology, W. Junk, Boston, Mass., 245-268, 1984.
- Akima, H., A method of bivariate interpolation and smooth surface filtering for irregularly-distributed data points, ACM Trans. Math. Software, 4(2), 148-159, 1978.
- Allen, R. G., Evaluation of estimating methods. In: Jensen, M. E., Burman, R. D. and Allen, R. G. (ed.), Evapotranspiration and Irrigation Water Requirements, ASCE manuscript, 1990.
- Ambroggi, R. P., Water. Sci. Amer. Sept. 1980: 91-101.
- Atwell, R. I. G., Some effects of Lake Kariba on the ecology of the Mid-Zambezi Valley of Rhodesia. Biol. Conserv. 2, 189-196, 1970.
- Balasubrahmanyam, S. and S. M. Abou-Zeid, Post-Itezहितzhi flow pattern of the Kafue in the Kafue Flats region. In: Proc. Nat. Sem. on Environment and Change: the Consequences of Hydroelectric Power Development on the Utilization of the Kafue Flats, University of Zambia, Lusaka, 63-67, 1978.
- Balek, J., Hydrology and Water Resources in Tropical Africa, Elsevier Scientific Publishing Company, New York, 1977.
- Balon, E. K. and A. G. Coche, Lake Kariba: A Man-Made Tropical Ecosystem in Central Africa., Monographiae Biologicae 24, W. Junk, The Hague, 767, 1974.
- Band, L.E., Distributed parameterization of complex terrain. In: E.F. Wood, ed., Land Surface-Atmosphere Interactions for Climate Modeling: Observations, Models, Analysis. Kluwer Academic, Dordrecht, Netherlands, 249-270, 1991.
- Barnes, D. L. and M. J. Franklin, Runoff and soil loss on a sandveld in Rhodesia. Proc. Grassld. Soc. Afr., 5: 140-144, 1970.

- Baumgartner, A., and E. Reichel, The World Water Balance, Elsevier, New York, 1975.
- Becker, A. and J. Nemeč, Macroscale hydrological models in support to climate research. In: The Influence of Climate Change and Climate Variability on the Hydrologic Regime and Water Resources, IAHS Publication #168, Vancouver, 431-441, 1987.
- Begg, G. W., The biological consequences of discharge above and below Kariba Dam. Proc. 11th Congr. Int'l Comm. for Large Dams, Madrid, 421-430, 1973.
- Bernacsek, G. M. and S. Lopes, Investigations into the Fisheries and Limnology of Cahora Bassa Reservoir Seven Years after Dam Closure (FAO/GCP/MOZ006/SWE FIELD doc.), 149, 1984.
- Bhagavan, M. R., The energy sector in SADCC countries. Ambio, 14: 214-19, 1985.
- Black, J., The distribution of solar radiation over the Earth's surface. In: Wind and Solar Energy, UNESCO, Paris, 138-140, 1956.
- Blackie, J. R., Hydrological effects of change in land use from rainforests to tea plantation in Kenya. In: Symposium on the Results of Research on Representative and Experimental Basins, IAHS/UNESCO Publication #97, Wellington, New Zealand, 312-329, 1972.
- Blaney, H. and W. Criddle, Determining consumptive use and irrigation requirements. USDA Tech. Bul. 1275, 59, 1956.
- Bolton, P., The Regulation of the Zambezi in Mozambique: A Study of the Origins and Impact of the Cabora Bassa Project. PhD, University of Edinburgh, 1983.
- Bolton, P., Sediment deposition in major reservoirs in the Zambezi basin. In: Challenges in African Hydrology and Water Resources, IAHS Publication #144, Harare, Zimbabwe, 559-567, 1984.
- Borchert, G. and S. Kempe, A Zambezi aqueduct. Mitt. Geol.-Palaont. Inst., Univ Hamburg, SCOPE/UNEP Sonderband Heft 58, 443-457, 1985.



- Brunskill, G. J., P. Campbell, S. Elliott, B. W. Graham, and G.W. Morden, Rates of transport of total phosphorus and total nitrogen in Mackenzie and Yukon watersheds, NWT and YT, Canada, Verh. Int. Ver. Theor. Angew. Limnol., 19, 3199-3203, 1975.
- Burges, S. J., Trends and directions in hydrology, Water Resour. Res., 22(9), 1S-5S, 1986.
- Campbell, A. and G. Child, The impact of man on the environment of Botswana. Botswana Notes and Records, 3: 91-111, 1971.
- Central African Power Corporation (CAPCO), Annual Report and Accounts, 1985.
- Chahine, M.T., GEWEX Continental-Scale Hydrological Field Experiment, Concept Paper, Jet Propulsion Laboratory, Pasadena, California, 1989.
- Choudhury, B. J., Relating Nimbus-7 37 GHz data to global land-surface evaporation, primary productivity and the atmospheric CO<sub>2</sub> concentration, Int. J. Remote Sens., 9(1), 169-176, 1988.
- Choudhury, B. J., and R. E. Golus, Estimating soil wetness using satellite data, Int. J. Remote Sens., 9(7), 1251-1257, 1988.
- Cluis, D. A., D. Couillard, and L. Potvin, A square grid transport model relating land use exports to nutrient loads in rivers, Water Resour. Res., 15(3), 630-636, 1979.
- Committee on Global Change, Toward an Understanding of Global Change, National Academy Press, Washington, D.C. 213, 1988.
- Correll, D., Watershed Research Perspectives, Smithsonian Institution Press, Washington, D. C., 1986.
- Davies, B. R., Stream regulation in Africa. In: Stanford, J. A. and Ward, J. V. (ed.), The Ecology of Regulated Streams, Plenum, N. Y., 113-143, 1979.
- Davies, B. R., A. Hall and P. B. N. Jackson, Some ecological aspects of the Cahora Bassa Dam. Biol. Conserv., 8: 189-201, 1975.

- Dickinson, R. E. and A. Henderson-Sellers, Modeling tropical deforestation: A study of GCM land-surface parameterizations. Q. J. R. Meteorol. Soc., 114: 439-462, 1988.
- DMAAC. Various years. Operational Navigation Charts. Defense Mapping Agency Aerospace Center, St. Louis, MO.
- Dooge, J. C. I., Looking for hydrologic laws. Wat. Res. Res., 22: 46S-58S, 1986.
- Dos Santos, J. F., Aproveitamento hidroelectrico de Cabora Bassa. Electricidade (Lisbon) 54: 236-47, 1968.
- du Toit, R. F., Soil loss, hydrological changes, and conservation attitude in the Sabi Catchment of Zimbabwe. Environ. Conserv., 12: 157-166, 1985.
- du Toit, R. F., Hydrological changes in the middle-Zambezi system. Zimb. Sci. News, 17: 121-125, 1983.
- Eagleson, P. S., The emergence of global-scale hydrology. Wat. Res. Res., 22: 6S-14S, 1986.
- Elder, J. F., Nitrogen and phosphorus speciation and flux in a large Florida river wetland system, Water Resour. Res., 21(5), 724-732, 1985.
- Elwell, H. A., An assessment of soil erosion in Zimbabwe. Zimb. Sci. News, 19: 27-29, 1985.
- Elwell, H. A., The degrading soil and water resources of the communal areas. Zimb. Sci. News, 17: 145-147, 1983.
- Elwell, H. A. and M. A. Stocking, Rainfall parameters to predict surface runoff yields and soil losses from selected field-plot studies. Rhod. J. Agric. Res., 11: 123-129, 1973.
- FAO/CSRC, Soil Map of the World, 1:5M, UNESCO, Paris. 1/2 Degree Digitization. Complex Systems Research Center, U.N.H., Durham, NH, 1974.
- FAO/UNDP, Multipurpose Surveys of the Kafue River Basin, Food and Agricultural Organization of the United Nations - United Nations Development Program, Rome, 45, 1968.
- FAO/UNESCO, Soil Map of the World, 1:5,000,000, Vol. I (Legend), Vol. VI (Africa), UNESCO, Paris, 1977.

- Fearnside, P. M., Human Carrying Capacity of the Brazilian Rainforest, Columbia University Press, New York, 1986.
- Fisher, T. R., N and P recycling in an Amazon River floodplain lake, paper presented at Symposium on Freshwater Wetlands and Wildlife, Univ. of Ga., Charleston, S. C., 1986.
- Gandolfi, C. and K. A. Salewicz, Multiobjective Operation of Reservoir Systems: The Zambezi Case Study, Working Paper, International Institute for Applied Systems Analysis, Laxenburg, Austria, 1990.
- Geiske A., Selaolo E., and S. McMullan, Groundwater recharge through the unsaturated zone of southeastern Botswana: A study of chlorides and environmental isotopes. In: Regionalization in Hydrology, IAHS Publ. No. 191. Proc. of the Ljubljana, Yugoslavia Conference. IAHS Press, Wallingford, UK, 33-44, 1990.
- Gentry, A. H. and J. Lopez-Parodi, Deforestation and increased flooding of the upper Amazon, Science, 210, 1354-1356, 1980.
- Gianessi, L. P., H. M. Peskin, and G. K. Young, Analysis of national water pollution control policies, 1, A national network model, Water Resour. Res., 17(4), 796-801, 1981.
- Gilbert Commonwealth International, Report on System Development Plan for Zimbabwe Electricity Supply Authority. Reading, UK, 1987.
- Gildea, M.P., B. Moore, C. J. Vörösmarty, B. Bergquist, J. M. Melillo, K. Nadelhoffer, and B. J. Peterson, A global model of nutrient cycling: I. Introduction, model structure, and terrestrial mobilization of nutrients. In: D. Correll (ed.), Watershed Research Perspectives, Smithsonian Institution Press, Washington, D.C., 1-31, 1986.
- Giorgi, F., Simulation of regional climate using a limited-area model nested in a General Circulation Model. Abstract #A11F-14. EOS, Trans. American Geophysical Union, 70: 1011, 1989.
- Goodison, B. E. (ed.), Hydrological Applications of Remote Sensing and Remote Data Transmission, International Association of Hydrological Sciences, Canada, Montreal, Ontario, 684, 1985.

- Goulding, M., Forest fishes of the Amazon, In: G. T. Prance and T. E. Lovejoy, Key Environments: Amazonia, Pergamon, New York, 267-276, 1985.
- Grotch, S. L., Regional Intercomparisons of General Circulation Model Predictions and Historical Climate Data, (DOE/NBB-0084). U.S. Department of Energy, 291, 1988.
- Gutowski, W. J., D. S. Gutzler and W.-C. Wang, Surface energy balances of three General Circulation Models: Implications for simulating regional climate change. Submitted to Journal of Climate, 1989.
- Guy, P. R., River bank erosion in the Mid-Zambezi Valley, downstream of Lake Kariba. Biol. Conserv., 19: 119-212, 1981.
- Hahn, J., S. G. Warren, J. London and J. L. Roy, Climatological Data for Clouds Over the Globe from Surface Observations., U.S. Department of Energy, Oak Ridge, Tennessee, 1988.
- Hall, A., B. R. Davies and I. Valente, Cahora Bassa: some preliminary physico-chemical and zooplankton pre-impoundment survey results. Hydrobiologia, 50: 17-25, 1976.
- Hansen, J. and S. Lebedeff, Global trends of measured surface air temperature. J. Geophys. Res., 92: 13,345-372, 1987.
- Hansen, J., D. Rind, A. DelGenio, A. Lacis, S. Lebedeff, M. Prather, R. Ruedy and T. Karl, Regional greenhouse climate effects. In: Coping with Climate Change, Proc. 2nd North American Conference on Preparing for Climate Change, Climate Institute, Washington D.C., 1988.
- Hansen, J., I. Fung, A. Lacis, D. Rind, S. Lebedeff, R. Ruedy, G. Russell and P. Stone, Global climate changes as forecast by Goddard Institute for Space Studies three-dimensional model. J. Geophys. Res., 93: 9341-9364, 1988.
- Harriss, R. C., S. C. Wofsy, M. Garstang, E. V. Browell, L. C. B. Molion, R. J. McNeal, H. M. Hoell, R. J. Bendura, S. M. Beck, R. L. Navarro, J. T. Riley, and R. L. Snell, The Amazon boundary layer experiment (ABLE 2A), J. Geophys. Res., 93, 1351-1360, 1988.

- Havel, J. J. and K. J. Bligh, Estimation of Water Yield Coefficients. In: Bennett, D. and Thomas, J. F. (ed.), On Rational Grounds: Systems Analysis in Catchment Land Use Planning, Elsevier, Amsterdam, 208-221, 1982.
- Herrera, R., Nutrient cycling in Amazonian forests, In: G. T. Prance and T. E. Lovejoy (Eds.), Key Environments Amazonia, Pergamon, New York, 95-108, 1985.
- Hoffer, R., D. F. Lozano-Garcia, D. D. Gillespie, P. W. Mueller, and M. J. Ruzek, Analysis of multiple incidence angle SIR-B data for determining forest stand characteristics, paper presented at the 2nd Space-Borne Imaging Radar Symposium, Jet Propul. Lab., Pasadena, Calif., May 1986.
- Hosier, R. H., Energy planning in Zimbabwe. Ambio, 15: 90-96, 1986.
- Huggins, L. F., and J. R. Burney, In: C. T. Haan (ed.), Surface runoff, storage and routing, In: Hydrologic Modeling of Small Watersheds, American Society of Agricultural Engineers, Monogr. 5, St. Joseph, Mich., 1982.
- Hutchinson, I. P. and D. C. Midgley, A mathematical model to aid management of outflow from the Okavanga Swamp. J. of Hydrol., 19: 93-112, 1973.
- Imhoff, M. L., C. Vermillion, M. H. Story, A. M. Choudhury, A. Gafoor, and F. Polcyn, Monsoon flood boundary delineation and damage assessment using space borne imaging radar and Landsat data, Photogramm. Eng. Remote Sens., 53(4), 405-413, 1987.
- International Geosphere-Biosphere Program, Toward an Understanding of Global Change, National Academy Press, Washington, D.C., 213, 1988.
- International Mathematical and Statistical Libraries, Inc., Houston, Tex., 1982.
- Jensen, M. and H. Haise, Estimating evapotranspiration from solar radiation. Amer. Soc. Civ. Engin., Jour. Irrig. and Drain, 89 (IR-4): 15-41, 1963.
- Johnson, A. I. (ed.), Hydrologic Applications of Space Technology, IAHS Publ. 160, Int. Assoc. of Hydrol. Sci., Gentbrugge, Belgium, 488, 1986.

- Junk, W. J., and C. Howard-Williams, Ecology of aquatic macrophytes in Amazonia, In: H. Sioli (ed.), The Amazon: Limnology and Landscape Ecology W. Junk, Boston, Mass., 269-293, 1984.
- Kellogg, W. W. and Z. Zhao, Sensitivity of soil moisture doubling of carbon dioxide in climate model experiments. Part I: North America. J. of Clim., 1: 348-366, 1988.
- Kenmuir, D. H. S., Fish production prospects in Zimbabwe. Zimbabwe Agric. J., 79: 11-17, 1982.
- Kiele, R. H., Irrigation development and the Kafue Flats. In: Proc. Nat. Sem. on Environment and Change of the Consequences of Hydroelectric Power Development on the Utilization of the Kafue Flats, University of Zambia, Lusaka, 69-73, 1982.
- Klemes, V., Sensitivity of Water Resource Systems to Climate Variations, World Meteorological Organization, WCP-98, 1-17, 1985.
- Korzoun, V. I., A. A. Sokolov, M. I. Budyko, K. P. Voskresensky, G. P. Kalinin, A. A. Konoplyantsev, E. S. Korotkevich and M. I. Lvovich, Atlas of World Water Balance, UNESCO, Paris, 1977.
- Krecek, J. and V. Zeleny, Effects of commercial forest logging upon streamflow processes in a small basin in the Moravian-Silesian Beskydy Mountains. In: The Influence of Man on the Hydrological Regime with Special Reference to Representative and Experimental Basins., IAHS/IASH Publication #130, Helsinki, 105-113, 1980.
- Leenaers, H., Estimating the Impact of Land Use Change on Soil Erosion Hazard in the Zambezi River Basin, IIASA Working Paper, Laxenburg, Austria. 26, 1989.
- Legates, D. R. and C. J. Willmott, Mean seasonal and spatial variability in gauge-corrected, global precipitation. Int'l. J. Climatology 10: 111-127, 1990.
- Legates, D. R. and C. J. Willmott, Terrestrial Water Budget Data Archive, U. of Delaware, Dept. of Geography, 1989.
- Leopold, L. B., M. G. Wolman,, and J. P. Miller, Fluvial Processes in Geomorphology, W. H. Freeman, New York, 1964.

- Lewis, L. A. and L. Berry, African Environments and Resources., Unwin Hyman Ltd., London. 404, 1988.
- Likens, G. E., F. H. Bormann, R. S. Pierce, J. S. Eaton and N. M. Johnson, Biogeochemistry of a Forested Ecosystem, Springer-Verlag, New York. 146, 1977.
- Machena, C. and P. Fair, Comparison of fish yields from prediction models between Lakes Tanganyika and Kariba. Hydrobiologia 137: 29-32, 1986.
- Makkink, G. F., Testing the Penman formula by means of lysimeters. Jour. Inst. Water Engin., 11: 277-288, 1957.
- Manabe, S. and R. T. Wetherald, Reduction in summer soil wetness induced by an increase in atmospheric carbon dioxide. Science 232: 626-28, 1986.
- Mather, J. R. and R. A. Ambroziak, A search for understanding potential evapotranspiration. Geogr. Review, 76: 355-370, 1986.
- Matthews, E., Global vegetation and land use. J. Clim. Appl. Meteor., 22: 474-487, 1983.
- McGuinness, J. L. and E.F. Bordne, A Comparison of Lysimeter - Derived Potential Evapotranspiration with Computed Values, United States Department of Agriculture, ARS, Tech. Bull. #1452, 71, 1972.
- Melack, J. M., and L. F. W. Lesack, Inputs of nitrogen and phosphorus to the flood plain of the Amazon River, paper presented at the Symposium on Freshwater Wetlands and Wildlife, Univ. of Ga., Charleston, S. C., 1986.
- Melack, J. M., and L. F. W. Lesack, Export of nitrogen and phosphorus from the central Amazon floodplain to the river, paper presented at the Chapman Conference on the Fate of Particulate and Dissolved Components within the Amazon Dispersal System: River and Ocean, Charleston, S. C., 1988.
- Mephram, J. S. and R. H. Mephram, Wetlands of the Zambesi Basin and the Lowlands of Mozambique. In: Symoens, J. J. and Burgis, M. J. (eds.), African Wetlands and Shallow Water Bodies: Directory, Institute de Recherche Scientifique pour le Developpement en Cooperation, Paris, France, 503-527, 1987.

- Meybeck, M., Total mineral dissolved transport by world major rivers. Hydrological Sci. Bull., 21: 265-284, 1976.
- Meybeck, M., Carbon, nitrogen, and phosphorus transport by world rivers. Amer. Jour. of Science, 282: 401-450, 1982.
- Milliman, J. D. and R. H. Meade, World-wide delivery of river sediment to the oceans. J. Geol., 91: 1-21, 1983.
- Minderhoud, P., Kafue Flats hydrological studies. In: Proc. National Sem. on Environ. and Change: The Consequences of Hydroelectric Power Development on the Utilization of the Kafue Flats, Lusaka, 59-622, 1978.
- Mintz, Y., and Y.V. Serafini, Global Monthly Climatology of Soil Moisture and Water Balance. Note Interne LMD #148, Laboratoire de Meteorologie Dynamique, Centre National de la Recherche Scientifique, Paris, 1989.
- Mitchell, J. F. B., C. A. Wilson and W. M. Cunningham, On CO<sub>2</sub> climate sensitivity and model dependence of results. Q. J. R. Meteorol. Soc., 113: 293-322, 1987.
- Mitchell, J. F. B., The seasonal response of a General Circulation Model to changes in CO<sub>2</sub> and sea temperatures. Quart. J. R. Met. Soc., 109: 113-152, 1983.
- Moore, B., M. P. Gildea, C. J. Vörösmarty, D. L. Skole, J. M. Melillo, B. J. Peterson, E. B. Rastetter and P. A. Steudler, Biogeochemical cycles. In: Rambler, M., Margulis, L. and Fester, R. (eds.), Global Ecology: Towards a Science of the Biosphere., Academic Press Inc., San Diego, CA, 113-142, 1989.
- Mwenya, A. N. and G. B. Kaweche, Wildlife conservation in the Kafue Flats in light of hydroelectric development. In: Proc. Nat. Sem. on Environment and Change of the Consequences of Hydroelectric Power Development on the Utilization of the Kafue Flats, University of Zambia, Lusaka, 129-35, 1982.
- NASA/EOS and Supplements, Earth Observing System. Science and Mission Requirements Working Group Report, Vol. 1, NASA, 51, 1984.
- National Aeronautics and Space Administration / Earth System Sciences Committee, Earth System Science, A Closer View, NASA, Washington, D. C., 208, 1988.



- National Aeronautics and Space Administration / Topographic Science Working Group, Topographic Science Working Group Report to the Land Processes Branch, Earth Science and Applications Division, NASA, 64, 1988.
- National Center for Atmospheric Research / NAVY, Global 10-minute elevation data, digital tape, Natl. Oceanic and Atmos. Admin., Natl. Geophys. Data Center, Boulder, Colo., 1984.
- Nemec, J. and J. Schaake, Sensitivity of water resource systems to climate variation. Hydrol. Sci., 27: 327-343, 1982.
- Nugent, C., The Zambezi River at Mana. Zimb. Sci. News, 22: 14-18, 1988.
- Obrdlik, P., A. Mumeka and J. M. Kasonde, Regulated rivers in Zambia - the case study of the Kafue River. Reg. Rivers: Res. and Management 3: 371-380, 1989.
- Olson, J. S., J. A. Watts and L. J. Allison, Carbon in Live Vegetation of Major World Ecosystems, (Publication # 1997), Oak Ridge National Laboratory, Oak Ridge, Tennessee, 1983.
- Oyebande, L., Effects of tropical forest on water yield. In: Reynolds, E. R. C. and Thompson, F. B. (ed.), Forests, Climate, and Hydrology, United Nations University, Tokyo, 16-50, 1988.
- Pastor, J., and W. M. Post, Calculating Thornthwaite and Mather's actual evapotranspiration using an approximating function, Can. J. For. Res., 14, 466-467, 1984.
- Pearce, A. J., L. K. Rowe and C. L. O'Loughlin, Effects of clearing and slash-burning on water yield and storm hydrographs in evergreen mixed forests, Western New Zealand. In: The Influence of Man on the Hydrological Regime with Special Reference to Representative and Experimental Basins., IAHS/IASH Publication #130, Helsinki, 119-127, 1980.
- Pinay, G., Hydrobiological Assessment of the Zambezi River System: A Review, WP-88-089, International Institute for Applied Systems Analysis, Laxenburg, Austria. 116, 1988.

- Pires, J. M., and G. T. Prance, The vegetation types of the Brazilian Amazon, In: G. T. Prance and T. E. Lovejoy (eds.), Key Environments Amazonia, Pergamon, New York, 109-145, 1985.
- Plamondon, A. P. and D. C. Ouellet, Partial clearcutting and streamflow regime of Ruisseau des Eaux-Volees Experimental Basin. In: The Influence of Man on the Hydrological Regime with Special Reference to Representative and Experimental Basins., IAHS/IASH Publication #130, Helsinki, 129-136, 1980.
- Plinston, D., A Review of the Hydrology of the Upper Zambezi. Inst. of Hydrology, Wallingford, UK, 1981.
- Quay, P. D., S. L. King, J. M. Lansdown, and D. O. Wilbur, Isotopic composition of methane released from wetlands: Implications for the increase in atmospheric methane, Global Biogeochem. Cycles, 2, 385-397, 1988.
- Raiche, J. W., E. B. Rastetter, J. M. Melillo, D. W. Kicklighter, P. a. Steudler, B. J. Peterson, A. L. Grace, B. Moore and C. J. Vörösmarty. 1991. Potential net primary productivity in South America: Application of a global model. Ecological Applications, (in press).
- Rastetter, E.B., M. G. Ryan, A. E. Russell, J. W. Raich, and C. J. Vörösmarty, Temporal aggregation of soil moisture models to improve consistency between daily and monthly estimates of moisture in drier soils. (In preparation, to : Water Resources Research), 1991.
- Reichle, D.E., ed, Dynamic Properties of Forest Ecosystems. Int'l Biological Programme 23. Cambridge Univ. Press, Cambridge, 683, 1981.
- Reeve, W. T. N. and D. T. Edmonds, Zambezi River flood hydrology and its effect on design and operation of Kariba Dam. Proc. Symp. on River Flood Hydrol., Instn. Civ. Eng., London, 169-186, 1966.
- Richards, K., Rivers: Form and Process in Alluvial Channels, Methuen, London, 1982.
- Richey, J. E., Interactions of C, N, P, and S in river systems: A biogeochemical model, In: B. Bolin and R. B. Cook (eds.), The Major Biogeochemical Cycles and Their Interactions, John Wiley, New York, 1983.

- Richey, J. E., R. H. Meade, E. Salati, A. H. Devol, C. F. Nordin, Jr., and U. dos Santos, Water discharge and suspended sediment concentrations in the Amazon River: 1982-1984, Water Resour. Res., 22(5), 756-764, 1986.
- Richey, J. E., L. A. K. Mertes, T. Dunne, R. L. Victoria, B. R. Forsberg, A. C. N. S. Tancredi and E. Oliveira, Sources and routing of the Amazon River flood wave. Global Biogeochem. Cycles, 3: 191-204, 1989.
- Richey, J. E., and M. N. G. Ribeiro, Element cycling in the Amazon Basin: A riverine perspective, In: R. Dickinson (ed.), The Geophysiology of Amazonia, John Wiley, New York, 245-250, 1987.
- Rzóska, J., On the Nature of Rivers, with Case Stories of Nile, Zaire and Amazon, W. Junk, Boston, Mass., 67, 1978.
- Salati, E., The Climatology and Hydrology of Amazonia. In: Prance, G. and Lovejoy, T. (ed.), Key Environments: Amazonia, Pergamon Press, Oxford, 18-48, 1985.
- Salati, E., and P. B. Vose, Amazon Basin: A system in equilibrium, Science, 225(4658), 129-225, 1984.
- Salati, E., and J. Marques, Climatology of the Amazon region, In: Harald Sioli (ed.), The Amazon: Limnology and Landscape Ecology, W. Junk, Boston, Mass., 85-126, 1984.
- Santa Clara, J. M. A., The hydrological operation of the Kariba hydroelectric scheme: Past, present, and future. Proc. Seizieme Congres des Grands Barrages, Q. 63, R. 29, Commission Internationale Des Grands Barrages, San Francisco, 449-478, 1988.
- Saxton, K. E., W. J. Rawls, J. W. Romberger, and R. I. Papendick, Estimating generalized soil water characteristics from texture, Soil Sci. Soc. Am. J., 50(4), 1031-1036, 1986.
- Schlesinger, W. H., J. F. Reynolds, G. L. Cunningham, L. F. Huenneke, W. M. Jarrell, R. A. Virginia and W. G. Whitford, New concepts in global desertification. Manuscript, 31, 1990.
- Schmidt, E. J., Water Quality Impact of Non-point Source Contaminants in Small Tidal Rivers, Ph.D. thesis, Univ. of N. H., Durham, 1981.

- Seagrief, S. C., The Lukanga Swamps - Northern Rhodesia. J. S. Afr. Bot., 28: 3-7, 1960.
- Sharma, T. C. and I. L. Nyumbu, Some hydrologic characteristics of the Upper Zambezi basin. In: Handlos, W. L. and G. W. Howard (ed.), Development Prospects for the Zambezi Valley in Zambia, Kafue Basin Research Committee, University of Zambia, 29-43, 1985.
- Shiklomanov, I. A. and O. I. Krestovsky, The influence of forest and forest reclamation practice on streamflow and water balance. In: Reynolds, E. R. C. and Thompson, F. B. (ed.), Forest, Climate and Hydrology, United Nations University, Tokyo, 78-116, 1988.
- Singh, V. P. (Ed.), Rainfall-Runoff Relationships, Water Resources Publications, Littleton, Colo., 1982.
- Sioli, H., The Amazon and its main affluents: Hydrography, morphology of the river courses and river types. In: H. Sioli (ed.), The Amazon: Limnology and Landscape Ecology of a Mighty Tropical River and Its Basin, Junk Publ., Dordrecht, Netherlands, 127-165, 1984.
- Sopper, N. E. and J. A. Lynch, Changes in water yield following partial forest cover removal on an experimental watershed. In: Symposium on the Results of Research on Representative and Experimental Basins, IAHS/UNESCO Publication #96, Wellington, New Zealand, 369-389, 1970.
- Stallard, R., and J. M. Edmond, Geochemistry of the Amazon, 2, The influence of geology and weathering environment on the dissolved load, J. Geophys. Res., 88, 9671-9688, 1983.
- Sutcliffe, J. V. and Y. P. Parks, Comparative water balances of selected African wetlands. Hydrol. Sci., 34: 49-62, 1989.
- Swank, W. T. and J. D. Helvey, Reduction of streamflow increases following regrowth of clearcut hardwood forests. In: Symposium on the Results of Research on representative and Experimental Basins., IAHS/UNESCO Publication #96, Wellington, New Zealand, 346-360, 1970.
- Swank, W. T. and D. A. Crossley, Forest Hydrology and Ecology, Ecol. Studies #66, Springer-Verlag, New York, 1988.

- Thornthwaite, C. W. and J. R. Mather, Instructions and Tables for Computing Potential Evapotranspiration and the Water Balance., Drexel Institute of Technology, Publications in Climatology, X(3), 1957.
- Thomsen, B. W. and H. H. Shumann, Water Resources of the Sycamore Creek Watershed, Maricopa County, Arizona, US Geological Survey Water Supply Paper #1861, 53, 1968.
- Tucker, C. J., J. R. G. Townshend, and T. Goff, Continental land cover classification using NOAA-7 AVHRR data, Science, 227, 369-375, 1986.
- Turc, L. , Evaluation des besoins en eau d'irrigation evapotranspiration potentielle. Ann. Agron., 12: 13-49, 1961.
- UNEP, Assessment of the Present and Future Activities Related to the Zambezi Action Plan, United Nations Environment Program - Report by the UNEP Mission of Experts to the Zambezi Countries, 115, 1986.
- UNESCO, Discharge of Selected Rivers of the World, Vol. III, Parts I-IV 1965-1979, UNESCO, Paris, 1971.
- UNESCO, Discharge of Selected Rivers of the World, Vol II, from start of observations to 1964, UNESCO, Paris, 1969.
- UNESCO, Discharge of Selected Rivers of the World, Vol. III, Mean Monthly and Extreme Discharges, part II, (1969-1972), UNESCO, Paris, 1974.
- UNESCO, Discharge of Selected Rivers of the World, Vol. III, Mean Monthly and Extreme Discharges, part III, (1972-1975), UNESCO, Paris, 1979.
- UNESCO, Discharge of Selected Rivers of the World, Vol. III, Mean Monthly and Extreme Discharges, part IV, (1976-1979), UNESCO, Paris, 1985.
- United Nations, River Inputs to Ocean Systems, UNIPUB, New York, 1981.
- US National Academy of Sciences, Climate, Climatic Change and Water Supply: Overview and Recommendations, Washington, DC., 1977.
- van Bennekom, A. J. and W. Salomons, Pathways of nutrients and organic matter from land to oceans through rivers. In: United Nations, River Inputs to Ocean Systems, UNIPUB, New York, 33-46, 1981.

- Van der Leeden, F., F. L. Troise, and D. K. Todd. 1990. The Water Encyclopedia, 2nd Edition. Lewis Publ., Chelsea, Michigan, 808, 1990.
- van der Lingen, M. I., Lake Kariba: Early history and South shore. In: Ackermann, W. C., White, G. F. and Worthington, E. B. (ed.), Man Made Lakes: Their Problems and Environmental Effects, American Geophysical Union, Washington, DC, 132-143, 1973.
- van der Wall Bake, Siltation and Soil Erosion Survey in Zimbabwe. In: Drainage Basin Sediment Delivery, IAHS Publ #159, Proc. Albuquerque Symposium, 69-80, August, 1986.
- Vannote, R. L., G.W. Minshall, K.W. Cummins, J.R. Sedell, and C.E. Cushing, The river continuum concept. Can. J. Fish. Aquat. Sci. 37: 130-37, 1980.
- Vörösmarty, C.J. and B. Moore III, Modeling basin-scale hydrology in support of physical climate and global biogeochemical studies: An example using the Zambezi River. Surveys in Geophysics, 12: 271-311, 1991.
- Vörösmarty, C. J., B. Moore, A. L. Grace and P. Gildea, Continental-scale models of water balance and fluvial transport: An application to South America. Global Biogeochem. Cycles, 3: 241-65, 1989.
- Vörösmarty, C.J., B. Moore, M.P. Gildea, B. Bergquist, J. M. Melillo, K. Nadelhoffer, and B. J. Peterson, A global model of nutrient cycling: II. Aquatic processing, retention and distribution of nutrients in large drainage basins. In: D. Correll (ed.), Watershed Research Perspectives, Smithsonian Institution Press, Washington, D.C., 32-56, 1986.
- Walling, D. E., Hydrological Processes. In: Gregory, K. J. and Walling, D. E. (ed.), Human Activity and Environmental Processes, John Wiley & Sons Ltd., Chichester, 53-85, 1987.
- Walling, D. E., The sediment yields of African rivers. In: Challenges in African Hydrology and Water Resources, IAHS Publication #144, Harare, Zimbabwe, 265-283, 1984.
- Ward, J.V. and J.A. Stanford, The serial discontinuity concept of lotic ecosystems. In: Fontaine III, T.D. and Bartell, S.M. (ed.), The Dynamics of Lotic Ecosystems, Ann Arbor Science Publishers, Ann Arbor, Michigan, 29-42, 1983.

- Ward, R. B., Sediment transport and a reservoir siltation formula for Zimbabwe-Rhodesia. Die Siviele Ingenieur in Suid Afrika, 9-13, 1980.
- Washington, W. M. and G. A. Meehl, Seasonal cycle experiment on the climate sensitivity due to a doubling of CO<sub>2</sub> with an atmospheric General Circulation Model coupled to a simple mixed-layer ocean model. J. Geophys. Res., 89: 9475-9503, 1984.
- White, E., Zambia's Kafue hydroelectric scheme and its biological problems. In: Ackermann, W. C., White, G. F. and Worthington, E. B. (ed.), Man Made Lakes: Their Problems and Environmental Effects, American Geophysical Union, Washington, DC, 620-629, 1973.
- White, F., The Vegetation of Africa., UNESCO 356, 1983.
- Whitlow, R., Man's impact on vegetation: The African experience. In: Gregory, K. J. and Walling, D. E. (ed.), Human Activity and Environmental Processes, John Wiley & Sons Ltd., Chichester, pp. 353-379, 1987.
- Willmott, C. J., S. G. Ackleson, R. E. Davis, J. J. Feddema, K. M. Klink, D. R. Legates, J. O'Donnell and C. M. Rowe, Statistics for the evaluation and comparison of models. J. Geophys. Res., 90: 8995-9005, 1985.
- Willmott, C.J. and S. M. Robeson, Climate, climatic change and their representation in the instrumental record. Proceedings: Resource Technology '90, Washington D.C., American Society for Photogrammetry and Remote Sensing, 1990.
- Willmott, C. J., and C. M. Rowe, Terrestrial Water Budget Data Archive: Version 1.01, Univ. of Del., Dep. of Geog., Newark, 1986.
- Willmott, C. J., C. M. Rowe, and Y. Mintz, Climatology of the terrestrial seasonal water cycle, J. Clim., 5, 589-606, 1985a.
- Willmott, C. J., Some comments in the evaluation of model performance. Bull. Amer. Meteor. Soc., 63: 1309-1313, 1982.
- Wiltshire, S. E., D. G. Morris, and M. A. Beran, Digital data capture and automated overlay analysis for basin characteristic calculation, Cartogr. J., 23, 60-65, 1986.

- Yair, A. and H. Lavee, Runoff generation in arid and semi-arid zones. In: Anderson, M. G. and Burt, T. P. (ed.), Hydrological Forecasting, John Wiley & Sons Ltd., 183-220, 1985.
- Yates, M. E., Effects of cultural changes in Makara Experimental Basin: Hydrological and agricultural production effects of two levels of grazing on unimproved and improved small catchments. In: Symposium on the Results of Research on Representative and Experimental Basins., IAHS/UNESCO Publication #97, Wellington, New Zealand, 270-291, 1972.



## APPENDIX

### ANALYSIS OF POTENTIAL ET FORMULAE

The following analysis tests some commonly-used methods for computing potential evapotranspiration (PET) and compares calculated results to site-specific data from the Zambezi region. The exercise will result in preliminary identification of a preferred method for calculating PET in the Water Balance Model described in the body of the text. The observed data is from FAO/UNDP (1968) which gives pan evaporation for a meteorological station located in the Kafue subcatchment at 15.0° S and 27.5° E.

Two of the methods are based on temperature. These are contrasted against three methods employing temperature, surface radiation and/or saturation vapor pressure. Results are presented in Figure III-6 along with a 0.8 \* Pan Evaporation timeseries.

The Thornthwaite and Mather (1957) technique is the first method based solely on temperature. The equations defining PET (mm/month) are:

$$PET = 16 d (10 T / I)^a \quad (A1a)$$

$$I = \sum_1^{12} (T/5)^{1.514} \quad (A1b)$$

$$a = 6.75 \times 10^{-7}I^3 - 7.71 \times 10^{-5}I^2 + 1.79 \times 10^{-2}I + 0.49 \quad (\text{A1c})$$

where T is temperature ( $^{\circ}\text{C}$ ), I is an annual heat index and a is an empirically-derived constant. The computed PET is then corrected for variable day and month length using d (standard = 12 hours and 30 days). After Thornthwaite (1948), the function takes the following form at or above  $26.5^{\circ}\text{C}$ :

$$\text{PET} = -0.43T^2 + 32.24T - 415.85 \quad (\text{A1d})$$

The Blaney and Criddle (1962) method is an agronomic tool established to determine crop irrigation requirements. The formula is posed as a function of temperature, but also has information on crop stage and requires the tracking of plant growth in order to accurately determine PET. It has the form:

$$\text{PET} = 25.4 D [(0.0173 T_f - 0.314) K T_f (D/D_s)] \quad (\text{A2a})$$

$$T_f = 1.8 T + 32 \quad (\text{A2b})$$

where  $T_f$  is mean daily air temperature ( $^{\circ}\text{F}$ ), K is the crop stage coefficient, and D is day length in hours and  $D_s$  is the sum of the day lengths over the year. Below  $1.7^{\circ}\text{C}$ , the first term within parentheses is set equal to 0.3. The monthly PET values using Blaney and Criddle method in the Kafue basin were provided by FAO/UNDP (1968).

The Turc (1961) method introduces an explicit radiation term into the PET determination:

$$PET = 0.40 T (R + 50) / (T + 15) \quad (A3)$$

The author has assumed that the term R refers to net ground-based radiation. This value was determined from a global net irradiance data set developed by Vörösmarty (unpublished). The data set was developed by taking radiation at the top of the atmosphere and correcting for cloudcover through the relationship of Black (1956):  $R = R_t (0.803 - 0.340 C1 - 0.458 C1^2)$ , where C1 = mean monthly cloudiness as a decimal fraction.

The Makkink (1957) method as reported in McGuinness and Bordne (1972) was used in this study. The equation is based on temperature, radiation and, implicitly, surface moisture effects:

$$PET = D [1.0213 \times 10^{-2} R ( / + \Psi) - 0.12] \quad (A4)$$

where is the slope of the saturation vapor pressure/temperature curve (mb/°C) and  $\Psi$  is the psychrometric constant, 0.66 (mb/°C).

The final method tested was that of Jensen and Haise (1963). It is a simple representation of PET as a function of radiation and temperature:

$$PET = 1.6742 \times 10^{-2} R D (0.014 [(1.8 T) + 32] - 0.37) \quad (A5)$$

with all variables as assigned previously. The first constant converts from radiation to equivalent depth of water.

The results are summarized in Figure III-6, for temperature- and temperature/radiation-based methods, respectively. There are considerable disparities among the methods. As a group the temperature-based methods reflect the timing of the temperature (see Figure III-5), which is not necessarily the timing shown by the pan ET timeseries. Assuming that 0.8\* pan value as given by FAO/UNDP (1968) is indeed the closest surrogate to PET, the Blaney/Criddle and Thornthwaite / Mather methods show annual values within, respectively, +15 % and -37 % of the "measured" PET. In contrast, the Turc, Makkink and Jensen/Haise techniques appear to more faithfully capture the timing of the pan ET curve, yet there are still substantial differences among the three sets of computed monthly values. The shape of the curves reflect the fact that each method accounts for the surface radiation shown in Figure III-5. On an annual basis, the Turc, Jensen/Haise and Makkink methods are within, respectively, -23 %, -10% and -33% of the annual pan ET. Based on this preliminary assessment, it would appear that the Jensen and Haise equation is most appropriate for use in a basin-scale model in the Zambezi region. The method may have wide applicability. In independent tests for a more humid tropical environment in South America

(Vörösmarty, unpublished data) the method performed well. Furthermore, the Jensen and Haise technique was judged to be among the best for temperature/radiation-based calculations in a comparative study by McGuinness and Bordne (1972) and by Allen (1990) using target lysimeter data for grasses. The latter study demonstrated that the method was suitable over a broad geographic range.